



EUROPEAN AVIATION SAFETY AGENCY
AGENCE EUROPÉENNE DE LA SÉCURITÉ AÉRIENNE
EUROPÄISCHE AGENTUR FÜR FLUGSICHERHEIT

Research Project EASA.2010/01

WAFCOLT - Water behaviour in aviation fuel under cold temperature conditions

Disclaimer

This study has been carried out for the European Aviation Safety Agency by an external organization and expresses the opinion of the organization undertaking the study. It is provided for information purposes only and the views expressed in the study have not been adopted, endorsed or in any way approved by the European Aviation Safety Agency. Consequently it should not be relied upon as a statement, as any form of warranty, representation, undertaking, contractual, or other commitment binding in law upon the European Aviation Safety Agency.

Ownership of all copyright and other intellectual property rights in this material including any documentation, data and technical information, remains vested to the European Aviation Safety Agency. All logo, copyrights, trademarks, and registered trademarks that may be contained within are the property of their respective owners.

Reproduction of this study, in whole or in part, is permitted under the condition that the full body of this Disclaimer remains clearly and visibly affixed at all times with such reproduced part.

WAFCOLT – Water in Aviation Fuel Under Cold Temperature Conditions

Final Report – Analysis And Recommendations

Edited by

Dr. Joseph K.-W. Lam
Airbus Operations Ltd

Contributions from

Mr. Mark D. Carpenter, Dr. Colleen Williams and Dr. Janice Hetherington
Cranfield Defence and Security, Shrivenham Campus

Dr. Liyun Lao, Dr. David Hammond, Prof. Colin Ramshaw and Prof. Hoi Yeung
Cranfield University, Cranfield Campus

Dr. Joseph K.-W. Lam
Airbus Operations Ltd

Report for

European Aviation Safety Agency
Ottoplatz 1
D-50679 Köln-Deutz
Deutschland

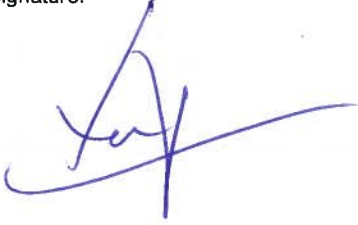
Contract reference

EASA.2010.OP.07

© AIRBUS OPERATIONS LIMITED 2013 ALL RIGHTS RESERVED

The copyright in this document, which contains information of a proprietary nature is vested in Airbus Operations Limited. The contents of this document/tape/disk/CDROM may not be used for any purposes other than for which it has been supplied and may not be reproduced either wholly or in part, in any way whatsoever, nor may it be used by, or its contents divulged to, any other person whatsoever without the prior written permission of Airbus Operations Limited.

Authorisation

Edited By:	Signature:  Joseph K.-W. Lam Fuel & Inerting R&T (EYUIR)	Date: 03 May 2013
Technical Approval:	Signature:  Stewart Ashworth Head of Refuel & Venting (EYUMR)	Date: 03 MAY 13
Technical Authorisation:	Signature:  Stephen Lisle-Taylor Head of Performance Integrity (EYUI)	Date: 03 May 13.

Issued by:

Airbus Operations Ltd.
 Golf Course Lane
 Filton
 Bristol BS99 7AR
 UK

Record of Revisions

Issue	Date	Reasons for revision
1.0	20 Jan 2012	<ul style="list-style-type: none">• Initial issue
2.0	20 Mar 2013	<ul style="list-style-type: none">• Fixed typos and minor format issues in all three parts• Added a record of revision• Further analysis and details added to Section 2.2.4 of Part 1• New results added to Part 2• Corrected Table 3 of Part 3 and the preceding text before the table• Corrected Section 2.3 of Part 3• New info/details added to Section 3 of Part 3• New info/details added to Section 4.3 of Part 3• Add the IMechE event brochure in Appendix D

Summary

This report constitutes the final report as stated in the technical proposal (SCF/SYS/GEN/98/2392) to EASA. It details Task 3 Analysis and Recommendations over the period from mid-June 2011 to December 2011. The report is divided into three parts:

- Part 1 is the contribution from the Shrivenham campus;
- Part 2 is the contribution from the Cranfield campus;
- Part 3 is the contribution from Airbus.

Laboratory testing was conducted in parallel at the two Cranfield campuses to ensure that the timescale of the project was met and to make the best use of the facilities and expertise at the two sites. Solubility tests were carried out at Shrivenham and ice accretion tests were carried out at Cranfield; Airbus coordinated the work conducted by Cranfield University. In addition to this work, results and analysis of icing tests conducted by Airbus outside this project are presented.

An executive summary is given for each part to highlight some of the main findings and recommendations.

Results from an additional ice accretion test conducted after the report was first issued to EASA are added to this updated report (issue 2).

Table of Contents

Authorisation	2
Record of Revisions.....	3
Summary	4
Table of Contents	5

Part 1: Analysis of Test Results & Recommendations – Shrivenham Campus..... 9

EXECUTIVE SUMMARY 10

1. INTRODUCTION..... 12

1.1 *Aims And Objectives* 14

1.2 *Methodology* 14

1.3 *Implementation* 15

2. WATER SOLUBILITY MEASUREMENTS 16

2.1 *Background*..... 16

2.2 *Experimental Work*..... 17

2.2.1 Fuel conditioning and standardisation..... 17

2.2.2 Water measurements in aviation fuel..... 19

2.2.3 Determination of water content in fuel using the multiple injection
technique with the KF 831 20

2.2.4 Results..... 21

2.3 *Discussion on Water Solubility Measurements* 28

2.4 *Summary and Conclusions on Water Solubility Measurements*..... 28

3. MICROSCOPY STUDY OF WATER DROPLET AND ICE FORMATION IN FUELS 30

3.1 *Background*..... 30

3.2 *Microscope and Cold Stage* 30

3.3 *Phase Contrast Microscopy* 31

3.4 *Sample Preparation and Selection*..... 32

3.5 *Cooling/Heating Regimes* 33

3.6 *Matrix of Tests Conducted* 33

3.7	<i>Microscopy Results</i>	34
3.8	<i>Discussion on Cold Stage Microscopy Observations</i>	41
3.9	<i>Summary and Conclusions on Cold Stage Microscopy</i>	43
4.	PARTICLE QUANTIFICATION USING THE JORIN VIPA	44
4.1	<i>Background</i>	44
4.2	<i>Jorin ViPA</i>	46
4.3	<i>Experimental Details</i>	46
4.4	<i>Darkening of the ViPA Field of View</i>	51
4.5	<i>Data Analysis</i>	52
4.6	<i>Discussion on Particle Quantification Tests</i>	60
4.7	<i>Summary and Conclusions on Particle Quantification Tests</i>	61
5.	DISCUSSION AND CONCLUSIONS	63
5.1	<i>Results And Discussions</i>	63
5.2	<i>Outcomes</i>	63
5.3	<i>Conclusions</i>	63
5.4	<i>Future Work</i>	64
	REFERENCES	65

Part 2: Analysis and Recommendations – Cranfield Campus..... **66**

	EXECUTIVE SUMMARY	67
1.	BACKGROUND	69
1.1	<i>Aims And Objectives</i>	70
2.	LITERATURE REVIEW	71
3.	METHODOLOGY	73
3.1	<i>Ice Accretion On Subcooled Surfaces</i>	73
3.2	<i>Ice Porosity</i>	74
3.3	<i>Adhesion Strength</i>	79
4.	IMPLEMENTATION	81
4.1	<i>Water Replenishment System</i>	81
4.2	<i>Specimen Blocks For Ice Accretion Tests</i>	85

4.3	<i>Modifications To The Simulated Fuel Tank</i>	86
4.4	<i>Chest Freezer</i>	88
4.5	<i>Experiment Processes</i>	89
5.	RESULTS	92
5.1	<i>Ice Accreted On Subcooled Surfaces In Fuel</i>	92
5.1.1	General observations.....	95
5.1.2	Quantification of accreted ice.....	101
5.2	<i>Properties Of Accreted Ice</i>	107
5.2.1	General observations.....	107
5.2.2	Quantification of porosity	108
5.2.3	Quantification of adhesion strength	110
6.	CONCLUSIONS	114
7.	RECOMMENDATIONS	116
8.	ADDITIONAL OBSERVATIONS	117
	REFERENCES	120

Part 3: Analysis of Test Results & Recommendations – Airbus..... 122

	EXECUTIVE SUMMARY	123
1.	INTRODUCTION	124
2.	SNOW-TO-LIQUID RATIO	125
2.1	<i>SLR Variability</i>	125
2.2	<i>Influence Of Fluid Medium On SLR</i>	128
2.3	<i>Influence Of Flow Velocity On SLR</i>	129
2.4	<i>Influence Of Growth Rate On SLR</i>	130
3.	ICING RISK REDUCTION	137
3.1	<i>Fuel System Icing Inhibitor</i>	137
3.2	<i>Fuel Warming</i>	139
3.3	<i>Onboard Water Separator</i>	140
3.4	<i>Fuel Line Anti-Icing</i>	142
3.5	<i>Insulating Material</i>	143
3.6	<i>Architecture Optimisation</i>	143

3.7	<i>Dehumidifying Ingress Air</i>	143	
3.8	<i>Displacing Ingress Air</i>	144	
3.9	<i>Fuel Dehydration</i>	145	
4.	CONCLUSIONS	147	
4.1	<i>Snow In Fuel</i>	147	
4.2	<i>Prevention Of Ice Formation In Fuel</i>	147	
4.3	<i>Outlook</i>	148	
	REFERENCES	152	
Appendix A: Response to Comments on the Literature Review – RP1115500, Issue 1			155
<i>Appendix A.1 Rationale For The Recent Revision To ASTM D7566</i>			169
<i>Appendix A.2 Water Phase Diagram</i>			171
<i>Appendix A.3 Methods Of Detecting Water In Aviation Fuel</i>			172
Appendix A.3.1 Aqua Glo.....			172
Appendix A.3.2 Shell Water Capsule			172
Appendix A.3.3 Karl Fischer Coulometry			173
Appendix A.3.4 Microseparometer Test.....			173
Appendix A.3.5 Particle Counting Techniques.....			174
Appendix B: Response to Comments on the Proposed Work Programme – PL1101812, Issue 1			175
<i>Appendix B.1 Compliance Matrix Between The Literature Review And The Proposed Testing Activities</i>			182
Appendix C: Test Fuels – Chemical & Physical Data Analysis Reports			185
<i>Appendix C.1 Air BP Filton Airfield Jet A-1</i>			186
<i>Appendix C.2 Chinese No. 3</i>			188
<i>Appendix C.3 Coryton High Aromatics Jet A-1</i>			190
<i>Appendix C.4 Russian TS-1 Aviation Kerosine</i>			192
<i>Appendix C.5 Sasol Fully Synthetic Jet A-1</i>			193
<i>Appendix C.6 JP-4 Wide-Cut Fuel</i>			198
Appendix D: IMechE Event Brochure – Managing Water and Ice in Aviation Fuel Under Cold Temperatures			200

Part 1: Analysis of Test Results & Recommendations – Shrivenham Campus

By

Mr. Mark D. Carpenter
Dr. Colleen Williams
Dr. Janice Hetherington

Cranfield Defence and Security
Shrivenham Campus
Swindon
SN6 8LA
UK

EXECUTIVE SUMMARY

The project was designed to evaluate the water dropout and ice formation characteristics of five jet fuels made to different national standards, which either comply with or are very similar to the Jet A-1 fuel specification; a key requirement was that one of the fuels was to be fully synthetic, i.e., not derived from conventional crude oil stocks. The work programme also required limited tests on a wide-cut fuel conforming to the JP-4 specification.

The WAFCOLT work programme conducted at Cranfield Shrivenham comprised two main elements. Firstly, a contribution to a literature review which summarised the relevant current knowledge and research on jet fuel composition, water shedding in fuels and low temperature studies of fuels. Secondly, a laboratory programme intended to confirm and generate new data where this was believed to be lacking, particularly for the new alternative jet fuels.

The laboratory work was concerned with making fundamental measurements and observations of the solubility of water in aviation fuels and determined what happened to this water as the fuel temperature was reduced. The tests were split into three areas:

- 1) Karl Fischer coulometric tests.
- 2) Cold stage microscopy tests.
- 3) Particulate measurements.

Information on the effects of water dropout on cooling fuel could be measured and observed directly. Measuring the response due to fuel composition was more difficult, owing to the complexity of fuel compositions, and measurements could only be made indirectly by comparing one fuel against another. The Karl Fischer tests yielded solubility curves for the current fuels. Cold stage microscopy observations and measurements corroborated previous observations of the behaviour of water in cooled fuels and confirmed dimensions of particles likely to be produced. Microscopy tests were useful for assessing and observing the likely physical changes but were not necessarily good predictors of how these changes might occur in larger bodies of fuel and/or the rates of those changes. The particulates study in a larger volume of fuel delivered data on the numbers of particles in the fuel and the dimensions of those particles. However, difficulties were encountered in resolving the nature of those particles, particularly as the temperature decreased.

No evidence of 'sticky' ice was observed, but some particles seemed to be more mobile than others. When ice particles were observed, these seemed to be in co-existence with water droplets. Under flowing conditions, supercooled water droplets might act as cement in bonding ice crystals to each other or to surrounding surfaces that they might come in to contact with. Based on the laboratory observations and measurements, it was considered that only limited icing would occur at temperatures above -20°C as a result of water shedding from aviation fuels.

The research findings will benefit anyone associated with designing fuel systems, developing strategies for avoiding icing in fuels or for those associated with developing fuels or additives which resist ice formation. In essence, the main beneficiaries will be airframe manufacturers, aircraft fuel system designers and fuel additive manufacturers.

1. INTRODUCTION

The WAFCOLT work programme conducted at Cranfield Shrivenham comprised two main elements:

- Firstly, a contribution to a literature review [1] which summarised the relevant current knowledge and research on jet fuel composition, water formation in fuels and low temperature studies of fuels.
- Secondly, a laboratory programme intended to cross-reference some areas raised by the literature review and generate new data where this was believed to be lacking, particularly for the new generation of alternative jet fuels.

This report details the laboratory research over the period from mid-June 2011 to November 2011, and covers three main areas:

- Water solubility measurements on the jet fuels supplied for this programme,
- Study of water droplet and ice formation in the jet fuels,
- Quantification of water droplet formation and particulates in jet fuel under conditions of reducing temperature.

Initial work involved familiarising staff with the various pieces of test equipment and performing checks to ensure that everything was working to specification. Tests were carried out using existing jet fuels and model hydrocarbons whilst waiting for fresh stocks of aviation kerosine fuels to arrive. A new Karl Fischer Coulometer was purchased for the project since this is an essential piece of equipment for measuring water content in liquids and would be key to assessing the water pick-up and shedding capabilities of the different fuels used in this test programme.

The laboratory work mostly followed the structure given in Part 1 of the proposed work programme [2]; however, a not insignificant amount of time was devoted to assessing water solubility in the different types of jet fuel so that solubility curves could be drawn to show the effects of temperature. Due to time constraints, it has not been possible to perform any work on the effects of additives to jet fuels.

The project was intended to evaluate the water dropout and ice formation characteristics of five jet fuels made to different national standards, which either comply with or are very similar to the Jet A-1 fuel specification; as far as possible, the fuels were to be sourced from the country from which that national standard originated. A further requirement was that one of the fuels was to be fully synthetic, i.e., not derived from conventional crude oil stocks. The work programme also included limited tests on a wide-cut fuel conforming to the JP-4 specification.

The Gantt chart for this project (Table 1) outlines the tasks to be addressed by the project and the indicative timescale.

Table 1 EASA WAFCOLT – Cranfield Shrivenham

Project Tasks	Jun 2011				Jul 2011				Aug 2011				Sep 2011				Oct 2011				Nov 2011				Dec 2011			
	1	2	3	4	1	2	3	4	1	2	3	4	1	2	3	4	1	2	3	4	1	2	3	4	1	2	3	4
TASK 2 LABORATORY TESTING																												
Task 2.3 Study of water droplet / ice formation																												
Training Colleen Williams																												
Fuel conditioning																												
Comparison tests with existing data																												
Karl Fischer measurements																												
Microscope cold stage measurements*																												
Freezer + Jorin measurements**																												
Effect of additives																												
TASK 3 ANALYSIS AND RECOMMENDATIONS																												
Task 3.1 Analysis of test results																												
Task 3.2 Final report																												
PROGRESS REPORTS/MEETINGS																												
Progress meeting																												
Final dissemination																												

* Tests will be repeated on up to six different fuels. Each fuel will take about 2 weeks to evaluate.

** Tests will be repeated on five different fuels; there are safety concerns about testing wide-cut fuel. Each fuel will take about 2 weeks to evaluate.

The date for the final dissemination was provisionally scheduled for January 2012. Due to delay of the project, the final dissemination will need to be re-scheduled.

1.1 Aims And Objectives

- The laboratory work largely followed the tasks detailed in the work proposal [2].
- Airbus procured all fuels detailed [2], but there were some delays.
- Fuel pre-conditioning as detailed.
- Cold stage microscopy. Ran all tests on current fuels as detailed. Some tests were duplicated to check for consistency. Some tests were not entirely satisfactory, e.g., due to out-of-focus images, which meant they had to be repeated. Results, in general, from this study were compared with results from previous tests, but exact like-for-like tests were not conducted. Did not attempt study of effects of particulates, FAME or HVO.
- Particulate analysis. Ran tests on current fuels as detailed but did not duplicate tests. Experiments were very time consuming, particularly the data analysis. However, an additional test was conducted to check the effect of partially drying one fuel.
- Additional work. A considerable amount of time was devoted to conducting Karl Fischer tests on the different fuels, in order to draw up water solubility curves. This information was used to help select the fuels for the larger scale tank testing at Cranfield.

1.2 Methodology

- This was fundamental research; it tried to make basic measurements of certain physical properties. Sometimes there are very few technical options in these situations.
- For instance, using the Karl Fischer coulometer, although time consuming, was an automated analytical system. Trying to achieve the same number of results using manual titration methods would have been even slower. Tried and accepted method of assessing water contents in fluids and materials.
- Cold stage microscopy. Direct observation of water dropout from fuels and re-solution. Occasionally, ice crystals could be observed. Possible to record time/temperatures at which events occurred and make dimensional measurements of particles observed. Providing the optical system is correctly calibrated, this is an accurate but labour intensive method of collecting data. Operator dependent, but a tried and proven method.
- Particulate analysis using the Jorin ViPA and freezer: This system had some known limitations, e.g., loss of optical transparency in fuel as it was cooled



(possibly an intrinsic feature of kerosine fuels) and difficulties with maintaining a constant temperature between the fuel siphon point in the fuel container and the optical measurement point. This experiment was difficult to conduct, has more variables and possibly a higher level of experimental scatter than the other experimental procedures. The ViPA is believed to be well characterised, but it is extremely difficult to prove that level of accuracy. Can only relate the results back to microscopy observations and external reports about using the ViPA.

1.3 Implementation

- Programme ran largely as planned, but with extra work due to water solubility tests on fuels.
- Starting the laboratory phase was delayed due to long delivery times on some of the fuels.
- Try to allow more time to complete tasks, in future research projects, to cover circumstances outside one's control.

2. WATER SOLUBILITY MEASUREMENTS

2.1 Background

The initial part of the test programme required an extensive assessment of the water pick-up and shedding characteristics of the supplied jet fuels; there was a requirement that the fuels should be freshly sourced since fuel compositions may change subtly with storage due to the formation of polar oxidation compounds such as organic acids. Some data on the water solubility behaviour is available in the open literature but this mostly dates back to the 1950s. Even data given in the CRC Handbook of Aviation Fuel Properties [3] (Fig 2-32) was found to pre-date 1984; the actual source of this data could not be verified [4] but looks similar to data presented by Crampton et al [5]. A limited amount of work has been conducted recently at Shrivenham on two jet fuels provided by a major UK oil refiner, but it was acknowledged that the scope of the work should be widened to take account of recent changes in fuel chemistry owing to the need to exploit less favourable crude oil reserves and the potential future use of alternative fuels.

Jet fuel does not have an exact chemical composition; it is produced to meet a set of properties. Its chemical composition will depend on the chemical species present in the parent crude oil that come over in the physical separation in the kerosine boiling range and on further chemical treatments that may be required to meet the jet fuel specifications. Jet fuels are often classed as 'Mercox treated', or 'hydrotreated', or 'straight run', reflecting the processes used in their production. The aromatics content of a fuel has been shown to have a significant effect on the affinity of the fuel for water but there are other constituents (impurities or additives) in the finished fuel, which may influence surfactancy tendencies.

Table 2 summarises the fuels available for this test programme.

Table 2 WAFCOLT test fuels

<i>Fuel and Specification</i>	<i>Abbreviated Name</i>	<i>Provenance</i>
Air BP Filton Airfield Jet A-1	Filton	Air BP UK Ltd
Chinese No 3	Chinese	PetroChina International (Hong Kong) Ltd
Coryton High Aromatics Jet A-1	Coryton	Coryton Advanced Fuels Ltd, UK
Russian TS-1 Aviation Kerosine	Russian	Blended by Coryton; tested/approved in Russia
Sasol Fully Synthetic Jet A-1	Sasol	Sasol, South Africa
JP-4 Wide-Cut Fuel	JP-4	Coryton Advanced Fuels Ltd, UK

Detailed chemical composition data and physical test data for all the fuels are given in the Appendix C. The kerosines were supplied to the normal commercial specification and included static dissipater additive (SDA), where shown. The JP-4 was actually supplied to the NATO F-40 (AVTAG/FSII) specification which includes requirements for lubricity improver, SDA and fuel system icing inhibitor.

2.2 Experimental Work

2.2.1 Fuel conditioning and standardisation

On receipt, the fuel transit containers were left to stand for at least one week in a dedicated flammables storage area. After standing, fuels were siphoned into 5 litre retention containers for laboratory use. The Chinese fuel was noted to show a fair degree of sediment in the bottom of the storage can. Fuels were filtered using nitrogen gas pressure through a Sartorius filter assembly fitted with Millipore HAWP04700 (0.45 μm) mixed cellulose filter; fuels were filtered in batches of approximately 1.2 litres. Plates 1 to 5 show the approximate colour and dirt retained by the filter after treating 1.2 litres; the filter colours were matched to the colour standards in Appendix X1 of ASTM D2276-06 and the rating is given for each plate. After filtering, all the fuels were noted to be water-white and would be classified as clear and bright.

Filtered fuels were stored in individual desiccators and dried over silica gel for at least one day. This procedure ensured that all the fuels had low concentrations of water and that re-humidification at temperatures below ambient temperature could be carried out without water coming out of solution from the fuel. The desiccators were stored inside a fume cupboard to minimise exposure to ambient light. The Chinese fuel was noted to be particularly susceptible to UV degradation, turning a noticeable yellow after a few days.

For the purposes of the test programme, the fuels were re-humidified in a closed vessel (a desiccator containing a small amount of distilled water throughout the process) at the appropriate test temperature; the aim was to achieve a 100% relative humidity (RH) environment without introducing bulk water. A Mercia Scientific Humidicab was used for tests at or above 5°C, as shown in Plate 6, and a Fisons FE 300H cabinet for temperatures below 5°C. In order to avoid over-saturating the fuels, each dried fuel sample was cooled to below the nominal conditioning temperature, transferred to the desiccator containing a small amount of distilled water and allowed to warm to the test temperature. Approximately 300 ml of fuel was treated in this way for each test. Fuel samples were gently stirred with a magnetic stirrer and the sample left to reach water saturated equilibrium at the relevant set temperature for at least one day. Previous work had shown this to be sufficient time for the system to reach equilibrium [6]. The desiccators were fitted with septum caps to allow sampling of the fuel without disturbing the equilibrium. A thermocouple was located in the fuel so that an accurate reading of the fuel temperature could be taken when sampled.

Plate 1 Air BP Filton Airfield Jet A-1
ASTM D2276-06 Appendix X1 colour rating:
G1

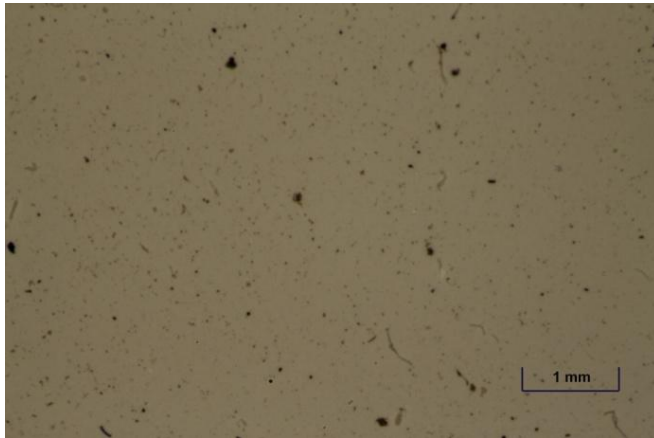


Plate 2 Chinese No 3 ASTM D2276-06
Appendix X1 colour rating: B1

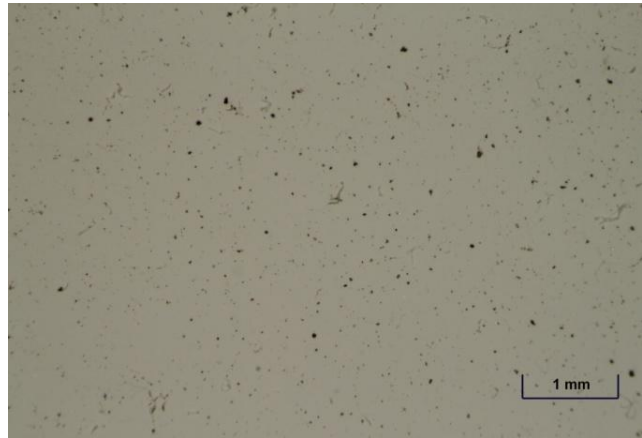


Plate 3 Coryton High Aromatics Jet A-1
ASTM D2276-06 Appendix X1 colour
rating: B3

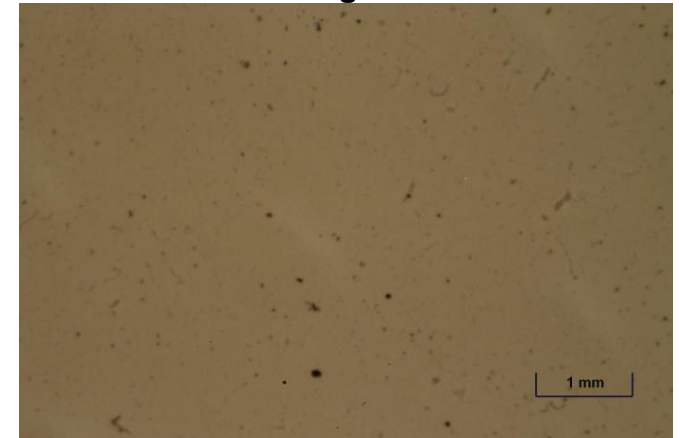


Plate 4 Russian TS-1 Aviation
Kerosine ASTM D2276-06 Appendix X1
colour rating: B1

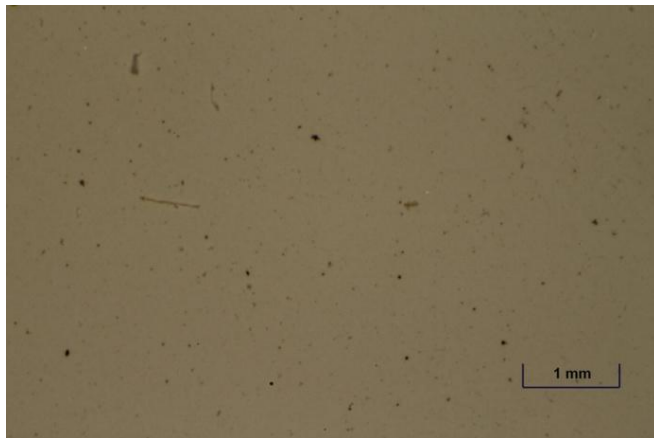


Plate 5 Sasol Fully Synthetic Jet A-1
ASTM D2276-06 Appendix X1 colour rating:
B0

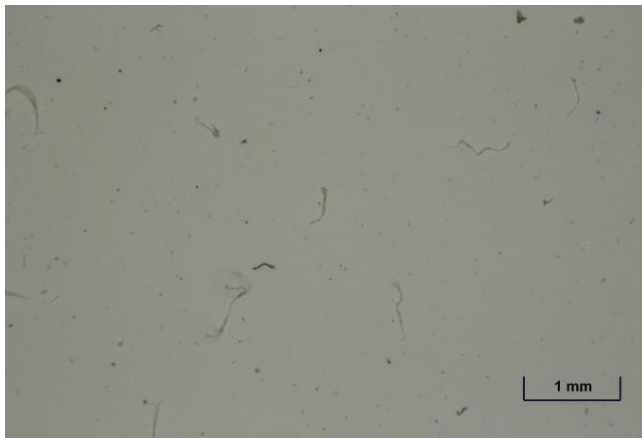


Plate 6 Mercia Scientific Humidicab with fuel samples and desiccators in position



2.2.2 Water measurements in aviation fuel

For this project, a new Metrohm Karl Fischer Coulometer (KF 831) was purchased, as shown in Plate 7. This was a substantial upgrade from the Metrohm KF 684 used previously and some experiments were necessary to ensure consistency of measurement between the two sets of apparatus. An SGE gas-tight 2.5 ml glass syringe with a long stainless steel luer needle was used for all injections. Metrohm recommended that a single injection under the surface of the anolyte solution was the best method for making the measurements. However, the method used previously for similar fuels work, and a technique also endorsed by Air BP, was a multiple injection sequence with the needle tip below the surface of the anolyte. A comparison of these two methods found that the multiple injection procedure gave a smaller spread of results than the single injection technique and so this method was adopted for all measurements [see Section 2.2.3]. Various anolytes were also evaluated as there were potentially three different ones that could be used for determination of the water content in aviation fuel. These were all manufactured by Sigma Aldrich under the Hydranal Coulomat brand; these were type AG-H, a solution of type A with chloroform (70:30) and Coulomat oil. Following experiments with all anolytes, it was found that type AG-H gave the most consistent results, with the least tendency to form a biphasic solution of fuel and anolyte. It should be noted that

measurements of the water content in fuels at temperatures below 5°C are nearing the limit of resolution by the Karl Fischer coulometric technique, due to the low concentration of water in the samples, and therefore are subject to a greater error.

Plate 7 Metrohm Karl Fischer Coulometer KF 831, with SGE glass syringe and needle in foreground



2.2.3 Determination of water content in fuel using the multiple injection technique with the KF 831

A clean, empty syringe of known weight was taken and the needle inserted into the Karl Fischer (KF) cell via a septum; AG-H anolyte solution was drawn into the syringe, then injected into the cell and a reading was taken of the water content. The syringe remained in position in the cell and AG-H solution was again drawn up into the syringe and then re-injected into the cell; this process was repeated until the water content measured was less than 1 ppm by mass. The syringe was removed from the KF cell and conditioned aviation fuel was drawn into the syringe and then weighed. The syringe containing fuel was inserted into the KF cell and the sample injected; a reading was taken of the water content. The calculated weight of fuel injected was entered via the KF 831 keypad, so that the water content of the fuel could be determined by mass. The syringe remained in the cell and AG-H solution was drawn up into the syringe, re-injected and a further reading of the water content was taken. This process was repeated a further two times to give a total of four readings. These readings were added together to give the total amount of water in

that sample of aviation fuel. The water content of each fuel was measured ten times at each temperature.

2.2.4 Results

To generate the water solubility curves, the saturated water content of each fuel was measured at nominal temperatures of -5 , 0 , 5 , 15 and 25°C . Each fuel was conditioned at the appropriate temperature and the water content was determined using the standard procedure given in Section 2.2.3. When fuel samples were taken at test temperatures below 5°C , the fuel in the conditioning desiccator tended to gradually warm up, typically by 1 to 3°C over the course of a set of measurements; this was due to the conditioning chamber door being opened multiple times to allow samples to be taken. Although individual readings of fuel temperature were made, for accuracy the KF measurements were always averaged over ten readings and therefore an average temperature is given for a set of readings at a particular temperature. For tests below 0°C , the temperature set point on the conditioning cabinet needed to be lower than the nominal test temperature to compensate for the warming effect due to the cabinet door being repeatedly opened and closed. Some of the data sets were repeated because there appeared to be a larger degree of scatter in the results than was considered satisfactory. There are a number of reasons for this; these might be related to laboratory temperature and/or humidity, condensation on the desiccator septum or syringe needle. It must be remembered that the concentrations of water being measured are very low, so even just traces of water can significantly skew the results.

The results presented are those from data sets which showed the most consistency, as reflected by the standard deviation. The water contents from the Karl Fischer measurements, averaged over ten readings at a particular temperature, are listed in Table 3. Table 4 gives an estimate of the water shed from each fuel on cooling a water saturated fuel at 25°C to 0°C and also to -20°C .

It is easier to look at trends graphically, so data from the tests were plotted as a series of curves of water content versus temperature. Since the water absorption characteristics of aviation fuels follows an exponential trend with increasing temperature, expressing water content on a logarithmic scale should yield a straight line relationship:

(1)

Here, w is the water solubility in fuel in ppm m/m, b is the base, n is the exponent coefficient and T is the fuel temperature in $^{\circ}\text{C}$. Trend lines were fitted to the data points for each fuel. Figure 1 illustrates the water solubility curves for averaged data given in Table 3. For comparative purposes, the curve for Jet A-1 from Figure 2-32 in the CRC Handbook [3] has also been added.

The standard deviation can be taken as a measure of the uncertainty in the measurements; the higher the standard deviation, the greater the spread of the measurements in the data set. Figure 2 illustrates the spread in the measurements for individual test sets. As the graph is on a logarithmic scale, it appears that there is

a greater degree of scatter at lower temperatures which accurately reflects the higher uncertainty in those measurements.

Table 3 Summary of Karl Fischer Test Results

Fuel	Conditioning Treatment Cabinet Temperature	Average Water Content (ppm by mass)	Standard Deviation	Average Sample Temperature* (°C)
Coryton High Aromatics Jet A-1	-9°C ~1 day	30	2.2	-5.5
	-3°C ~3 days	33	0.7	-0.5
	5°C ~1 day	44	2.1	5.0
	15°C ~3 days	67	1.6	14.5
	25°C ~1 day	104	1.2	25.0
Chinese No 3	-5°C ~1 day	24	1.0	-3.0
	-2.5°C ~5 days	30	1.1	-0.5
	5°C ~1 day	40	0.7	6.0
	15°C ~2 days	61	0.6	15.0
	25°C ~1 day	96	1.5	25.0
Russian TS-1 Aviation Kerosine	-8°C ~1 day	22	1.2	-3.5
	-3°C ~1 day	28	0.6	0.5
	5°C ~1 day	38	0.6	5.0
	15°C ~3 days	53	1.3	14.0
	25°C ~2 days	93	1.4	25.0
Air BP Filton Airfield Jet A-1	-9°C ~1 day	20	0.9	-5.5
	-3°C ~3 days	27	1.0	-0.5
	5°C ~1 day	33	0.9	5.0
	15°C ~3 days	50	0.6	14.0
	25°C ~1 day	86	0.8	25.0
Sasol Fully Synthetic Jet A-1	-5°C ~1 day	19	1.2	-1.0
	-2.5°C ~4 days	19	0.6	1.0
	5°C ~1 day	29	0.7	5.0
	15°C ~2 days	43	0.5	14.0
	25°C ~3 days	73	0.7	25.5
JP-4 Wide-Cut Fuel	5°C ~3 days	64	0.9	5.0
	15°C ~1 day	74	2.6	14.5
	25°C ~6 days	90	2.9	25.0

* This was the average fuel sample temperature, at the time of sampling, expressed to the nearest 0.5°C

Table 4 Estimated Water Dropout from Fuels on Reducing Temperature based on Karl Fischer Results

The aromatics contents were taken from the certificates of analysis for the fuels

<i>Fuel</i>	<i>Aromatics</i>	<i>Average Water Content (ppm by mass)*</i>			<i>Water Dropout (ppm by mass)*</i>	
	<i>% v/v</i>	<i>At 25°C</i>	<i>At 0°C</i>	<i>At -20°C</i>	<i>Cooling from 25°C to 0°C</i>	<i>Cooling from 25°C to -20°C</i>
<i>Coryton High Aromatics Jet A-1</i>	24.1	104±2	36±2	15±2	68±4	89±4
<i>Chinese No 3</i>	16.4	97±2	29±2	11±2	68±4	86±4
<i>Russian TS-1 Aviation Kerosine</i>	13**	93±2	27±2	10±2	66±4	83±4
<i>Air BP Filton Airfield Jet A-1</i>	13.7	86±2	26±2	10±2	60±4	76±4
<i>Sasol Fully Synthetic Jet A-1</i>	12.4	73±2	20±2	7±2	53±4	66±4
<i>JP-4 Wide-Cut Fuel</i>	10.3	89±2	58±2	41±2	31±4	48±4

* These values were derived from trendline gradient data given in Figure 1

** % m/m

Water Solubility versus Temperature for Various Jet Fuels
 Best fit curves through average of data for each fuel

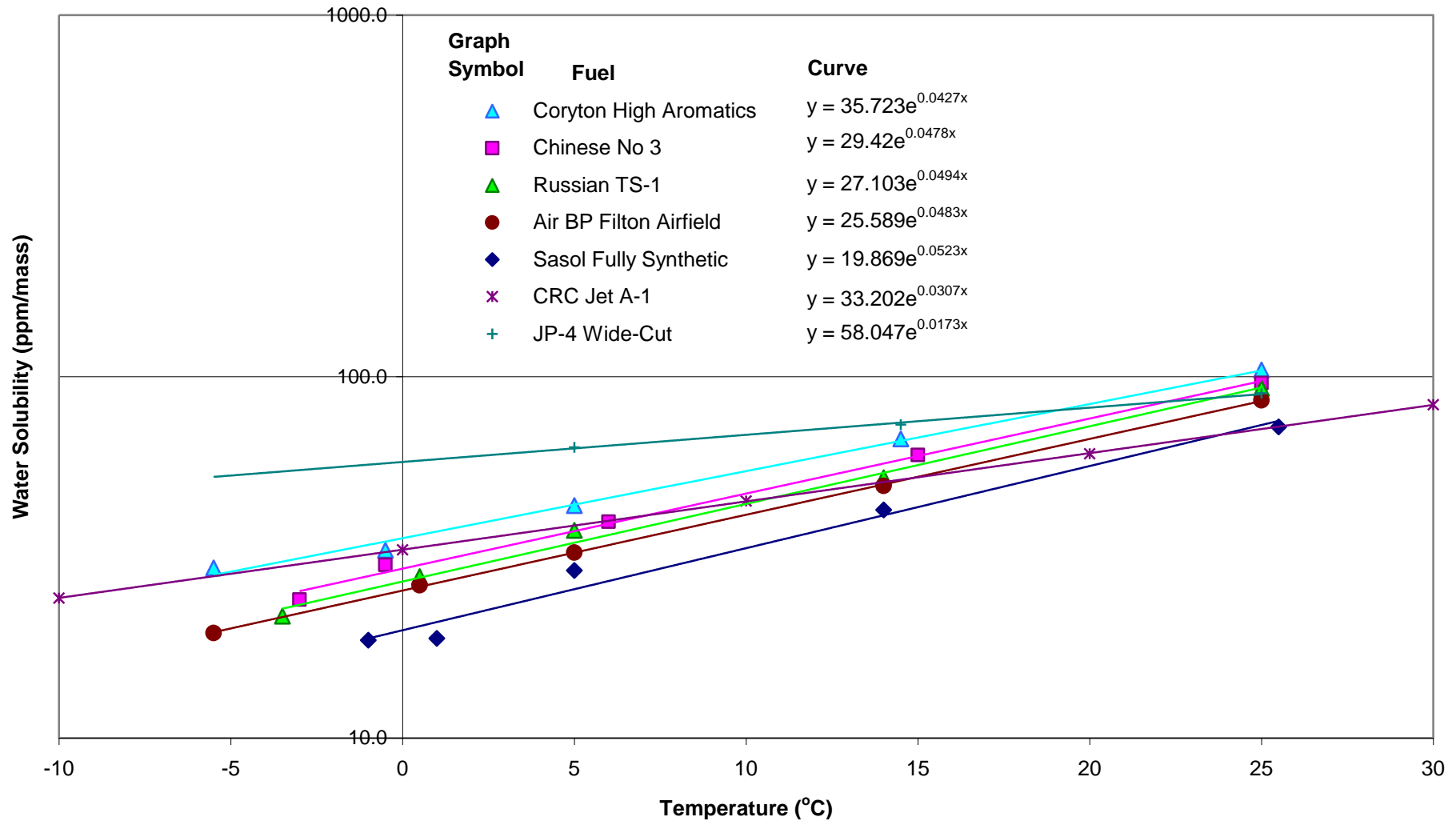


Figure 1 Water Solubility Curves Using Averaged Water Content Data

Water Solubility versus Temperature for Various Jet Fuels
Best fit curves, showing spread of data points

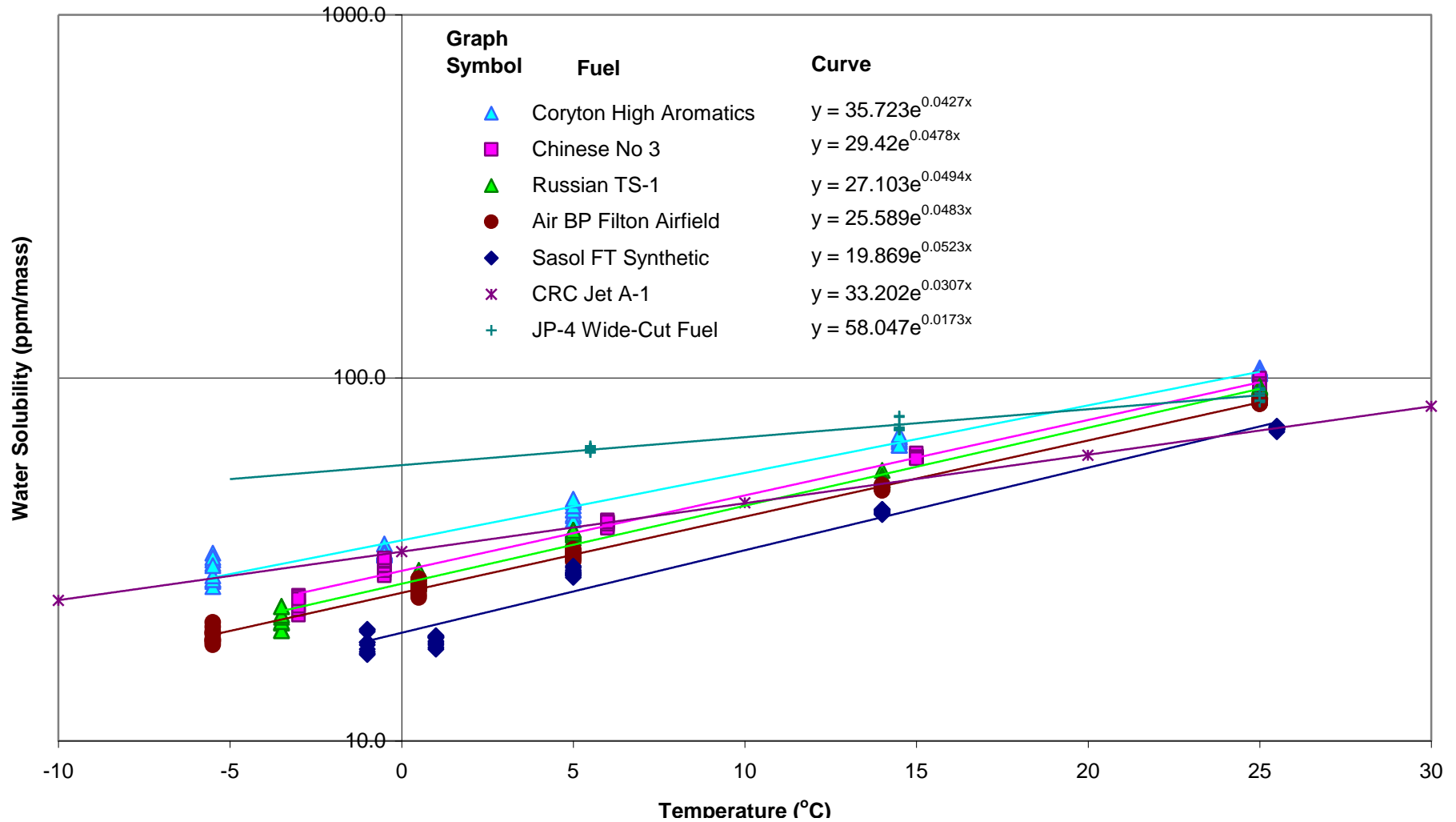


Figure 2 Water Solubility Curves Showing Degree of Scatter in Water Content Data

The ranking of the Jet A-1 fuels with respect to their affinity for water is quite clear from Figures 1 and 2. Sasol has the lowest affinity for water with the smallest base for the exponential function (19.869), followed by Filton, then Russian and Chinese, with Coryton having the highest affinity and the largest base for the exponential function (35.723). With the possible exception of the Coryton high aromatics fuel, the exponent coefficients of the exponential functions (or gradients of the curves) are very similar (Table 5) but do not follow the same trend as the affinity for water.

Table 5 Ranking of Kerosine Fuels with Respect to their General Affinity for Water

<i>Affinity for Water</i>	<i>Fuel</i>	<i>Exponent Coefficient</i>	<i>Deviation from the Mean Exponent Coefficient</i>
Highest	Coryton High Aromatics Jet A-1	0.0427	-0.0058
↓	Chinese No 3	0.0478	-0.0007
	Russian TS-1 Aviation Kerosine	0.0494	0.0009
	Air BP Filton Airfield Jet A-1	0.0483	-0.0002
Lowest	Sasol FT Fully Synthetic Jet A-1	0.0523	0.0038
	Mean	0.0485	-

Mean exponent is the average exponent of the Chinese, Russian and Filton fuels. The maximum exponent (Coryton fuel) and the minimum exponent (Sasol fuel) are ignored in the mean calculation.

The experimental solubility curves for the five kerosine fuels generated from the Karl Fischer determinations are of similar order to the solubility curve for the generic Jet A-1 fuel given in Figure 2-32 of the CRC Handbook [3]. However, the latter fuel has a much shallower gradient than the other curves, which tends to overestimate the water content at temperatures below 5°C and leads to an underestimate at temperatures above 15°C.

The JP-4 fuel showed a much shallower gradient than the other fuels with an exponent (0.0173) which was lower than the other fuels, but a base of the exponential function (58.047) which was much higher. The underlying reasons for this are covered in the discussion. The gradient is of similar order and ranking to the solubility curve for the generic JP-4 fuel given in Figure 2-32 of the CRC Handbook [3].

Figures 3 and 4 show the base, a , and the exponent coefficient, b , plotted against aromatics in % v/v. The Russian data were not included since the aromatics were given in % m/m. The trendlines in Figures 3 and 4 provide an estimate to a and b given the concentration of aromatics in % v/v.

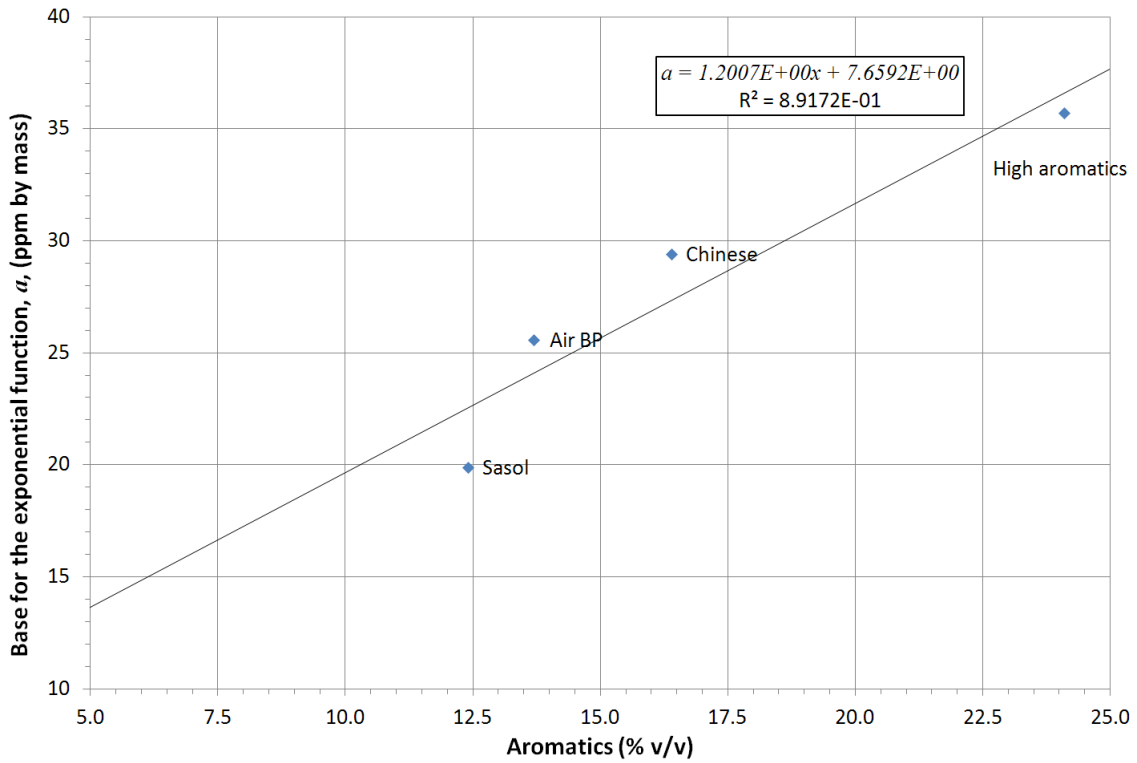


Figure 3 Bases, a , for the exponential function, Eqn. 1, plotted against aromatics

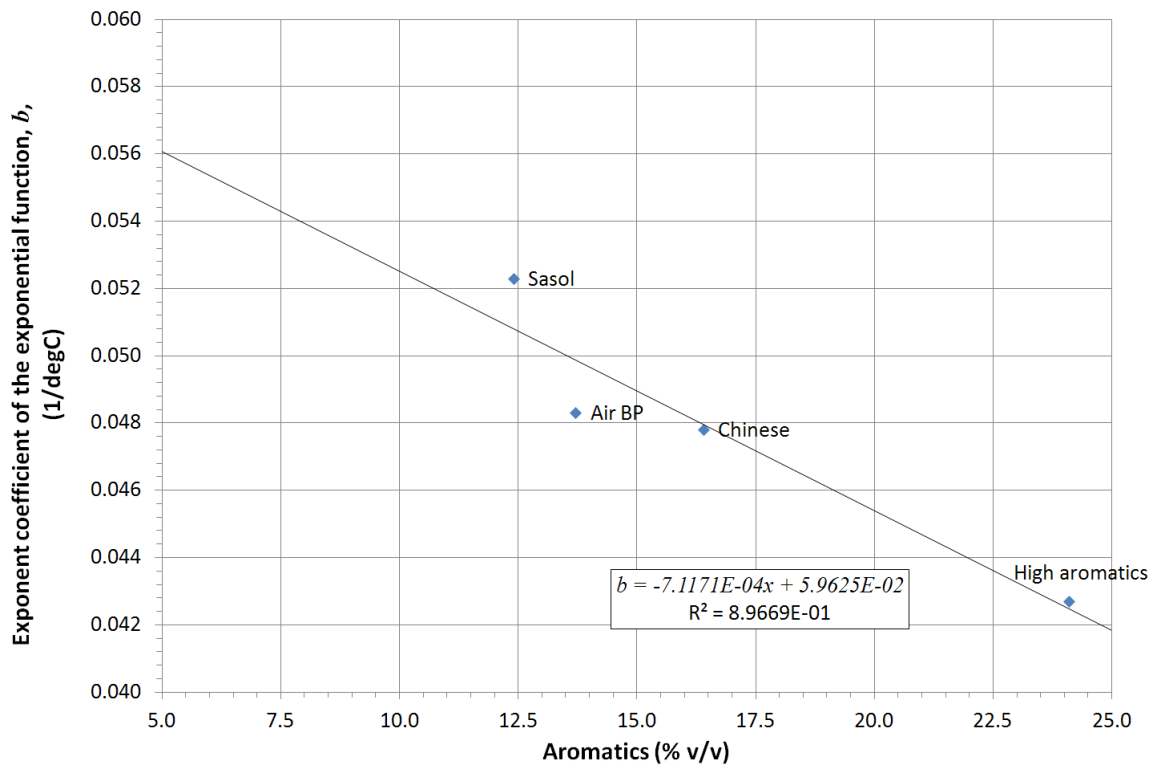


Figure 4 Exponent coefficients, b , of the exponential function, Eqn. 1, plotted against aromatics

2.3 Discussion on Water Solubility Measurements

As expected, the ability of each fuel to hold water in solution diminishes with decreasing temperature, as shown in Tables 3 and 4 and Figures 1 and 2.

The Coryton fuel, which had the highest aromatics content of the kerosine fuels, had the highest concentration of water over the entire temperature range of this work. This agrees with previous studies by the authors [6] comparing the water content of a number of hydrocarbons where aromatic hydrocarbons were found to dissolve larger quantities of water than linear hydrocarbons of similar molecular mass.

The Sasol fuel with its low aromatics content had the lowest concentration of water over the entire temperature range of this work. Again this agrees with the previous work on model hydrocarbons.

Extrapolating the Karl Fischer results to lower temperatures suggests that a fuel with a high aromatics content is likely to shed a larger quantity of water as the temperature decreases than a fuel with a low aromatics content. This suggests that icing problems are likely to be greater for fuels with high concentrations of aromatic hydrocarbons.

In Table 3, the Sasol fuel has the same water content at the two lowest temperatures -5°C and 0°C. This has been attributed to the inability of the Karl Fischer Coulometer to accurately determine very low concentrations of water and this led to a larger uncertainty over these results than that suggested by the standard deviation.

JP-4 fuel is specified for gas turbine propulsion systems but is now only used in consistently cold climates. It contains a proportion of lighter hydrocarbon molecules (naphtha or gasoline fraction) and is often termed a wide-cut fuel. The lighter fraction improves the fuel relight ability at altitude and reduces its freezing point but also contributes significantly to the fire risk due to a low flash point; JP-4 is therefore not directly comparable to the kerosine fuels.

The JP-4 fuel supplied for testing was made to the NATO F-40 (AVTAG/FSII) specification. This includes various additives that are used for military fuels but are not normally included in fuels for commercial aviation purposes. The fuel system icing inhibitor (FSII) interacts with free water to form a non-freezing solution; however, it may indirectly have a beneficial effect on water solubility. It is known that smaller hydrocarbon molecules tend to be slightly better at holding water in solution. It was clear from the Karl Fisher tests that the JP-4 was less likely to shed water than the kerosine fuels but it was not possible to say whether the effect was mainly due to the smaller hydrocarbons or the FSII.

2.4 Summary and Conclusions on Water Solubility Measurements

Water solubility – temperature curves were experimentally created for five aviation fuels and one wide-cut fuel. The Karl Fischer Coulometer method was used to

determine the saturated water content of each fuel over a range of temperatures between -5°C and 25°C.

The affinity for water of each fuel with respect to the other fuels was measured, with the Coryton High Aromatics Jet A-1 having the highest affinity and the Sasol Fully Synthetic Jet A-1 having the lowest affinity for water. The JP-4 wide-cut fuel had a moderately high affinity for water at ambient temperatures, but showed the least tendency of any of the fuels to shed water as the temperature decreased.

The Coryton fuel shed the greatest quantity of water as the temperature decreased. This suggests that icing problems will be greatest for fuels with a high concentration of aromatic hydrocarbons.

There was difficulty discerning the water content of the Sasol fuel at temperatures below 0°C due to the very low concentration of water in the fuel and the limitations of the Karl Fischer apparatus.

The experimental solubility curves are comparable to the water solubility curves of the Jet A-1 and JP-4 fuels reported in the CRC handbook [3].

3. MICROSCOPY STUDY OF WATER DROPLET AND ICE FORMATION IN FUELS

3.1 Background

Cold stage phase contrast optical microscopy was considered to be the most appropriate method to fulfil this part of the project. Cold stage systems give accurate temperature control of small test specimens and, theoretically, can offer control over a wide temperature range from the boiling point of liquid nitrogen to well above ambient temperature. The microscope, in phase contrast mode, can yield sharp and bright images of features that would not normally be distinguishable by the human eye. Limitations of this technique are the requirements for high levels of system cleanliness, limited depth of field when viewing specimens (hence the need for precise focussing) and problems associated with contamination or micro-fogging of the cold stage windows.

3.2 Microscope and Cold Stage

A Leica DM LM compound microscope was selected for this part of the project and matched with a Linkam Examina Dynamix cold stage system. This microscope has a trinocular head which allows simultaneous viewing of specimens whilst recording the field of view via a camera. The microscope was fitted with a revolving turret with 5x, 10x and 20x objective lenses; the 10x and 20x lenses could be used in phase contrast mode. The lower magnification lenses were used for setting up and aligning the system whilst all observations and measurements were made at 20x magnification.

The Linkam Examina Dynamix system comprised a THMS600 cold stage linked to an automated liquid nitrogen cooling system, a QICam fast digital camera and Linksys control software. Specimen temperature control was achieved with a small silver block, within the cold stage chamber, that could be heated electrically or cooled with liquid nitrogen. Specimens were placed in a small container that sat directly on the silver block.

The control software was programmed so that images of the sample were recorded at pre-defined intervals. This permitted images to be examined on completion of the experiment and measurements made of any features observed. It is also possible to link the images together to give a time-lapse video effect.

Before using the microscope, it was serviced by Leica, which involved dismantling and rigorous cleaning of all lenses, prisms, filters and the camera to reduce aberrations from dirt particles. Despite this precaution, it was not possible to remove every dirt particle and there are five particles in the optical systems that are visible in some images.

Plate 8 shows the microscope with cold stage, temperature control system and camera.

Plate 8 Leica DM LM Compound Microscope Fitted with Linkam THMS600 Cold Stage and Associated Cooling Control System



3.3 Phase Contrast Microscopy

Phase contrast microscopy uses differences in density and refractive index to differentiate between transparent components in a mixture such as water droplets suspended within a fuel. Using this technique, with the microscope described in Section 3.2, enabled water droplets to be distinguished as white spots against the blue background of the fuel. Phase contrast microscopy works well with extremely thin specimens or small particles. Thicker features or particles that are not precisely focussed will appear to show a halo which can confound the image; in addition, interacting halos can give the image a type of mosaic effect. This is particularly the case when examining mobile particles and some images recorded were considered less than ideal.

Phase contrast illumination consists of a phase ring located behind the front lens element of the microscope objective lens and a matching ring in the aperture plane of the condenser lens. It is essential to correctly centre these two elements and for

this reason a phase centring telescope, temporarily replacing one of the eyepieces, is used in the initial set up.

Throughout this work, a 20x phase contrast objective lens was used for sample observations and measurements. This lens, in conjunction with other lenses in the camera optical path, yielded a recorded image of the field of view of 0.5 mm by 0.37 mm (0.185 mm²).

3.4 Sample Preparation and Selection

Sample preparation and cleanliness of the sample holder are of paramount importance for optical microscopy, especially where nucleation of crystals at low temperature is to be studied.

For all the results presented in this report, the sample was contained in a small quartz crucible approximately 15 mm diameter by 2.2 mm deep fitted with a cover slip; this contained a volume of about 400 µl of fuel. A rigorous cleaning regime was adopted for the crucible and cover. On each occasion, prior to use, they were cleaned with Decon 90, in an ultrasonic bath, rinsed twice in distilled water and dried in a glass drying cabinet. The crucible was filled to the brim with the fuel being studied to minimise the inclusion of visible air bubbles when the cover slip was applied. In practice, this was difficult to achieve without slight escape of fuel. It was important to avoid external contamination of the crucible or cover slip, since even slight traces of fuel could adversely affect the quality of the optical images.

The crucible was placed in a crucible carrier within the cold stage to allow visual scanning of the sample without opening the cold stage. The carrier allowed some control of the position of the crucible within the cold stage.

To prevent condensation from forming on the windows of the cold stage as the temperature was reduced, the interior was purged with dry nitrogen prior to cooling. In operation, nitrogen from the Linkam system, and an external gas bottle, was blown across the external surfaces of the top and bottom windows to minimise fogging.

Each of the fuels detailed in Table 2 was studied using the microscope/cold stage system. Observation of the behaviour of the fuels was conducted at approximately the geometric centre of the crucible (middle of the crucible, away from any surfaces) and on the bottom surface of the crucible. These two positions approximate to the bulk properties of fuel (with associated convection currents and free motion of fuel and particles) and a chilled surface with micro-scratches (or defects) that might assist in the nucleation of water or ice crystals from the fuel.

The fuels were filtered and conditioned at 25°C as described in Section 2.2.1.

3.5 Cooling/Heating Regimes

Tests were conducted using three different cooling/heating regimes as detailed in Table 6.

The maximum freezing temperature specified for Jet A-1 is -47°C and the fuel temperature during flight should always be 3°C above the recorded fuel freezing temperature. For this reason, -44°C was chosen as the lowest temperature for any of the fuel microscopy studies.

The fast cooling rate was chosen as 10°C per minute, since this was the highest rate used in previous work [6]. A slower cooling rate of 1°C per minute was selected for the second regime to see if there were any time dependency effects on nucleation of water or ice crystals.

The third cooling profile was based on the fuel temperature during the last flight of G-YMMM from Beijing to London Heathrow prior to a hard landing at Heathrow Airport. Details of the fuel temperature over the course of that flight are given in the AAIB report [7] of the incident. This cooling regime was adopted to find out if anomalous icing occurred under such conditions.

Table 6 Cooling and Heating Regimes Used in the Microscopy Studies

<i>Thermal regime</i>	<i>Details</i>
Fast cool/heat cycle	Hold at 25°C for 2 min Cool at $10^{\circ}\text{C}/\text{min}$ from 25°C to -44°C Hold at -44°C for 30 min Heat at $10^{\circ}\text{C}/\text{min}$ from -44°C to 25°C
Slow cool/heat cycle	Hold at 25°C for 2 min Cool at $1^{\circ}\text{C}/\text{min}$ from 25°C to -44°C Hold at -44°C for 30 min Heat at $1^{\circ}\text{C}/\text{min}$ from -44°C to 25°C
AAIB report cooling/heating regime [7]	Hold at 25°C for 2 min Cool at $1^{\circ}\text{C}/\text{min}$ from 25°C to -2°C Hold at -2°C for 40 min Cool at $0.15^{\circ}\text{C}/\text{min}$ from -2°C to -20°C Cool at $0.05^{\circ}\text{C}/\text{min}$ from -20°C to -34°C Hold at -34°C for 80 min Heat at $2^{\circ}\text{C}/\text{min}$ from -34°C to 25°C

3.6 Matrix of Tests Conducted

Table 7 details the cold stage tests conducted; each test required a fresh sample of fuel. Some tests were repeated if the experimental set-up was unsatisfactory, e.g., due to slight wicking of fuel or due to problems with the recorded image quality.

Table 7 Summary of Cold Stage Microscopy Tests on Fuels

<i>Fuel (conditioned at 25°C)</i>	<i>Position in Crucible</i>	<i>Thermal Regime</i>		
		<i>Fast Cool</i>	<i>Slow Cool</i>	<i>AAIB Regime</i>
<i>Coryton High Aromatics Jet A-1</i>	Middle	X	X	
	Bottom	X		*
<i>Chinese No 3</i>	Middle	X	X	
	Bottom	X	X	X
<i>Russian TS-1 Aviation Kerosine</i>	Middle	X		
	Bottom	*	X	X
<i>Air BP Filton Airfield Jet A-1</i>	Middle	X		
	Bottom	X	X	X
<i>Sasol Fully Synthetic Jet A-1</i>	Middle	X	X	
	Bottom	X	X	X
<i>JP-4 Wide-Cut Fuel</i>	Middle	X		
	Bottom	X	X	X

* Unsatisfactory test - limited data - to be repeated

3.7 Microscopy Results

In general terms, all the fuels behaved in a similar way, although there were detail differences in the temperature at which water droplets first appeared from solution, the numbers of particles and whether any ice crystals were observed over the course of the test. There were also differences between tests where observations were made in the centre of the crucible as opposed to the bottom of the crucible. Table 8 summarises these differences.

Water droplets came out of solution in the fuel as the temperature was reduced. Water droplets nucleated first on the bottom of the crucible, typically becoming visible between 18°C and 10°C; a representative image is shown in Plate 9. Floating droplets generally were not observed until the temperature reached 5°C but, for some tests, the temperature had to drop to -2°C. It is difficult to put exact figures on this since, in some consecutive tests on the same fuel, there could be a 3°C to 4°C difference in the temperature that droplets first appeared.

The initial droplets were typically less than 5 µm across but occasional larger droplets up to 10 µm were seen; the largest droplet noted measured 13 µm. Droplets nucleating on the base of the crucible were generally slightly larger than the floating droplets. Particles precipitated out of solution in the middle of the crucible were not static, but drifted up and down or across the field of view indicating the presence of convection currents. Some of the droplets that nucleated on the base of the crucible remained stationary but others seemed to be more mobile and were able to migrate to a limited extent. Only limited numbers of the larger droplets (greater than 4 µm) seemed to be formed; within the field of view (0.185 mm²), less than twenty-five larger droplets were noted and often it was much less than this. Particles precipitated from kerosine fuels seemed to remain isolated with no tendency to cluster or amalgamate. Those precipitated from JP-4 showed a tendency towards

clustering, as illustrated by Plate 10, where in several instances, droplets have migrated together but individual droplet outlines are still visible.

Table 8 Summary of Cold Stage Microscopy Particle Observations

<i>Fuel (conditioned at 25°C)</i>	<i>Position in Crucible</i>	<i>Water/Ice Particle Size (µm)</i>		
		<i>Fast Cool</i>	<i>Slow Cool</i>	<i>AAIB Regime</i>
<i>Coryton High Aromatics Jet A-1</i>	Middle	Largest 6.5 Mostly <3*	Largest 11 Few <6 Mostly <3**	
	Bottom	Largest 10 Few <5 Mostly <3		
<i>Chinese No 3</i>	Middle	Mostly <3	Mostly <3	
	Bottom	Largest 6 Mostly <3	Largest 13 Few <6 Mostly <2.5***	Largest 12 Few <6 Mostly <2.5
<i>Russian TS-1 Aviation Kerosine</i>	Middle	Mostly <3		
	Bottom		Largest 6 Mostly <2	Largest 5 Mostly <2***
<i>Air BP Filton Airfield Jet A-1</i>	Middle	Largest 8.5 Few <6 Mostly <3		
	Bottom	Mostly <4	Largest 13 Few <8 Mostly <2.5	Largest 11 Few <7 Mostly <3**
<i>Sasol Fully Synthetic Jet A-1</i>	Middle	Largest 4 Mostly <2***	Largest 8 Mostly <2.5	
	Bottom	Largest 7 Mostly <2	Largest 7 Mostly <2	Largest 5 Mostly <2***
<i>JP-4 Wide-Cut Fuel</i>	Middle	Largest 6.5 Mostly <3		
	Bottom	Largest 8 Mostly <3	Largest 10 Few <7 Mostly <3	Largest 7 Mostly <3

Notes (see text for detail):

* 'Cracked' droplets

** Clear evidence of ice crystal formation

*** Tentative evidence of ice crystal formation

Droplets seemed to grow slightly in size as the temperature reduced, but reached a limiting dimension (as noted above) and the preferential mode for water precipitation appeared to be for more water particles to nucleate. Typically this took the form of a haze of micro droplets of between 1 µm and 3 µm. For some of the tests, this almost looked like a shower of micro droplets, since very large numbers of particles were nucleated almost simultaneously. The onset of haze formation occurred at around

-2°C and became more prominent by -10°C; Plate 11 illustrates the appearance of micro droplet formation. As the temperature was reduced further, some of the micro droplets appeared to grow slightly, possibly to 4 µm, but no further significant growth changes were noted. As the temperature decreased, some of the droplets developed a pink or blue hue or even a dark blue/black centre.

For most of the tests, there was no clear evidence of ice crystal formation. The two exceptions were the Filton fuel (bottom of crucible, AAIB regime – see Plate 12) when crystals were clearly noted to have developed on cooling to -29°C and Coryton (middle of crucible, slow cool) when starting to warm up, crystals were noted at -41°C. However, even where crystals were observed, not all of the droplets appeared to have frozen. Ice crystals were typically up to 8 µm across, but one cluster of crystals was noted in the Filton fuel which measured 20 µm across.

In four other tests, Chinese (bottom of crucible, slow cool), Russian (bottom of crucible, AAIB regime) and Sasol (bottom of crucible, AAIB regime and middle of crucible, fast cool), droplets with crystalline-like features or irregular outlines were noted but could not be clearly identified as ice crystals. Coryton (middle of crucible, fast cool) showed a few spherical droplets that looked as though they had cracked; these are difficult to discern, but a few cracked droplets are just visible in Plate 13. JP-4 was the only fuel to show no sign of any crystal formation.

On reheating the fuel samples, the water droplets went back into solution. The haze of micro droplets (less than 3 µm) were the first particles to go back into solution and this typically occurred over the temperature range of -8°C to 4°C. Larger droplets of water were more persistent, and the fuel had to warm to between 10°C and 19°C for all of these to re-dissolve.

For fuels that seemed to show droplets with crystalline-like features, any evidence of angular or irregular edges tended to soften as the fuel warmed up and the particles reverted to spherical droplets; this process was not consistent for all fuels but seemed to occur over a temperature range from -18°C to -2°C. The angular features disappeared most readily from the Coryton samples, but it was not apparent if this was just a coincidence.

Plate 9 Russian TS-1 Aviation Kerosine, on cooling to 8.5°C,
showing formation of first droplets

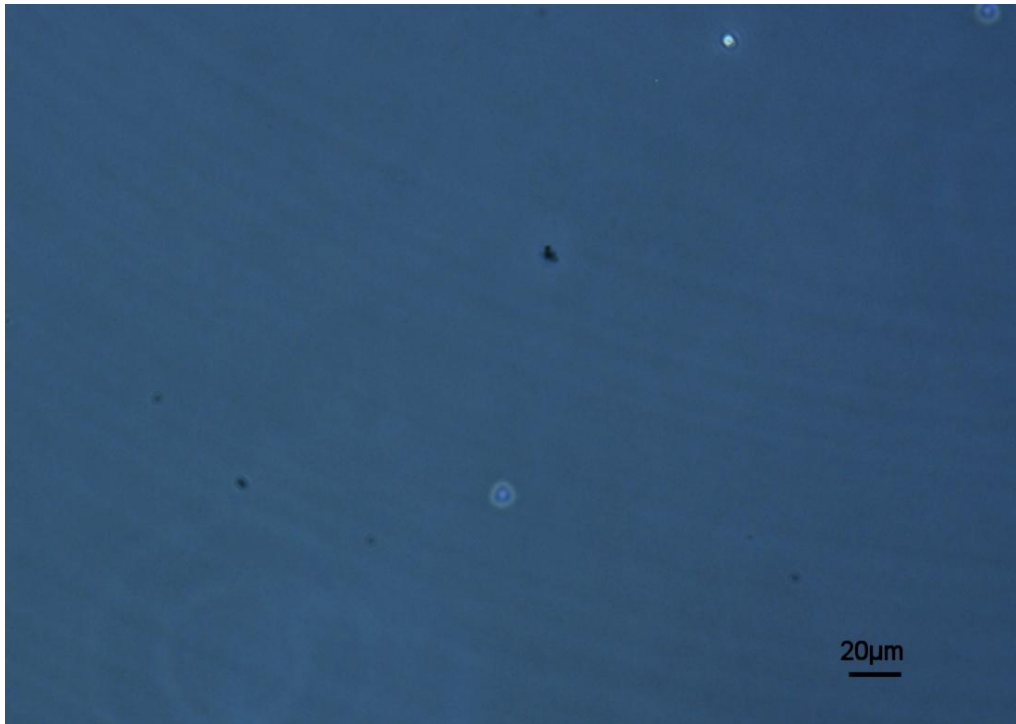


Plate 10 JP-4 Wide-Cut Fuel, on cooling to -2°C, showing
clustering of droplets on bottom of crucible

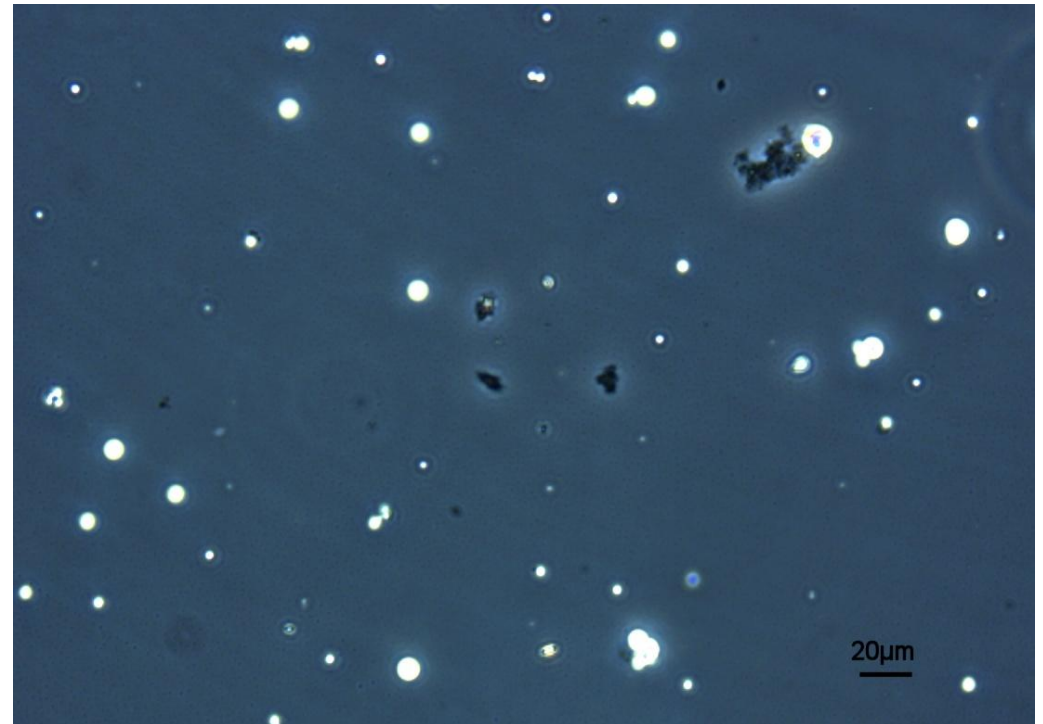


Plate 11 Air BP Filton Airfield Jet A-1, on cooling to -3.8°C , showing larger droplets and development of microdroplet formation on bottom of crucible

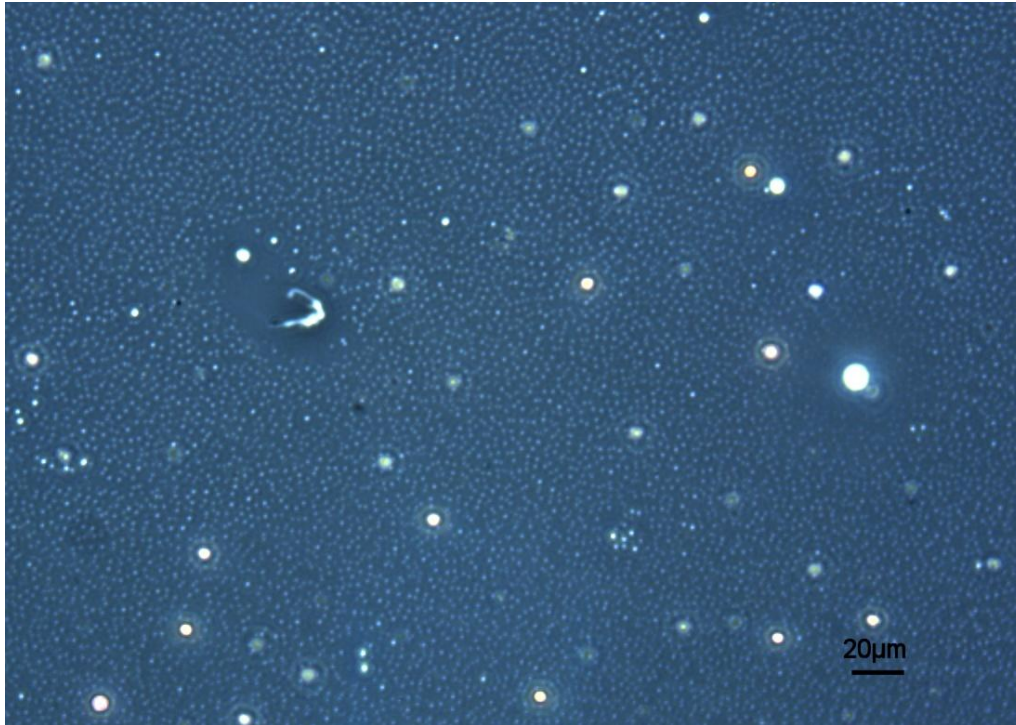


Plate 12 Air BP Filton Airfield Jet A-1, on holding at -34°C , showing small ice crystals in coexistence with water droplets on bottom of crucible

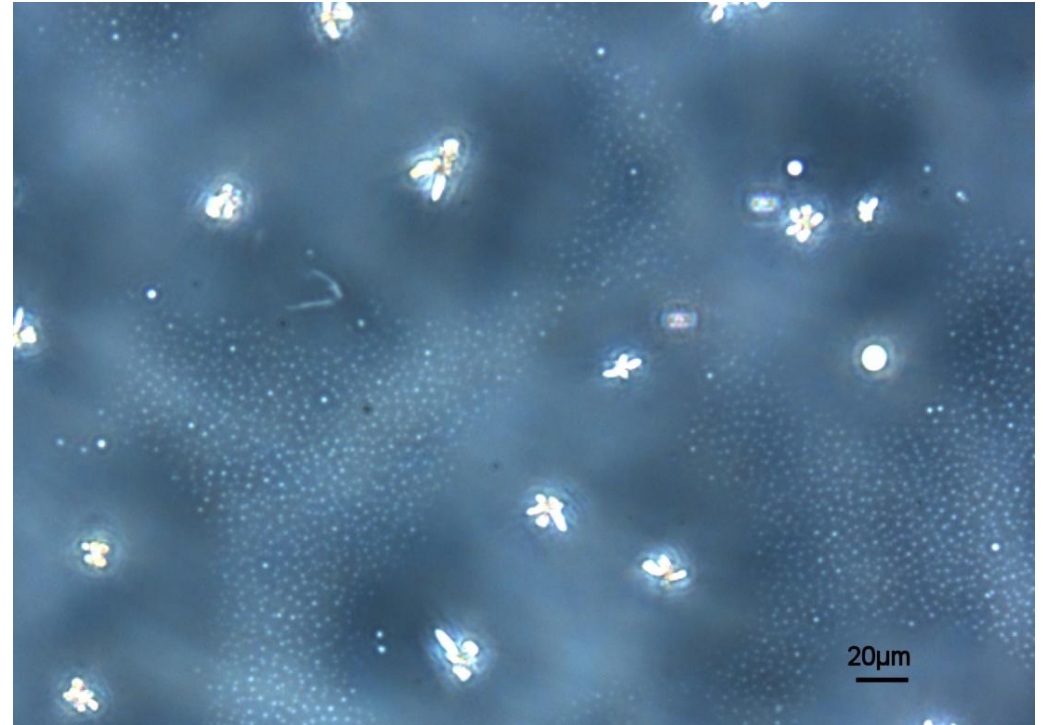


Plate 13 Coryton High Aromatics Jet A-1, on warming to -38°C , showing spherical droplets, a few of which appear to be 'cracked'

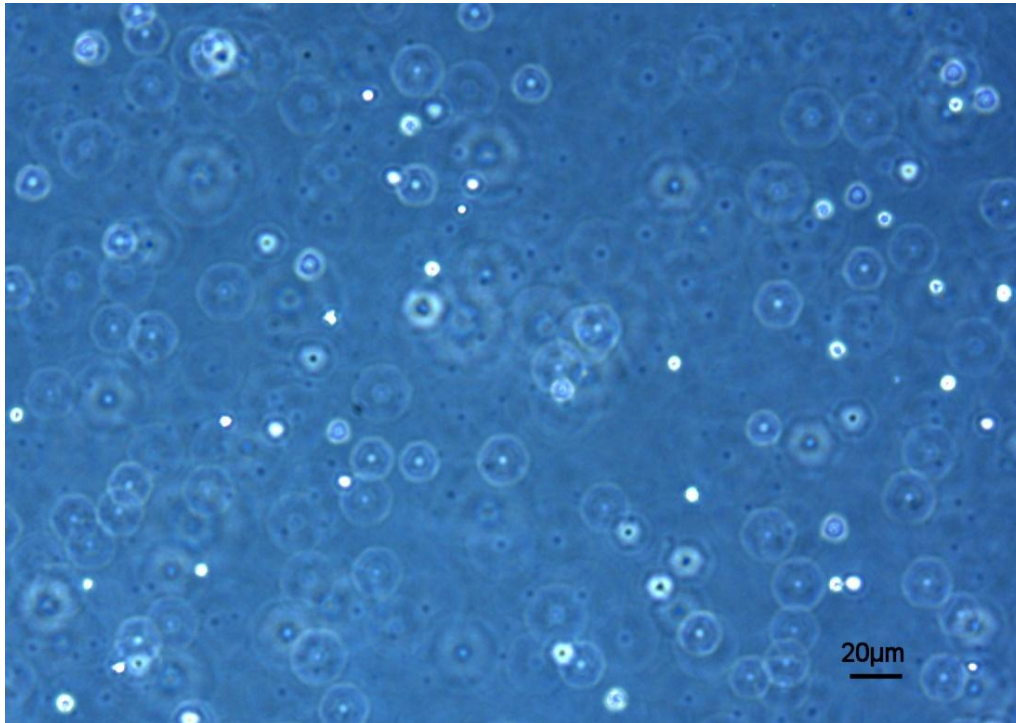


Plate 14 Air BP Filton Airfield Jet A-1, on warming -10°C , showing original crystal formations, but most microdroplets have redissolved

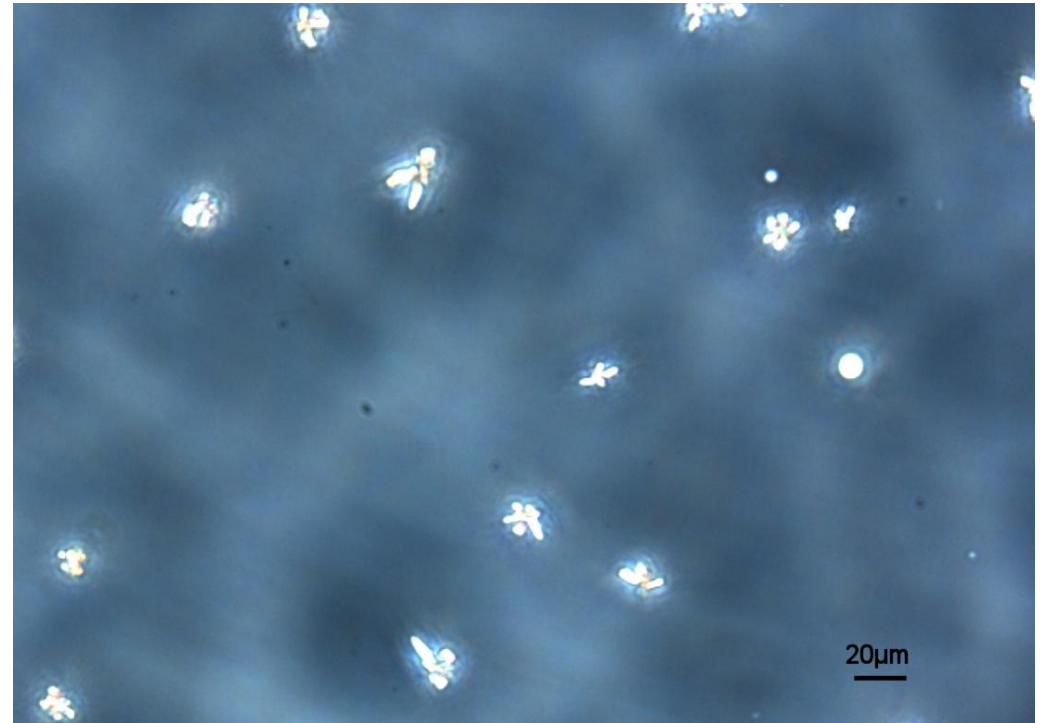


Plate 15 Air BP Filton Airfield Jet A-1, on warming -2°C , showing softening of crystal formations

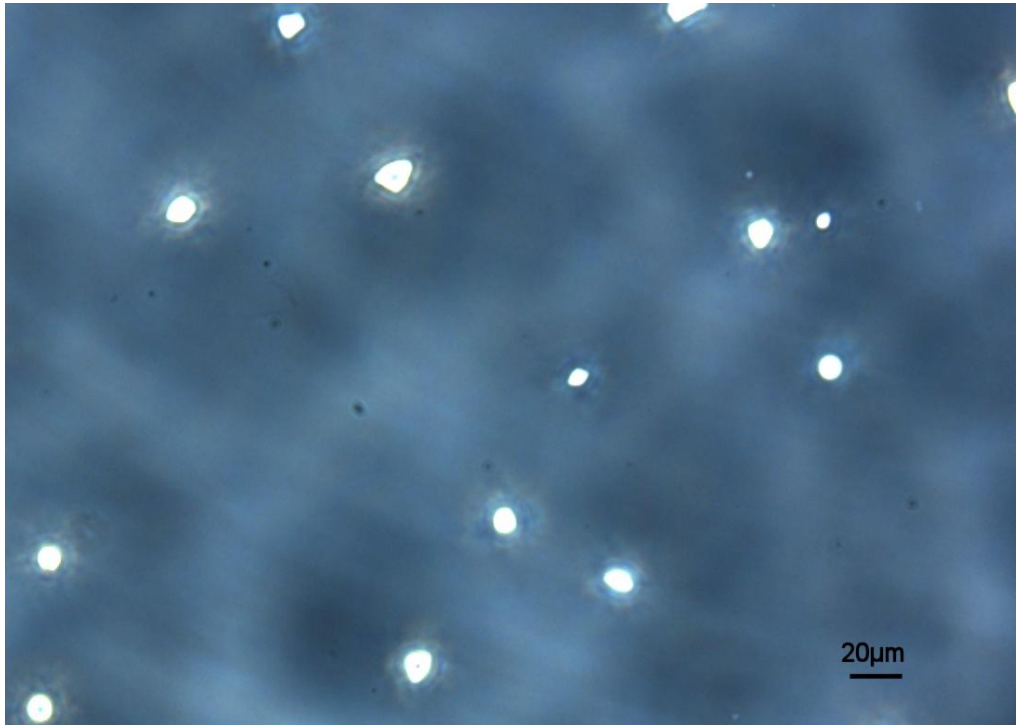
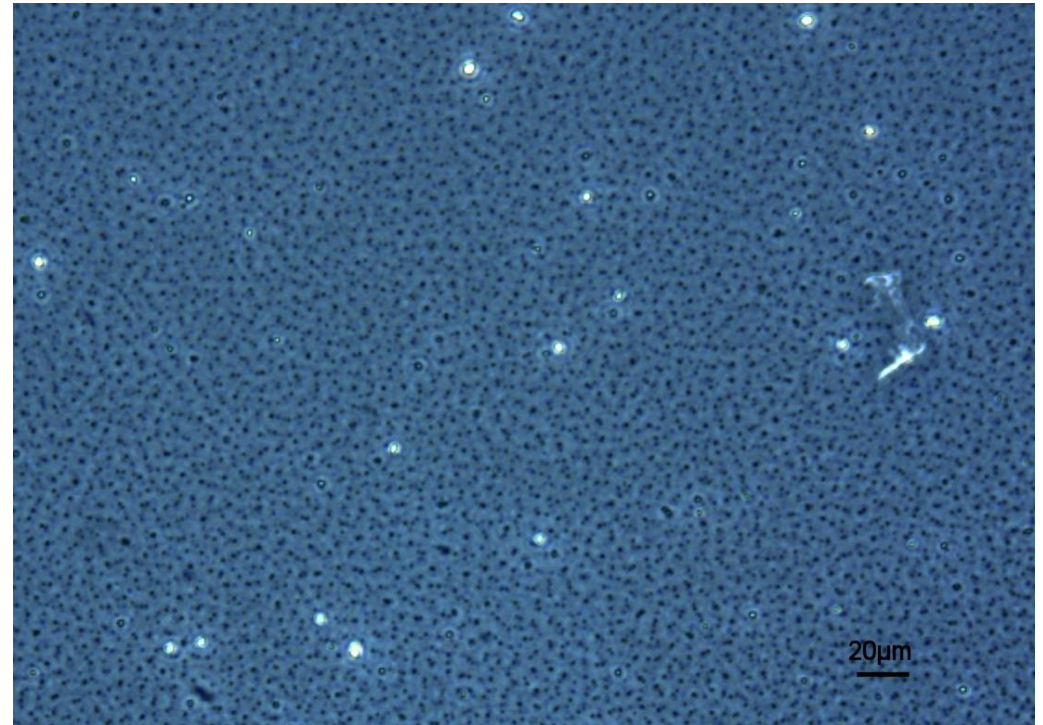


Plate 16 JP-4 Wide-Cut Fuel, on warming to 25°C , on completion of the first AAIB regime test. The white particles were static, but the black particles oscillated with Brownian-like motion



The Filton fuel (bottom of crucible, AAIB regime), which clearly showed ice crystals, behaved slightly differently. After initial formation of ice crystals at -29°C , the crystals seemed to grow, but reached limiting sizes (typically $8\ \mu\text{m}$) as the system settled at the holding temperature of -34°C . Zones of water droplet depletion were visible around the crystals. On reheating, the water droplets went back into solution preferentially and by -10°C , the main ice crystals were virtually the only particles left in view; see Plate 14. By -2°C , the crystals were shrinking slightly and losing their angular features as illustrated by Plate 15. However, there was still slight evidence of crystalline features at 8°C and it was not until 10°C that all traces of crystallinity had vanished. The water droplets formed from these crystals were back in solution by 18°C .

The first AAIB regime test run on the JP-4 produced an odd result when the fuel returned to room temperature. A very large number of small, dark particles (about $3\ \mu\text{m}$ diameter) were observed on the bottom of the crucible; by racking the microscope up and down, it was estimated that the depth of this layer could be as much as $60\ \mu\text{m}$. The particles were not static but oscillated in a way reminiscent of Brownian motion. It was not clear whether the particles were due to one of the additives in this fuel or whether these were microscopic air bubbles. The particles seemed to be quite stable and did not change appreciably over 3 days. The AAIB regime test on JP-4 was repeated but the effect could not be replicated.

An experiment was run to confirm whether FSII was present in the water droplets released from JP-4 fuel, two centrifuge tubes containing 10 ml of JP-4 conditioned at 25°C and two centrifuge tubes containing 10ml of JP-4 conditioned at 5°C were placed in the laboratory freezer at -44°C ; a thermocouple was inserted into one tube to check the temperature. Once the fuel had reached -44°C , it was held at that temperature for 2 hours. The tubes were removed from the freezer, allowed to warm up to ambient temperature and then centrifuged (60,000 rpm for 5 minutes). After centrifuging, in two tubes it was noted that a minute quantity of denser liquid had separated from the fuel. 2 ml of distilled water was added to all four tubes and each tube was shaken for 20 seconds. The tubes were centrifuged again at 60,000 rpm for 5 minutes. After centrifuging, the fuel was drawn off and the water layers combined to give enough material for gas chromatography mass spectrometry (GC-MS) analysis. The spectra produced by the GC-MS showed the presence of large amounts of various hydrocarbon species that masked traces of other compounds; diethylene glycol monomethyl ether was not present in sufficient quantity to be seen above the hydrocarbon 'noise'. This result will need to be investigated further.

3.8 Discussion on Cold Stage Microscopy Observations

There were no really clear-cut differences between the ways the individual fuels behaved in these tests. The Russian and Sasol fuels seemed to nucleate slightly smaller water droplets and the slower cooling regimes probably resulted in slightly larger particles but it is not certain that these observations are statistically significant. Water droplet nucleation was more likely to occur initially on the base of the crucible. This is partly due to the presence of microscopic scratches in the surface of the

crucible, which can act as nucleation sites, and partly due the thermal flux at that interface.

With fuels conditioned and saturated at 25°C, initial droplet formation (on the base of the crucible) typically started within the range 18°C to 10°C. There was no clear ranking between the fuels when this happened, possibly because the gradients of the water solubility curves are very similar, although JP-4 might have been expected to show delayed onset of water nucleation. As the temperature decreased, there was some growth of the initial particles, but the preferred mode of water shedding became nucleation of free-floating particles.

Small numbers of floating droplets, typically less than 8 µm, started to appear below 5°C, but it was really on reducing the temperature to below -2°C that the large-scale nucleation process seemed to begin. On a microscopic basis, this event sometimes looked like a shower of particles, but macroscopically it could be termed as the onset of haze formation. The initial haze particles were rather small (less than 2 µm) and indistinct but, by -10°C, the droplets became more prominent, whiter and easier to observe. It is probable that the haze formation process started at a slightly higher temperature than -2°C but could not be resolved by the microscope.

After haze formation, the fuels seemed to stabilise and, apart from slight growth of water droplets, there were no notable changes to be observed. Ice crystal formation was by no means a certainty although, in these tests, two fuels showed clear evidence of this. It is possible that at lower temperatures some particles had frozen as spherical droplets. Plate 13 shows what are believed to be micro droplets that have frozen and cracked, but Coryton (middle of crucible, fast cool) was the only sample noted to show this feature. Four other fuel tests resulted in some particles with crystalline-like features, but these could not be clearly identified as ice crystals.

The water droplet and ice crystal features noted during these tests have been observed before in tests on model hydrocarbons and jet fuels [6]; water droplet and haze formation are recognised phenomena as jet fuels are cooled. Water droplets formed in this way are typically very small and will not settle under gravity. Clean, microscopic water droplets are able to supercool to considerably below the normal melting point of water, and these tests have re-confirmed previous observations that the particles could remain liquid at temperatures as low as -44°C. Even when ice crystals were noted to be present, there appeared to be coexistence between ice and water particles.

The JP-4 might be expected to behave slightly differently to the other fuels in two respects. Firstly, it has a proportion of lighter hydrocarbon molecules, which help to keep more water in solution, and secondly, it was reported to contain 0.126% FSII, an additive used to interact with free water and prevent it from freezing at low temperatures. The standard chemical used for FSII is diethylene glycol monomethyl ether - DiEGME. There was evidence of clustering of the precipitated water droplets and it is believed that this was due to the presence of DiEGME.

As noted from the Karl Fischer tests, the water solubility of JP-4 was about the same as the other fuels at 25°C, but the gradient of the solubility curve was much shallower and therefore would be assumed to have a lesser tendency to shed water as the

temperature was reduced. Under the microscope, the early water shedding behaviour looked similar to the kerosines and the JP-4 produced a haze of microscopic droplets at temperatures comparable to the other fuels; however, it was difficult to say whether fewer particles were nucleated. The JP-4 did not show any evidence of ice formation and it was assumed that this was due to the FSII addition. Owing to an unusual droplet formation on completion of one of the tests, efforts were made to identify what might have been the cause. The initial results from these analytical tests were inconclusive; in particular it was hoped to detect traces of DiEGME. The spectrum from the GC-MS tests suggested that other hydrocarbon species were masking its presence but this observation will need further investigation.

3.9 Summary and Conclusions on Cold Stage Microscopy

There were no really clear-cut differences between the ways the individual fuels behaved in these tests. The Russian and Sasol fuels seemed to nucleate slightly smaller water droplets and the slower cooling regimes probably resulted in slightly larger particles but it is not certain that these observations were statistically significant.

Initial droplet formation (on the base of the crucible) typically started within the range 18°C to 10°C but there was no clear ranking between the fuels on when this happened. JP-4 behaved similarly in this respect to the kerosine fuels.

As the temperature decreased, small numbers of floating droplets started to appear below 5°C; when the temperature was reduced to below -2°C the large-scale nucleation process began. This was considered to be the onset of haze formation. The haze became more prominent as the temperature reduced further.

The initial droplets precipitated were typically less than 5 µm but occasional larger particles up to 13 µm were noted. Haze particles were rather small – generally less than 2 µm.

Ice crystal formation was observed in two fuels. Slight evidence of ice crystals were noted in four other tests but could not be categorically confirmed. It is possible that at lower temperatures some particles had frozen as spherical droplets; one of the Coryton fuel tests showed what looked like cracked droplets.

The JP-4 was expected to behave slightly differently to the other fuels owing to its different chemical composition and the FSII addition. Water dropout appeared to be similar to the other fuels but there was no evidence of any ice formation.

4. PARTICLE QUANTIFICATION USING THE JORIN VIPA

4.1 Background

A bespoke particle analyser with cooling system, previously developed for analysing particle distributions in cooled aviation fuels, was used for this part of the work. The system combines a Jorin ViPA (Visual Process Analyser), modified for low temperature use, and an Arctiko LTF325 super deep freezer rated to operate as low as -60°C . The Jorin ViPA system is designed to view particulates in fluid flows. It is normally not intended to operate below 0°C although the viewing cell should easily be capable of operating at temperatures of -60°C . The cell is housed within a sealed enclosure filled with dry air, so limiting the potential for condensation, and includes a heating element to gently warm the camera and associated electronics.

The Arctiko LTF325 freezer has been modified with a front access port to allow access for tubing, wiring and thermocouple connections. The short term cooling capacity of the freezer can be assisted by installation of up to 145 kg of aluminium plate. Air can be circulated around the freezer cabinet to improve heat exchange and allow experiments to be run within a reasonable timeframe (less than 5 hours).

The fuel container used for these tests was fabricated from 1.6 mm thick stainless steel sheet with a thicker base and removable flanged lid, to facilitate cleaning. The container was of elliptical cross-section (internal major/minor dimensions of 225 x 100 mm and 235 mm high) and has a nominal capacity of 4 litres. The internal surface of the container was coated with PPG F580-2080 (a greenish-yellow epoxy primer coating), used to coat the internal surfaces of aircraft fuel tanks. The lid was provided with a number of ports to allow temperature measurement and sampling of fuel from different positions within the container, as shown in Plate 17.

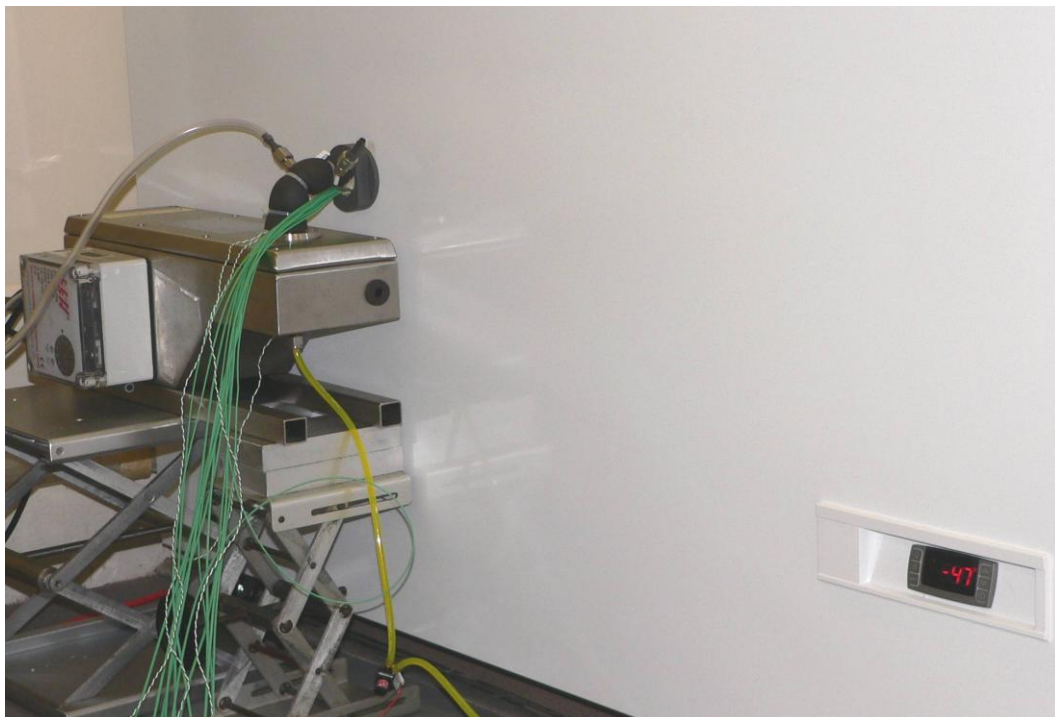
The port connector in the front of the freezer has twelve thermocouple connections and three tubing connections. The tube used to sample fuel from the container was thickly insulated and has thermocouples embedded at strategic intervals to assess any temperature change between the fuel container in the freezer and the ViPA. The vent connection on the fuel container was connected to atmosphere via a desiccant trap to prevent atmospheric moisture from condensing and freezing in the vent tube. In operation, fuel is 'sucked' through the ViPA, using a micropump on the discharge side; the intention is to avoid altering particle distributions and damage to any ice crystals that might be entrained in the fuel flow. A further tube connection permits backfilling the freezer cabinet with nitrogen, to minimise any risk of fuel vapour ignition.

The general arrangement of the ViPA and freezer is shown in Plate 18. The ViPA flow cell is contained within the stainless steel casing; fuel is fed into the top of the flow cell and passes downwards. The black insulated tube is the fuel feed from the freezer and waste fuel is discharged through the yellow tube to a suitable container. The green wires are the thermocouple connections.

Plate 17 Stainless steel fuel container, prior to final bolting



Plate 18 Jorin ViPA coupled to fuel container inside freezer. The port connector facilitates fluid and thermocouple connections inside the freezer. Data from the system is displayed on a remote computer



4.2 Jorin ViPA

The Jorin ViPA is a particle size analysis system designed to operate in-line at process temperature and pressure; the flow cell and associated casing are of robust construction. It uses a backlit flow cell and video microscope to capture images of discrete objects in a process stream. Image analysis techniques and user-defined parameters are then applied to differentiate between the different object populations present by assessing the measurable characteristics of these populations; particle detection thresholds are preset by running background calibrations and then checked with live flows that particles of interest are being detected correctly. The system offers a real-time display and stores data for subsequent analysis.

The camera has a CCD of 1024 x 778 pixels; as configured, the pixel size equates to a real-world dimension of 0.47 μm . This means that the maximum field of view in the flow cell is about 0.48 x 0.365 mm; the depth of the flow cell is 0.3 mm. In practice the system should be able to resolve particles of dimensions between 0.5 and 250 μm , although it is believed that the true lower limit of resolution is about 1.5 μm .

In use, the video system operates at 20 frames per second. It performs a background calibration of 100 frames and then a burst of 361 frames in image analysis mode. On completion of the imaging cycle, the data is stored to hard disk drive and the sequence repeated. Each cycle takes about 39 s and, for the purposes of this test programme, was repeated ten times at each test interval. The flow rate through the cell was set to about 20 ml/minute; this was a balance between conserving fuel and ensuring that the flow rates were high enough so that the same particles were not counted twice in consecutive images.

4.3 Experimental Details

1.5 mm diameter mineral insulated type K thermocouples were fitted to the lid of the fuel container and inserted to different depths, between 15 and 150 mm above the base of the container; Plate 17 gives an idea of their relative positions. The fuel siphon point was set to approximately 75 mm above the base of the container to avoid drawing up any contaminants or ice particles that may have settled at the bottom. Three thermocouples were set at the same depth as the siphon point, but at different points within the container, to measure the fuel temperature at the take-off point and to assess whether mixing and convection currents were occurring within the body of fuel.

The freezer was filled with approximately 70 kg of aluminium plate and the cabinet temperature set to -54°C for all experiments; the internal circulating fan was not used for these tests. For each test, the fuel container was filled with approximately 3.75 litres; all fuels were filtered using the method described in Section 2.2.1. With the exception of the test on the dried Filton fuel, the fuels were not given any extra drying or humidification treatments. Table 9 summarises the fuels tested.

Table 9 Fuels Evaluated by Particle Size Analysis

<i>Fuel</i>	<i>Conditioning</i>	<i>Average Water Content on Test Completion (ppm by mass)</i>
<i>Coryton High Aromatics Jet A-1</i>	As-received condition, filtered and exposed to ambient air for 18 hours	93
<i>Chinese No 3</i>	As-received condition, filtered and exposed to ambient air for 18 hours	88
<i>Russian TS-1 Aviation Kerosine</i>	As-received condition, filtered and exposed to ambient air for 18 hours	NM
<i>Air BP Filton Airfield Jet A-1</i>	As-received condition, filtered and (partly) dried above a bed of silica gel desiccant	28
<i>Air BP Filton Airfield Jet A-1</i>	As-received condition, filtered and exposed to ambient air for 18 hours	NM
<i>Sasol Fully Synthetic Jet A-1</i>	As-received condition, filtered and exposed to ambient air for 18 hours	63

NM – not measured

After filling, the top of the fuel container was largely covered with Parafilm and the fuel was allowed to 'breathe' at ambient temperature (~23°C) and humidity for 18 hours. Before starting each test, the Parafilm was removed and the lid bolted down; the fuel container was then located in the freezer and the thermocouple and fluid connections were made.

The system fuel lines were purged by dispensing about 150 ml fuel, and then the flow was stopped. An initial background test was performed with the ViPA under no flow conditions, and repeated under flow conditions, to assess initial fuel and system 'cleanness'. After this, a sequence of ten sets of measurements were made, at between 20 and 30 minute intervals as the fuel cooled down, until all the fuel accessible to the pick-up tube had been consumed. The flow rate through the cell was set to about 20 ml/minute.

A typical fuel cooling profile is given in Figure 5. It can be seen that temperature stratification occurred within the fuel container and that fuel near the bottom cooled faster than fuel in the middle of the container. The temperature of the fuel sampled for these tests approximated to the bulk fuel temperature (red curve in Figure 5). The tubing inside the freezer connecting the fuel container to the ViPA flow cell was carefully insulated but, owing to its small dimensions, tended to cool down faster than the bulk fuel temperature. On the other hand, the ViPA, with its heavy cell construction, cooled more slowly. These factors made it difficult to assess the true temperature of the fuel at the point of particle counting; for the purpose of analysing the data, the bulk fuel temperature at the time of sampling was taken to be

representative since this would be the temperature at which any water droplets or ice particles would be formed.

Air BP Filton Airfield Jet A-1
Typical fuel cooling profile during particle analyser tests. Freezer setpoint: -54°C

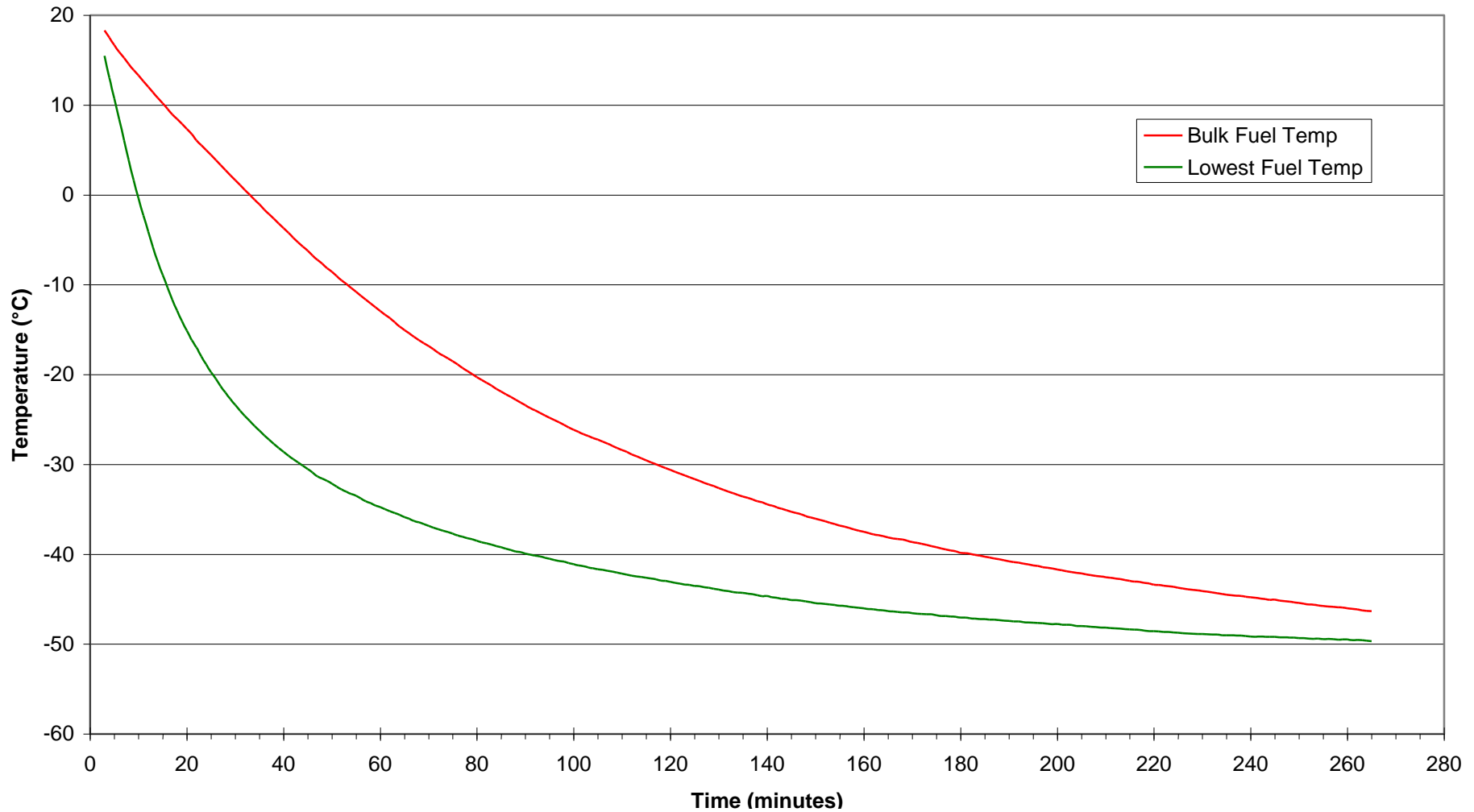


Figure 5 Typical Fuel Cooling Profile Achieved with Experimental Set-up

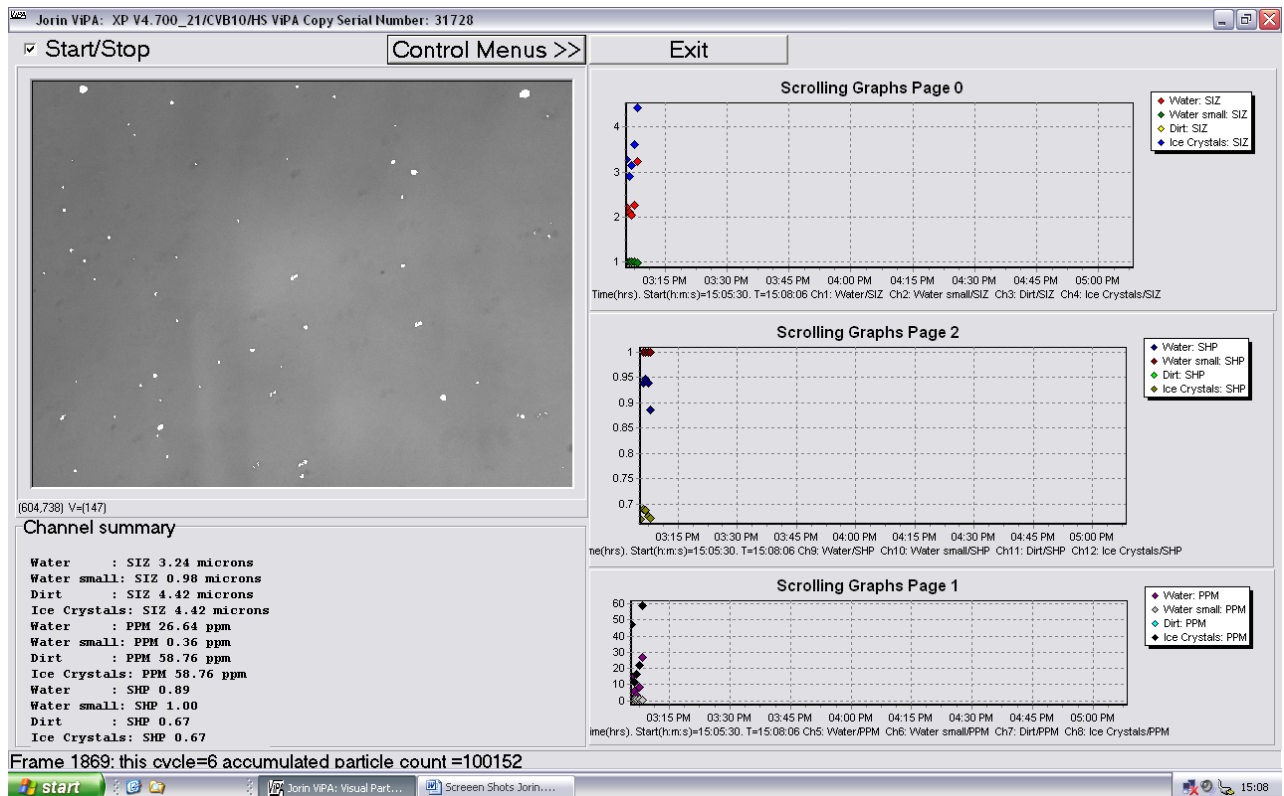


Figure 6 Jorin ViPA Screenshot whilst Evaluating Air BP Filton Airfield Jet A-1

Data from the ViPA flow cell was passed to a computer giving the operator a screen displaying real-time detection of particles; the system offers options for displaying other data relevant to the current experiment. Figure 6 was a screenshot of the system in operation whilst evaluating the Filton fuel; particles detected by the system are highlighted in white. The system was configured to display real-time information on size, shape factor (SF) and concentration of particles in the flow stream. In particular, the system showed that particles fell into three shape categories, i.e.,

- spherical (SF = 1),
- slightly less than spherical (SF ≈ 0.95) and
- angular/irregular (SF ≈ 0.7);

this finding seemed to be common to all fuels.

The ViPA system worked satisfactorily although difficulties were experienced as the fuel temperature decreased; the image became darker, due to loss of transparency in the fuel and it was noted that the analyser was not detecting all particles at lower temperatures. Adjustments were made to the detection threshold and the camera gain settings to determine if these could improve matters. Slight improvements in detection were achieved, but it was considered unsatisfactory to alter instrument

settings mid-way through a test run since it was not known what effect these changes might have had on detection accuracy at higher temperatures.

Differences between the fuels were apparent as experiments progressed. For instance the Sasol fuel was noted to show far larger numbers of particles than the other fuels, but these were generally smaller. The vast majority of particles observed were small (well under 30 μm) and the cut-off for data analysis purposes was taken as 15 μm . Two fuels (Chinese and Russian) showed occasional larger particles in the flow stream which exceeded 100 μm .

On completion of an experiment, the lid was removed from the fuel container. In all cases, the residual fuel had a cloudy-opaque appearance; samples of fuel were taken in four instances for Karl Fischer analysis of water content; results are given in Table 9. Data from the tests captured by the ViPA was examined and the relevant portions extracted for further analysis.

4.4 Darkening of the ViPA Field of View

Darkening of the field of view within the ViPA system has been observed before but the causes were not categorically identified; however, it has certainly been associated with operating the system at below ambient temperatures. Loss of transparency in aviation fuels has been reported before and has been ascribed to haze formation due to precipitation of water micro droplets [8].

A test was conducted to compare the performance of dried Filton fuel against Filton fuel exposed to ambient air. The fuel was filtered and dried in a desiccator in approximately 1 litre batches, using the system described in Section 2.2.1, and then transferred to the stainless steel fuel container. This was stored in a large Perspex specimen cabinet (with o-ring sealed door and silica gel desiccant) until sufficient fuel had been dried for the test; the silica gel desiccant in the cabinet had to be regenerated every 24 hours. Apart from drying the fuel, the test was run in same way as the tests on the other fuels exposed to ambient air.

Figures 13 and 14 illustrate the particle counts and mean particle sizes for this test. In respect of image darkening at lower temperatures, the dried Filton fuel was possibly slightly better than the ambient air conditioned Filton fuel, but this was not conclusive.

Karl Fischer coulometer tests were conducted on the fuel when the test was completed; these showed that the water content was about 28 ppm by mass. This was considerably drier than the standard Filton fuel but not as good as the carefully dried fuel used for the Karl Fischer water solubility tests.

4.5 Data Analysis

The ViPA generates large quantities of data based on particle detection and measurements of the dimensions of detected particles (Figures 7 to 20). Mean particle size is a fundamental measurement performed by an image analysis system and requires accurate recognition of particles of interest and speedy assessment of the area of the particle presented to view.

Four measurements of the diameter of each particle detected were made at 45° intervals (feret diameters). The average feret diameter was reported as the size of the object and the feret diameters were used to compute shape factor. Further calculations were used to compute the volume of particles and their concentration in the flow stream. Whilst this latter computation is of interest, it is not an absolute measure since there is an assumption that all particles within a field of view have been detected and assessed. Mean particle data from most of the fuels seemed to be fairly consistent, but the results from the Russian fuel seemed to be skewed by the presence of a few large particles. Information on concentration has therefore not been included in this report.

Data from each test has been segregated into two categories: particles that could be clearly identified as water and 'other particles'. This latter category could include water (particularly where two or more droplets are almost aligned one in front of the other in the flow cell), dirt particles, ice or components in the jet fuel which precipitated out of solution at lower temperatures. For the purposes of data presentation, an 'all particles' category has also been included to give an idea of the total number of particles.

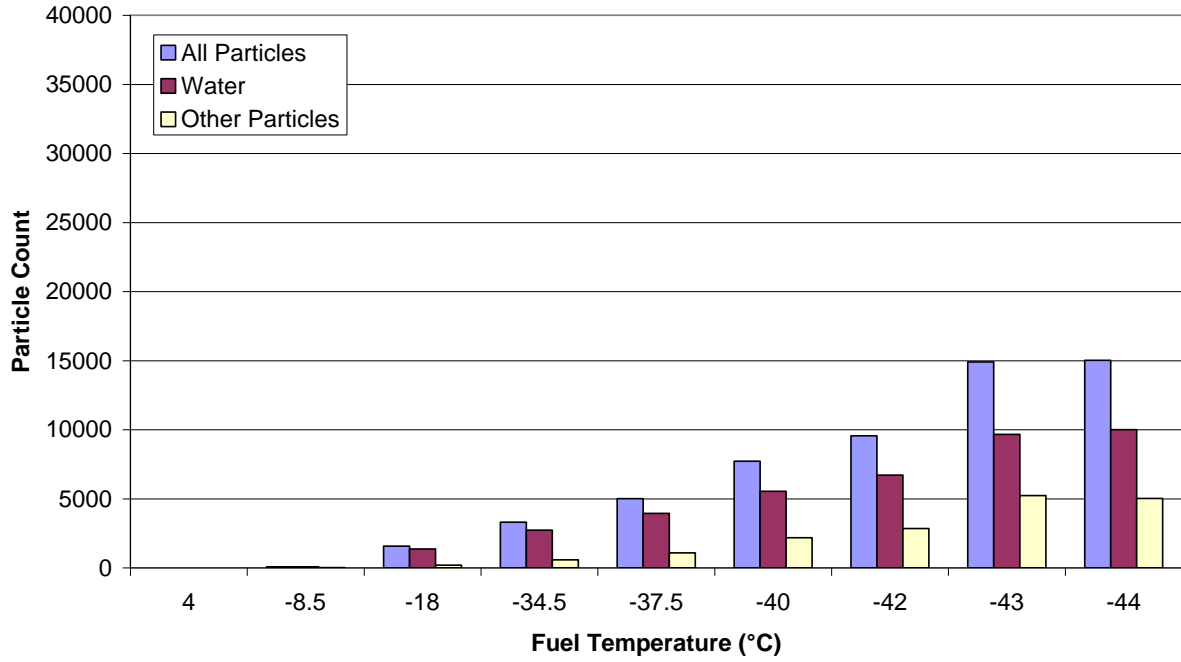


Figure 7 Coryton High Aromatics Jet A-1 showing variation in particle count with decreasing temperature

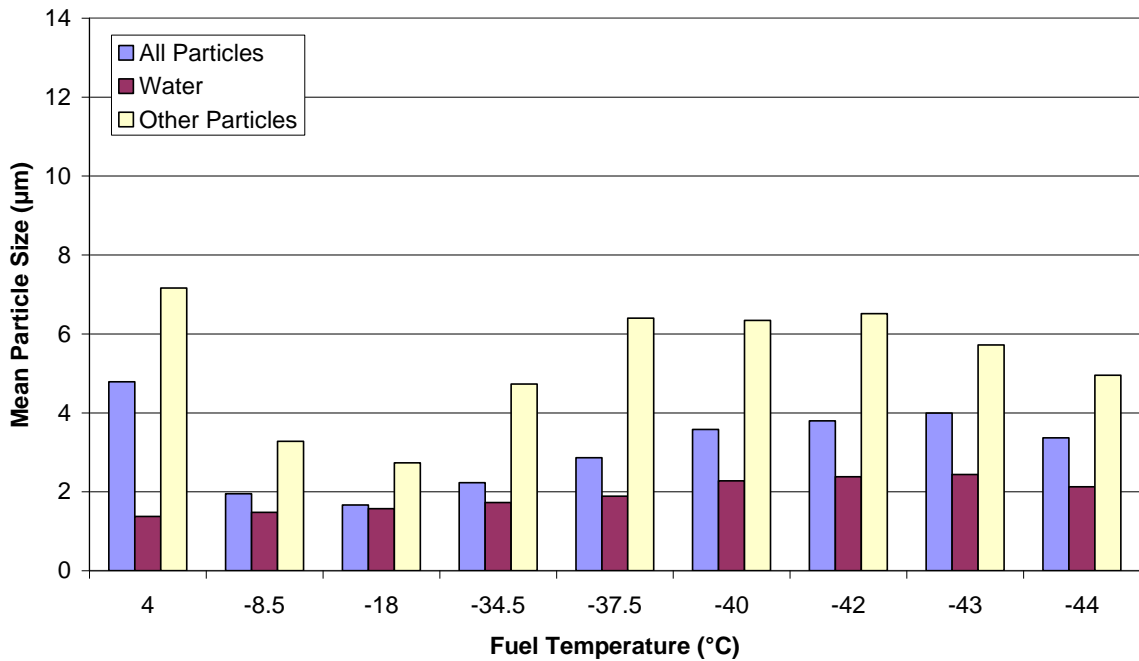


Figure 8 Coryton High Aromatics Jet A-1 showing variation in mean particle size with decreasing temperature

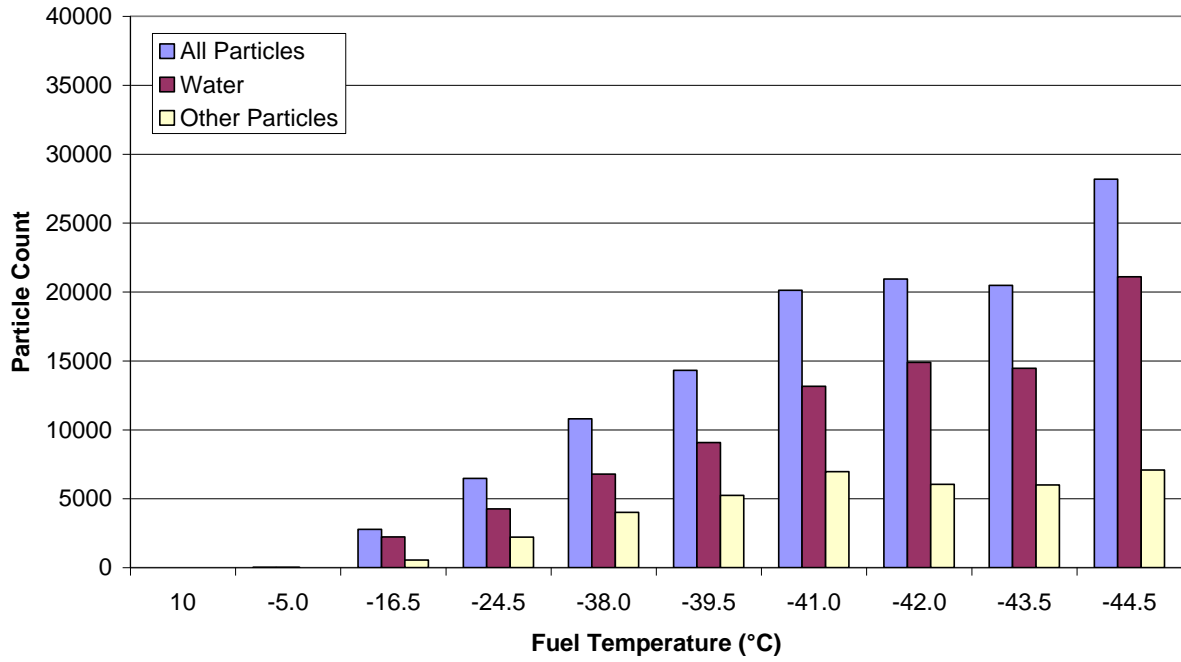


Figure 9 Chinese No 3 showing variation in particle count with decreasing temperature

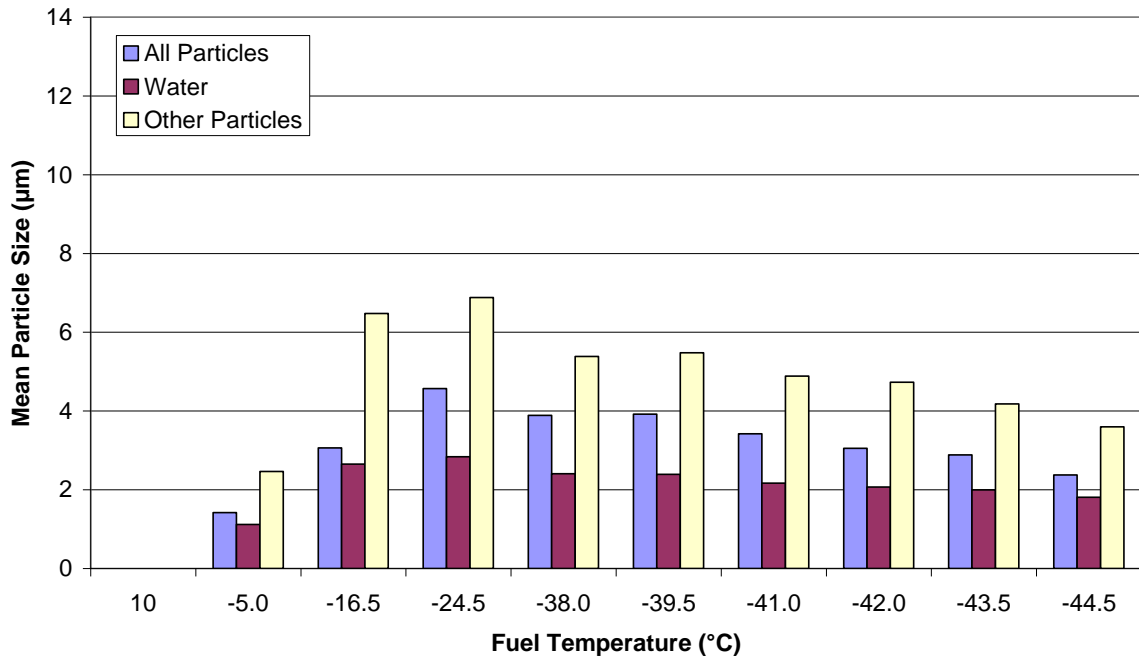


Figure 10 Chinese No 3 showing variation in mean particle size with decreasing temperature

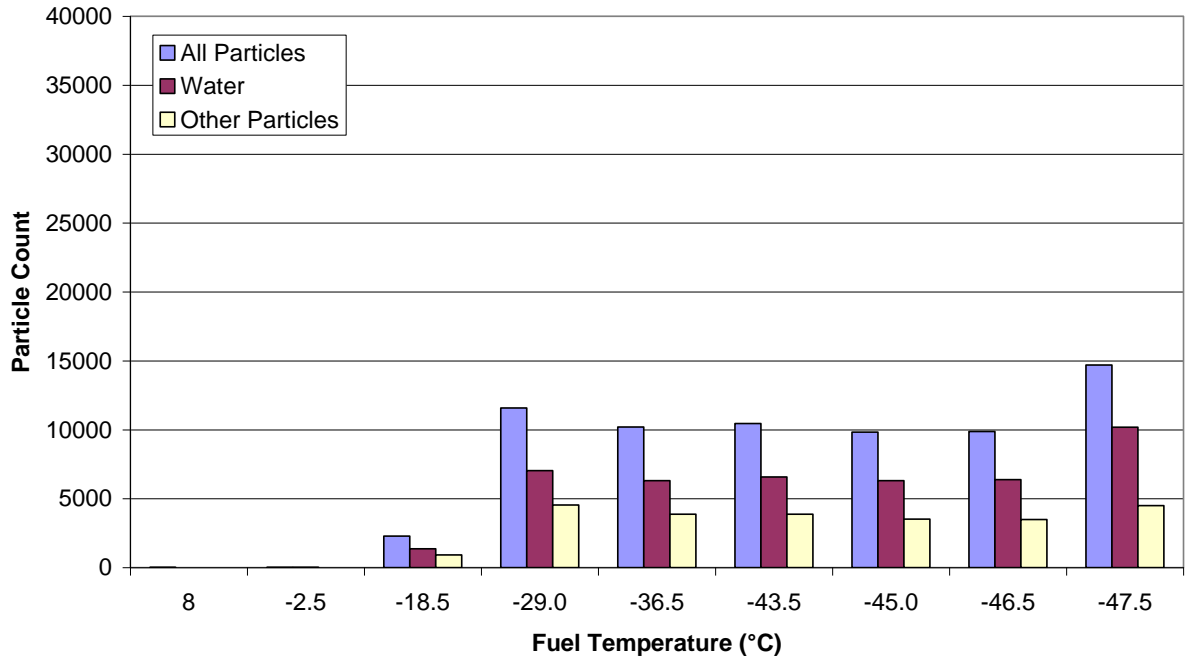


Figure 11 Russian TS-1 Aviation Kerosine showing variation in particle count with decreasing temperature

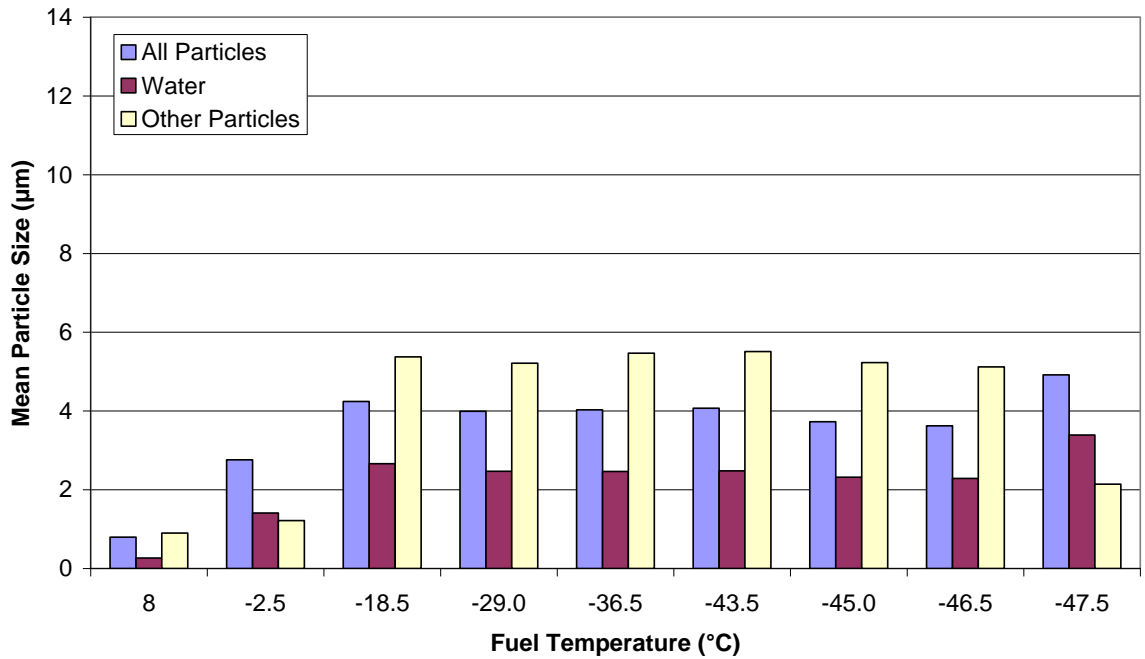


Figure 12 Russian TS-1 Aviation Kerosine showing variation in mean particle size with decreasing temperature

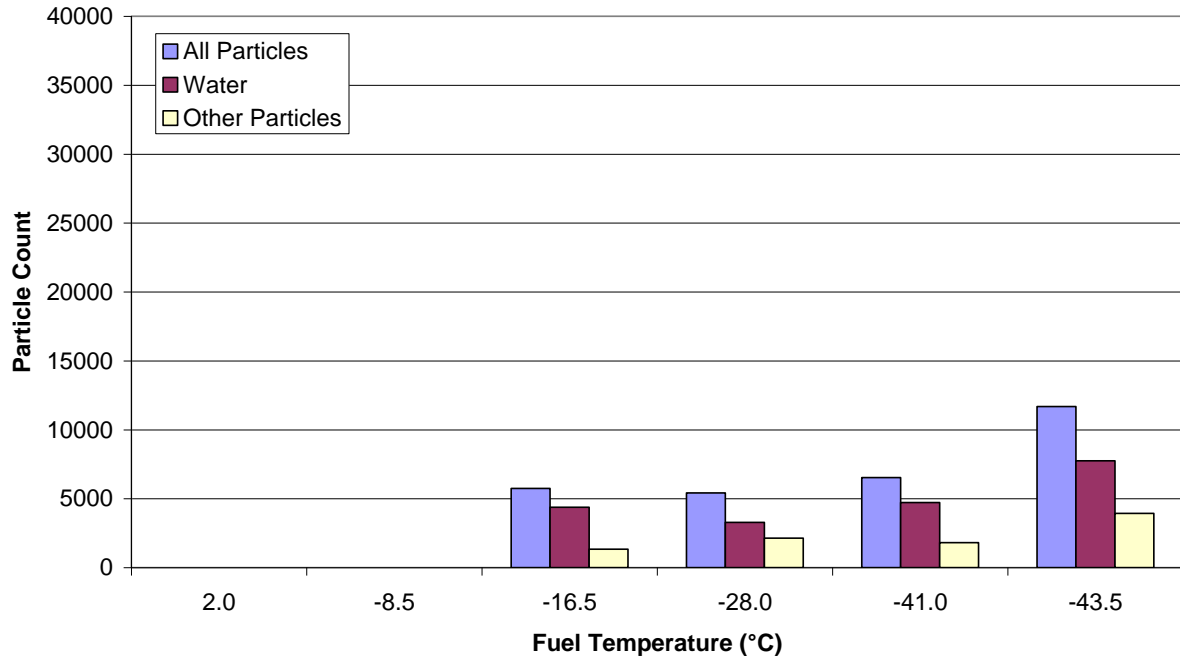


Figure 13 Air BP Filton Airfield Jet A-1 (partially dried) showing variation in particle count with decreasing temperature

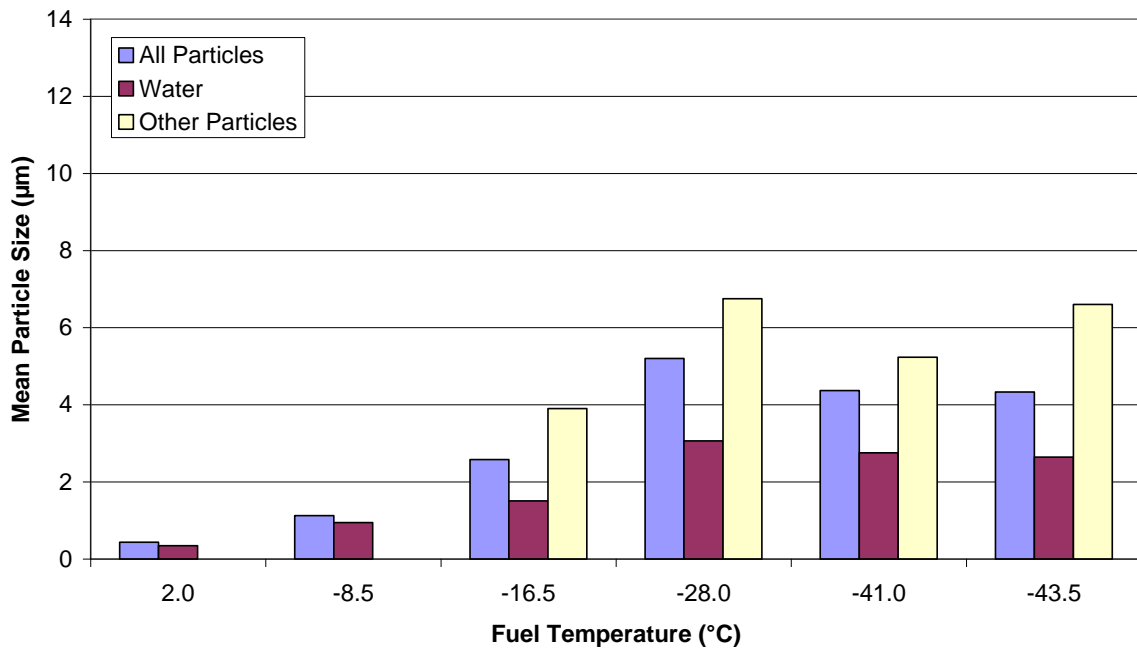


Figure 14 Air BP Filton Airfield Jet A-1 (partially dried) showing variation in mean particle size with decreasing temperature

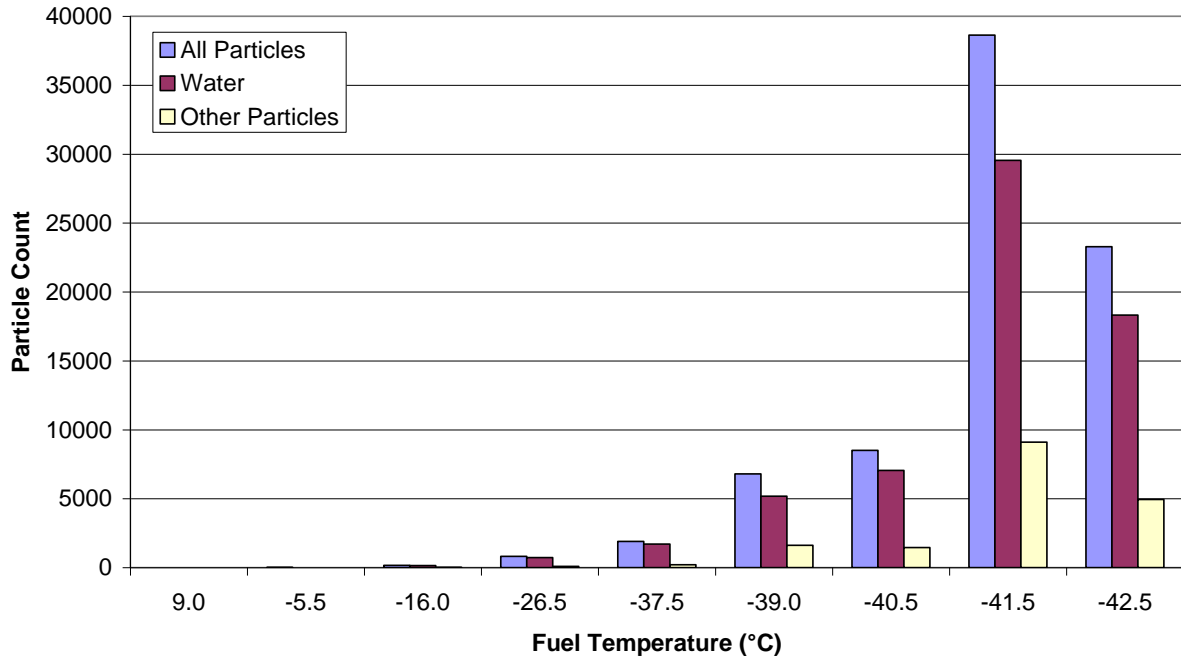


Figure 15 Air BP Filton Airfield Jet A-1 showing variation in particle count with decreasing temperature

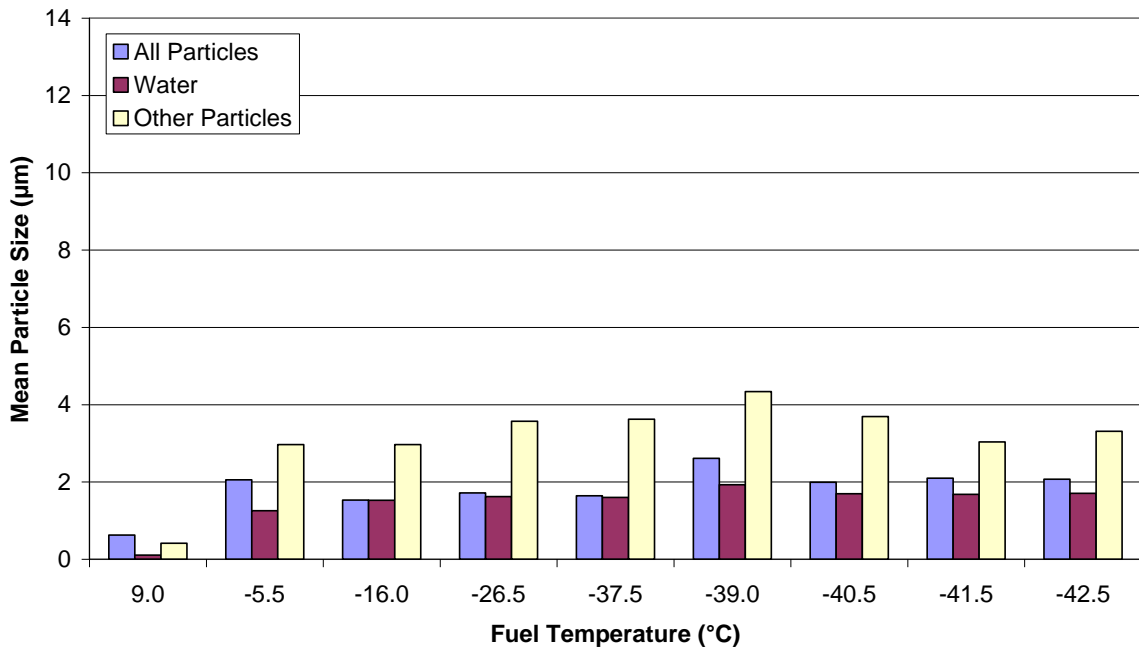


Figure 16 Air BP Filton Airfield Jet A-1 showing variation in mean particle size with decreasing temperature

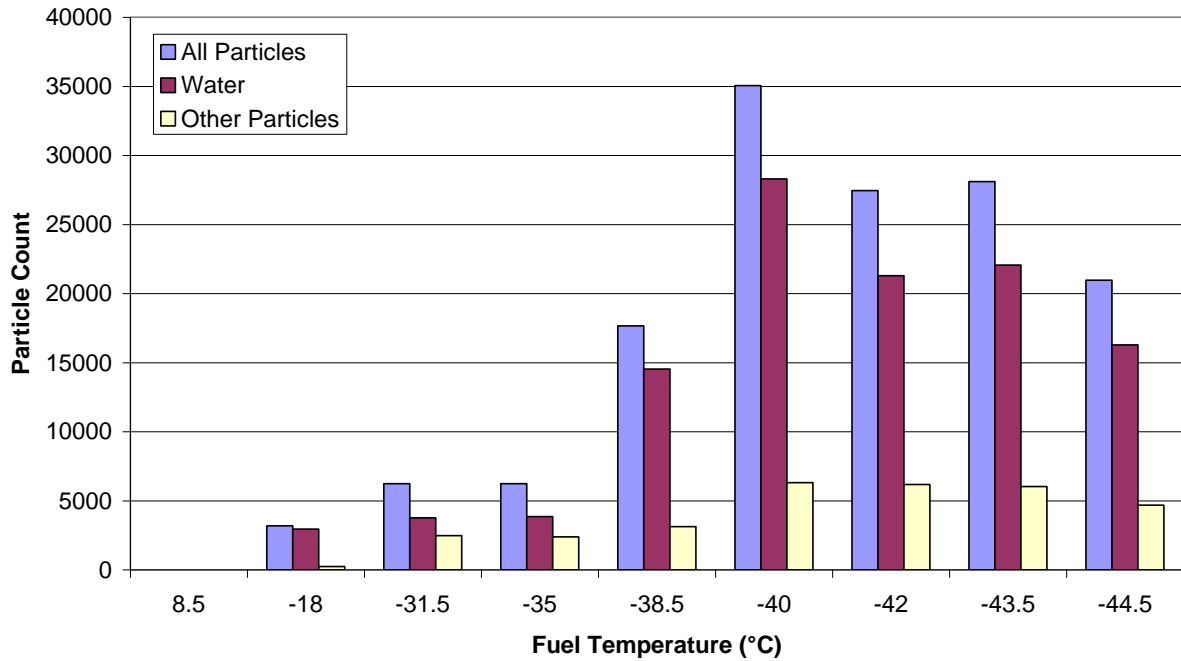


Figure 17 Sasol Fully Synthetic Jet A-1 showing variation in particle count with decreasing temperature

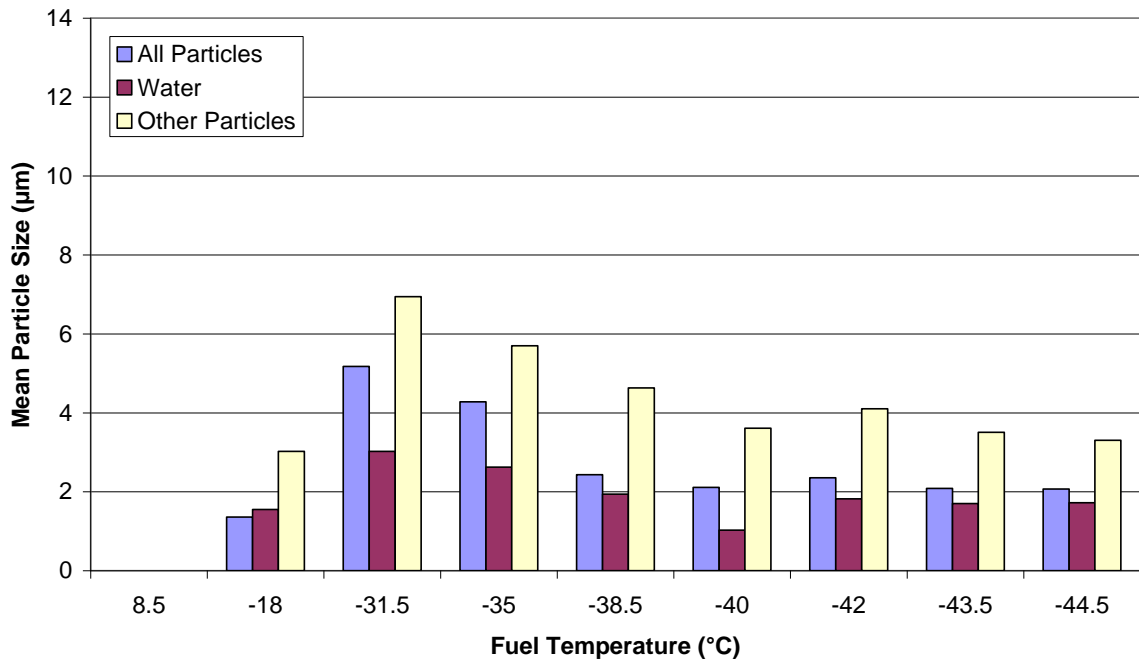


Figure 18 Sasol Fully Synthetic Jet A-1 showing variation in mean particle size with decreasing temperature

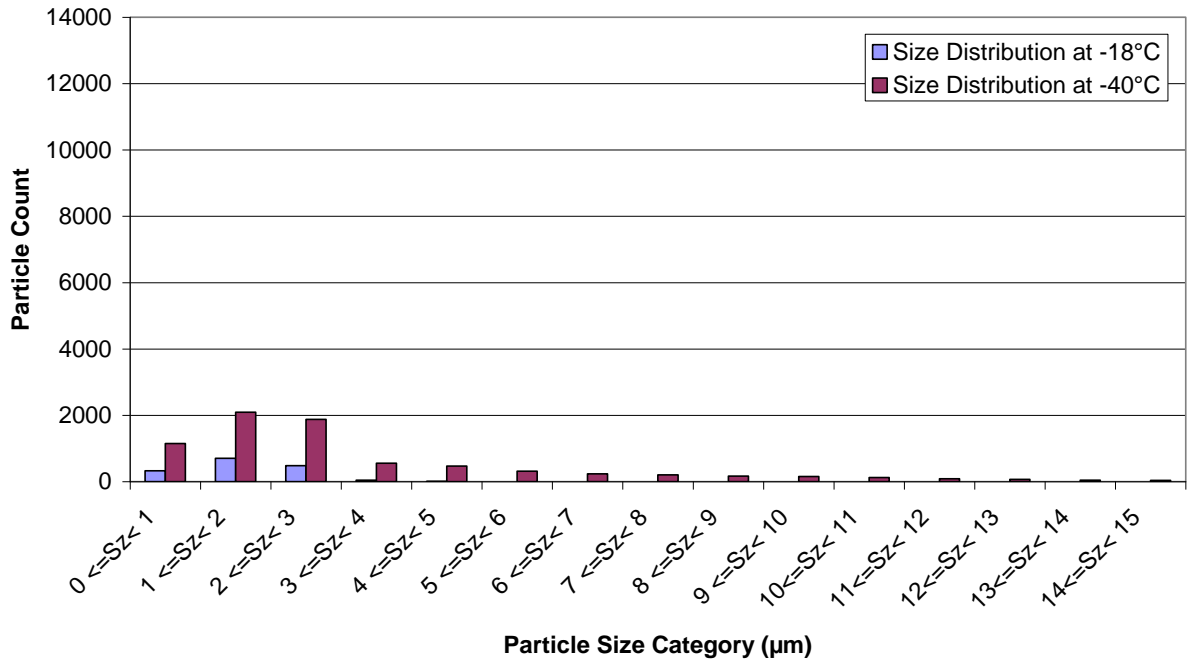


Figure 19 Coryton High Aromatics Jet A-1 showing ‘All Particles’ size distributions at bulk fuel temperatures of -18°C and -40°C

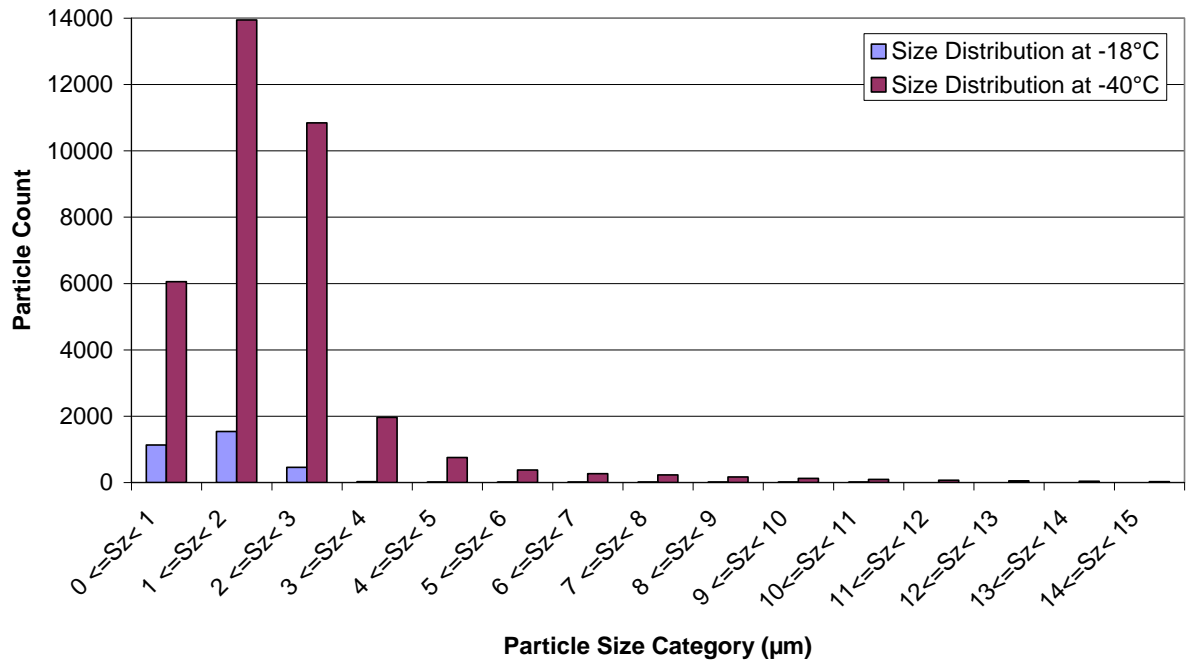


Figure 20 Sasol Fully Synthetic Jet A-1 showing ‘All Particles’ size distributions at bulk fuel temperatures of -18°C and -40°C

4.6 Discussion on Particle Quantification Tests

In general terms, the particle quantification measurements tied in with data from the cold stage microscopy tests. The ViPA system seemed to be good at discerning the very small water droplets that would be responsible for haze formation. It did not fare quite so well at classifying larger particles or at discriminating between particles and the background at lower temperatures. Data generated by the ViPA was linked to the temperature of the bulk fuel since this was the temperature at which any particles would have been formed. It has not been possible to confirm how much change may have occurred in transit from the fuel siphon point to the flow cell in the ViPA, but it was intended that the flow rate would have been high enough so that this was not a significant issue.

The ViPA system relies on being able to discriminate between the background and particles of interest; the user sets the detection threshold at a level that is considered appropriate. The degree of contrast between particles and background was considered adequate at ambient temperature but decreased as the temperature was reduced and this reduced the detection efficiency of the system. At bulk fuel temperatures below about -40°C , darkening of the field of view became more prominent, and affected data collection, particularly for the Filton and Sasol fuels.

The test comparing the performance of the dried Filton fuel against Filton fuel exposed to ambient air was not entirely conclusive. Darkening of the ViPA images was experienced in both cases, but the dried fuel possibly showed less reduction in transparency; it was not absolutely certain if this was due to too high a water content in the dried fuel. Whilst steps were taken to dry the fuel, difficulties were experienced in maintaining that dryness; the indicator in the silica gel showed that it needed to be regenerated at least once per day. This was probably due to the conditioning cabinet being not completely air-tight and limitations in the way that the fuel container could be handled. Karl Fischer tests on the fuel showed that the water content was about 28 ppm by mass which was considerably drier than the standard fuel but not ideally dry.

Initial background tests showed that the fuels were virtually particle-free and that any contaminants were at insignificant levels compared to particle counts when the temperature was reduced. A reduction in fuel temperature caused particles to start precipitating from solution and the numbers of particles increased as the temperature decreased. However, significant numbers of particles were not noted until the bulk fuel temperature had decreased to -15°C . Modest differences were noted between the fuels in terms of the numbers of particles precipitated from solution but the partially dried Filton fuel generated the least in this respect. Superficially, the Coryton fuel showed relatively low particle counts but closer examination showed that the particles were mostly larger and that the overall volume of material precipitated was actually the highest of all the fuels. The Sasol fuel appeared to shed the highest number of particles, but these were very small and, overall, approximately 65% the total volume of particles precipitated by the Coryton fuel.

As has been noted, the ViPA possibly experienced difficulties with categorising some of the particles. This raised concerns, particularly where these particles were detected at higher temperatures when ice formation was unlikely to have occurred.

From consideration of shape factor, there seemed to be three distinct populations of particle passing through the system: spherical, slightly sub-spherical and angular/irregular. The most plausible reason for classification as irregular particles is that when large numbers of water droplets are passing through the flow cell, two or more spherical particles could be aligned so that they appear to have an irregular outline. Like the Leica optical microscope, the ViPA has a focal plane within the flow cell, which limits the in-focus depth of field. Particles which are not in this focal plane would appear blurred or hazy and therefore should not be detected. The optical depth of field is not known for this system, but the flow cell has a depth of 0.3 mm, so there is ample prospect for several particles of micron dimensions to be passing through the cell in parallel.

Once the bulk temperature of the fuel dropped below 0°C (typically about 35 minutes after starting the experiment), the possibility of ice particles in the flow stream could not be discounted. Ice is likely to be formed at temperatures higher than those noted in the cold stage microscopy tests, principally because in an actively cooled larger body of fuel, there will be convection currents, geometric features such as thermocouple probes and occasional dirt particles, all of which will assist heterogeneous nucleation of ice crystals. Having noted this, 'other particles' represented only a tiny percentage of all the particles detected until the bulk fuel temperature reached approximately -20°C. Even if all these particles were due to ice, the tests suggested that serious icing due to precipitated water droplets was unlikely to occur above a bulk fuel temperature of -20°C.

4.7 Summary and Conclusions on Particle Quantification Tests

Generally, the particle size measurements tied in with data from the cold stage microscopy tests. Most particles detected were around 2 µm and relatively few were observed that were above 5 µm. However, occasional much larger particles were recorded.

Initial background tests showed that within the operating resolution of the ViPA (0.5 µm to 250 µm), the fuels were virtually particle-free and that contaminants were at insignificant levels compared to particle counts when the temperature was reduced. Fuel filtering was considered to have been effective.

Modest differences were noted between the fuels in terms of the numbers of particles precipitated from solution but the partially dried Filton fuel generated the least. The Coryton fuel showed relatively low particle counts but shed larger particles so that the overall volume of material precipitated was actually the highest of all the fuels. The Sasol fuel precipitated the highest number of particles, but these were very small and, overall, the least volume of material from the fuels exposed to ambient air.

The ViPA system seemed to be good at discerning the very small water droplets that would be responsible for haze formation. It was possibly not so good at classifying larger particles or at discriminating between particles and the background at low

temperatures (bulk fuel temperatures below about -40°C) due to darkening of the field of view.

The test to identify whether water droplets were the cause of darkening of the ViPA field of view (due to haze formation) was not entirely conclusive. In tests comparing the dried Filton fuel with Filton fuel exposed to ambient air, both fuels showed some darkening although the dried fuel was possibly marginally better in this respect. Difficulties were experienced with drying the volume of fuel required for this test and maintaining a dry environment whilst assembling the fuel container.

The possibility of ice particles in the flow stream could not be discounted but ice was not categorically identified from the particle quantification tests.

5. DISCUSSION AND CONCLUSIONS

5.1 Results And Discussions

The project was about making fundamental measurements of the solubility of water in aviation fuels and what happened to this water as the temperature was reduced.

Information on the effects of cooling rates could be measured and observed directly; monitoring the effects of fuel composition was more difficult (owing to the complexity of fuel composition) and measurements could only be made indirectly by comparing one fuel against another. Microscopy tests were useful for assessing and observing the likely physical changes but were not necessarily good predictors of how these changes might occur in larger bodies of fuel and/or the rates of those changes. Tests on the 4 litre container of fuel yielded useful information on particle sizes and distributions but difficulties were encountered in resolving the nature of those particles, particularly as the temperature decreased.

The project delivered measurements and data sets on the water solubility of current jet fuels from several sources. Cold stage observations and measurements corroborated previous observations of the behaviour of water in cooled fuels and confirmed dimensions of particles likely to be produced. The particulates study in a larger volume of fuel delivered data on the numbers of particles in the fuel and the dimensions of those particles which should help with modelling the behaviour of water in fuels and estimation of the prospects for ice deposition.

5.2 Outcomes

The research will benefit anyone associated with designing fuel systems, developing strategies for avoiding icing in fuels or for those associated with developing fuels or additives which resist ice formation. In essence the main beneficiaries will be airframe manufacturers, aircraft fuel system designers and fuel additive manufacturers.

The methodology was considered sound, as far as it went but, as was noted earlier, a lot of this work was of a fundamental nature designed to capture basic, yet unknown, scientific information.

5.3 Conclusions

No evidence of 'sticky' ice was observed, but some particles seemed to be more mobile than others. When ice particles were observed, these seemed to be in co-existence with water droplets. Under flowing conditions, supercooled water droplets might act as cement in bonding ice crystals to each other or to surrounding surfaces that they might come in to contact with. Based on the laboratory observations and

measurements, it was considered that only limited icing would occur at temperatures above -20°C as a result of water shedding from aviation fuels.

5.4 Future Work

The scope of the project could be widened and additional tests could be carried out on the larger-scale analysis of particulates. A particular interest would be to establish why jet fuel loses its optical transparency; this is of significance when using optical techniques to make measurements.

The way that the freezer and ViPA system was operated needs to be reviewed to consider how the system could be improved or extended. For instance, as fuel is being withdrawn from the fuel container, fresh (warm) fuel could be introduced so that it behaves more like the continuous fuel supply system of an aircraft.

Further tests could be run on the JP-4 samples, particularly with reference to the fuel system icing inhibitor, to identify what the actual mechanism of FSII is.

REFERENCES

1. Airbus report no RP1115500, Issue 1, *WAFCOLT – Water in Aviation Fuel Under Cold Temperature Conditions, A Literature Review*, ed. J K-W Lam, May 2011.
2. Airbus report no RP1101812, Issue 1, *WAFCOLT – Water in Aviation Fuel Under Cold Temperature Conditions, Proposed Work Plan*, ed. J K-W Lam, July 2011.
3. CRC Report No 635, 2004, *Handbook of Aviation Fuel Properties*.
4. Private communications with Tedd Biddle (Pratt & Whitney), Melanie Thom (Baere Aerospace) and Jean-Phillipe Belières (Boeing).
5. A B Crampton, R F Finn, J J Kolfenbach, *What Happens to the Dissolved Water in Aviation Fuels?*, SAE Summer Meeting, New Jersey, June 1953.
6. M D Carpenter, J I Hetherington, L Lao, C Ramshaw, H Yeung, J K-W Lam, S Masters, S Barley, *Behaviour of Water in Aviation Fuels at Low Temperatures*, 12th International Conference on Stability, Handling and Use of Liquid Fuels, Sarasota, USA, October 2011.
7. AAIB, Aircraft Accident Report 1/2010, EW/C2008/01/10, *Report on Accident to Boeing 777-236ER, G-YMMM at London Heathrow Airport on 17 January 2008*.
8. L Lao, C Ramshaw, H Yeung, M Carpenter, J Hetherington, J K-W Lam, S Barley, *Behaviour of Water in Jet Fuel in a Simulated Fuel Tank*, paper no. 2011-01-2794, SAE 2011 AeroTech Congress & Exhibition, Toulouse, France, October 2011.

Part 2: Analysis and Recommendations – Cranfield Campus

By

Dr. Liyun Lao
Dr. David Hammond
Prof. Colin Ramshaw
Prof. Hoi Yeung

Cranfield University
Cranfield Campus
Bedfordshire
MK43 0AL
UK

EXECUTIVE SUMMARY

The WAFCOLT project comprised a literature study and an experimental investigation program. The experimental work carried out by the research team at Cranfield main site, investigated the behaviour of accreted ice on subcooled surfaces submerged in fuels. The main results and findings from this part of the experimental study are summarised in this report.

The ice accretion on subcooled surfaces submerged in fuels with a moderate convection, has been simulated and observed in a 20-litre aluminium tank with chilled plates and glass windows. A water replenishment system was used to circulate and add dissolved water to the fuel sustaining the water content in fuel while growing ice on subcooled surfaces in the tank. The tank was also fitted with an array of thermocouples to measure various temperatures at points of interest. Ice accretion and growth on bare aluminium, painted aluminium and composite surfaces at three cooling plate temperatures (-25°C, -35°C and -55°C) have been examined.

A method to estimate the accreted ice porosity has been developed. Ice layer thickness and the coverage area were estimated. The mass of water in the ice collected was measured, and hence, the porosity could be estimated.

A method to evaluate the strength of accreted ice using a jet of fuel has been developed. The fuel jet dislodged the accreted ice and the pressure required to dislodge the accreted ice was estimated from the jet velocity.

In an ice slip event, it provided an alternative way to estimate the adhesion strength. The ice accumulated on a vertical surface slip down under its own weight.

The main findings from this study are as follows:

- The lower the subcooled surface temperature relative to the bulk fuel temperature, the larger the amount of ice accretion.
- The composite surface accreted relatively less ice, due to its lower thermal conductivity preventing it from being cooled to the same equilibrium temperatures as the bare and painted aluminium surfaces.
- Fuel with a higher aromatic content generally has a greater ability to dissolve water. As the fuel was cooled, it gave a relatively higher quantity of ice accretion.
- The accreted ice on vertical surfaces was very fluffy, soft and had very little mechanical strength. In this study, the SLR (i.e. snow to liquid ratio, a parameter used to indicate the ice porosity) and strength of the ice on subcooled vertical surfaces were estimated.
 - The estimated average SLR was 23.3;
 - The estimated adhesion strength was of the order of 1 Pa.

- When the fuel temperature was less than -40°C , ice accreted on subcooled horizontal surfaces was fine and gritty.

As this study was mainly concerned with ice accretion from dissolved water in a relatively static flow field, ice accretion in flowing fuel should be investigated in the future. The fate of dislodged ice should also be investigated to examine the conditions where ice is found to be “*sticky*” and could be accumulated in a fuel system. In addition, the role of moisture in the ullage space and free water in fuel should also be studied.

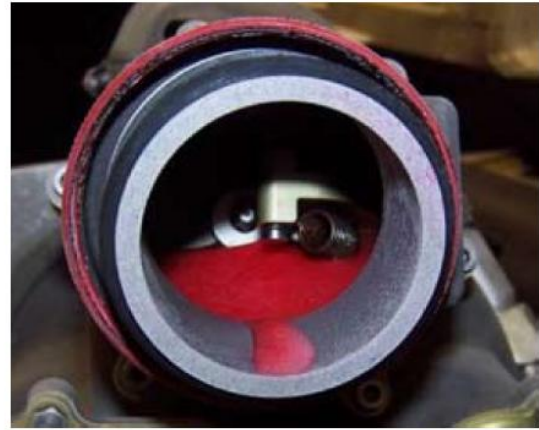
1. BACKGROUND

In January 2008 a British Airways Boeing 777 lost power to its engines and crash landed during approach to London's Heathrow Airport. Investigation by the Air Accident Investigation Branch (AAIB) [1] postulated that at fuel temperatures between -5°C and -20°C , water shed from fuel might form ice that adheres to fuel system surfaces. Under certain conditions, a substantial amount of ice could accumulate on the inner surfaces of the fuel feed system. This ice could be dislodged during high fuel flows. Dislodged ice might collect at restrictions in the system such as at the Fuel Oil Heat Exchangers (FOHE) feeding the engines, causing a restriction in fuel flow, leading to a reduction in available thrust.

Figure 1 shows a number of locations in the fuel feed system where ice was accumulated in the tests carried out during the investigation.



(a) Ice in a hose at the rear of the strut.



(b) Dyed ice in a check valve housing.



(c) Ice on the inlet face of the FOHE.

Figure 1 Accreted ice in the fuel feed system [1].

The investigation has led the AAIB to make recommendations towards airworthiness authorities for further research into aspects related to water and ice in fuel. Both the

European Aviation Safety Agency (EASA) and Federation Aviation Administration (FAA) have agreed a common approach to tackle the AAIB recommendations.

1.1 Aims And Objectives

The WAFCOLT – Water in Aviation Fuel Under Cold Temperature Conditions project covers the literature survey and laboratory testing for the formation and characterisation of ice crystals in aviation fuel. The main objectives and scope are [2]:

- Identify and review existing data/reports concerning the presence of water and ice in aviation jet fuel;
- Collect a set of jet fuels encompassing the different manufacturing processes and standards for testing and analysis;
- Laboratory testing to characterise:
 - The formation of ice crystals in aviation jet fuel and the influence of several key parameters,
 - The type and related mechanical properties of ice crystals in fuel;
- Derive recommendations for preventive actions as to ice formation in jet fuel.

The project was divided into three stages known as:

- Task 1 – Literature review and design of experiment;
- Task 2 – Laboratory testing;
- Task 3 – Analysis and recommendations.

Task 2 was further subdivided into the following sub-tasks:

- Task 2.1 – Collection of fuel samples;
- Task 2.2 – Study of ice crystal structure in fuel;
- Task 2.3 – Study of water droplet / ice formation;
- Task 2.4 – Study of ice accretion.

Details of the tasks are given in [2]. The research team at Cranfield University main site was assigned to contribute to Task 1, Task 2.4 and Task 3.

2. LITERATURE REVIEW

Research on water in jet fuel at low temperatures can be dated back to the 1950s [3 - 5]. However, there has been very little literature in the public domain on the subject since then.

As a part of a wider Airbus research programme, Airbus launched an experimental investigation on ice deposition on subcooled surfaces in fuels carried out at Cranfield University in collaboration with EADS Innovation Works [6, 7]. The freezing phenomena experienced in aircraft fuel tanks at cruise had been modelled with a 20 litre glass-windowed aluminium tank with a fuel cooling system and a laser based particle sizer system (Figure 2). The tank has two cooling plates, a fixed bottom cooling plate and a moveable upper cooling plate. The upper cooling plate may be adjusted vertically to allow the fuel tank to have a variable aspect ratio and a variable ullage space.

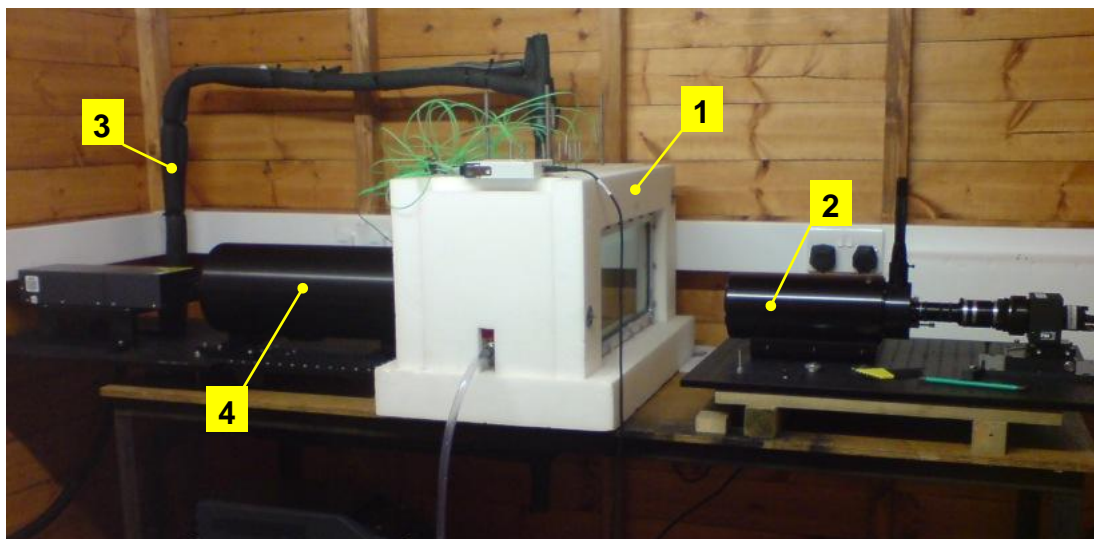


Figure 2 The simulated fuel tank experimental rig [8]. Key: 1 – simulated fuel tank; 2 – camera with long rang microscope lens; 3 – coolant supply tubing (with insulation); 4 – laser and diffuser.

Notable results from this study were [8]:

- The observed ‘fog’ phenomena in the fuel tank was shown to be due to excess dissolved water precipitating out as fine water droplets as water solubility in the fuel decreased when the temperature was reduced. The fog pattern was closely related to the cooling mode. The top cooling mode, although not relevant to flight operation, nevertheless will provide a homogeneous fog distribution since the cooling is dominated by convection; the convection enhanced mixing in the fuel. The bottom cooling mode associated with a fuel tank with ullage space will provide a stratified fog layer since the cooling is dominated by conduction.

- Visualisation of water deposition on a subcooled horizontal aluminium surface was carried out. Preliminary results from the study suggested that the deposition is by the Bergeron process. There were at least two different type of deposition on the subcooled surface when the fuel was cooled down:
 - Ice crystals of hexagonal habit grow in areas with sharp surface features from the dissolved water phase, when the fuel temperature was lower than -10°C .
 - Spherical ice particles, believed to be of cubic habit, deposited on the surface directly from the dissolved water phase.

A literature review [9] carried out as the first stage of the current project (WAFCOLT) confirmed that there is a lack of information in the public domain on the ice accretion onto subcooled surfaces in fuel, including physical properties of the accreted ice, the influence of physical conditions, e.g. surface properties, temperature variations of fuel, fluid velocity and fuel components on the ice accretion. The physical properties, such as the typical porosity and mechanical strength, are essential for understanding and modelling the accumulation and shedding processes of the accreted ice, which in turn is critical for improvements of water management in fuel systems.

3. METHODOLOGY

Task 2.4 – Study of Ice Accretion was divided into two phases. They were:

- Experimental set-ups to grow ice on subcooled surfaces submerged in fuel by using a simulated fuel tank with a water replenishment system were explored. The success of this phase was essential for ice property tests in the next phase.
- Determination of the mechanical properties of the accreted ice on the subcooled surface submerged in fuel.

3.1 Ice Accretion On Subcooled Surfaces

Characteristics of ice accretion on subcooled surfaces were studied by visualisation. The growth rate and ice texture were of particular interest. The process of ice accretion was monitored through the observation windows of the simulated fuel tank. The following parameters were investigated:

- **Fuel temperature**

Ice accretion tests were carried out at three different temperatures which were defined by the temperature set point of the cooling plate in the simulated fuel tank. The cooling plate was set to:

- -25°C;
- -35°C;
- -55°C.

- **Fuel**

Due to time constraints, only three jet fuels were used in the ice accretion tests. Two fuels were selected from the five Jet A-1 fuels used in the laboratory testing at Shrivenham under the WAFCOLT project (see Part 1 of this report). They were selected based on water solubility data and the aromatic content. The three fuels used were:

- *Merox treated Jet A-1*
This was one of the fuels used in a previous study. This was used as the control fuel. The aromatic content of the fuel was 16.6% m/m. In terms of the aromatic content, it sat between the Coryton high-aromatic Jet A-1 fuel and the SASOL fully synthetic Jet A-1 fuel.
- *Coryton high-aromatic Jet A-1*
This was one of the five Jet A-1 fuels tested at Shrivenham. The aromatic content of the fuel was 24.1% v/v. In terms of the aromatic content, it was virtually at the upper limit for the Jet A-1 specification.

- *SASOL fully synthetic Jet A-1*
This was another fuel from the Jet A-1 fuels tested at Shrunvenham. The aromatic content of the fuel was 12.4% v/v. In terms of the aromatic content, it had the lowest content of the three selected fuels.

One of the factors influencing water solubility in fuel is the aromatic content. Fuel with a high aromatic content should hold more dissolved water than fuel with a lower aromatic content at the same temperature (see Part 1 of this report). The three fuels used had a range of aromatic contents and therefore should represent the likely range of water solubility in fuel.

- **Surface**

Three specimens with different surface properties were tested. The specimens were based on aluminium blocks of the same design. Details of the test specimens are given in a later section. The surface properties tested were:

- *Bare aluminium*
This was used as the control.
- *Painted aluminium*
This represented the generic fuel tank surface properties. The ice accretion surfaces of the aluminium block were painted with a representative fuel tank paint supplied by Airbus.
- *Painted composite*
This represented the alternative fuel tank surface properties. Composite strips were bonded on a base aluminium block and painted at Airbus.

The specimens were placed on the cooling plate in the simulated fuel tank. They made good thermal contact with the cooling plate. During testing, they would have different surface temperatures due to the material thermal properties at the surface and would result different degrees of subcooling relative to the bulk fuel temperature.

3.2 Ice Porosity

Measurement of the porosity of accreted ice proved to be very challenging. As the ice was extremely soft and loose, it deformed or collapsed if disturbed. Compaction takes place when sampled into a container. It was difficult to apply conventional density measurement methods for this application.

Two major challenges needed to be overcome in order to carry out the porosity tests. They were:

- To accrete sufficient ice for the test;

- To determine the real porosity value without changing the ice structure and liquid contents.

As the simulated tank used in the current project contains up to 20 litre of fuel, the amount of dissolved water in the fuel was therefore limited. A water replenishment system was developed to continuously add dissolved water to the fuel in the tank. Details of the water replenishment system are given in a later section.

A well established parameter known as the Snow to Liquid Ratio (SLR) [10] in the field of atmospheric physics was adopted to characterise the accreted ice porosity in the current application. SLR is inversely proportional to the snow density, ρ_s . This means that as the snow density increases, i.e. more mass for the same volume, the SLR diminishes, and vice versa. Definitions of the snow density and SLR are given below:

$$\rho_s = \frac{m}{V} \tag{1}$$

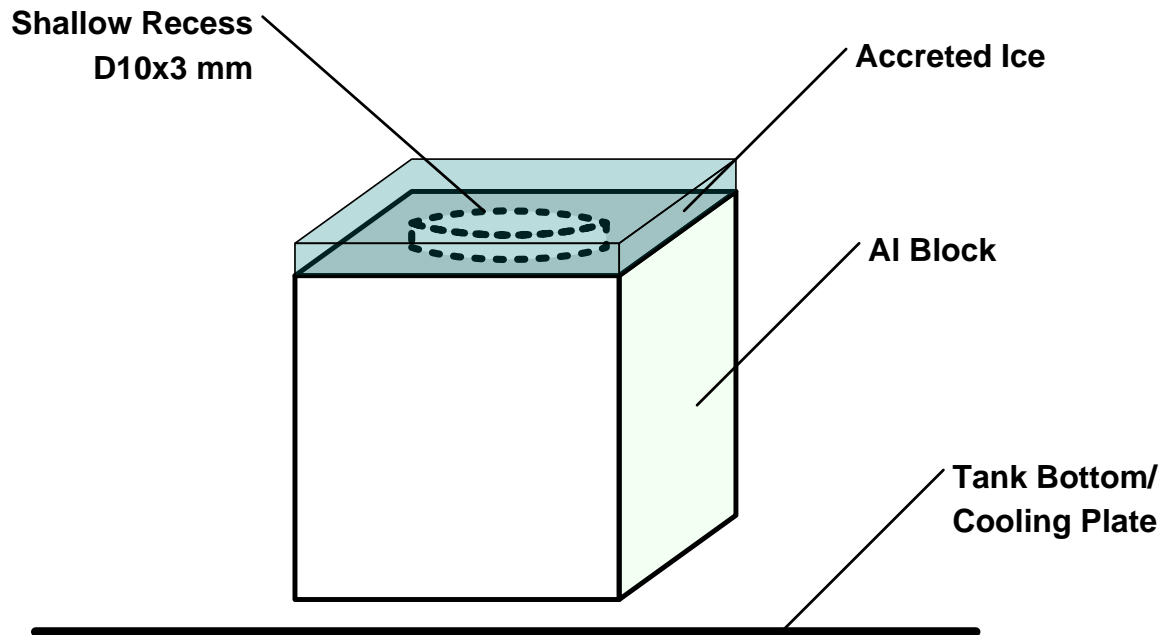
$$SLR = \frac{m}{V \rho_w} \tag{2}$$

where V is the occupied volume of the snow; m and V are the mass and volume of water when the ice is melted; and ρ_w is the reference density of water (1000 kg/m³).

The mass of water in the collected fuel/melted water mixture can be measured by using KF coulometric titration, if it is less than 50 milligrams; otherwise, the water in the ice can be separated from the entrapped fuel by melting and re-freezing to obtain a solid ice lump and weighing the ice lump directly.

A number of ideas to collect a known volume of accreted ice have been tried. One attempt is illustrated in Figure 3a. A recess of known volume was machined into the top surface of an aluminium block. When excess ice had accumulated in the recess, the aluminium block was removed from the tank. The ice adhering to the top and sides was cleared off using a blade. This left the ice in the recess undistributed and the ice was allowed to melt in the recess. When melted, the liquid mixture (containing both water and fuel) was analysed to determine the amount of water and fuel in the liquid mixture.

A 168-hour ice accretion run did not fill the recess with sufficient ice (Figure 3b). Since the ice did not fill the recess completely, the volume of ice in the recess was therefore undetermined, and it was not possible to compute the snow density, and hence the SLR.



(a) Schematic of ice accretion for porosity estimation – a recess in a subcooled aluminium block.



(b) Top view of the recess with accreted ice.

Figure 3 Ice accretion in a recess of a specifically designed aluminium block for ice porosity estimation.

A contingency method, which applied equally to the specimen blocks and the specially made aluminium block, was adopted. With water being continuously replenished into the tank, a layer of ice built up over the block surfaces (c.f. Figure 3b). Once the ice on the top surface had been scraped off carefully, the thickness of the ice layer at the top of the vertical surfaces could be seen clearly (Figure 4).

The thickness of the ice layer could be estimated with the aid of a thickness gauge (Figure 4b). The gauge comprised of a handle and a tri-blade head. The three blades on the tri-blade head have steps with heights of 2, 4 and 6 mm, respectively. By prodding a blade with the most appropriate step in the ice layer, the ice layer thickness could be estimated with some level of confidence.

Figure 4c shows that the ice layer on the vertical surfaces was thinning out towards the foot. For simplicity, the ice layer thickness on the vertical surfaces was assumed to have a linear profile with the maximum thickness at the top of the vertical surfaces and zero thickness at the foot.

The volume of the ice layer on the vertical surfaces could be calculated since the dimension of the block and the ice layer thickness are known. When the fuel was drained out from the tank, the accreted ice on the vertical surfaces was collected and its water content was measured. The snow density and the SLR were calculated from Eqn. 1 and Eqn. 2.



(a) The ice layer thickness at the top of the vertical surfaces could be seen clearly from the picture.



(b) The thickness gauge with its tri-blade head.



(c) Ice covered area on the vertical surfaces. Thinning of the ice layer towards the foot of the vertical surfaces is observed.

Figure 4 Contingency method to estimate the ice volume and hence the ice porosity by estimating the ice layer thickness with the aid of a thickness gauge.

3.3 Adhesion Strength

A number of methods to determine ice strength had been proposed and discussed at the beginning of the project [11]. These methods included the use of specially designed meters to measure adhesion, compression, tensile and breaking strengths and an instrumented plough to measure the force required to scrape the ice from the surface. The most challenging requirement was that tests have to be performed in situ so that the properties of the ice will not be changed due to removal/sampling.

While measurements have to be carried out in situ, easy access to the accreted ice is required. This led to lowering of the top cooling plate to the bottom of the tank. Details of this modification are given in Section 4.3.

As the accreted ice was found to be very loose, these initial proposed ideas proved to be not viable for the application. An alternative approach using a liquid jet of fuel to assess the adhesion strength was evaluated. Since a low jet velocity could be maintained and controlled accurately, the method was well suited for the current application where adhesion was expected to be very weak. The schematic of the method is shown in Figure 5.

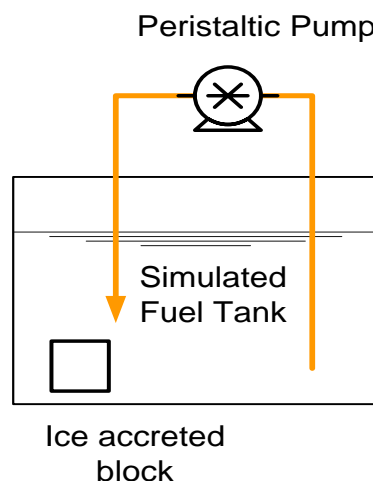


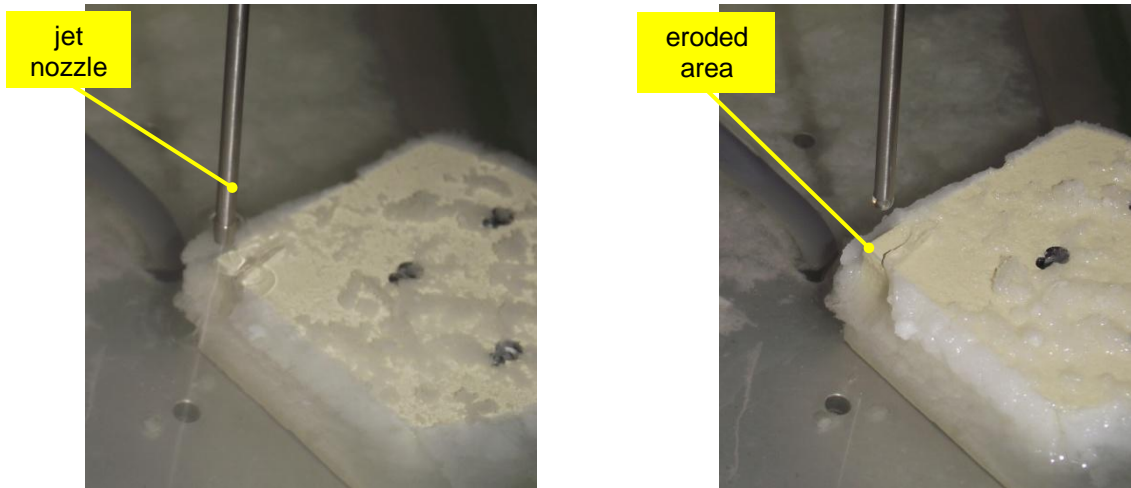
Figure 5 Schematic of the jet method to evaluate the ice adhesion strength.

The fuel jet was driven by a peristaltic pump which took some fuel from the simulated fuel tank and injected back at a selected target as a jet through a specially designed nozzle. The pump has a digital controller to control the fuel volume flow rate. The range is controllable from 6 to 800 ml/min. This is equivalent to a mean jet velocity, , at the nozzle outlet from 0.024 to 3.2 m/s.

The jet was directed vertically downward. The jet nozzle was positioned at a distance, , from the target. The centreline jet velocity, , at a distance, , from the nozzle is given by [12]:

(3)

where Re is the nozzle Reynolds number; d is the inner diameter of the nozzle (2.3 mm in this application) and ν is the kinematic viscosity of the fuel.



(a) Fuel jet in operation in fuel. The jet had dislodged the accreted ice at the corner of the block submerged in fuel.

(b) Fuel has been drained away showing the area of erosion.

Figure 6 Fuel jet method to evaluate the ice adhesion strength.

Figure 6a shows the jet nozzle and a test specimen block submerged in the fuel. Ice had been grown on the test specimen block. It can be seen that the accreted ice around the targeted corner of the test specimen block was dislodged. Figure 6b shows ice distribution after the fuel in the tank was drained. The adhesion strength of the accreted ice was evaluated based on the estimated velocity of the jet and the area of the erosion.

4. IMPLEMENTATION

4.1 Water Replenishment System

The initial amount of dissolved water in the fuel in the simulated tank was not sufficient to form noticeable amount of ice on the subcooled surfaces. It was therefore necessary to continuously replenish the dissolved water in the fuel during the test. It was important that the water was replenished in the fuel in the dissolved form. This allowed the project to focus on investigations on ice accretion from fuel with dissolved water only. The development of the water replenishment system was critical to the success of this experimental study. Much effort was made towards the development of this system.

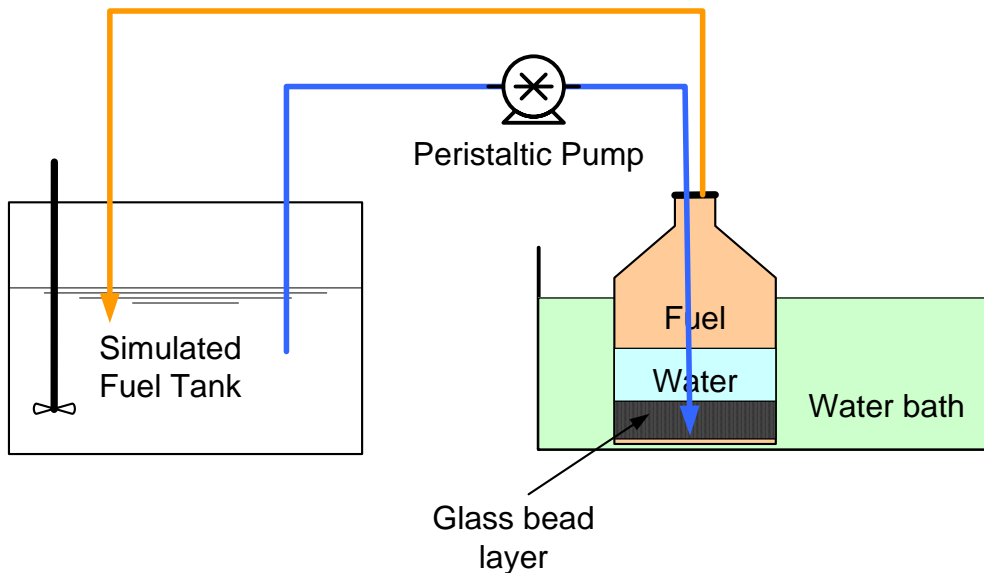


Figure 7 A schematic showing the initial water replenishment system setup.

Figure 7 shows the initial design of the water replenishment system. In the replenishment process, fuel from the simulated fuel tank was extracted from the tank, pumped through a “saturator” and returned to the simulated fuel tank. The saturator had a volume of around 500 ml and sat in a warm water bath; the water bath temperature was controlled. The saturator was partly filled with de-ionised water and partly with fuel. There was a layer of glass beads at the bottom of the saturator to disperse the incoming fuel into small droplets. As the fuel droplets rose through the water layer in the saturator, the fuel droplets warmed up and absorbed water with them. Water absorption also took place at the interface between the water layer and the fuel layer. Fuel was then taken from the upper end of the fuel column in the saturator and re-introduced back to the simulated fuel tank.

A stirrer was fitted in the fuel tank to enhance the mixing of water and temperature.

The initial design proved to have a number of problems. Two major concerns were:

- Some free water was entrained in the fuel in the saturator. The fuel returned to the simulated fuel tank was therefore contaminated with suspended water droplets.
- Since the saturator was connected to the pump outlet, the saturator was therefore pressurised. In some instances, it caused fuel leakage at the connector of the saturator and was therefore a flammable hazard concern.

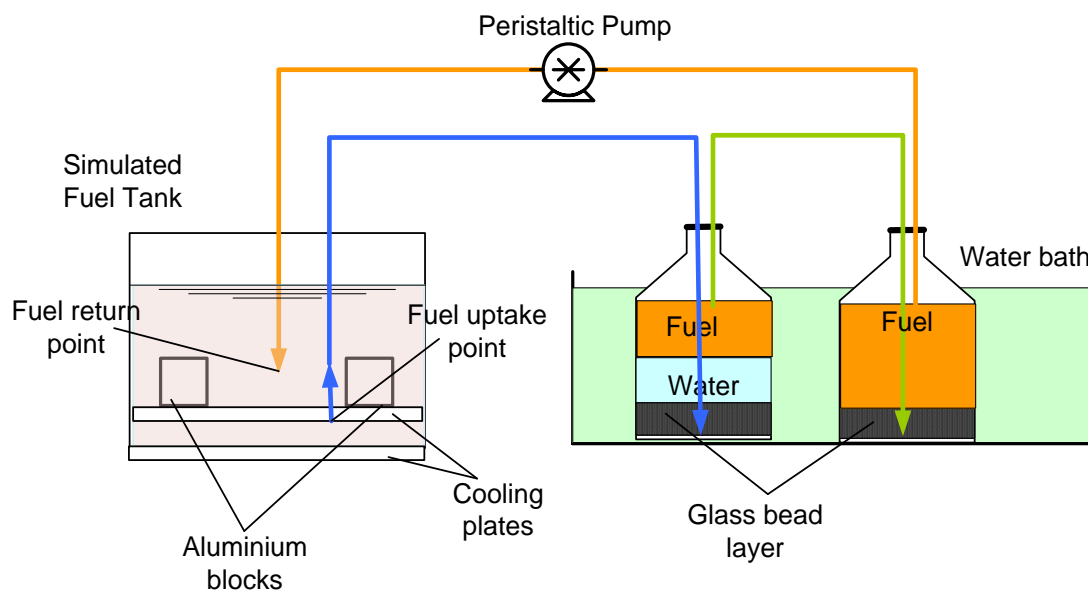


Figure 8 A schematic showing the revised water replenishment system setup.

A two-stage suction system was developed to overcome these deficiencies. Two major changes were made to the original design. A schematic of the revised water replenishment system is shown in Figure 8. Two bottles were used in this system to minimise the risk of entrained free water. The bottles were placed in a warm water bath. In the first bottle (the bottle on the left in Figure 8) was the saturator. It was made up in a similar way to the saturator in the initial design. In the saturator, the glass bead layer was approximately 30 mm high, the water/fuel interface was about 60 mm high and the fuel/air interface was about 90 mm high. The second bottle (the bottle on the right in Figure 8) was the recuperator. It was made up similarly to the saturator but filled with fuel only.

The system was reconfigured so that the bottles were on the suction side of the pump. This avoided pressurising the bottles and therefore eliminated the risk of fuel leakage.

In operation, water depleted cold fuel from the simulated fuel tank was passed through the saturator to replenish the water content. Fuel outflow from the saturator could contain some free water suspended as fine water droplets. The fuel from the saturator was therefore passed through the recuperator where the fuel was warmed up further. It served as a buffer zone preventing fuel with suspended free water return to the simulated tank directly. The warmer fuel also allowed the suspended water droplets more time to be dissolved in the fuel. In addition, the glass bead layer in the recuperator encouraged coalescence of any water droplets to bigger droplets which settled out to the bottom of the recuperator.

The fuel pick-up point was in the gap between the two cooling plates. The fuel return point was in the geometric centre of the fluid (fuel) body. The pick-up point and the return point are depicted in Figure 8. The positions of the pick-up point and the return point were strategically selected to ensure a good symmetrical temperature profile and fluid dynamic profile so that the specimen blocks placed in the four quadrants of the tank experienced the same operating conditions. The stirrer used in the initial configuration (Figure 7) was removed, since it would create an undesirable flow pattern in the tank.

It can be seen in Figure 9 that the fuel in the second bottle was clear. This suggested that there was a negligible amount of suspended water in the fuel. The fuel, replenished with dissolved water, was passed back into the simulated fuel tank.

Figure 10 shows the measured water content in the returning fuel from the water replenishment system during a 7-day ice accretion experiment for Test #2 and Test #5. Definitions of the tests are given in the ice accretion test matrix in Table 1 in Section 4.5. The results for Test #2 are fairly consistent. If a best fit line is fitted to the results, it would be a flat line of a constant value of approximately 56 ppm by volume (71 ppm by mass). The ppm by volume to ppm by mass conversion was calculated by assuming the water to fuel density ratio was $1.23 = 1000/810$ where water density was taken as 1000 kg/m^3 and the fuel density was taken as 810 kg/m^3 [13]. However, the results for Test #5 showed an upward trend with time. It increased from 57 ppm by volume (70 ppm by mass) on day-1 to 75 ppm by volume (92 ppm by mass) on day-7. It is not clear why the water content in the returning fuel increased significantly on day-7 in Test #5. A possible explanation may be water contamination in the recuperator. During the replenishing process, some free water may be carried over from the saturator to the recuperator. Over a period of time, the contamination might build up to a level that could result in a noticeable increase in the total water concentration (dissolved and suspended) in the returning fuel. Although the incoming fuel temperatures of Test #2 and Test #5 were very similar, -5.1°C and -3.4°C , respectively, but the incoming fuel from Test #2 was drier than Test #5 because more ice was accreted in Test #2 compared to Test #5 (see Figure 22 in Section 5.1.1). Since the incoming fuel from Test #2 was drier, it resulted less free water entrained during the replenishing process because the fuel was able to dissolve the entrained free water. For Test #5, since the fuel was wetter, the fuel was not able to dissolve the entrained free water as in Test #2. Thus, Test #5 was more likely to have a contaminated recuperator over a long period of operation.

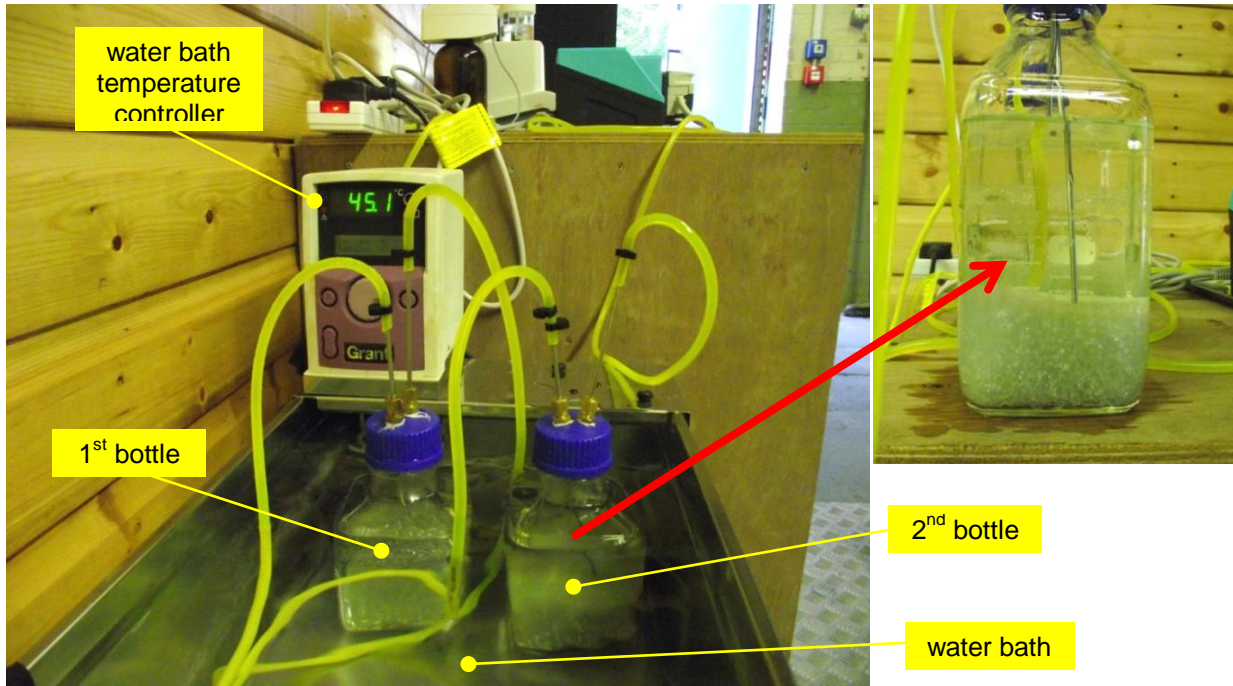


Figure 9 Left: Water replenishment system in operation; Right: Second bottle taken out of the water bath to show the fuel clarity.

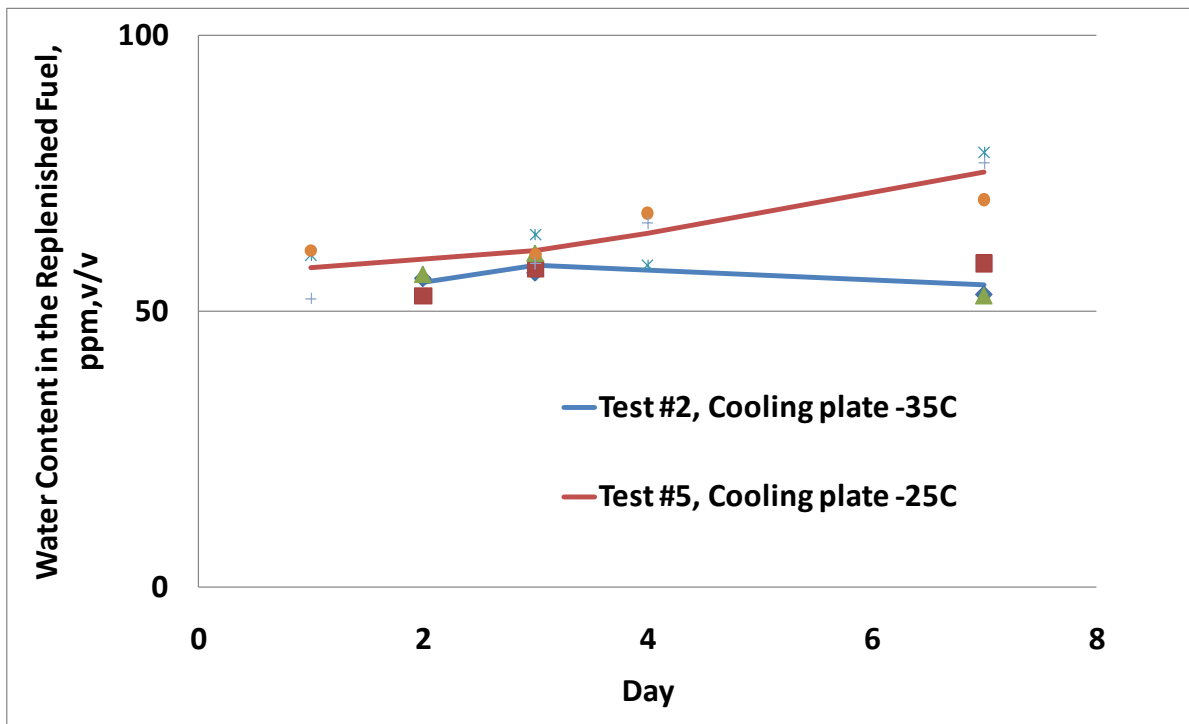


Figure 10 Water content in the returning fuel from the water replenishment system during a 7-day run for Test #2 and Test #5. Fuel used: Coryton High Aromatics; water bath temperature set point: 40°C; and fuel circulation rate: 200 ml/min

4.2 Specimen Blocks For Ice Accretion Tests

To observe the ice accretion process on different subcooled surfaces, three specimen blocks of different surface finishes were prepared. The three specimen blocks were based on a baseline aluminium block of the dimensions shown in Figure 11.

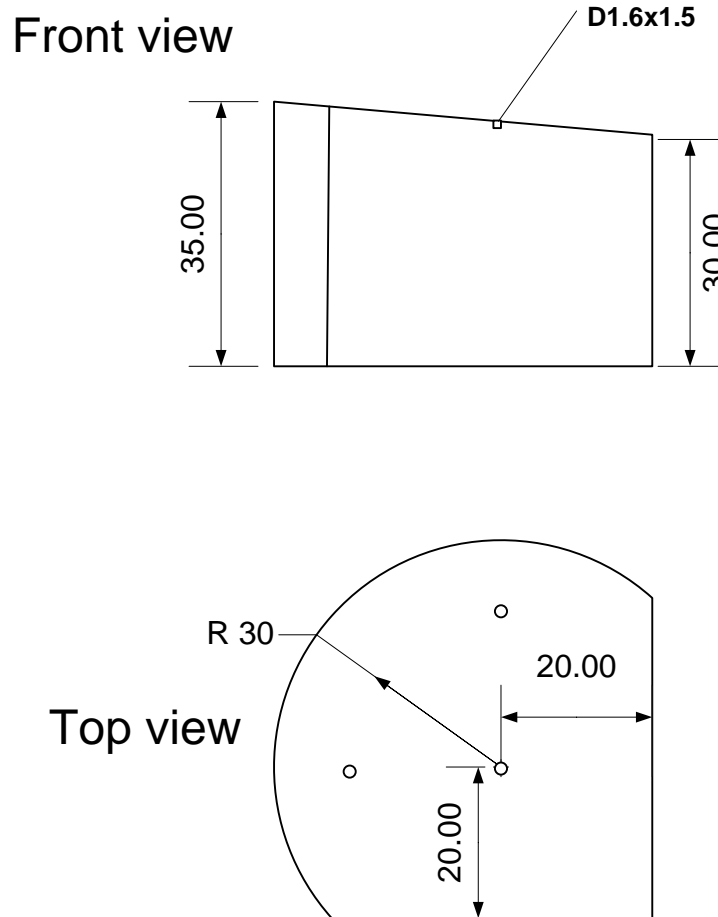


Figure 11 Design of the aluminium block used for ice accretion experiments. Units are in mm.

The top surface of the baseline aluminium block was slightly inclined to allow laser imaging. Laser imaging was initially proposed to capture the ice accretion process, but was found not to be practical because of the heavy fog due to high water content in fuel and the long experimental periods. Laser imaging was therefore abandoned and basic observation was used instead.

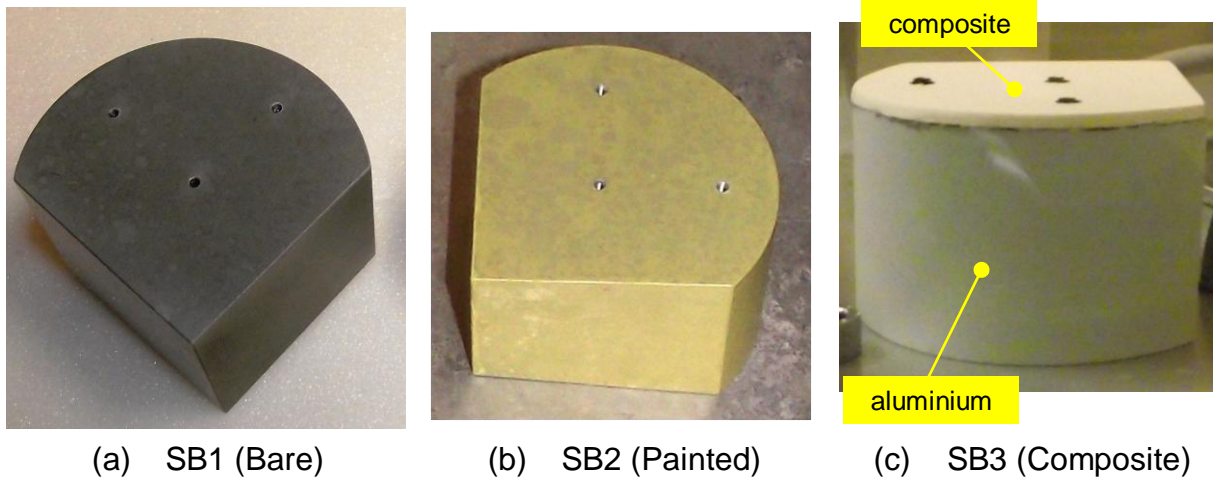


Figure 12 Specimen blocks. (a) Bare aluminium block; (b) Painted aluminium block and (c) Composite strips bonded on the top and one of the flat vertical faces of the baseline aluminium block.

Three specimen blocks are shown in Figure 12. They were:

- The first specimen block was bare aluminium. This was the control specimen block. This was designated as SB1 (bare).
- The second specimen block was painted on all surfaces except the bottom surface using a representative fuel tank paint supplied by Airbus. The bottom surface was left bare to give good thermal contact with the cooling plate that it was resting on. The thermal contact was expected to be similar to that of the control specimen block. This was designated as SB2 (painted).
- The third block had a composite strip bonded to the top surface and one of the flat vertical sides. The block was painted similarly to the second block. The bottom surface was left bare like the second specimen block to provide good thermal contact. This was designated as SB3 (composite).

On the top surfaces of the three specimen blocks, holes were drilled to accommodate thermocouples for surface temperature measurements.

4.3 Modifications To The Simulated Fuel Tank

Originally the simulated fuel tank had a pair of windows constructed for the purposes of visual observation/imaging for the laser illumination and camera system. The windows were double glazed with a 6 mm thick inner panel of toughened glass, a 10 mm air gap and an 8 mm thick laminated heated outer glazed panel. After several long runs, cracks developed in the heated glass panel of both windows. Investigation in conjunction with the fabricator concluded that the cracks were caused by thermal stress due to uneven heating of the laminated panels.

Two modifications were then made to the simulated fuel tank:

1. The laminated heated glass panels were removed. The new windows were now constructed using double glazed toughened glass panels only. A nitrogen purging setup was used for long runs. The windows were shrouded in a hood and nitrogen was introduced to minimise water condensation on the windows and thus reducing excessive frost build. A hot air gun was used to defrost the windows when visual observations were required.
2. Inherited from the previous icing study, the simulated fuel tank had two cooling plates; a fixed bottom plate and a moveable upper plate. The design allowed the position of the upper cooling plate to be adjusted vertically. To improve access to the specimen blocks inside the simulated fuel tank, the top cooling plate was lowered to the bottom of the tank. Effectively, two cooling plates were stacked on top of each other at the bottom of the tank (Figure 13). Test specimen blocks were placed on top of the 'top' cooling plate at the bottom of the tank during tests (Figure 14).

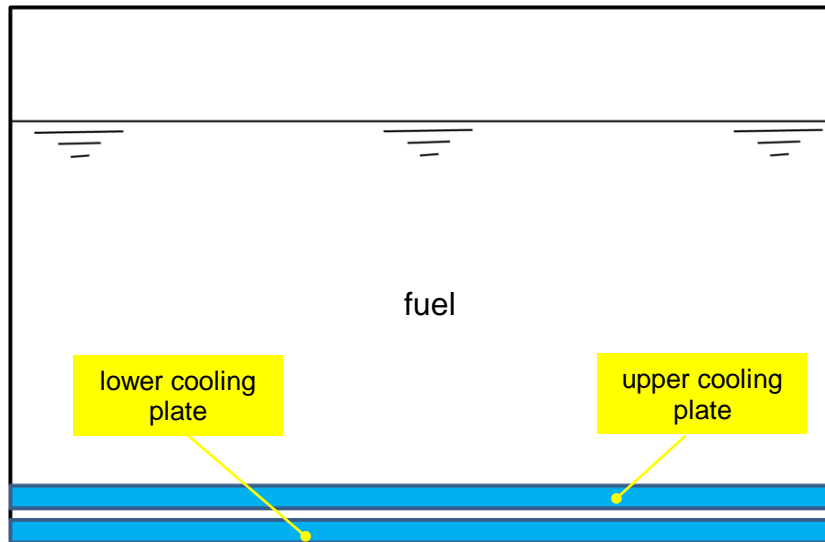


Figure 13 Schematic of the cooling plate arrangement.

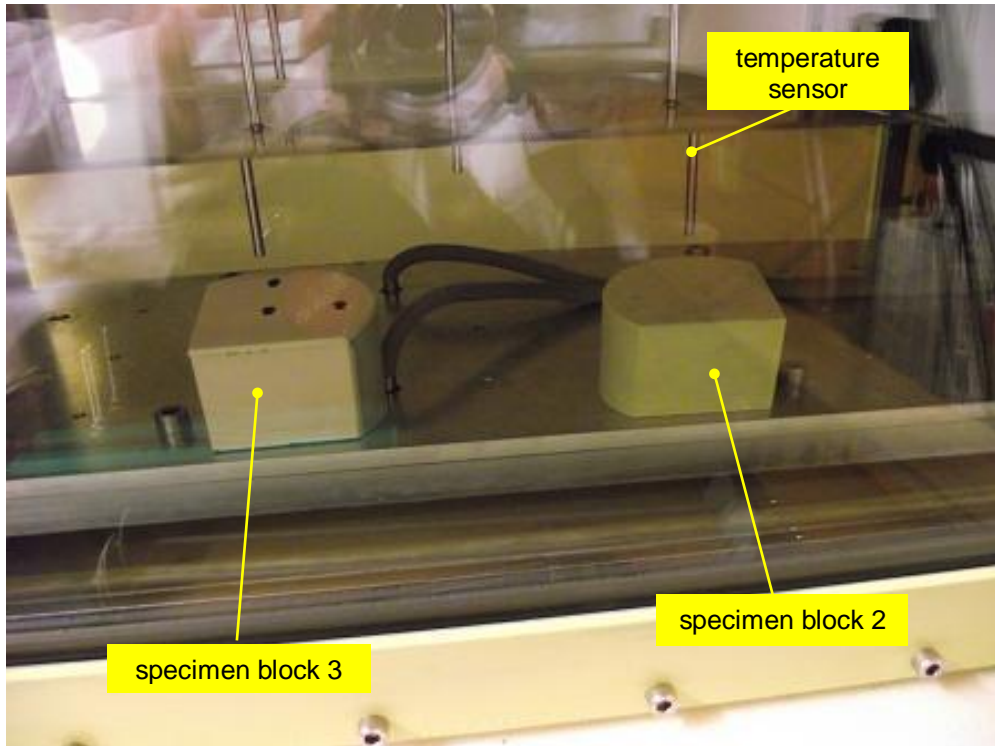


Figure 14 Simulated fuel tank with specimen blocks sitting on the ‘top’ cooling plate lowered to the tank bottom.

4.4 Chest Freezer

A chest freezer (Figure 15) was purchased for storage of collected accreted ice and also to provide a working chamber for handling and analysing the ice in a controlled cold environment.

The chest freezer, with two transparent lids on its top, allowed convenient access to the inside. It provided a space of 250 litres at a temperature of -26°C for work to be carried out. The accreted ice covered specimen blocks were transferred into the freezer once removed from the simulated fuel tank.

Since the melting point of pure ice is 0°C, the freezer preserved the ice in its original state as far as possible, without melting. Although some vaporization from or deposition onto the stored accreted ice would be inevitable, the processes were expected to be slow if the air in the freezer was not disturbed too much. Substantial changes to the accreted ice were not expected within a short period, i.e. a few minutes, while analysis was being conducted.



Figure 15 A chest freezer for storage of collected accreted ice.

4.5 Experiment Processes

All experiments comprised of two phases, the ice growth phase and the evaluation phase. Details of the two phases are:

- *Ice Growth Phase*
 Conditions for ice accretion, e.g. fuel type, cooling plate temperature, duration of ice growth period, flow rate of the water replenishment system and the water bath temperature, were set as required. During the ice growth phase, temperatures at different locations in the simulated fuel tank were logged and the water content of the fuel was monitored using a Karl Fisher coulometer.
- *Evaluation Phase*
 At the end of the ice growth phase, ice was collected from the specimen blocks for analysis to evaluate the effects of surface finish, fuel type and degree of subcooling on ice accretion. For the ice porosity estimation and adhesive strength tests, the procedures have been detailed in sections 3.2 and 3.3, respectively.

Table 1 Ice accretion test matrix

<i>Fuel</i>	<i>Cooling Plate Temperature</i>		
	<i>-25°C</i>	<i>-35°C</i>	<i>-55°C</i>
<i>Jet A-1 Mercox treated</i>	-	#1	-
<i>Coryton High Aromatics Jet A-1</i>	#5	#2	#3
<i>SASOL Fully Synthetic Jet A-1</i>	-	#4	-

Table 1 shows the proposed ice accretion test matrix. Five ice accretion tests were conducted. Test #1 was a trial test to develop the experimental set-up and procedure. Test #2 and Test #3 were designed to investigate the effect of the fuel temperature. Test #2 and Test #4 were designed to investigate the effect of the aromatic content. Test #5 was added after the initial issue of the final report (dated 20 January 2012) to EASA. Test #5 was designed to enrich the exiting results and conclusions. It provided an additional test point for a higher cooling plate temperature at -25°C.

Figure 16 shows the layout of the specimens for an ice accretion experiment in the simulated fuel tank. All the specimen blocks were placed on the central area of the cooling plate to ensure the specimen blocks would be subjected to similar conditions. The specially designed aluminium block with a recess at the top surface initially designed for ice porosity estimation was also placed in the central area of the cooling plate similarly to the specimen blocks. As discussed in Section 3.2, ice porosity estimation would be estimated from the ice layer thickness on the vertical surfaces of the specimen blocks directly. Thus, the specially designed aluminium block was redundant. It was placed in the tank to ensure a symmetrical layout as far as possible.

Additionally, two shallow plates were placed on the cooling plate. One shallow plate was placed directly under the fuel return point. The other shallow plate was placed away from the centre at a remote corner of the tank. The plates were used to collect ice that grew on them. The ice that grew on the plate under the fuel return point would experience a jet impingement. The ice that grew on the plate at a remote corner of the tank would experience a pseudo-static condition. The contrast of the ice found on the two plates would be of interest.

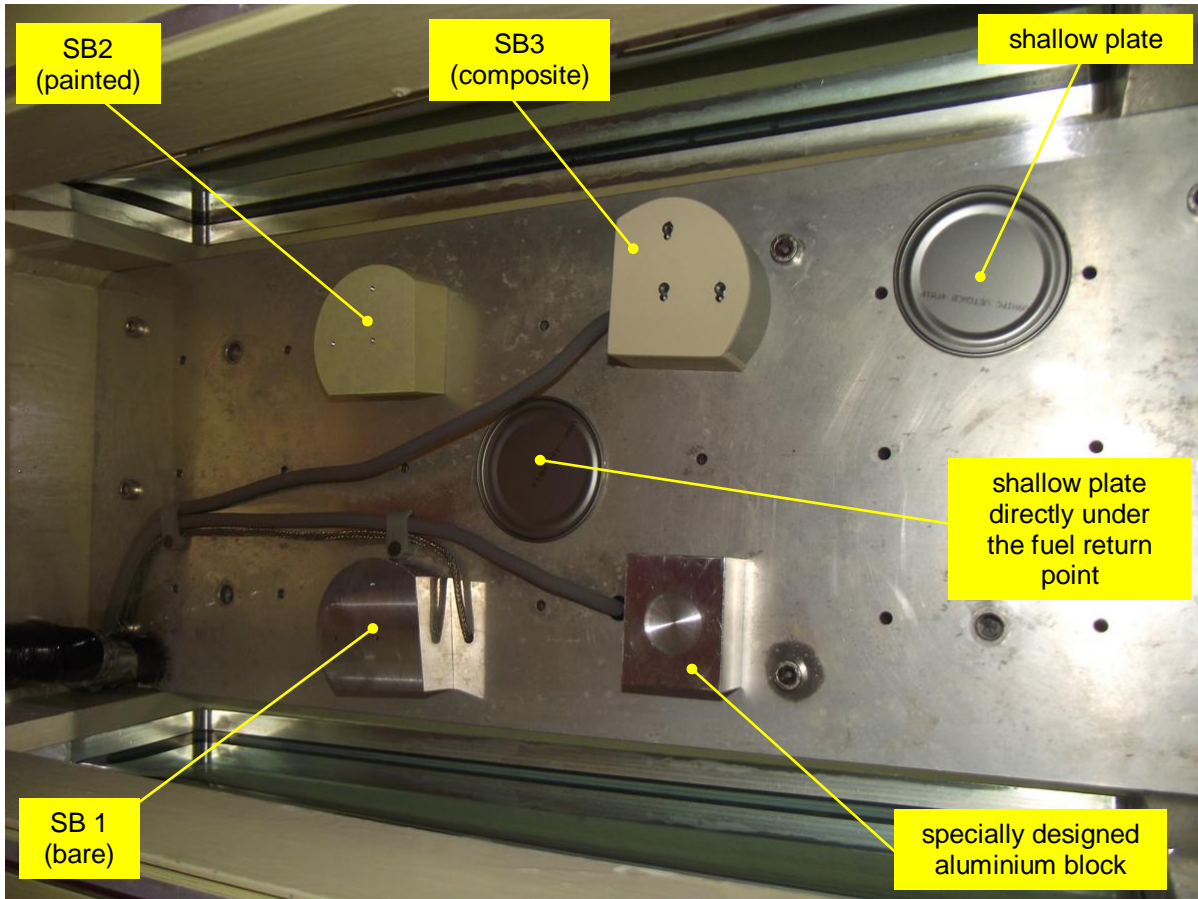


Figure 16 Top view of the specimen layout on the cooling plate.

5. RESULTS

5.1 Ice Accreted On Subcooled Surfaces In Fuel

As stated in Section 4.5, Test #1 was a trial test to develop the experimental set-up and procedure. In the test, the ice growth phase lasted for ~240 hours. This was found to be excessive. A shorter ice growth phase could produce sufficient ice for the evaluation phase. The subsequent tests, Test #2, Test #3, Test #4 and Test #5, had a reduced ice growth phase duration of ~168 hours. This enabled the tests to be done at a quicker turnaround time to meet the schedule. Unfortunately, the results of Test #1 were not like-for-like to those of Test #2, Test #3, Test #4 and Test #5, since it had a much longer ice growth phase. Test #1 results are therefore not included in the main discussion in the report. The results are referenced where applicable.

For a long haul flight, such as a flight from Beijing to Heathrow, the flight duration is ~10.5 hours [1]. The ice growth phase in the tank on board of the aircraft would be ~8 hours if the fuel uploaded on the aircraft is cold (see Part 3 Figure 9). In comparison, the ice growth phase duration in a typical long haul flight is much less than that in the ice accretion tests in this study. The discrepancy is mainly due to the limit of the water replenishment.

The simulated fuel tank has a volume of 20 ltr only. This is a fraction of the volume of a typical fuel tank on an aircraft. Reducing the tank volume reduces the volume to surface area ratio. A larger tank would potentially accrete more ice since it has a larger volume to surface area ratio, i.e. more water available to deposit on the surface. Recognising the scaling effect, a water replenishment system was introduced to top up the water content in the tests (Section 4.1). The water replenishment had a fuel flow rate of 200 ml/min. A low fuel flow rate was used for the water replenishment system to ensure the fuel in the simulated fuel tank to remain undisturbed as much as possible. During the 168 hours of ice growth in the tests, the total volume of fuel exchanged would be 2016 () ltr. It should be noted that the water replenishment system was relatively inefficient, since the fuel returned was only topped up a fraction of the saturated value (see Section 4.1). Hence, a large volume of fuel needs to be exchanged to build up a sufficient ice layer thickness for evaluation.

During the ice growth phase, typical temperatures and temperature differences relative to the fuel temperature at 3 cm above the cooling plate in the fuel at various locations in the simulated fuel tank are tabulated in Table 2. The temperature differences are referred to as the degree of subcooling in this study. The top surface temperature of the SB1 (bare) had the lowest top surface temperature of the three specimen blocks. The paint provided a degree of thermal insulation and thereby gave a slightly warmer top surface temperature in SB2 (painted) compared to SB1 (bare). The composite strip on SB 3 (composite) had good thermal insulation and gave the highest top surface temperature compared to the other two specimen blocks.

Table 2 **Temperatures at various locations in the simulated fuel tank in Tests #1 to #5.**

Locations	Tests #1, #2 and #4		Test #3		Test #5	
	Temperature, °C	Degree of subcooling relative to [a], °C	Temperature, °C	Degree of subcooling relative to [a], °C	Temperature, °C	Degree of subcooling relative to [a], °C
Tank bottom	-24.2	-19.1	-47.1	-3.6	-19.0	-15.6
3 cm above the cooling plate, [a]	-5.1	0.0	-43.5	0.0	-3.4	0.0
Top surface of SB1 (bare)	-17.3	-12.2	-46.2	-2.7	-11.2	-7.8
Top surface of SB2 (painted)	-13.7	-8.6	-45.0	-1.5	-8.3	-4.9
Top surface of SB3 (composite)	-10.0	-4.9	-43.7	-0.2	-6.5	-3.1
Room temperature	17.7	22.8	14.8	58.2	16.9	20.3

In Test #1, Test #2, Test #4 and Test #5, the fuel temperature immediately next to the cooling plate at the bottom of the tank was much lower than the fuel temperature at a position of 3 cm above the cooling plate. The degree of subcooling was -19.1°C for Test #1, Test #2 and Test #4 and -15.6°C for Test #5 (Table 2). The cooling plate temperature was set to -35°C in Test #1, Test #2 and Test #4 and to -25°C in Test #5. Due to a higher cooling plate temperature in Test #5, the degree of subcooling for Test #5 was lower than that in Test #1, Test #2 and Test #4. Since the fuel was cooled by the cooling plate at the bottom of the tank, a stable vertical temperature gradient was established. The temperature was stratified such that the fuel in the upper part was appreciably warmer than that at the bottom. As demonstrated in the previous investigation [6, 8] with this mode of cooling, heat transfer was predominately through conduction. The water replenishment system should have a very limited influence on the fuel fluid dynamic in the tank, since the water replenishment system fuel flow rate was low.

In Test #3, the cooling plate was set to a much lower temperature of -55°C compared to a temperature of -35°C in Test #1, Test #2 and Test #4 and a temperature of -25°C in Test #5 (Table 1). Due to a much lower operating temperature, the external surfaces of the simulated fuel tank were much more prone to have ice formed on them from condensation of warm humid air in the laboratory. With a long test run time (168 hours), the ice could grow to a significant thickness. The ice obscured the viewing into the tank. It also hindered access to the specimen blocks by freezing the lid shut. Although measures such as nitrogen purging and hot air gun were deployed (Section 4.3), they were ineffective in this case.

A workaround was to cover the simulated fuel tank with thermal insulation foam in Test #3. This eliminated the ice problem by preventing the ambient air to come into direct contact with the cold external surfaces of the simulated fuel tank. The effect of the thermal insulation foam can be seen from the temperatures in Table 2. In Test #3, the tank bottom temperature was only 3.6°C lower than the fuel temperature at 3 cm above the cooling plate. The temperature differential was much lower than the same in Test #1, Test #2 and Test #4, where the temperature differential was -19.1°C and in Test #5, the temperature differential was -15.6°C

The temperature differential observed in Table 2 can be explained by thermal energy balance. The thermal energy flowed out of the simulated fuel tank through the cooling plate is given by, $Q_{out} = h_c A (T_{fuel} - T_{cooling})$, where A is the surface area of the cooling plate, h_c is the heat transfer coefficient, and T_{fuel} and $T_{cooling}$ are the bulk fuel temperature and the cooling plate temperature. The thermal energy flowed into the simulated fuel tank may be summed up by a single parameter, Q_{in} . At equilibrium the thermal energy flowed into the tank is balanced with the thermal energy flowed out of the tank, $Q_{in} = Q_{out}$. Take h_c and A to be constants in all tests:

- **Test #3, with good thermal insulation covering the tank**
 was expected to be small due to good thermal insulation, and it resulted a small temperature differential, $\Delta T = 3.6^{\circ}\text{C}$.
- **Test #1, Test #2, Test #4 and Test #5, with poor thermal insulation covering the tank**

was expected to be large due to poor thermal insulation, and it resulted a large temperature differential,

With very little heat flowed from the ambient to the fuel in Test #3, the walls and the ceiling of the simulated fuel tank were at a very similar temperature to the cooling plate. The ullage temperature was found slightly lower than the fuel temperature. This confirmed the ullage was being cooled by the cold ceiling, which was expected to have a similar temperature to the cooling plate. The fuel in the tank was therefore cooled from all sides. This cooling mode was different to that in Test #1, Test #2, Test #4 and Test #5 where cooling was predominately from the bottom. The different in cooling mode should be noted when comparing results with Test #3.

5.1.1 General observations

Figure 17 shows the ice accretion on a vertical composite strip bonded surface of SB3 (composite) in Test #1; the ice layer gets thinner towards the bottom. This characteristic appeared on all vertical surfaces of all the specimen blocks. It is postulated that one or both of the following factors could be in play creating this characteristic:

- The subcooled vertical surfaces created a local down draught bringing a relatively warmer and wetter fuel in contact with the surfaces. As the fuel flowed downward over the vertical surfaces, ice was accreted on the surfaces and the fuel became cooler and drier. Less water was therefore available for ice accretion toward the lower part of the vertical surfaces.
- Since the dissolved water content is closely linked to the fuel temperature, the dissolved water concentration therefore is expected to stratify in a similar manner to the fuel temperature. As discussed previously, the fuel was cooled at the bottom, and thereby created a vertical temperature gradient and hence a water concentration gradient. The upper part of the vertical surfaces would be sitting in a relatively warmer and wetter fuel compared to the lower part of the vertical surfaces.

The top surfaces and the upper part of the vertical surfaces sat in a relatively warmer and wetter fuel. They should have similar amount of accreted ice. However, the ice accreted on the top surfaces was much less than that on the upper part of the vertical surfaces; it does not support the stratified argument. The down draught was believed to be the dominant factor.



Figure 17 Ice accreted on a vertical composite surface of SB3 (composite) in Test #1.

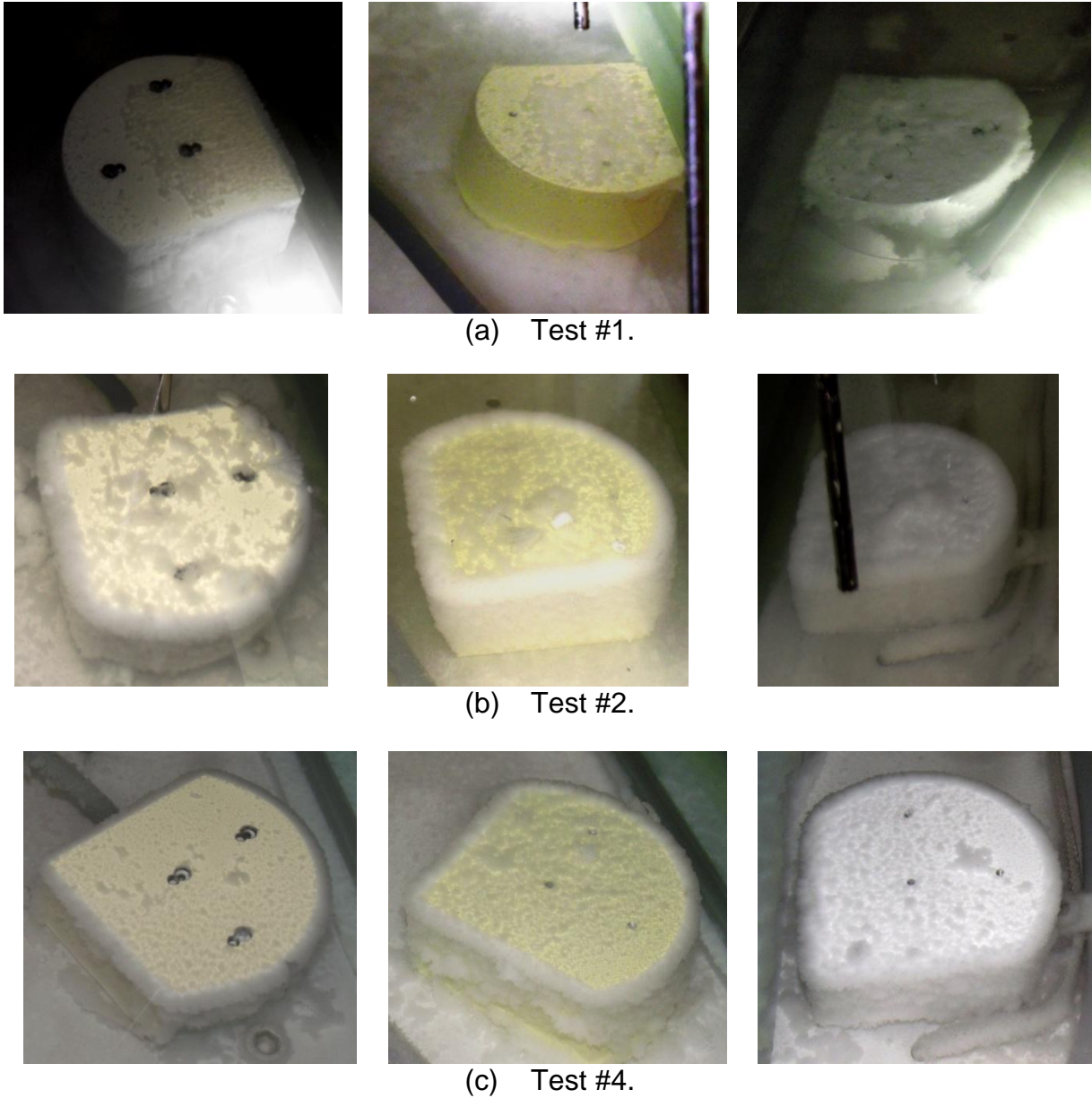


Figure 18 Ice accreted on top surfaces of the specimen blocks in (a) Test #1, (b) Test #2 and (c) Test #4. Left: SB3 (composite); Middle: SB2 (painted); Right: SB1 (bare).

Figure 18 shows ice accreted on the top surfaces of the specimen blocks in Test #1, Test #2 and Test #4. From the photographs, the following general observations can be made:

- For Test #1, Test #2 and Test #4, SB3 (composite) had the least amount of ice accreted on the top surface, while SB1 (bare) had the most ice accreted on the top surface. SB2 (painted) had an intermediate amount of accreted ice. This characteristic is postulated to be attributed to the degree of subcooling of the surfaces. Due to the effectiveness of thermal insulation of the different surface finishes, SB3 (composite) showed the least subcooling, whilst SB1 (bare) the most subcooling and SB2 (painted) an intermediate subcooling (Table 2). The degree of subcooling seems to correlate well with the amount of ice accreted.
- In Test #2, the accreted ice on the specimen blocks was noticeably greater compared to the counterparts in Test #4. In Test #2, Coryton High Aromatics Jet A-1 was used. The fuel had an aromatic content of 24.1% v/v [13]. In Test #4, SASOL fully synthetic Jet A-1 was used. The fuel had an aromatic content of 12.4 % v/v [13]. As discussed previously [9] and confirmed with testing [13], there seems to be a positive correlation between the fuel's aromatic content and its water solubility. With a higher aromatic content and thereby a higher water solubility, for the same amount of fuel, more water is available for ice accretion at low temperature conditions.
- It was observed that a significant amount of ice was formed on the edges of specimen blocks. This may be due to two reasons:
 - Sharp corners favour nucleation;
 - Mass transfer due to flow pattern around edges is more prominent.
- It is worth noting that there was not much ice on the vertical surfaces of the specimen blocks in Test #1 (Figure 18a). This was because the ice on some of the vertical surfaces was dislodged and had fallen onto the bottom of the tank when the lid of the tank was opened. Adjustment to the operating procedure was made subsequently to minimise disturbance to the accreted ice. As a result, in Test #2 (Figure 18b), the vertical ice layers on the specimen blocks remained almost intact.



(a) Test #5



(b) Test #2

Figure 19 Ice accreted on the top surfaces of SB1 in (a) Test #5 and (b) Test #2.

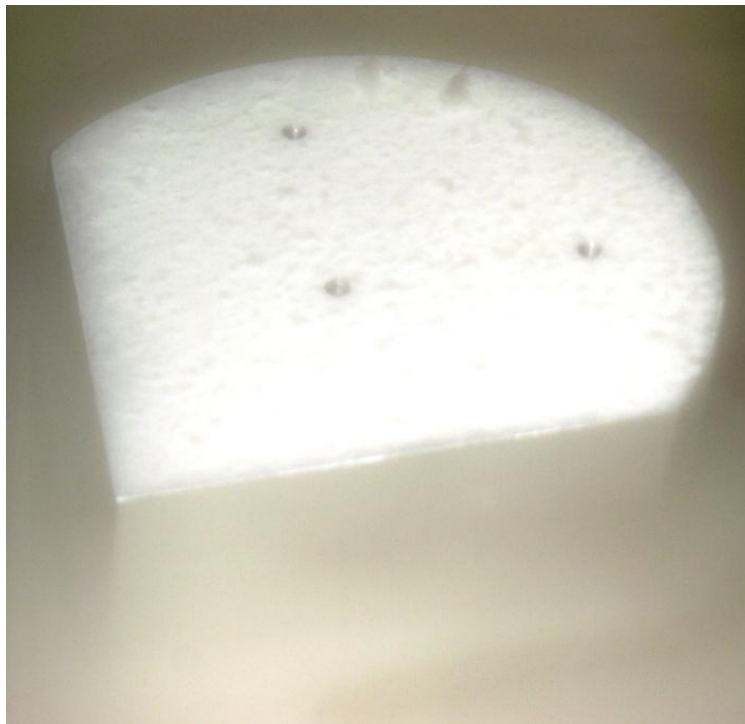


Figure 20 Fine gritty ice ducted on the top surface and no ice on the vertical surfaces of SB1 (bare) in Test #3.

The ice accreted on the top surfaces of SB1 (bare) in Test #5 and Test #2 is shown in Figure 19. One can see the similarity of the appearance of the ice between the two cases. The ice was thinner in the centre than at the edges as discussed earlier. The amount of ice on the top surface in Test #5 seems to be less than that in Test #2. Quantification and discussion of the amount of accreted ice on the specimen blocks are discussed in the next section.

Test #3 revealed a different ice accretion phenomenon. At the end of a 168-hour ice growth phase, the top surfaces of the specimen blocks were dusted with fine gritty ice and there was no ice accreted on the vertical surfaces of the specimen blocks (Figure 20). Since the surfaces of the specimen blocks were only a few degrees (a maximum of 2.7°C for bare aluminium surface) cooler than the fuel temperature, there was insufficient energy potential to overcome the energy barrier for ice deposition on the subcooled surfaces by the Bergeron process. This is evident from lack of snow deposition on the vertical subcooled surfaces.

The fuel temperature in Test #3 was around -43.5°C. At this temperature, the dissolved water concentration was ~6 ppm by mass (Part 1 Figure 1). Water would have come out from fuel as water droplets and ice particles. The mean water droplet size and ice particle size were ~2.4 µm and ~5.7 µm, respectively (Part 1 Figure 6). The ice particles would have a settling rate of much less than m/s [15]. Given a long test duration (168 hours) and a relatively small distance for settling (i.e. small tank), it was plausible that some ice particles could settle on the top surfaces of the specimen blocks.

5.1.2 Quantification of accreted ice

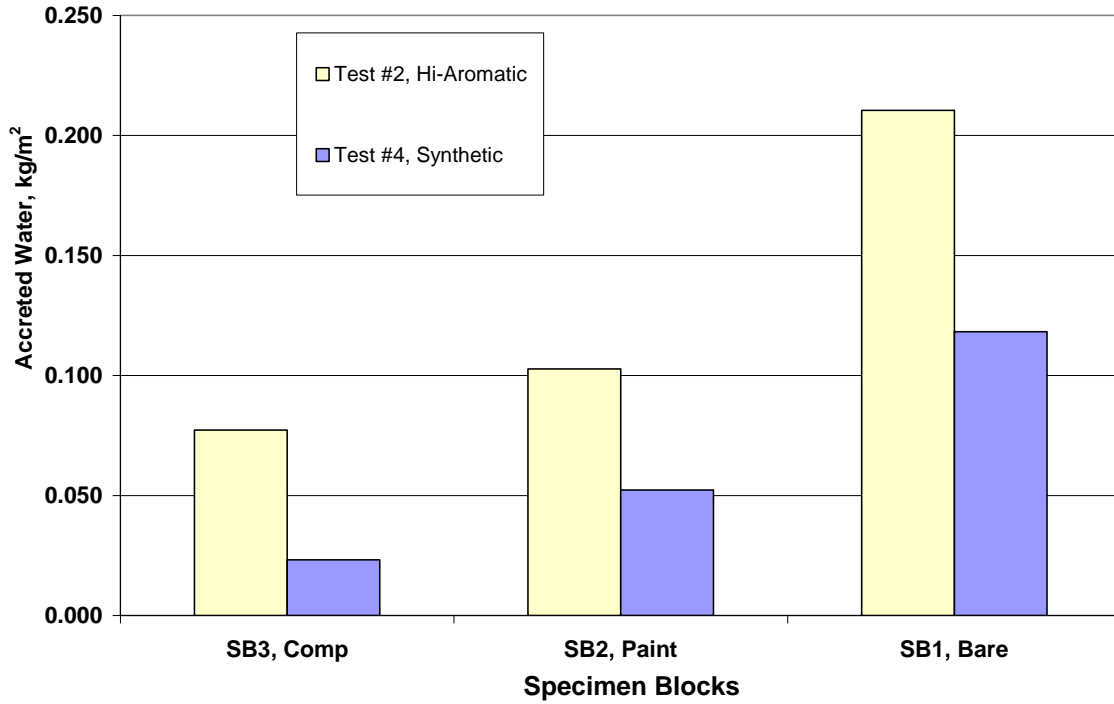
The amount of ice accreted on a subcooled surface in fuel is difficult to define. The mass of accreted ice is not an appropriate measure, as the ice entraps a large volume of fuel within its structure. The volume of the accreted ice is also not an appropriate measure because it is difficult to measure accurately. Therefore, it was proposed to use the amount of water in the melted accreted ice as a quantifiable measure for the accreted ice.

Ice was collected from the surfaces. When the ice was melted, the amount of water was determined by an appropriate method. The mass of melted water from the accreted ice on the top surfaces of the specimen blocks in Test #2 and Test #4 are plotted in Figure 21a; and in Test #2 and Test #3 are plotted in Figure 21b. The water is referred to as accreted water for the discussion in this report.

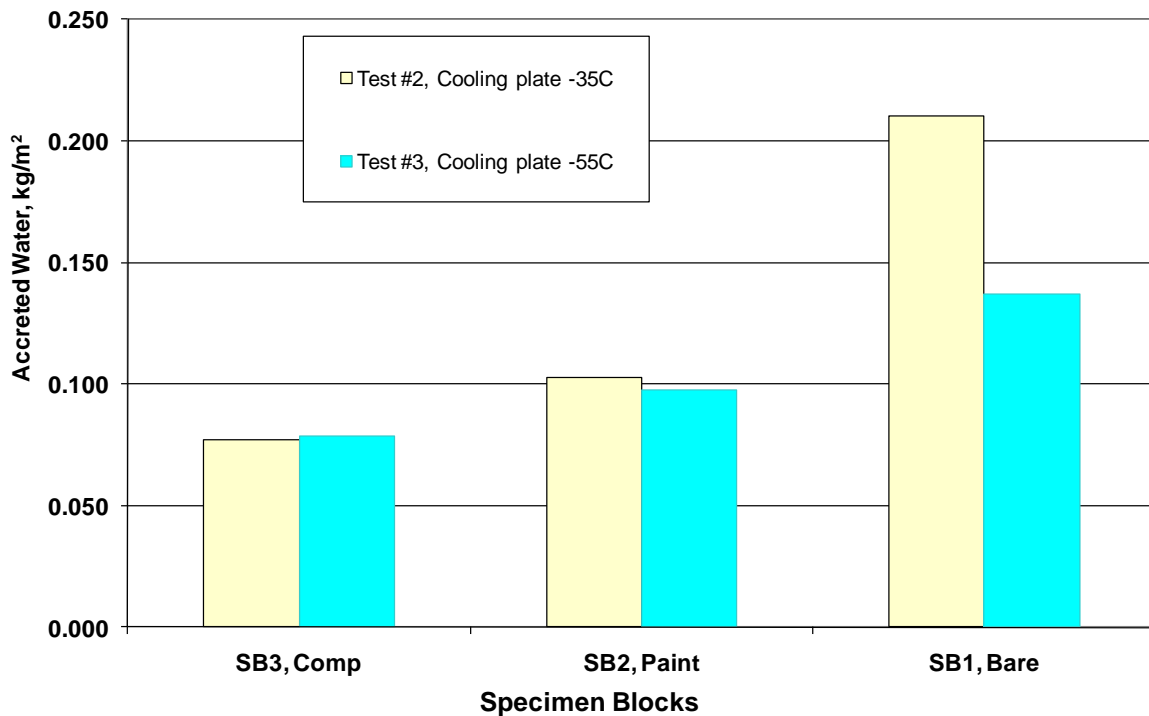
From Figure 21a, it can be seen that there are significant differences in accreted water between the specimen blocks and between the two fuels used. The effect of the fuels was as expected and it was consistent with the observations noted in Part 1. Fuel with a higher aromatic content has higher water solubility, and would therefore give more accreted ice when cooled. The effect of surface subcooling was also in line with expectation. Surfaces with a higher degree of subcooling has higher energy potential to drive the Bergeron process at a higher rate for ice deposition, and would therefore give more accreted ice.

From Figure 21b, it can be seen that the mass of accreted water in Test #3 was similar to that in Test #2 for SB2 (painted) and SB3 (composite). The mass of accreted water for SB1 (bare) in Test #3 was significantly lower than the same in Test #2. As discussed in Section 5.1.1, since there was no accreted ice on the vertical surfaces but a fine gritty ice blanket was found on the top surfaces of the specimen blocks in Test #3, it was hypothesised that the main ice accretion mechanism was settling of the ice particles in Test #3.

In theory, the settling mechanism should be independent of the surface subcooling in a static environment. However, the mass of accreted water on the top surfaces of the specimen blocks in Test #3 was far from constant and varied from specimen block to specimen block. There seems to be a positive correlation between the accreted water and the degree of subcooling of the surfaces. The observed correlation could be attributed to the local environment of the specimen blocks. The downward natural convection generated by the subcooled specimen blocks changed the fluid dynamics around them. The downward convection aided the settling of the ice particles on the specimen blocks.

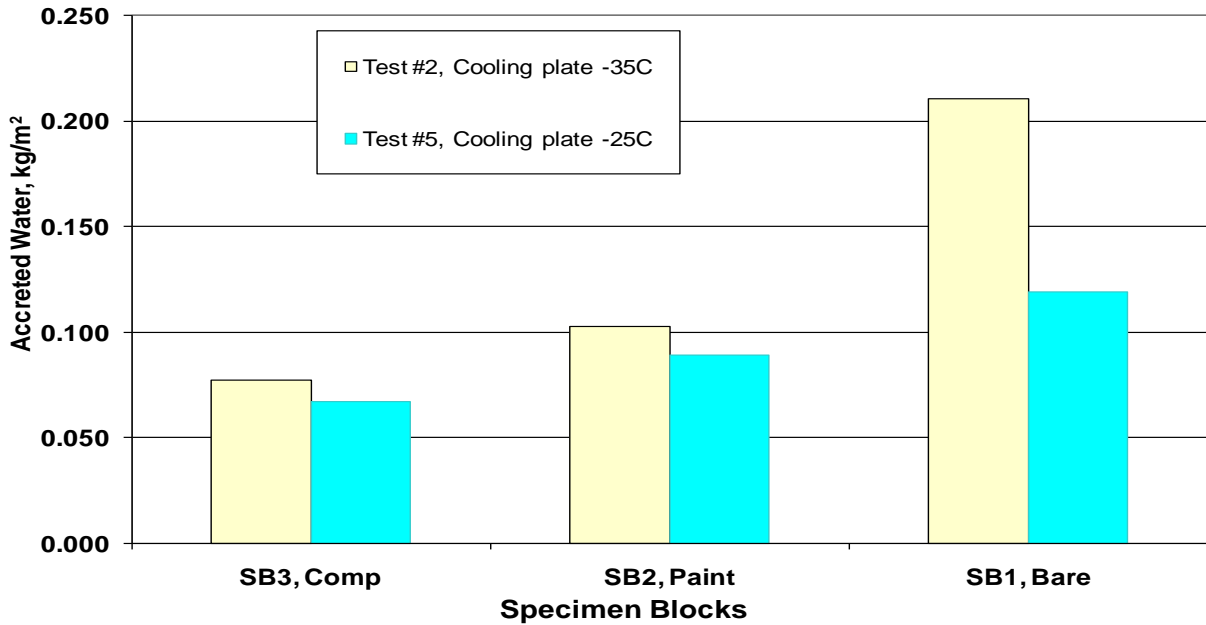


(a) Melted water from the accreted ice on the top surfaces of the specimen blocks in Test #2 and Test #4

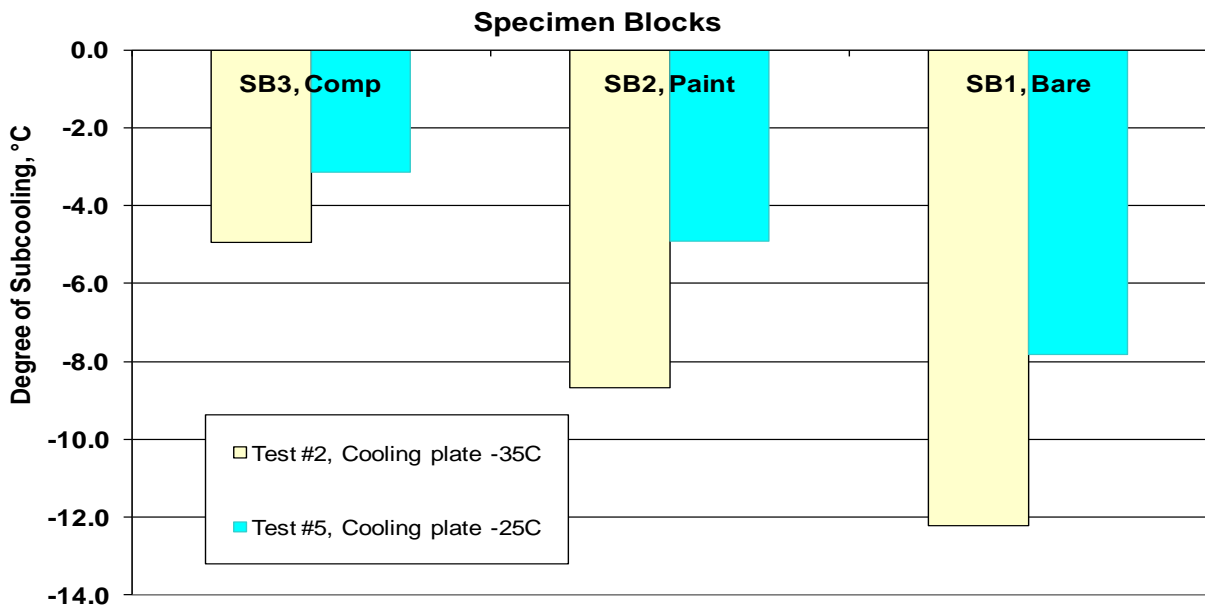


(b) Melted water from the accreted ice on the top surfaces of the specimen blocks in Test #2 and Test #3

Figure 21 Comparison of the melted water from the accreted ice on the top surfaces of the specimen blocks in different conditions.



(a) Melted water from the accreted ice on the top surfaces of the specimen blocks in Test #2 and Test #5



(b) Degree of subcooling on the top surfaces of the specimen blocks in Test #2 and Test #5

Figure 22 Comparison of the accreted water and temperature on the top surfaces of the specimen blocks in Tests #2 and Test #5.

A strong downward convection local to the block would promote more ice particles to settle on the block by bringing in more ice particles to the block from the surrounding and increasing the settling rate. Since SB1 (bare) had the highest degree of subcooling, it would have a relatively stronger downward convection local to the block and therefore would expect to have more ice particles settled on the block. Similarly, since SB3 (composite) had the lowest degree of subcooling, it would have a relatively weaker downward convection local to the block and therefore would expect to have less ice particles settled on the block. This postulation seems to support the observed correlation.

In Figure 22a, it shows a comparison of accreted water between Test #2 and Test #5. As with previously observation in Figure 21, SB3 (composite) had the least accreted water and SB1 (bare) had the most accreted water. Furthermore, Test #2 had more accreted water than Test #5 for the same specimen block. Figure 22b shows the degree of subcooling of the specimen block surfaces. The observation clearly shows that there is a positive correlation of the amount of accreted water and the degree of subcooling of the surfaces.

Table 3 summaries the amount of accreted water, degree of subcooling and water dropout for Test #2 and Test #5. Water dropout is defined as the amount of free water precipitated out from a fully saturated fuel for a given decrease in temperature. In Figure 23, by plotting the amount of the accreted water against the water dropout, a positive linear correlation can be seen. As discussed earlier, since the test duration is long (i.e., ~168 hours), ice particle settling may be a significant contributor to the total accreted water. However, in aircraft fuel tank, due to a much shorter duration and the dynamic in the tank, ice particle settling is negligible.

Table 3 Summary of the subcooling, water dropout and accreted water in Test #2 and Test #5.

<i>Fuel</i>	<i>Test #5</i>			<i>Test #2</i>		
	<i>SB1 (bare)</i>	<i>SB2 (painted)</i>	<i>SB3 (composite)</i>	<i>SB1 (bare)</i>	<i>SB2 (painted)</i>	<i>SB3 (composite)</i>
<i>Subcooling, °C</i>	-7.8	-4.9	-3.1	-12.2	-8.7	-4.9
<i>Fuel Temperature at 3 cm above the cooling plate, °C</i>	-3.4			-5.1		
<i>Water Dropout, ppm by mass</i>	7.1	5	3.1	9.4	7.1	4.4
<i>Accreted Water on the Top Surface of the specimen Block, kg/m²</i>	0.119	0.089	0.067	0.210	0.103	0.077

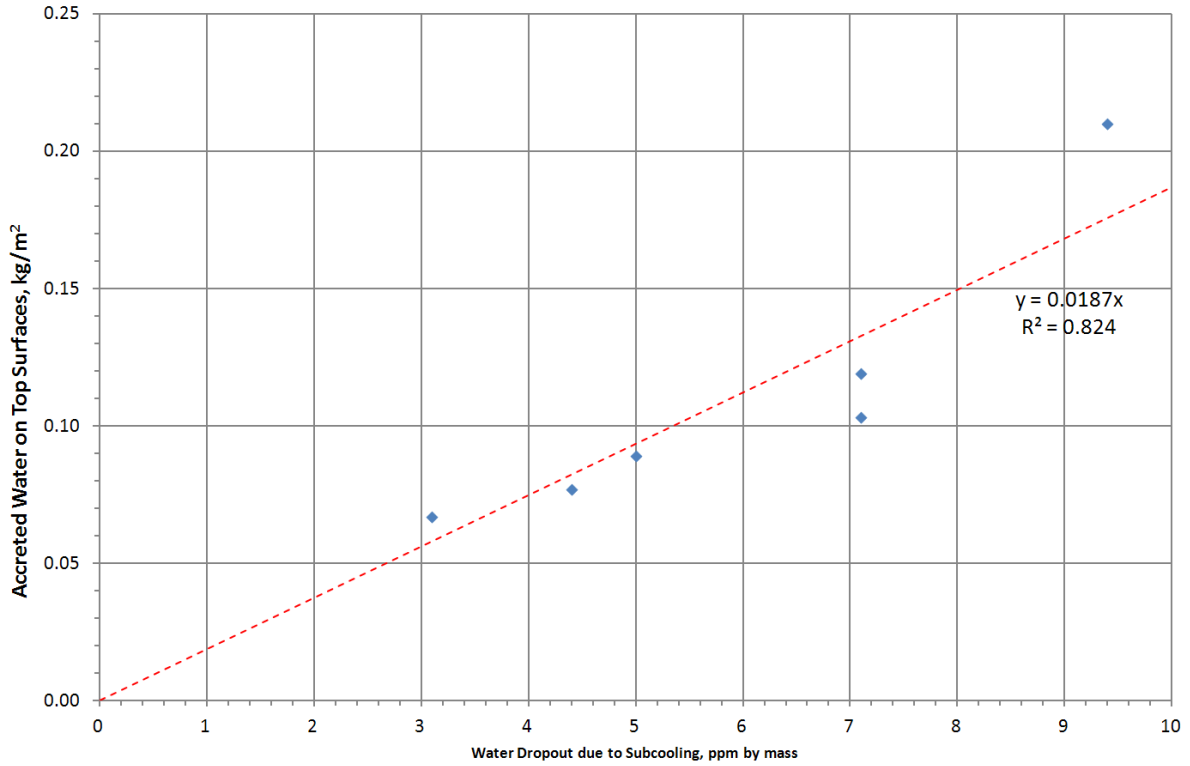


Figure 23 Accreted water vs water dropout due to subcooling on the top surfaces with data from Tests #2 and Test #5. A best fit line is plotted for reference.

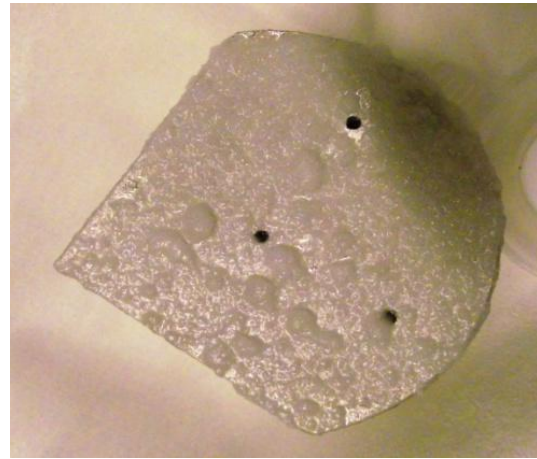
5.2 Properties Of Accreted Ice

5.2.1 General observations

Ice accreted on subcooled surfaces in fuel had a fluffy appearance (Figure 24a). When the ice was taken out from the fuel (Figure 24b), the fluffy ice collapsed giving an appearance of a heavy wet ice.



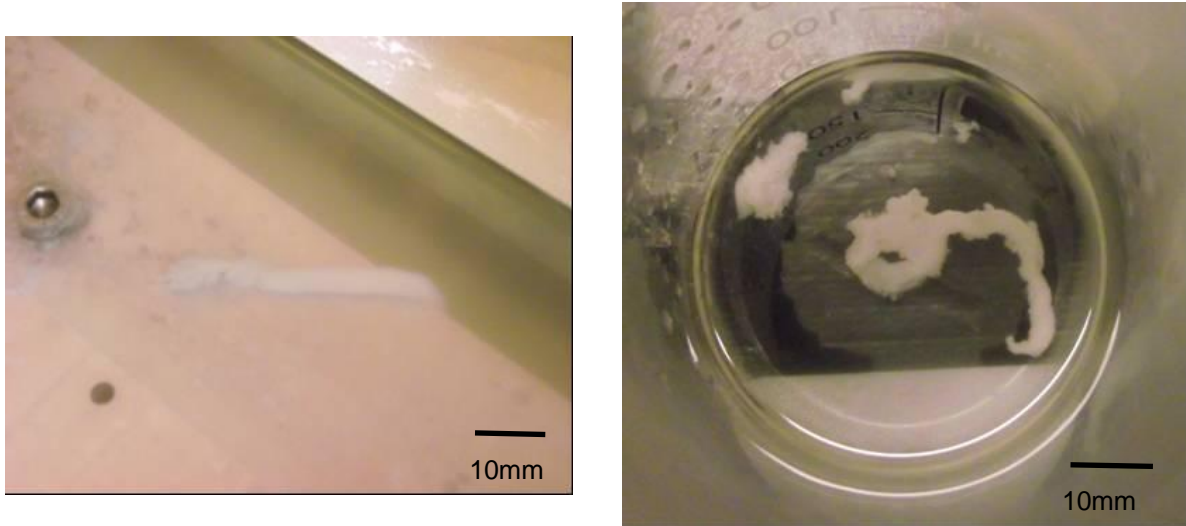
(a) Accreted ice in fuel showing a fluffy appearance.



(b) Accreted ice out of fuel showing a heavy wet appearance.

Figure 24 Accreted ice on SB1 (bare). (a) In fuel; and (b) out of fuel.

The adhesion strength of the accreted ice was very weak. A gentle disturbance to the fuel around the accreted ice on the vertical surfaces caused the ice to dislodge and slid down the vertical surfaces to the bottom. In some cases, the sliding action could change to a tank-treading action [14] where the ice clusters tumbled and/or rolled down the vertical surfaces. This could give rise to an ice “rope” as shown in Figure 25a. Due to the tumbling and/or rolling, the ice compacted a little. The initial fluffy appearance changed to a dense appearance. Furthermore, the compaction seemed to enhance the ice structural rigidity. The ice “rope” was strong enough that it could be scooped up with fuel from the bottom of the simulated fuel tank using a beaker (Figure 25b). It remained intact when slightly touched with a finger.



(a) Ice “rope” slid off from a specimen block and resting on the cooling plate.

(b) Collected ice “rope” in a beaker.

Figure 25 Ice “rope” from the SB2 (painted). (a) On the cooling plate; and (b) Collected sample in a beaker.

5.2.2 Quantification of porosity

The porosity of the ice, defined as SLR, was estimated from the procedures discussed in Section 3.2. Accreted ice was collected in a container. The ice was allowed to melt in the container in a warm environment. Melt water separated out from the fuel/water mixture at the bottom of the container over time. The container was then exposed to a cold environment to allow the melt water collected at the bottom of the container to freeze. When the water was frozen to solid, the fuel was drained out and the weight of the frozen water was measured by an electronic balance.

The volume of the accreted ice was calculated from the ice coverage area and the ice layer thickness. The ice layer thickness was estimated with the aid of the ice depth gauge (see Figure 4b). The ice coverage area was estimated from the known geometry dimensions.

Table 4 shows the estimated SLR of the accreted ice on the vertical surfaces of the specially designed aluminium block (see Figure 4c) for Test #2, Test #4 and Test #5. The estimated SLR of the accreted ice on the flat vertical surfaces of SB1 (bare) for Test #4 is also given for reference. The calculation steps are tabulated in Table 4 for clarity and if applicable, clarification would be given.

Table 4 SLR estimation and computation

<i>Parameter</i>	<i>Test #2</i>	<i>Test #4</i>		<i>Test #5</i>
	<i>Ice collected from all vertical surfaces of the specially designed aluminium block</i>	<i>Ice collected from all vertical surfaces of the specially designed aluminium block</i>	<i>Ice collected from the two flat vertical surfaces of SB1 (bare)</i>	<i>Ice collected from a vertical surface of the specially designed aluminium block</i>
<i>Mass of water in the collected ice [] (Measured with an electronic balance)</i>	0.530 g	0.341 g	0.298 g	0.131 g
<i>Total horizontal length of the ice collection area [L] (Obtained from the geometry dimensions of the block)</i>	152 [= (35+42)x2] mm	152 [= (35+42)x2] mm	82 [= 41x2] mm	42 mm
<i>Vertical height of the ice collection area [H] (Estimated from observation)</i>	30 mm	27 mm	29 mm	28 mm
<i>Total ice coverage area [A_{tot} = LxH]</i>	4620 mm ²	4104 mm ²	2378 mm ²	1176 mm ²
<i>Ice layer thickness at the top of the vertical surfaces [] (Estimated from observation)</i>	6.0 mm	4.0 mm	5.0 mm	5.0 mm
<i>Ice layer thickness at the bottom of the vertical surfaces [] (Estimated from observation)</i>	0.0 mm	0.0 mm	0.0 mm	0.0 mm
<i>Mean ice layer thickness for calculation of the ice volume []</i>	3.0 mm	2.0 mm	2.5 mm	2.5 mm
<i>Collected ice volume []</i>	13860 mm ³	8208 mm ³	5945 mm ³	2940 mm ³
<i>Snow density [], Eqn. 1</i>	38.2 kg/m ³	41.5 kg/m ³	50.1 kg/m ³	44.6 kg/m ³
<i>SLR [], Eqn. 2</i>	26	24	20	22
<i>Average SLR</i>	23			

5.2.3 Quantification of adhesion strength

The adhesion strength of the accreted ice was evaluated by a jet method described in Section 3.3. Figure 26 shows a fuel jet targeting a corner of a specimen block covered with accreted ice at various jet velocities. The jet nozzle was at a distance 10 mm vertically from the block corner. The centreline jet velocity at the target, v_c , was calculated from the nozzle velocity, v_n , using Eqn. 3. The jet nozzle velocity, v_n , and the centreline jet velocity, v_c , together with their associated dynamic pressure are shown under each sub-figures in Figure 26. The dynamic pressure, P_d , of the jet was calculated by:

$$P_d = \frac{1}{2} \rho_f v_c^2 \quad (4)$$

where ρ_f is the fuel density and v_c is the centreline jet velocity.

With a very moderate centreline velocity of 5 mm/s, the fluffy ice on the top surface was dislodged with ease (Figure 26a). With the centreline velocity increased to 13 mm/s, the cleared area on the top surface was significantly enlarged (Figure 26b). When the centreline velocity was increased to 45 mm/s, the fluffy ice on the edge was dislodged (Figure 26c). With the centreline jet velocity increased to 138 mm/s, the cleared area on the vertical sides of the block corner had a diameter of about 10-15 mm (Figure 26d).

From the results, order of magnitude of the adhesion strength could be estimated from the dynamic pressure of the centreline jet velocity. Two critical velocities are noted from Figure 26. They are:

- The accreted ice on the top surface of the block (Figure 26b) was cleared by a centreline jet velocity of 13 mm/s or a dynamic pressure of 0.07 Pa. The adhesion strength of the accreted ice was estimated to be of the order of 0.1 Pa.
- The accreted ice on the edge of the block (Figure 26c) was cleared by a centreline jet velocity of 45 mm/s or a dynamic pressure of 0.82 Pa. The adhesion strength of the accreted ice was estimated to be of the order of 1 Pa.



(a) $u_m = 24 \text{ mm/s}$; $u = 5 \text{ mm/s}$; $P_{dyn} = 0.01 \text{ Pa}$



(b) $u_m = 40 \text{ mm/s}$; $u = 13 \text{ mm/s}$; $P_{dyn} = 0.07 \text{ Pa}$



(c) $u_m = 80 \text{ mm/s}$; $u = 45 \text{ mm/s}$; $P_{dyn} = 0.82 \text{ Pa}$



(d) $u_m = 160 \text{ mm/s}$; $u = 138 \text{ mm/s}$; $P_{dyn} = 7.72 \text{ Pa}$

Figure 26 Accreted ice on SB3 (composite) was dislodged by a fuel jet at various velocities. Fuel density, ρ_i , was assumed to be 825 kg/m^3 at a temperature -5°C for the calculation of the dynamic pressure, P_{dyn} .

Figure 27 shows progression of ice accretion on a vertical bare aluminium surface during the ice growth phase in Test #5. While generally less ice accreted towards the bottom, it can be seen that the accreted ice appeared to have slipped downwards under its own weight in Figure 27c and Figure 27d.

Considering the balance between the buoyancy force and the gravitational force on the ice layer and the adhesion force between the ice layer and the vertical surface, the force balance equation is:

where ρ_{ice} and ρ_{fuel} are the density of ice and fuel, respectively; ϕ is the volume fraction of ice in fuel (); g is the acceleration of gravity; t is the ice layer thickness; A is the ice accretion area and τ is the adhesion strength. Rearrange for τ , the equation becomes:

With typical values for the parameters, i.e. $\rho_{ice} = 920 \text{ kg/m}^3$, $\rho_{fuel} = 810 \text{ kg/m}^3$, 4.3% (SLR = 23 from Table 4), and $t = 5 \text{ mm}$, the adhesion strength between ice and the vertical surface is estimated to be 0.23 Pa. This is in the same order of magnitude of the estimated adhesion strength reported earlier. It provides further support to the initial findings using an alternative approach.

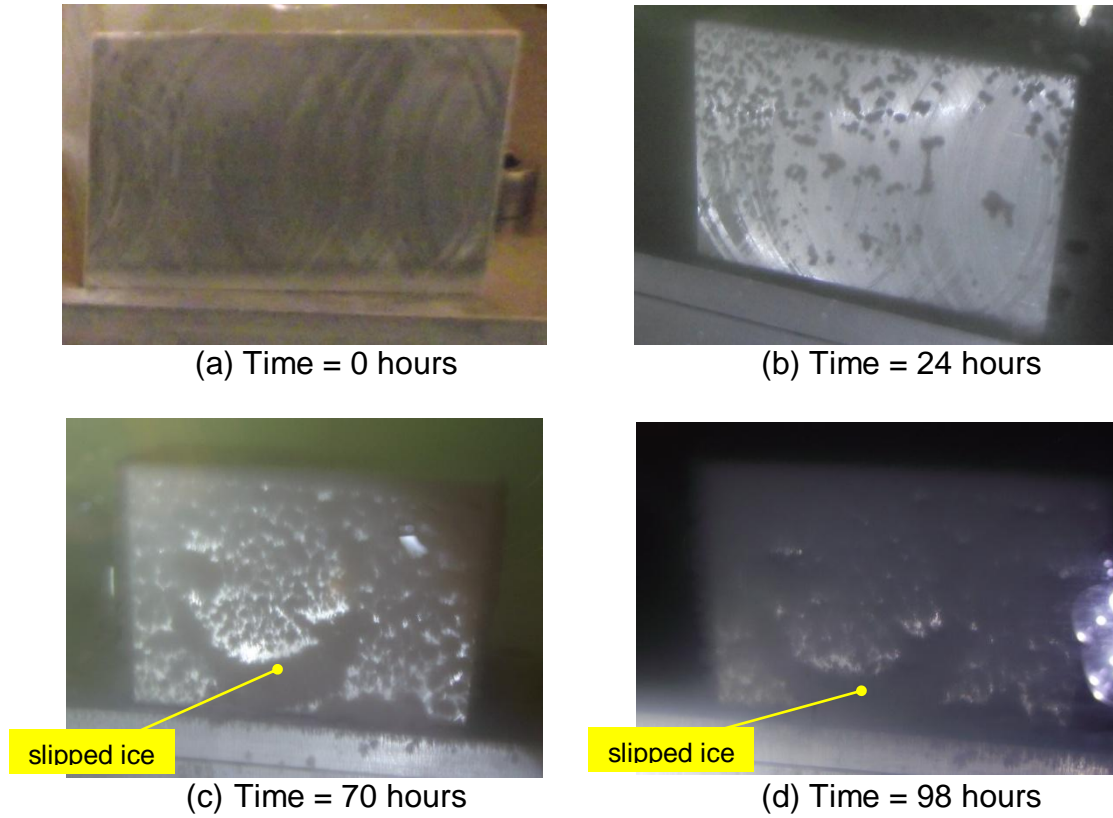


Figure 27 Progression of ice accretion on a vertical bare aluminium surface during the ice growth phase in Test #5.

6. CONCLUSIONS

Ice accretion on subcooled surfaces in fuel had been simulated using a 20-litre aluminium tank with chilled plates and glass windows. The simulated fuel tank was fitted with an array of thermocouples to measure temperatures at points of interest. To sustain the water content of the fuel while growing ice on the subcooled surfaces in the simulated fuel tank, a water replenishment system was developed. The water replenishment system continuously circulated fuel from the simulated fuel tank through a saturator and a recuperator which added just dissolved water to the fuel.

The accreted ice grown on different surfaces (bare aluminium, painted aluminium and composite) and different fuels (Jet A-1 Mercox treated, Coryton high aromatics Jet A-1 and SASOL fully synthetic Jet A-1) was examined.

The main findings from this study are:

- For a higher degree of subcooling with the same fuel at the same bulk fuel temperature, more accreted ice will result. Since the solubility of water in fuel is non-linear and varies from fuel to fuel, subcooling temperature does not readily give a one-to-one relationship to the amount of accreted ice. A more appropriate parameter to correlate with the accreted ice is the amount of water dropped out due to subcooling. A linear correlation is observed between the amount of water dropout due to subcooling and the mass of accreted ice.
- Of the three specimen blocks used in the tests, the highest ice accretion rate was found with the bare aluminium specimen block (SB1, bare), while the lowest rate with the composite specimen block (SB3, composite). Composite material has good thermal insulation properties. When compared with painted and bare aluminium surfaces, the composite strips bonded on the aluminium blocks showed the least subcooling, and hence, they gave the smallest quantity of accreted ice.
- Fuel with a higher aromatic content generally is able to dissolve a larger amount of water, i.e. higher water solubility. High aromatic fuels are likely to absorb more water at an increased temperature, and hence, shed more water as the temperature is decreased. This leads to increased ice accretion.
- The main mechanism of ice accretion is through the Bergeron process. Although ice particle settlement was observed in the tests, however it was not representative of aircraft application. Ice particle settlement is not applicable in aircraft fuel tanks because a typical long haul flight duration is not long enough for the ice particles to settle out and the fuel in the tanks is far from static.
- The accreted ice was found to be very fluffy, soft and had very little mechanical strength. Its average snow to liquid ratio (SLR) was estimated at 23. In atmospheric physics, this is classified as light snow in a three-snow category classification system [10]. Its adhesive strength was estimated to be of the order of 1 Pa using the jet method. The observed slippage of accreted



ice on a vertical surface under its own weight in Test #5 further confirmed the weak adhesion strength reported.

- When the fuel temperature was less than -40°C , ice accreted on the top surfaces of the specimen blocks was found to be fine and gritty. The ice was believed to be from ice particle settlement. Due to the low degree of subcooling, there was no fluffy ice formed from the main ice accretion mechanism (Bergeron process).
- There was evidence to suggest that the dislodged ice, if subjected to tumble and/or roll, could become more compact and also mechanically stronger. This postulates that ice clusters in a fuel flow, where the ice clusters may be subjected to tumble and/or roll, could be more compact and mechanically stronger.

7. RECOMMENDATIONS

The work reported was concerned with ice accretion on subcooled surfaces in fuel due to the dissolved water in fuel. The accreted ice was found to be very fluffy and very weak mechanically. It has very little adhesion strength and therefore can be dislodged easily from any surfaces.

Areas of interest for further investigation are:

- There was evidence to suggest that the dislodged ice, if subjected to tumble and/or roll, could become more compact and also stronger mechanically. The effect of flow velocity on accretion process and ice properties should be investigated.
- The fate of dislodged ice should also be investigated to find out how the ice is carried by the fuel in the fuel system and where it accumulates.
- The interaction between moisture (water) content in the ullage and cool fuel needs to be investigated as there is no or very little literature published on the subject.
- Ice accretion due to free water in the fuel tank should also be investigated.

8. ADDITIONAL OBSERVATIONS

During the tests, a number of different forms of ice in the fuel were observed. Visual observation showed that the physical properties of the ice seemed to be quite different from that of the ice accreted on the specimen blocks (which has been described in previous sections). These ice forms, described below, are not within the scope of current project. However, for information, we would like to report these related observations as additional notes.

Figure 28 showed different forms of ice built up around a cold stainless tubing (o.d. 2.5 mm) in the fuel (left) and in air space above the fuel inside the simulated fuel tank (right). The tubing was used to withdraw cold fuel beneath the cooling plate to the water replenishment system (see Figure 8). The tube came up through the fuel volume, the ullage space above the fuel before exiting the top cover of the simulated fuel tank. As it was from just beneath the cooling plate, the fuel had a lower temperature than the fuel surrounding the tubing. The surface temperature of the tube was thus lower than the surrounding fuel and air.

Ice was formed on all sides of the cold tubing in both fuel and air. In fuel the cloudy appearance of the liquid made the form of the ice growth difficult to determine but the generally diffuse/lumpy appearance of the ice suggested a branching or loose agglomeration phase (perhaps similar to the fluffy ice found on the specimen blocks). In air, solid and gritty ice formed around the tube. Where the pipe emerged from the surface of the fuel, the ice was less thick, perhaps a result of a drier or less mobile air layer immediately above the fuel/air interface. Towards the top of the picture, the ice surface became rough, breaking up into a series of tooth like features.

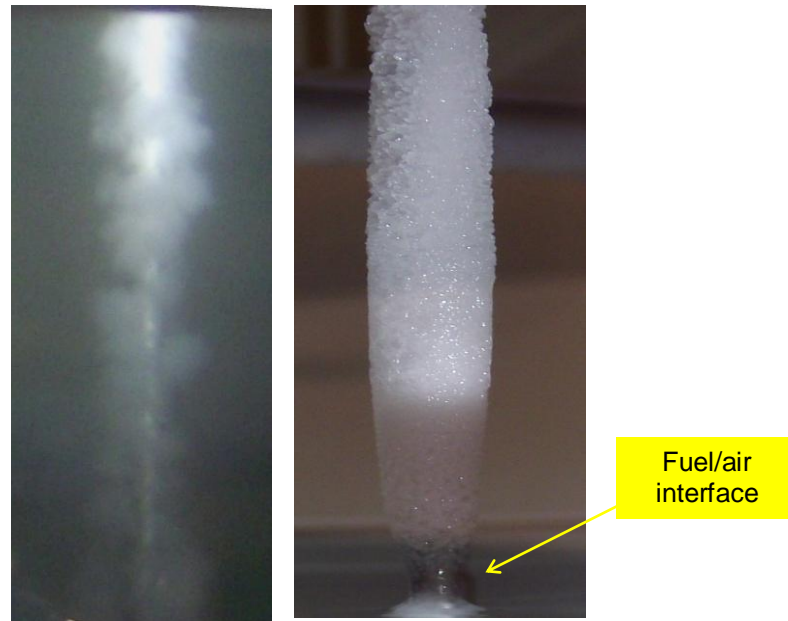


Figure 28 Ice formed around a cold stainless tubing in the simulated fuel tank during the ice growth phase in Test #4. The cold fuel beneath the cooling plate was withdrawn via this tubing to the water replenishment system for saturation. Left: in fuel; Right: in the air space just above the fuel body.

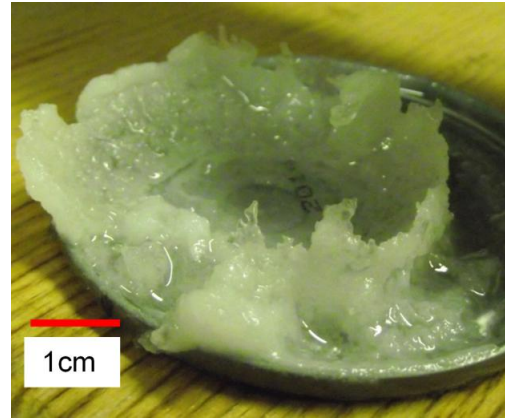
A crater of compacted ice was seen to form at the water replenished fuel return. It formed directly beneath the incoming fuel jet where the jet (still slightly warm) was deflected by the cooling plate and the cone of water rich fuel formed by the impact of the jet mixed with the surrounding cool fuel, as shown in Figure 29. This ice was translucent and looked very much like the ice which forms when water droplets coalesce or impinge in conditions close to freezing point, like a hail particle or glaze ice on an aircraft wing.

In some aircraft fuel systems, fuel is used to cool the lubrication, hydraulic and integrated drive generator (IDG) oil systems in aircraft turbine engines [16]. The fuel and the oil systems are connected via a fuel cooled oil cooler (FCOC). In some operation conditions, fuel in excess to the engine demand is pumped to the FCOC to cool the oil. The excess fuel is returned to the fuel system. The return fuel is warm and may pick up some water in the FCOC from ice that accumulated in the FCOC. If the return fuel impinges on a subcooled surface in the fuel system, potentially, it may give rise to ice similar to that observed in Figure 29.

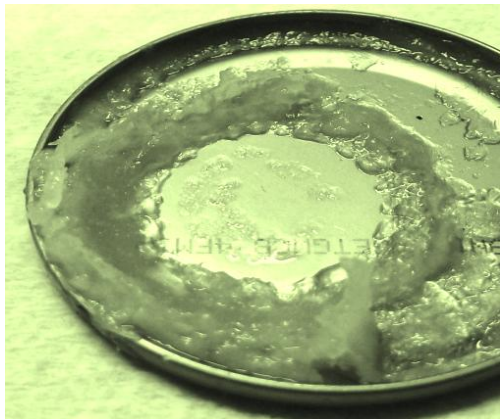
Figure 30 shows ice nodules accreted on a specimen block in a test. The ice of the ice nodules had similar appearance to the ice from the crater. It is postulated that some ice from the crater may be sheared off as ice nodules. The convection carries the ice nodules and deposits them on the specimen block surface. The ice nodules seemed to be able to stick well even on a vertical surface.



(a) Test #1



(b) Test #2



(c) Test #5

Figure 29 Craters of compacted ice were found at the water replenished fuel return. They formed directly beneath the incoming fuel jet. (a) Crater from Test #1; (b) Crater from Test #2 and (c) Crater from Test #5.

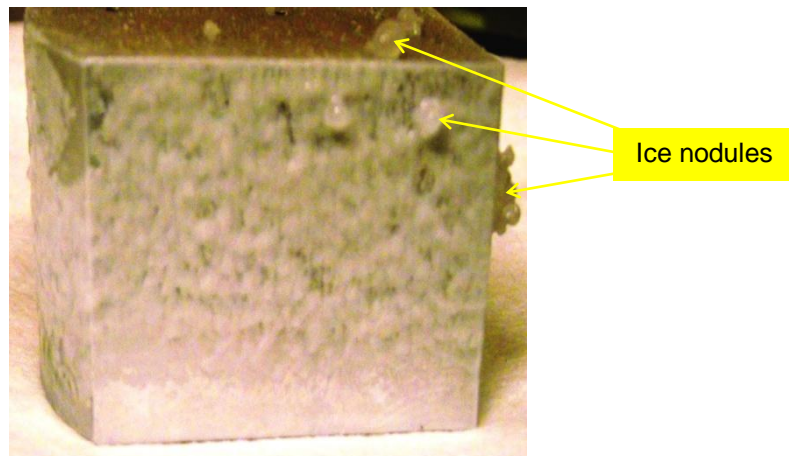


Figure 30 Ice nodules found accreted on a specimen block in a test. The ice had similar appearance to that from the crater.

REFERENCES

1. AAIB (2010). *Report on Accident to Boeing 777-236ER, G-YMMM at London Heathrow Airport on 17 January 2008*. Aircraft Accident Report 1/2010, EW/C2008/01/10.
2. Lam JK-W (2010). *Water in Aviation Fuel Under Cold Temperature Conditions – Technical Proposal*. Airbus Operations Ltd., Report No. SCF/SYS/GEN/98/2392, for European Aviation Safety Agency, Tender Reference EASA.2010.OP.07, 29 July 2010.
3. Krynitsky JA, Crellin JW & Carhart HW (1950). *The Behavior of Water in Jet Fuels and Clogging of Micronic Filters at Low Temperatures*. Report 3604, Naval Research Laboratory, Washington DC, USA.
4. Crampton AB, Finn RF & Kolfenbach JJ (1953). *What Happens to the Dissolved Water in Aviation Fuels?* SAE Summer Meeting, Atlantic City, New Jersey, USA, June 7-12, 1953.
5. Ragozin NA (1961). *Jet Propulsion Fuels*. Pergamon Press.
6. Lao L, Ramshaw C & Yeung H (2010). *Experimental Investigations Using a Simulated Fuel Tank*. Cranfield University, Process Systems Engineering Group, Report No. 10/LL/560 for EADS Innovation Works, 12 January 2011. [Commercial in confidence]
7. Hetherington JI and Carpenter MD (2010). *Water and Ice Morphology Study*. Cranfield University, Shrivenham, Report No. DEAS/JIH/MDC/1580/11 for EADS Innovation Works, 14 January 2011. [Commercial in confidence]
8. Lao L, Ramshaw C, Yeung H, Carpenter M, Hetherington J, Lam JK-W and Barley S (2011). *Behaviour of Water in Jet Fuel Using a Simulated Fuel Tank*. SAE 2011 AeroTech Congress & Exhibition, Paper No. 11ATC-0156/2011-0102794, Toulouse, France, 18-21 October 2011.
9. Hetherington JI, Carpenter MD, Lao L, Hammond D, Ramshaw C, Yeung H and Lam JK-W (2011). *WAFCOLT – Water in Aviation Fuel Under Cold Temperature Conditions: A Literature Review*. Airbus Operations Ltd., Report No. RP1115500, Issue 1, for European Aviation Safety Agency, edited by Lam JK-W, 17 May 2011.
10. Ware EC, Schultz DM, Brooks HE, Roebber PJ and Bruening SL (2006). *Improving Snowfall Forecasting by Accounting for the Climatological Variability of Snow Density*. Weather and Forecasting, vol. 21, p. 94-103, February 2006.
11. Carpenter MD, Williams C, Lao L, Hammond D, Ramshaw C and Yeung H and Lam JK-W (2011). *WAFCOLT – Water in Aviation Fuel Under Cold Temperature Conditions: Proposed Work Programme*. Airbus Operations Ltd., Report No. PL1101812, Issue 1, for European Aviation Safety Agency, edited by Lam JK-W, 15 July 2011.

12. Da C Andrade EN and Tsien LC (1937). *The Velocity Distribution in a Liquid into Liquid Jet*. Proceedings of Physical Society, vol. 49, no. 4, July 1937.
13. Carpenter MD, Williams C, Lao L, Hammond D, Ramshaw C and Yeung H and Lam JK-W (2011). *WAFCOLT – Water in Aviation Fuel Under Cold Temperature Conditions: Second Intermediate Report – Laboratory Testing*. Airbus Operations Ltd., Report No. RP1136539, Issue 1, for European Aviation Safety Agency, edited by Lam JK-W, 14 October 2011.
14. Chan KY, Gajjar J and Lam JK-W (2011). *Water Drop Runoff in Fuel Tank Vent Pipes with Air Flow Shear*. Industrial Mathematics Shorter Knowledge Transfer Partnership (KTP) Case Study, Knowledge Transfer Networks, 2011.
15. CRC. *Handbook of Aviation Fuel Properties*, 3rd Edition. CRC Report No. 635, 2004.
16. Sterifinger H (1998). *Fuel/Oil System Thermal Management in Aircraft Turbine Engines*. RTO AVT Symposium on Design Principles and Methods for Aircraft Gas Turbine Engines, held in Toulouse, France, 11-15 May 1998, and published in RTO MP-8.

Part 3: Analysis of Test Results & Recommendations – Airbus

By

Dr. Joseph K.-W. Lam

Airbus Operations Limited

Filton

Bristol

BS99 7AR

UK

EXECUTIVE SUMMARY

Part 3 includes results and analysis of some of the icing tests conducted at Airbus outside this project and expand on some of the topics discussed in Part 1 and Part 2.

The snow-to-liquid ratio (SLR) was briefly introduced in Part 2 of this report as a parameter for the porosity of the accreted ice on the subcooled surfaces in the simulated fuel tank. The variability of SLR of the snow found in the test rig, in icing tests conducted at Airbus outside this project, is not too dissimilar to that of snowfall events in the atmosphere. The mean SLR for snow in an aircraft fuel system is 19.7. This is classified as “*Very Light*” snow in a six-snow category classification system. In contrast, the mean SLR of snow in the atmosphere is 15.6 and is classified as “*Light*” in the same classification system. Similarly, the SLR of snow in the simulated fuel tank (Part 2) was 23.0 and is classified as “*Ultra Light*” in the same classification system.

The apparent lightness of the snow found in fuel is discussed. The lightness is hypothesised to:

- **Fluid medium**
Since fuel has similar density to water and ice, the snow crystals grow in an almost weightless environment.
- **Crystal habit**
Fuel gives a favourable environment for prism (i.e. needle) ice growth due to its high thermal conductivity but low molecular diffusion. The aggregated needles form a very open structure.

A number of ice prevention concepts are outlined in Section 3. The concepts may be divided into two classes.

- **Class 1**
Dealing with the ice directly, i.e. treating the symptoms. Proposed concepts such as FSII, fuel heating, onboard water separation and fuel line anti-icing are described.
- **Class 2**
Elimination of sources of water, i.e. treating the causes. Proposed concepts such as dehumidifying ingress air, displacing ingress air and fuel dehydration are described.

More focused research activities to investigate other parameters that may have an influence on water/ice in fuel should be carried out. These research activities may be pursued through a combination of funded PhD studies and post-doc research studies.

1. INTRODUCTION

Descriptions of the laboratory tests and analysis of the test results have been presented in Part 1 and Part 2 of this report from Shrivenham and Cranfield, respectively. In Part 3, it is aimed, where possible, to include results and analysis of some of the icing tests conducted at Airbus outside this project. Correlation between the results from the Airbus icing tests and from the Shrivenham and Cranfield laboratory tests is discussed. Some of the topics discussed in Part 1 and Part 2 are expanded in Part 3.

2. SNOW-TO-LIQUID RATIO

The snow-to-liquid ratio (SLR), or sometime simply referred as the snow ratio, is a well defined parameter commonly used in atmospheric physics [7]. The ratio was briefly introduced in Part 2 of this report as a parameter for the porosity of the accreted ice on the subcooled surfaces in the simulated fuel tank.

To recap, the definitions of the snow density and SLR are given below:

$$\rho_s = \frac{m_s}{V_s} \tag{1}$$

$$SLR = \frac{m_s}{m_w} = \frac{\rho_s V_s}{\rho_w V_w} \tag{2}$$

where V_s is the occupied volume of the snow; m_s and m_w are the mass and volume of water when the ice is melted; and ρ_w is the reference density of water, 1000 kg/m³.

2.1 SLR Variability

Measurements of freshly fallen snow indicate that the SLR may vary from 3 to 100 [8]. Figure 1 shows the distribution of observed SLR from 1650 12-hour snowfall events. The mean and median SLR are 15.6 and 14.1, respectively. For the purpose of diagnosis, SLR are categorized according to three specified classes, heavy, average and light, that reflect the distinct density characteristics in [8].

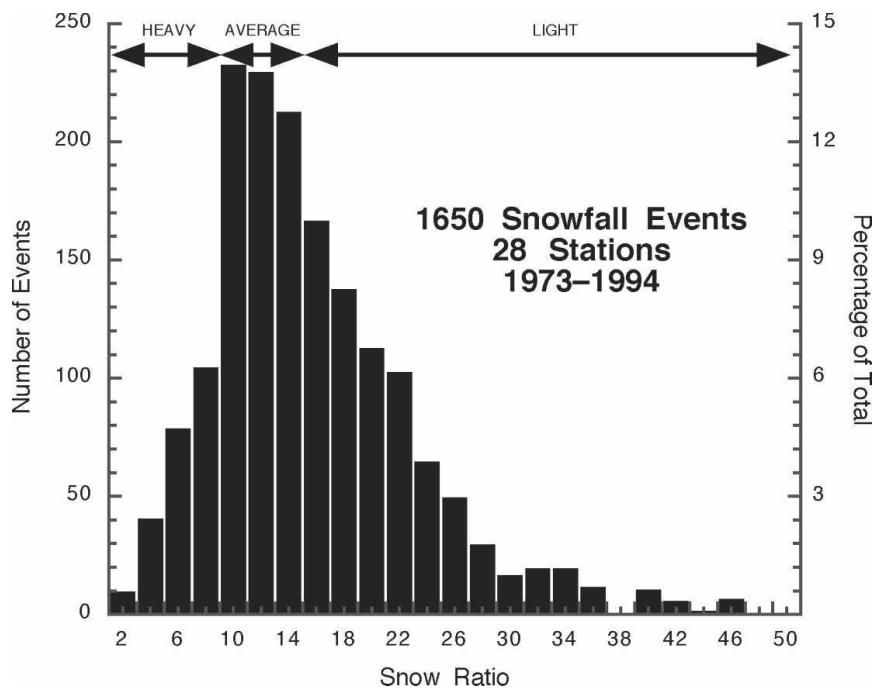


Figure 1 Distribution of observed SLR from 1650 12-h snowfall events [8].

In a test campaign conducted between October 2009 and January 2011, at the Airbus Fuel Test Facility, Filton, UK, water composition of ice slush collected in the test rig was analysed [6]. Fuel was drained from the test rig to allow access inside the test rig for the collection of the ice slush. The ice slush collected was left to melt to give a liquid mixture with water settled at the bottom and fuel at the top. The volume of the liquid mixture and the water volume were measured. The volume data collected did not allow the SLR (Equation 2) to be calculated directly, since both the water volume and the snow volume were required.

To approximate the SLR, the snow volume was inferred from the liquid mixture volume. The snow volume was conservatively assumed to be equal to the liquid mixture volume. When the fuel was drained, the structure of the ice slush might collapse and thereby forced some fuel out of the structure. As a result, the liquid mixture volume would be less than expected, and the SLR would be under-predicted using this assumption.

Figure 2 shows the distribution of estimated SLR from 47 test points of the test campaign. The mean and median SLRs are 19.7 and 14.3, respectively. The variability of SLR of the snow found in the test rig does not seem to be out of place with that found in the atmosphere.

It has been reported that the snow formed in the simulated fuel tank has a SLR of 23.0 (see Part 2 of this report). This value is within the variability of SLR shown in Figure 2. It is classified as ultra light snow under the 6-snow-category (Table 2).

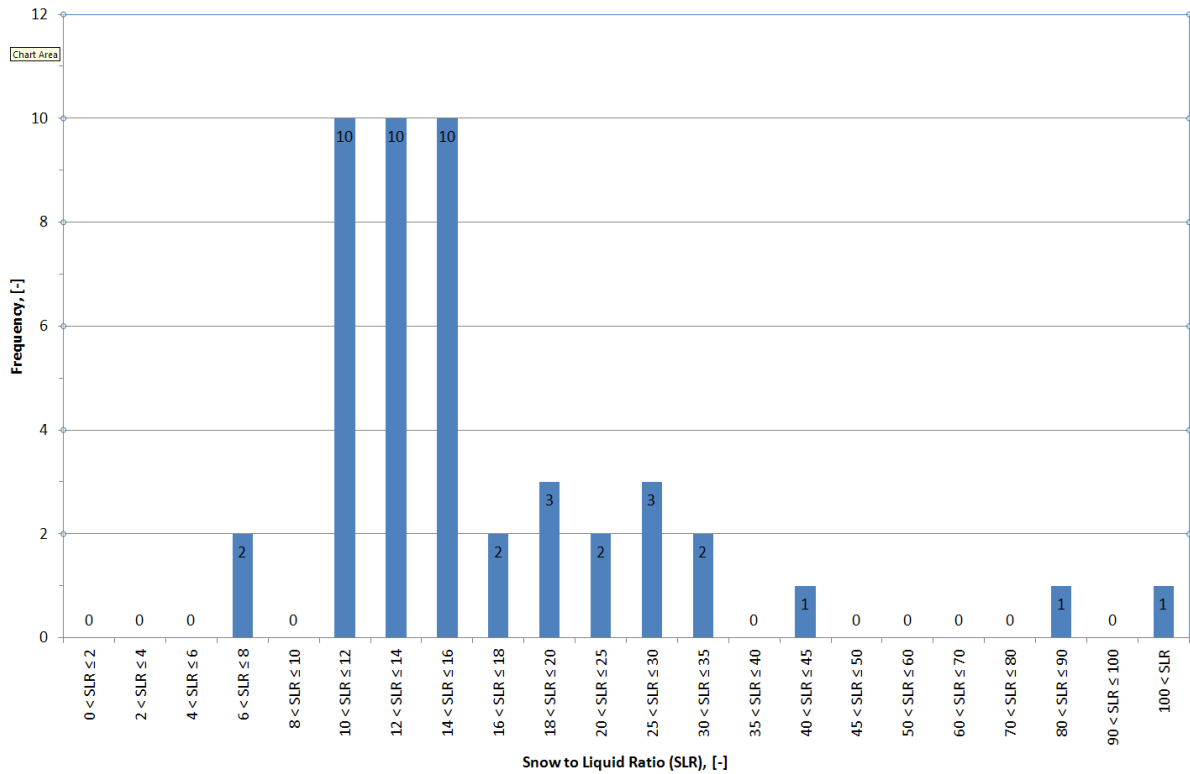


Figure 2 Distribution of estimated SLR from 47 test points in a test campaign conducted between October 2009 and January 2011, at the Airbus Fuel Test Facility, Filton, UK.

2.2 Influence Of Fluid Medium On SLR

With fallen snow on the ground, the lower layer supports the weight of the snow above. This leads to a gradual increase of compaction from the snowpack surface to the bottom of the snowpack [9]. Smaller SLR is expected at the lower layer of the snowpack compared to that at the upper layer of the snowpack.

In fuel, the density ratio of ice and fuel is approximately 1.14 (ice density $\sim 920 \text{ kg/m}^3$ at melting point; fuel density $\sim 810 \text{ kg/m}^3$ at room temperature). Ice is only slightly denser than fuel and may be considered almost neutrally buoyant in fuel. This implies that the weight of the ice is almost balanced by the buoyancy force; the effective weight acting downward under gravity is therefore negligible. This almost weightlessness effect allows ice crystals in fuel to form a very open structure without fracturing their dendrites under their own weight. This leads to a relatively higher SLR.

Table 1 Comparison of the occurrence of the three categories of snow [8] between the snowfall events [8] and Airbus fuel icing test campaign [6].

Snow Category	SLR Band	Proportion of Cases	
		Snowfall Events [8]	Airbus Fuel Icing Test Campaign [6]
Heavy	$\text{SLR} \leq 9$	14%	4%
Average	$9 < \text{SLR} \leq 15$	41%	55%
Light	$15 < \text{SLR}$	45%	41%

Table 2 Comparison of the occurrence of the six categories of snow [9] between the snowfall events [8] and Airbus fuel icing test campaign [6].

Snow Category	SLR Band	Proportion of Cases			
		Snowfall Events [8]		Airbus Fuel Icing Test Campaign [6]	
Very heavy	$\text{SLR} \leq 5.5$	17%	6%	4%	0%
Heavy	$5.5 < \text{SLR} \leq 8.5$		11%		4%
Average	$8.5 < \text{SLR} \leq 12.5$	28%	28%	28%	28%
Light	$12.5 < \text{SLR} \leq 17.5$	55%	26%	68%	40%
Very light	$17.5 < \text{SLR} \leq 22.5$		16%		9%
Ultra light	$22.5 < \text{SLR}$		13%		19%

Table 1 and Table 2 show the SLR bands of the three and six categories of snow, respectively. A comparison of the snow class distribution between the snowfall events [8] and the Airbus fuel icing test campaign [6] is also shown in the tables. In the three snow category classification (Table 1), the classification is too broad to be able to distinguish any subtle different. In the six snow category classification (Table 2) with a narrow band for each classification, a trend starts to emerge. The Airbus

fuel icing test campaign has a significantly lower proportion of snow in the combined categories of *Very Heavy* and *Heavy* snow compared to that for the snowfall event. At the same time, the Airbus fuel icing test campaign has a significantly higher proportion of snow in the combined categories of *Light*, *Very Light* and *Ultra Light* snow compared to that for the snowfall event. It should be noted that the SLR is under-estimated for the Airbus fuel icing test campaign. The real trend is therefore skewed more toward the light snow end.

2.3 Influence Of Flow Velocity On SLR

Surface wind can affect the SLR of fallen snow on the ground. At a critical wind speed over 9 m/s, ice crystals at the surface may be fractured mechanically during saltation [7, 8]; this process decreases the SLR. The surface wind speed only plays a minor role among other atmospheric factors by decreasing SLR with increasing wind speed [7].

The equivalent critical flow speed in a fuel flow application may be estimated to get a feel for the effect of the fuel flow on the SLR of the accreted ice in fuel. For flow similarity, the dynamic pressure for the fuel flow application is matched with that for the surface wind. The dynamic pressure for the fuel flow application, $\rho_f v_f^2$, and the surface wind, $\rho_a v_w^2$, are:

$$\rho_f v_f^2 = \rho_a v_w^2 \quad (3)$$

$$\rho_f v_f^2 = \rho_a v_w^2 \quad (4)$$

where v_f and v_w are the fuel and air (wind) velocities, respectively; and ρ_f and ρ_a are the fuel and air densities, respectively. Equating the fuel and wind dynamic pressures, the fuel velocity, v_f , may be expressed in terms of the wind (air) velocity, v_w , and the fuel and air densities, ρ_f (810 kg/m³) and ρ_a (1.2041 kg/m³ at 0°C):

$$v_f = v_w \sqrt{\frac{\rho_a}{\rho_f}} \quad (5)$$

From Equation 5, the equivalent critical flow speed in a fuel flow application is approximately 0.35 m/s (= 0.0386 x 9 m/s). In the test campaign [6], most tests were conducted with a nominal fuel mass flow rate, 5700 lb/hr (2586 kg/hr), with a fuel pipe test element of 2.5 inches (0.0635 m) diameter. This gave a mean fuel flow velocity in the pipe of approximately 0.28 m/s with a nominal fuel density of 810 kg/m³ (i.e. same density as in Section 2.2).

This fuel flow velocity was of the same order of magnitude of the computed critical velocity of 0.35 m/s. It was at approximately 20% (= (0.35 – 0.28) / 0.35 x 100%) below the critical velocity. Although the reported SLR from the Airbus fuel icing test

campaign (see Section 2.1) is lower than that reported for the simulated fuel tank (see Part 2 of this report), however as discussed in Section 2.1, the method used to compute the Airbus fuel icing test SLR is thought to under-estimate the true value. It is not possible to say whether the observed lower SLR was due to the compaction by the fuel flow or not. Nevertheless, since the fuel flow rate is below the critical velocity, the influence of fuel flow on the SLR was considered to be marginal if any.

2.4 Influence Of Growth Rate On SLR

As discussed in the Literature Review [4], temperature is one of the main factors controlling the habit of ice crystals. Figure 3 shows ice habits at various temperatures at saturation with respect to liquid water. Dendrites, which grow between -10°C and -20°C, have large open spaces in the crystal structure, thereby yielding a high SLR [7, 8]. Needles are the next lightest crystal habit [8] since they tend to aggregate forming mesh-like structures which have open spaces. Columns and plates are the densest form [8]. Figure 4 shows the dendrite, needle, column and plate ice habits.

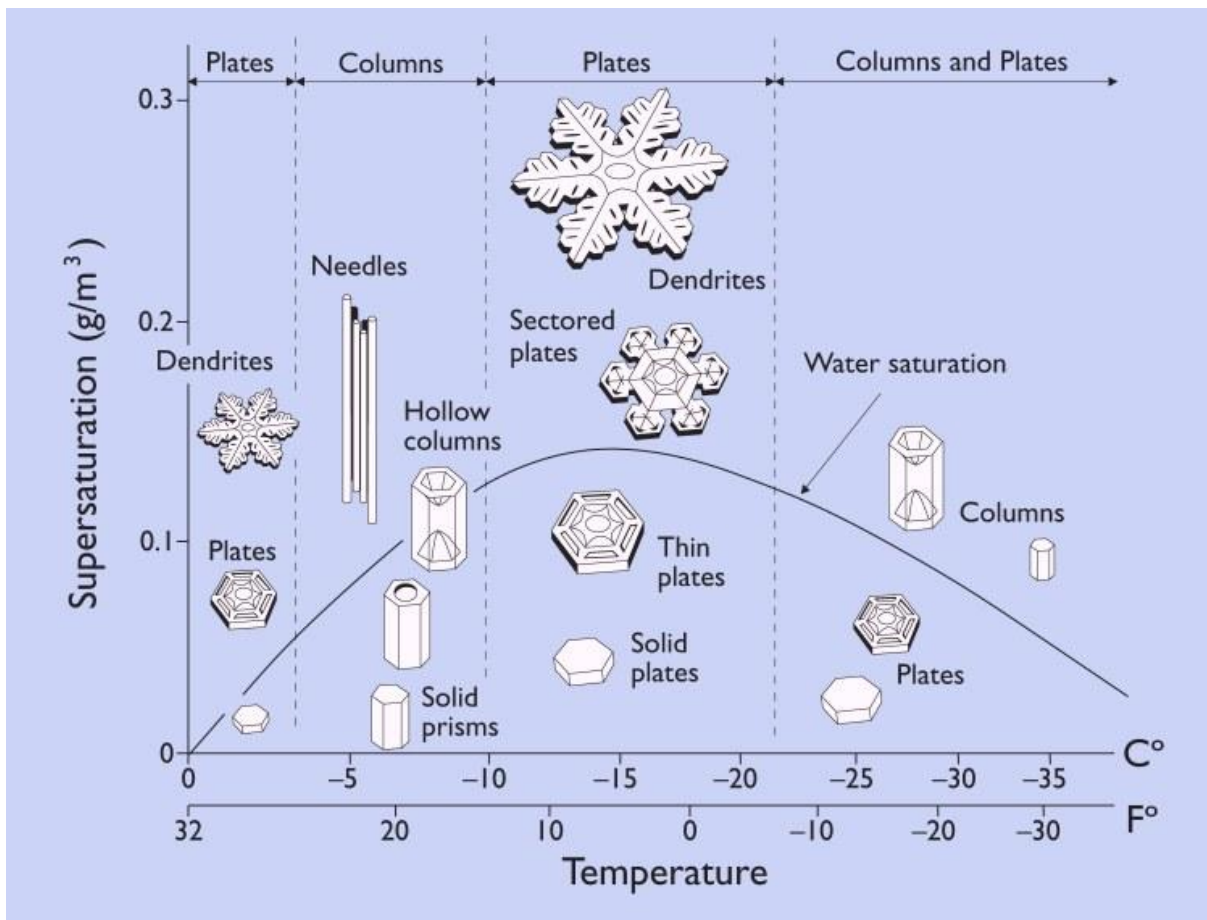


Figure 3 Diagram showing the growth habits of ice crystals as a function of temperature and supersaturation [13].

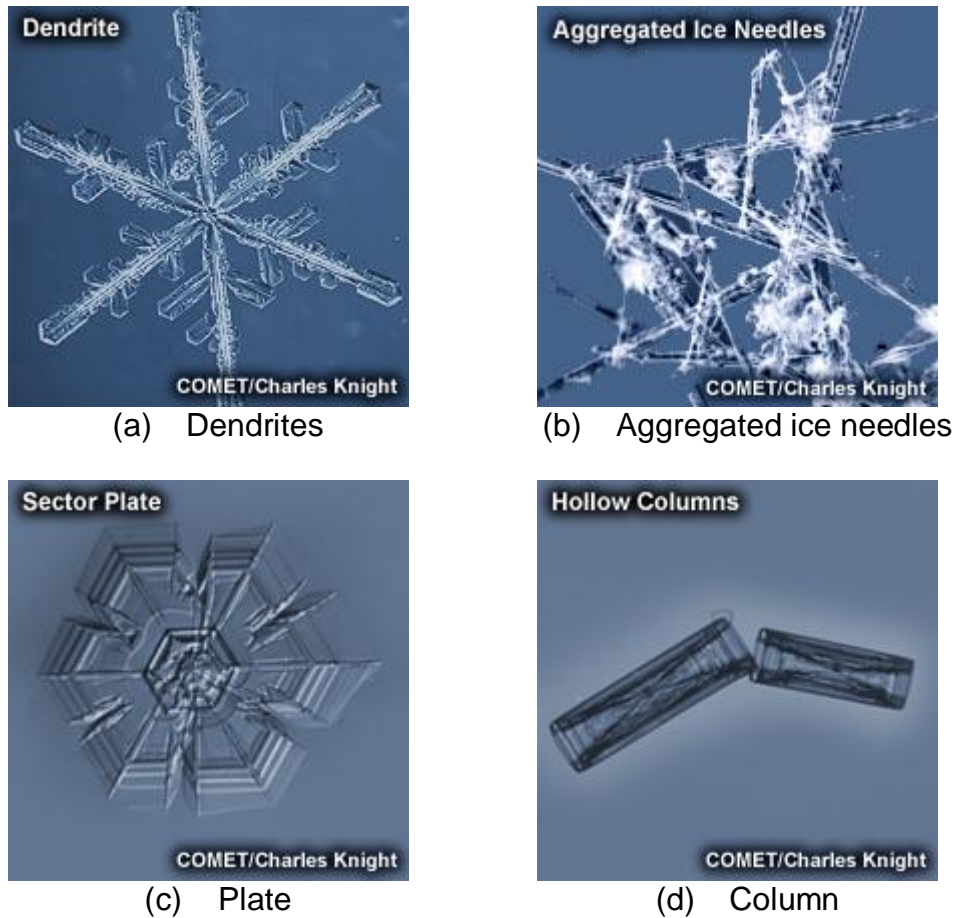
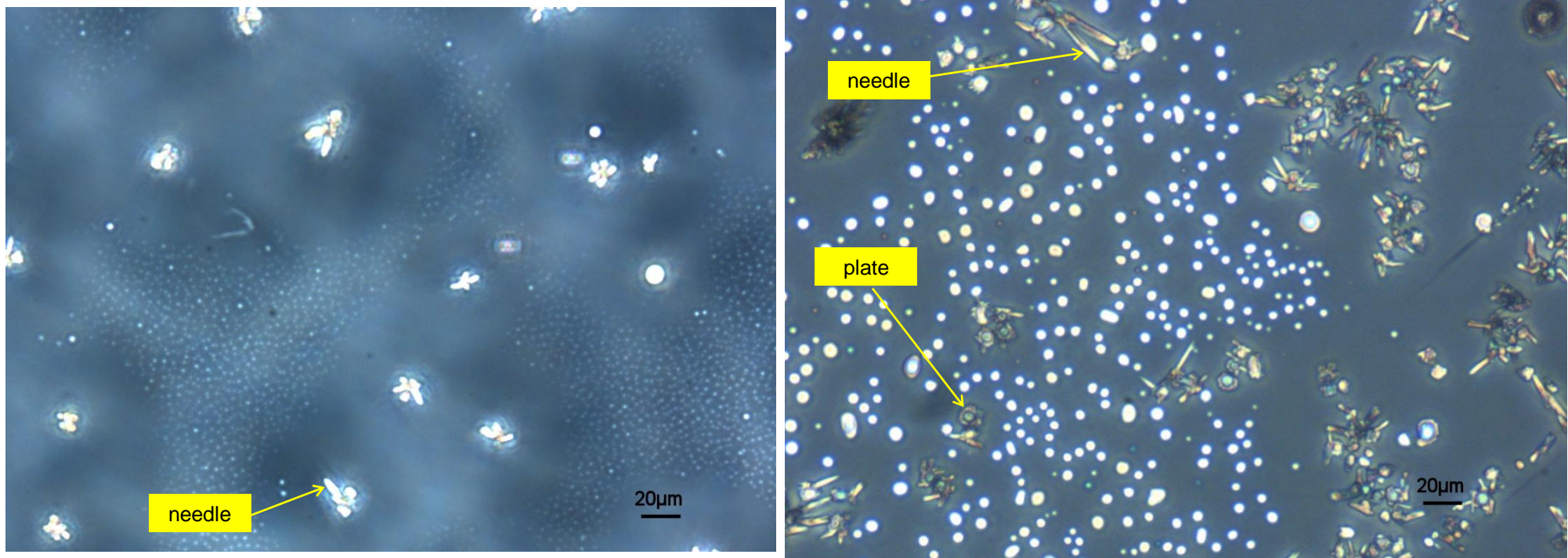


Figure 4 Ice crystal habits [11].

In a previous study [12] and in the current study (see Part 1 of this report), an optical microscope fitted with a cold stage was used to observe ice crystals formed as the fuels were cooled. Figure 5 shows ice crystals in coexistence with water droplets on the bottom of the crucible. Ice crystals of needle habit and plate habit are found in Figure 5b, but ice needles dominated in Figure 5b. Snow formed from aggregation of the ice crystals in Figure 5b would be expected to give a relatively high SLR.



(a) Air BP Filton Airfield Jet A-1, on holding at -34°C (AAIB cooling regime), showing small ice crystals in coexistence with water droplets on the bottom of the crucible [Part 1 of this report].

(b) Toluene on slow cooling to -35°C , showing ice crystals and 2-12 μm water/ice droplets on the bottom of the crucible [12].

Figure 5 Ice crystal habits in fuel.

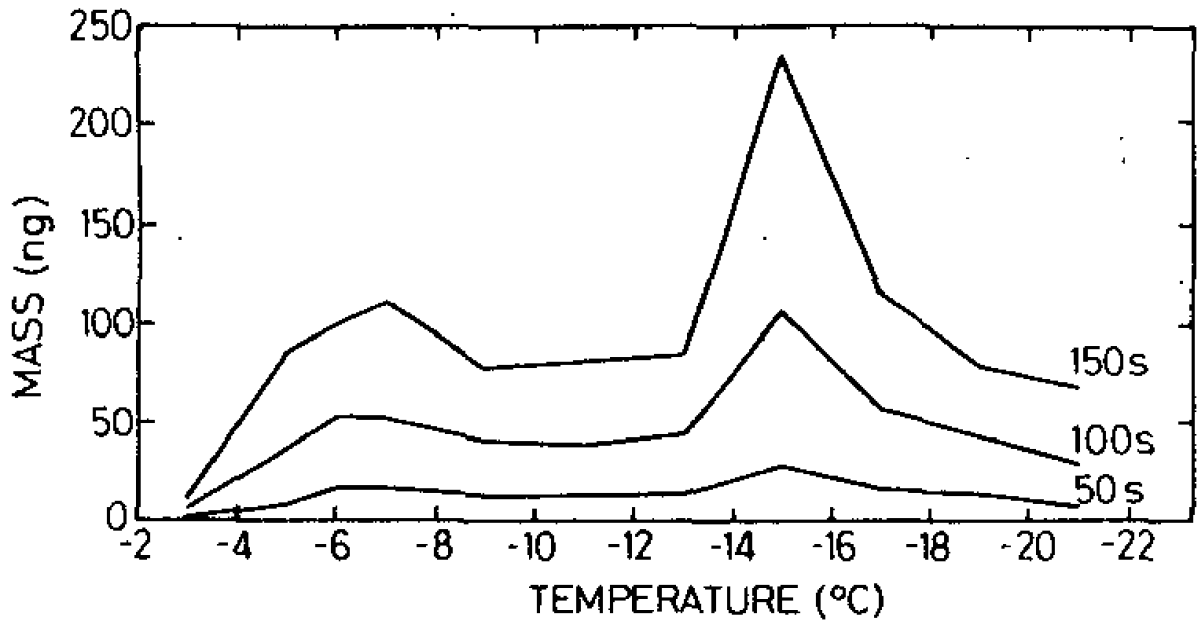


Figure 6 Variation of estimated crystal mass with temperature at 50, 100 and 150 s after seeding [16].

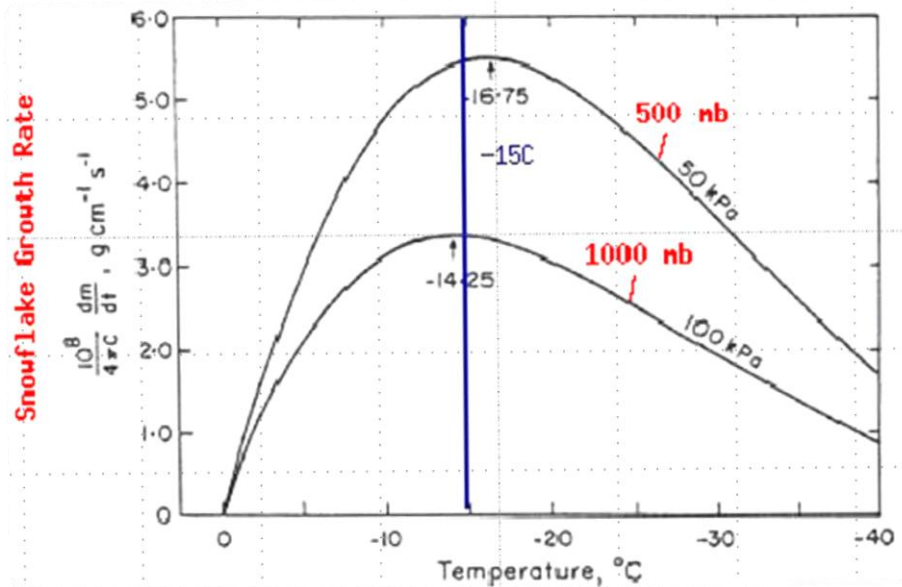


Figure 7 Normalised ice crystal growth rate as a function of temperature [14].

Another factor affecting SLR is crystal size. Long ice needles aggregate to form a relatively large mesh structure with much void spaces giving a relatively high SLR, whereas short ice needles aggregate to form a relatively small mesh structure giving a relatively low SLR. Aggregation is most active close to the melting point, i.e. between 0°C and -4°C, as the liquid-like layer is at maximum thickness [9, 15]. Liquid-like layer was discussed in detailed in the literature review [4]. At contact points, snowflakes join together by fusion and freezing of the liquid-like layers. At lower temperature, i.e. -12°C to -18°C, aggregation is mostly due to entanglement of jammed branches of snowflakes [9]. Snowflakes are interlocked together by their branches rather than fused together as at higher temperatures.

Dendrite snow crystals have branches that make them very effective in jammed aggregation. Needle snow crystals that have been aggregated to mesh structures are equally effective in jammed aggregation. The open ended needles from one aggregated ice needle structure may be locked into another aggregated ice needle structure. Aggregation of crystals like dendrites or needles would result in snow of a relatively higher SLR than crystals like plates and columns.

The size of the crystal at a specific time depends on the growth rate from post-nucleation up to the time of interest. Many factors affect the growth rate [8, 9]:

- Growth duration time;
- Degree of supersaturation with respect to ice;
- Temperature; and
- Pressure.

Figure 6 shows the variation of estimated crystal mass with temperature and time. The maximum size occurs at temperature around -15°C. This temperature corresponds to the maximum growth rate by the Bergeron process. Ice-crystal growth by the Bergeron process is dependent primarily on temperature and with pressure playing a secondary effect [14]. Figure 7 shows the normalised ice crystal growth rate as a function of temperature. At 100 kPa, the maximum growth rate occurs at around -14°C; and at 50 kPa, the maximum growth rate occurs at -17°C [14].

Figure 5a shows ice crystals in coexistence with water droplets on the bottom of the crucible in Air BP Filton Airfield Jet A-1. Figure 5b shows the same in Toluene. The Air BP Filton Airfield Jet A-1 underwent the AAIB cooling regime [see Part 1 of the report]. The Toluene underwent the slow cooling regime [4]. At the critical temperatures for ice crystal growth, i.e. -2°C to -20°C, the cooling rates for the AAIB cooling regime and the slow cooling were -0.15°C/min and -1°C/min, respectively. The AAIB cooling rate was much slower than the slow cooling rate in this critical temperature range.

To reach the same end temperature, a slow cooling rate would take a longer time than a fast cooling rate. Growth duration is noted as one of the factors that affect the crystal size. With longer ice growth duration, fuel that underwent a slow cooling

regime was expected to produce ice crystals relatively larger than that produced under a fast cooling regime. The longest needles in Figure 5a and Figure 5b are about 11 μm [see Part 1 of the report] and 35 μm , respectively. Despite undergoing a much slower cooling regime, and hence longer growth duration, the ice crystals in Figure 5a are in general much smaller and more rounded than those in Figure 5b.

Toluene is an aromatic hydrocarbon. The saturated solubility of water in Toluene at 25°C was reported to be about 566±10 ppm by mass [4]. The concentration in ppm by mass is multiplied by the density ratio, ρ_t/ρ_w ($= 870 / 1000 = 0.87$, where ρ_t is the Toluene density and ρ_w is the water density) to give the concentration in ppm by volume. This gives 492 ($= 566 \times 0.87$) ppm by volume. This value is much higher than the accepted value of 330 ppm by volume [17] or 379 ($= 330 / 0.87$) ppm by mass. This suggests that the 566±10 ppm by mass reported in [4] may be erroneous.

The saturated solubility of water in Air BP Filton Airfield Jet A-1 at the same temperature is about 86±2 ppm by mass [Part 1 of this report]. It is reasonable to assume that solubility of water in Toluene behaves in a similar way as jet fuels with temperature, i.e. water solubility decreases exponentially with decreasing temperatures, and the solubility of water in Toluene may be expressed as a function of temperature in the following form:

(6)

where S is the water solubility in ppm by mass; A is the coefficient for the exponential function and it is the water solubility in ppm by mass at 0°C; B is the exponent coefficient; and T is the fuel temperature in °C. With no available data to determine the exponent coefficient, B , the average mean exponent coefficient, 0.0485, for the five Jet A-1 fuels used in this study was assumed [Part 1 of this report]. The coefficient for the exponential function, A , may be determined from the water solubility 25°C with the assumed exponent coefficient. Table 3 shows the values for the coefficients in Equation 6 for, and the solubility of water in, Toluene and Air BP Airfield Jet A-1 at 25°C and -34°C. It should be noted that the solubility of water in Toluene from Chemical net [17] is used in the calculation in Table 3. It can be seen that water dropout between 25°C and -34°C for Toluene is approximately 4.4 times that for Air BP Filton Airfield Jet A-1. This suggests that ice crystal growth in Air BP Airfield Jet A-1 (Figure 5a) may be constrained by the availability of water in comparison to that in Toluene (Figure 5b). It resulted in smaller crystals in Air BP Airfield Jet A-1 and larger crystals in Toluene. The availability of water is linked to the degree of supersaturation. It is one of the factors that affect the crystal growth.

Aggregated snow from smaller ice crystals in Air BP Filton Airfield Jet A-1 would produce a relatively lower SLR compared to aggregated snow from larger ice crystals in Toluene.

Table 3 Values for the coefficients in Equation 6 for, and the solubility of water in, Toluene and Air BP Airfield Jet A-1 at 25°C and -34°C.

	<i>Toluene</i>	<i>Air BP Filton Airfield Jet A-1</i>
, Equation 6 [ppm by mass]	112.7	25.589
, Equation 6 [1/°C]	0.0485	0.0483
Solubility at 25°C [ppm by mass]	379	86
Solubility at -34°C [ppm by mass]	22	5
Water dropout between 25°C and -34°C [ppm by mass]	357	81

3. ICING RISK REDUCTION

Two principal classes of concepts are in play to reduce the icing risk. The first class category is to tackle the ice directly, i.e. treating the symptoms. The second class category is to eliminate sources of water, i.e. treating the causes. A number of examples from each class are presented in the following subsections.

Table 4 Icing risk reduction – Concept classification.

<i>Class 1 – Tackling the ice</i>		<i>Class 2 – Eliminating sources of water</i>	
Section 3.1	Fuel System Icing Inhibitor	Section 3.7	Dehumidifying Ingress Air
Section 3.2	Fuel Warming	Section 3.8	Displacing Ingress Air
Section 3.3	Onboard Water Separation	Section 3.9	Fuel Dehydration
Section 3.4	Fuel Line Anti-Icing		
Section 3.5	Insulating Materials		
Section 3.6	Architecture Optimisation		

3.1 Fuel System Icing Inhibitor

Fuel system icing inhibitor (FSII) may be used to prevent free water from freezing in aircraft fuel systems; however, there is a desire to reduce the use of FSII in aviation [4]. FSII is chemically aggressive and can cause corrosion and deterioration of fuel tanks and fuel system components.

DiEGME (DiEthylene Glycol Monomethyl Ether) is the only FSII approved for jet fuels [18]. DiEGME is slightly soluble in fuel and must be blended in the fuel as fine droplets to ensure a large surface area to promote rapid and complete dissolution of the additive.

If a pool of water is present in the sump of a fuel tank, i.e. accumulation from previous operation, the DiEGME will preferentially dissolve in the pool of water. It results in a lower than expected concentration of DiEGME in fuel and a pool of water in the sump containing a high concentration of DiEGME. With a below optimal concentration of DiEGME in fuel, free water that comes out from fuel as the fuel is cooled would not have sufficient DiEGME to prevent it from freezing.

NAME	Fuel System Icing Inhibitor	
	APISOLVE 76	APITOL 120
Chemical Composition	Ethylene Glycol monomethyl Ether	Diethylene Glycol Monomethyl Ether
Cas No.	109-86-4	111-77-3
Appearance	Clear, bright and free from solid mater	Clear, bright and free from solid mater
Colour, Platinum-Cobalt	10.0 Max.	10.0 Max.
Specific Gravity 20/20 °C	0.963 - 0.967	1.021 - 1.025
Distillation Initial Boiling Point Dry Point	123.5 °C Min. 125.5 °C Max.	191.0 °C Min. 198.0 °C Max.
PH of 25% solution in water 25 ± 2 °C	5.0 to 7.0	5.5 to 7.5
Flash Point (°C)	43.3 °C Min.	85 °C Min.
Water Content %	0.15 Max.	0.15 Max.
Molecular Weight	76.1	120.15
Acidity % w/w (as Acetic Acid)	0.01 Max.	0.01 Max.
Viscosity at 20 °c	1.7 cps.	3.9 cps.
Solubility In water	Soluble	Soluble
Nato Code	S-748	S-1745
Diethylene Glycol Contain (% m/m)	-	0.5 Max. (DEF STAN 68-252/2)
Ethylene Glycol Contain (% m/m)	0.025 Max.	0.5 Max. (MIL - DTL - 85470B)
Joint Service Designation	AL-31	AL-41
USAF Military Specification	MIL - DTL - 27686G	MIL - DTL - 85470B
British Military Specification	DERD 2451/issue3	DEF STAN 68-252/2

Figure 8 FSII general properties [19].

3.2 Fuel Warming

Heat has to be removed from various onboard systems (i.e. avionics, hydraulic system, inerting system etc...) so they may continue to operate efficiently and reliably. Currently, various aircraft use heat exchangers to cool different aircraft systems [5]. The two main coolants commonly used on aircraft are fuel and air. Fuel is a convenient heat sink and most aircraft systems already channel their waste heat to the fuel.

By maintaining the fuel above the ice melting temperature, 0°C, ice is completely eliminated in the fuel system. The bulk fuel temperature in the wing tanks is generally assumed to follow the outside ambient air temperature. From Figure 9, it can be seen that with initial fuel temperatures at 60°F (15.6°C), 80°F (26.7°C) and 100°F (37.8°C), it takes approximately 0.7 hours, 1.2 hours and 1.6 hours, respectively, for the fuel to reach the 0°C (32°F).

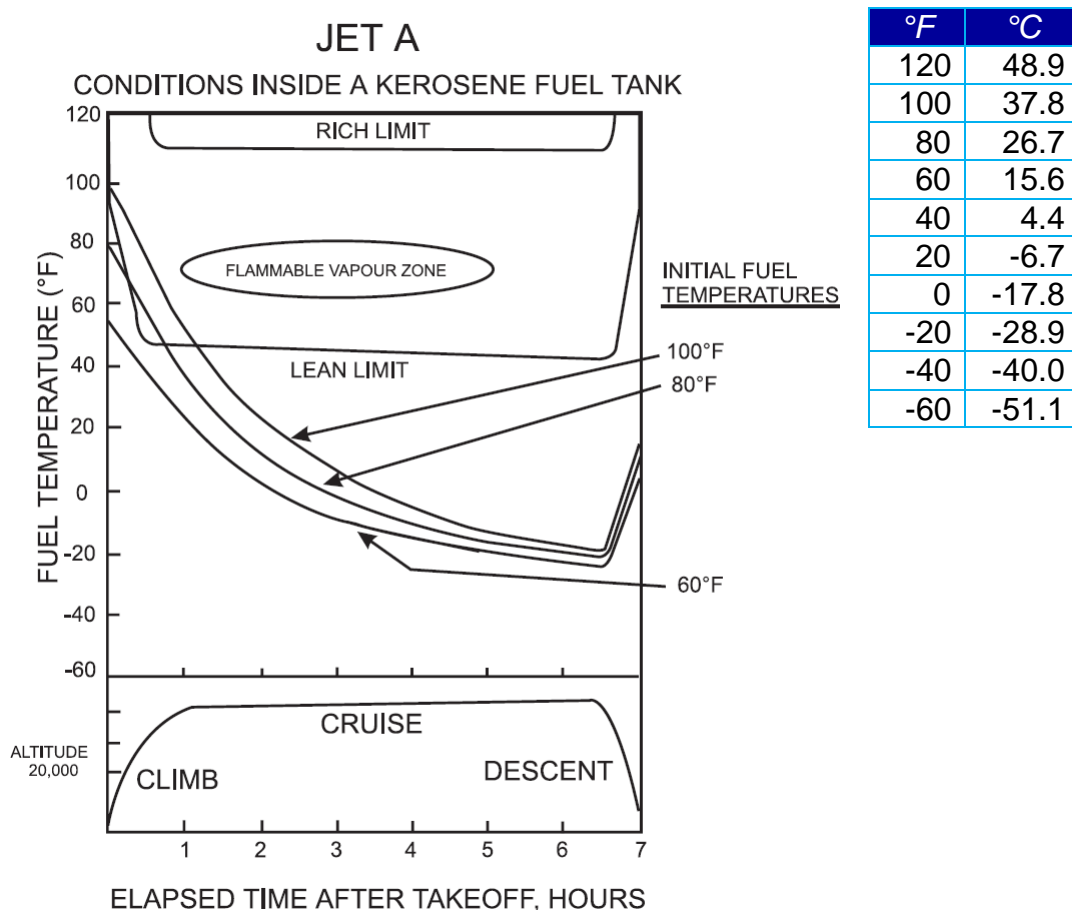


Figure 9 Typical Jet A fuel temperature in flight [20].

For short haul flights with flight duration less than 3 hours, waste heat from various onboard systems, in general, should be adequate to maintain the fuel temperature above the ice melting temperature, 0°C.

For long haul flights (flight duration more than 6 hours), onboard systems would be struggling to provide sufficient waste heat to keep the fuel temperature above the ice melting temperature for the whole duration of the flight. Dedicated fuel heaters may be required to provide the heat shortfall. Fuel heaters have an impact on the flight operation efficiency. They add weight to the aircraft and drain energy from onboard power plants.

3.3 Onboard Water Separator

Since the solubility of water in aviation jet fuel decreases with decreasing temperature, during aircraft cruise, water shed from fuel as the fuel temperature decreases. It forms small droplets of the order of 1-3 microns (see Part 1 of this report). The droplets remain suspended in the fuel and create a mist or fog-like phenomenon in fuel [28]. The settling rate of a micron size droplet in a static fuel tank environment is less than 1×10^{-5} m/s at 15.5°C [29]. The fuel in onboard fuel tanks is far from static due to aircraft motion, fuel transfer and vibration.

The mist or fog-like phenomenon in fuel tends to clear with time [30]. Drier (water unsaturated) fuel dissolves the suspended water droplets. The suspended water feeds the growth of the ice by the Bergeron process [12, 28]. If the water droplets are collected and disposed of as early as possible in the flight, it would greatly reduce the risk of ice building up in the fuel system since the source of water for ice growth is limited.

Apparatus such as a cyclonic separator [27] and water coalescer [26] have been proposed to remove the suspended water droplets in the fuel and dispose the collected water in a safe and efficient way. The cyclonic separator or the water coalescer, is connected within a fuel system onboard.

For the cyclonic separator, fuel from a fuel tank is fed into the cyclonic separator, which spins the fuel into an intense cyclonic spiral, and centrifugal force separates the suspended water droplets from the fuel. For the water coalescer, fuel from a fuel tank is fed into the water coalescer, which causes suspended water droplets in the fuel to agglomerate into larger droplets, which settle out under gravity. In both cases, the "*purified*" fuel is returned to the tank and the water is collected in a separate area to be disposed of appropriately. The "*purified*" fuel has a much lower suspended water concentration and therefore has a very limited water content to contribute to the growth of deposited ice on subcooled surfaces in the tank.

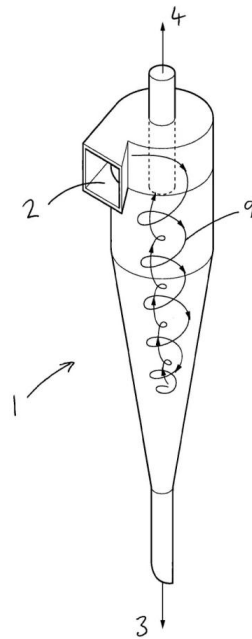
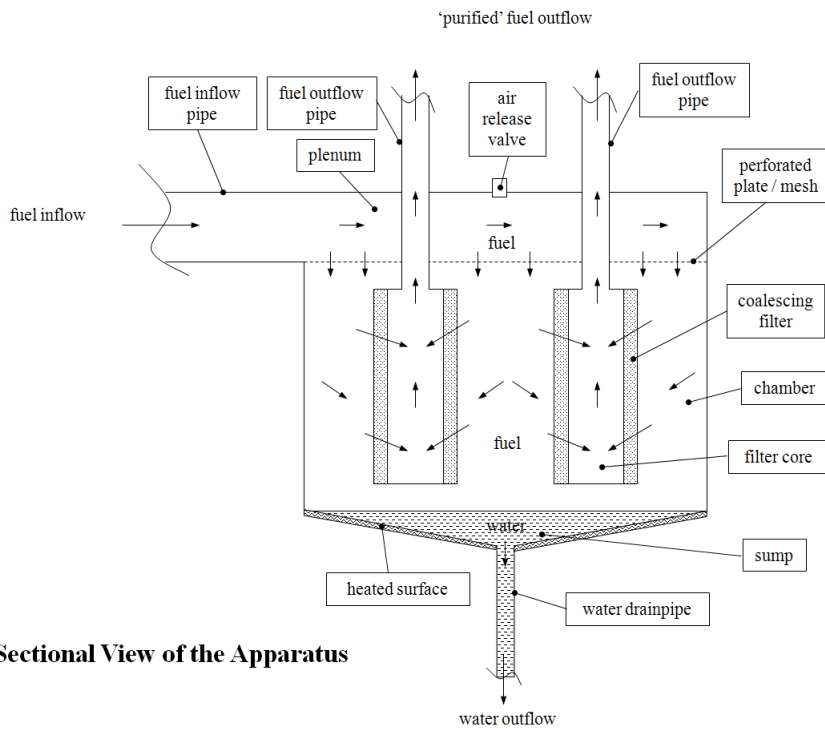


Figure 10 A schematic 3D view of the flow within the cyclonic separator during operation [27]. Key: 1 – cyclonic separator; 2 – flow inlet; 3 – water/fuel outlet; 4 – “purified” fuel outlet; 9 – spiral flow streamlines.



A Sectional View of the Apparatus

Figure 11 A schematic section side view through a coalescing filter [26].

3.4 Fuel Line Anti-Icing

The primary function of a Fuel Oil Heat Exchanger (FOHE) is to cool the engine oil. Since fuel is used as the coolant, fuel is heated up by the oil in the FOHE. The heating of the fuel prevents ice from building up downstream in engine intake strainers in the fuel line that feed fuel from the tanks to the wing mounted engines.

Heat moves inward from the heated surface by conduction and convection to warm the fuel. The rate of heat transfer is limited and the heating is not uniform. In a non-optimal design of heat exchanger, the fuel in the core of the flow stream may remain cold and any ice clusters in the core of the flow stream would not be melted.

A microwave de-icing and anti-icing system for a fuel line carrying fuel has been proposed [21]. It suppresses ice formation in a fuel line by transmitting microwaves along the fuel line to energize water and ice carried with the fuel in the fuel line. The microwaves interact with water to efficiently heat the water by a process known as dielectric heating. The dielectric heating effect on the fuel and on the water is proportional to their respective dielectric constants. Aviation fuel has a dielectric constant of around 1.7 [22], water has a dielectric constant of around 80.4 [22], and ice has a dielectric constant of around 3.15 [23]. The heating effect on ice is approximately twice ($= 3.15 / 1.7 \sim 1.85$) that of fuel. Ice would heat up preferentially over fuel. Once the ice has melted, the water would heat up quickly. The heating effect on water is approximately fifty times ($= 80.4 / 1.7 \sim 47.3$) that of fuel. The heat from the water would dissipate into the fuel and thereby warm the fuel.

Figure 12 shows the schematic of the proposed system. The fuel line is tuned as a waveguide to contain the microwave energy in the fuel line. Microwave receivers, RX, are placed at each end of the fuel line to absorb residual microwave energy and to measure and control the transmitted energy levels. The proposed system is more efficient and effective since it heats the ice/water directly.

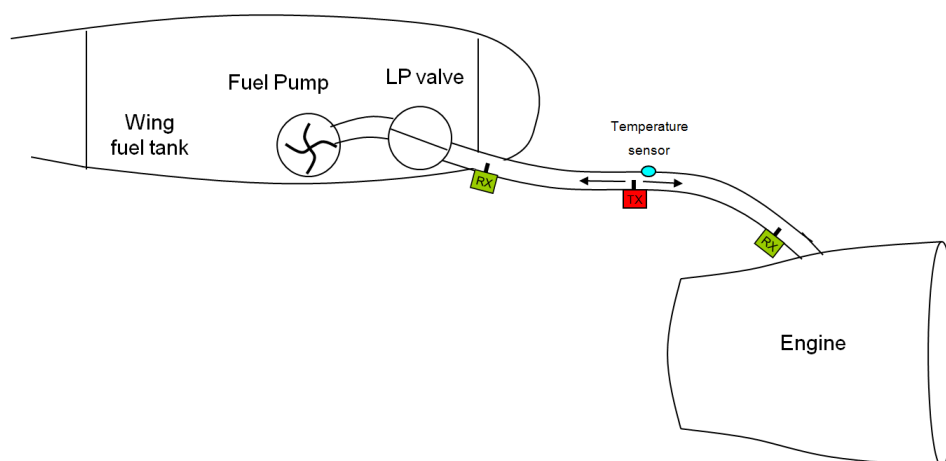


Figure 12 Schematic of the proposed microwave de-icing and anti-icing system for fuel line. RX – microwave receiver; TX – microwave transmitter; LP – low pressure.

3.5 Insulating Material

As observed in Part 2, Section 5.1.1, of this report, due to effectiveness of thermal insulation of the different surface finishes, the composite specimen block showed the least subcooled and thereby have the least accreted ice. Intuitively, a composite fuel pipe would therefore have less ice accreted compared to the same for a metal pipe.

3.6 Architecture Optimisation

In addition to the use of insulating materials, noted in Section 3.5 above, to reduce the degree of subcooling and thereby reducing the accreted ice, fuel system architecture may be optimised to achieve the same goal. Desirable fuel system architecture may have a small temperature variation in the system such that the fuel in the fuel pipe is at more or less the same temperature as the environment around the fuel pipe. This reduces the degree of subcooling and induces less accreted ice in the pipe.

3.7 Dehumidifying Ingress Air

Water may enter aircraft fuel tanks from varying sources; primarily from fuel uplifted to the aircraft fuel tanks during refuel and from air entering the aircraft fuel tanks via the vent system. Depending on the environmental conditions, water ingress with vent air is suggested to contribute up to 30-40% of the total water accumulated in the fuel system [24]. Hence, about 60-70% of the total water accumulated in the fuel system is from water uplifted during refuelling.

During aircraft descent, due to increasing external atmospheric pressure there is a net inflow of ambient air through the ventilation system to maintain pressure equilibrium. The ingress of ambient air during descent brings relatively warm, humid air into the fuel system, and hence a significant volume of water enters the fuel tank.

A number of systems have been proposed [24, 25] to remove water effectively from air entering the aircraft fuel tank. By this mean, one of the primary sources of water, water ingress from vent, is eliminated and thereby the content of water in the fuel tank can be kept low. This improves fuel system reliability, reduces maintenance activities, and above all, reduces icing risk.

Figure 13 shows a general ventilation system architecture for a three-tank configuration of an aircraft fuel system. Each surge tank includes a NACA vent which opens to the atmosphere on the lower aerodynamic surface of the aircraft wing. The surge tanks further include a vent protector and a dehumidifying device (proposed apparatus).

The dehumidifying device may be of desiccant type [25], refrigerating type [24] or other types of dehumidifying devices. The water collected in the dehumidifying device should be disposed of effectively to ensure the water is not introduced into the fuel tanks. It is important that the dehumidifying device should be maintenance-free as much as possible to eliminate additional burden on aircraft operation.

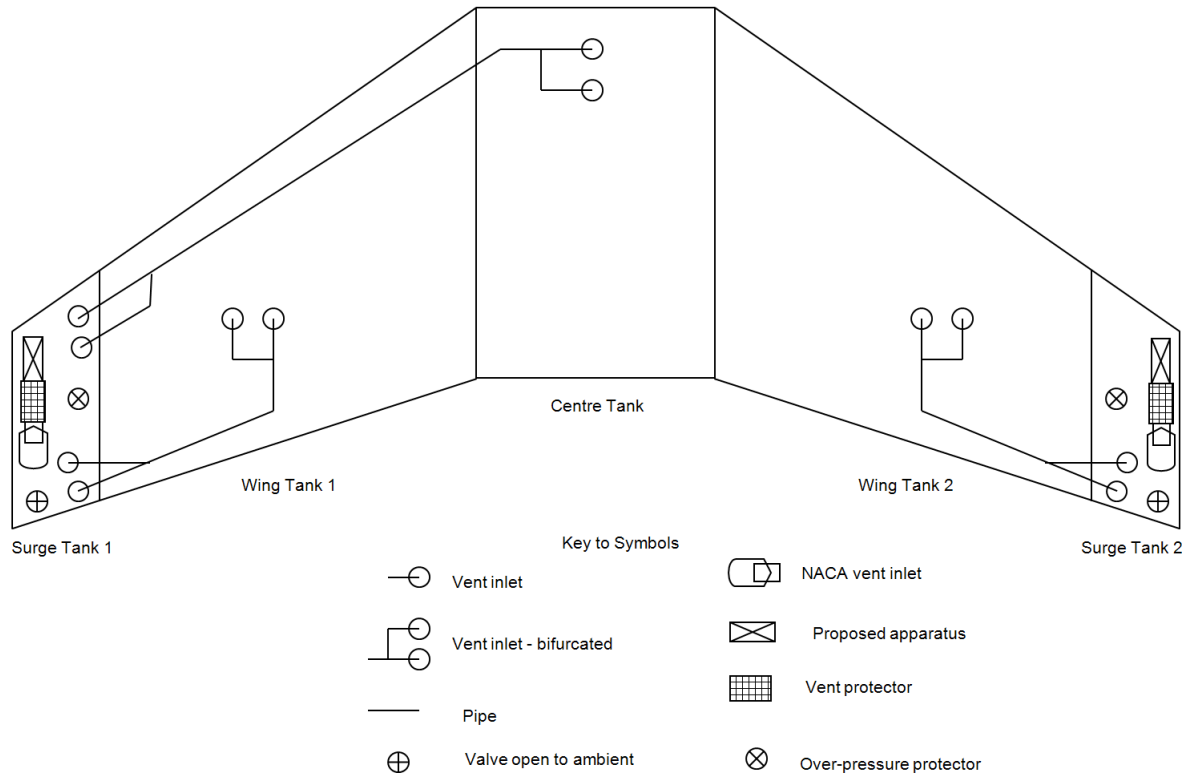


Figure 13 Schematic a general ventilation system architecture for a three-tank configuration of an aircraft fuel system showing the proposed installation of the dehumidifying device (proposed apparatus).

3.8 Displacing Ingress Air

The introduction of Fuel Tank Inerting Systems (FTIS) on aircraft brings an additional opportunity for water management. Since the TWA accident (17th July 1996), there has been a significant effort to reduce fuel tank fire risks. The atmosphere in the ullage contains combustible components such as fuel vapour and oxygen, which in conjunction with an ignition source could cause an explosion if the fuel/air mixture is within the flammable region. Inerting attempts to reduce the oxygen content and fuel vapour content in the ullage atmosphere by displacing the ullage air with an inert gas. Inert gas, i.e. argon, nitrogen or carbon dioxide, could be injected into the ullage.

Typically, an On-Board Inert Gas Generation System (OBIGGS) is used to generate Nitrogen Enriched Air (NEA) from engine bleed air for inerting. Conditioned bleed air is passed through a hollow fibre membrane in an Air Separation Module (ASM). The process removes oxygen, water vapour and other gases in the bleed air.

The OBIGGS may be tuned such that the NEA injected in the fuel system at descent is more than sufficient to equalise the ambient pressure so that there is very little or no air ingress. With very little or no ingress of warm humid air at descent, it eliminates one of the primary sources of water, water ingress from vent and thereby keeps the content of water in the fuel tank low. This improves fuel system reliability, reduces maintenance activities, and above all, reduces icing risk in the same way as the proposed methods in the previous section.

3.9 Fuel Dehydration

It has been proposed to take further benefit from the OBIGGS by using NEA to dehydrate the fuel onboard [1].

Figure 14 shows a schematic of the proposed arrangement. Dry NEA is injected in the fuel and the ullage for optimized water management in the tank. NEA injected in the fuel forms bubbles, which rise through the fuel. Diffusion of water from the fuel into the gas bubbles occurs until equilibrium is reached. This dehydrates the fuel as the bubbles rise to the fuel surface. By reducing the concentration of dissolved water in the fuel, there is a reduction of water that may precipitate out of the fuel as the fuel is cooled during a flight.

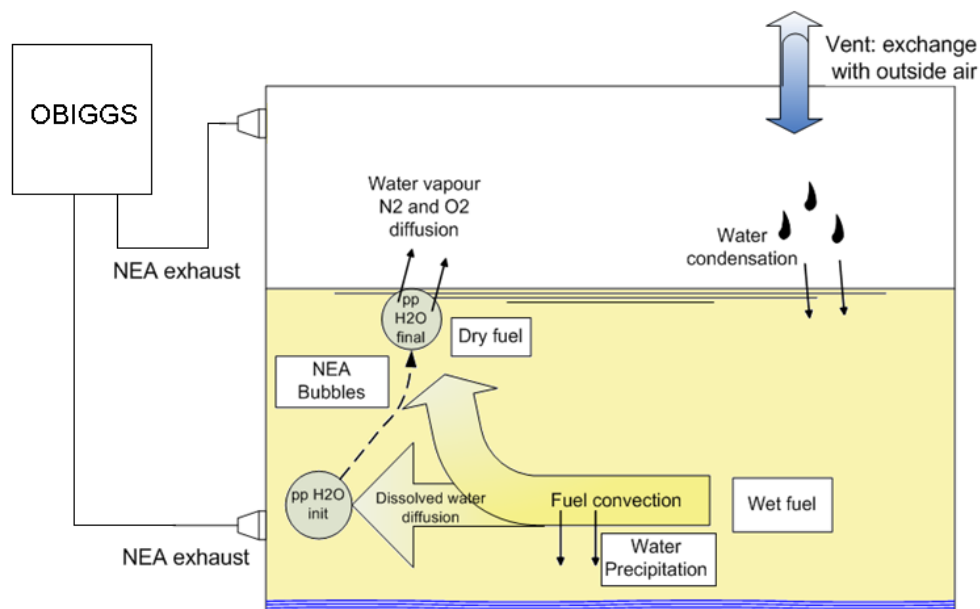


Figure 14 Schematic of the proposed dehydration system for dehydrating fuel within the fuel tanks.

When the water vapour laden NEA bubbles release from the fuel at the fuel surface, the wet NEA helps to maintain a low oxygen level in the ullage by displacing the ullage atmosphere. Since water vapour is an inert gas, water vapour has no abatement effect on the inerting function of the NEA. Dry NEA is also injected into the ullage to ensure an effective distribution of NEA and mixing with the ullage atmosphere. It is also used to control the humidity in the ullage atmosphere preventing it from becoming over-saturated with water vapour. By limiting the water vapour saturation in the ullage atmosphere, there is a reduction in the amount of water that may precipitate out of the atmosphere due to condensation.

A preliminary modelling study of a dual-use OBIGGS for fuel dehydration and fuel tank inerting has been conducted [2]. The modelling study shows the optimal flow split ratio, whereby one part is injected in the fuel to dehydrate the fuel and the other part is injected in the ullage to prevent condensation, is between 0.3 to 0.6. The split ratio is defined as the ratio of NEA injected in the fuel to the total NEA injected in the tank. If the split ratio is 1, 100% of the NEA is injected in the fuel; and if the split ratio is 0, 100% of the NEA is injected in the ullage. With a split ratio of 0.3, 70% of NEA is injected in the ullage and thereby giving a bulk ullage relative humidity (RH) of around 30%. This maintains a fairly low RH in the ullage to stay below the dew point, to prevent condensation forming on the underside of the (cold) top wing skin.

Laboratory experiments, verified and compared with theory, have demonstrated the critical function and provided characteristic proof of the proposed fuel system dehydration concept [3]. NEA sparging can provide complete fuel dehydration with appropriate NEA flow. This is approximately one unit volume of NEA to one unit volume of fuel. Theoretically, this can prevent water precipitating out from fuel at all temperatures. It should be noted that the dual-use of NEA, for fuel dehydration and for inerting, has a different requirement for the NEA flow at different phases of the flight. Fuel dehydration requires a high NEA flow at an early phase of the flight; but inerting requires a high NEA flow at descent. A proper system design and optimization are needed to ensure the dehydration objective and inerting objective are achieved.

The proposed method eliminates both main sources of water, uploaded dissolved water in fuel and water ingress from vents. It keeps the fuel system dry (in terms of water), and greatly improves fuel system reliability, reduces maintenance activities, and above all, reduces icing risk.

4. CONCLUSIONS

4.1 Snow In Fuel

The SLRs of ice slush collected in the test rig of a test campaign conducted between October 2009 and January 2011, at the Airbus Fuel Test Facility, Filton, UK, were presented to show the variability of SLRs found in an aircraft fuel system. The variability is not too dissimilar to that of snowfall events in the atmosphere. The mean SLR for snow in an aircraft fuel system is 19.7. This is classified as “*Very Light*” snow in a six-snow category classification system. In contrast, the mean SLR of snow in the atmosphere is 15.6 and is classified as “*Light*” in the same classification system.

The apparent lightness of the snow in an aircraft fuel system may be due to a number of factors. The prime factors may be:

- Ice is only slightly heavier than fuel and may be considered almost neutrally buoyant in fuel. The almost weightlessness effect allowed ice crystals in fuel to form in a very open structure without fracturing their dendrites under their own weight. This leads to a relatively higher SLR.
- Snow crystal growth dynamics is typically dominated by attachment kinetics in combination with molecular diffusion and thermal diffusion [31]. Molecular diffusion brings water molecules to the growing crystal. Thermal diffusion removes latent heat generated from solidification. Since fuel has a high thermal diffusivity but a low molecular diffusivity compared to air, this reduces the mechanism of snow crystal growth to attachment kinetics with molecular diffusion controlled only [31]. At low water concentration, as in the case in fuel, molecular diffusion is limited and the crystal growth is dominated by attachment kinetics. Prism ice growth is preferential over dendritic ice growth in fuel. It results predominately in needles and plates in fuel. Aggregated needles may form a very open structure that gives rise to a relatively large SLR.

4.2 Prevention Of Ice Formation In Fuel

A number of ice prevention concepts have been outlined in Section 3. The concepts may be divided into two classes.

- Class 1
This deals with the ice directly, i.e. treating the symptoms. Proposed concepts such as FSII, fuel warming, onboard water separation and fuel line anti-icing have been described.
- Class 2

This eliminates sources of water, i.e. treating the causes. Proposed concepts such as dehumidifying ingress air, displacing ingress air and fuel dehydration have been described.

The pros and cons of the proposed concepts are difficult to quantify. It depends on the aircraft fuel system architecture, flight mission, airline operation procedure, and many other factors.

4.3 Outlook

The presence of water in aviation jet fuel has been a topic of concern for the aviation industry for many decades. The incident of a 2-engine large commercial aircraft, the Boeing 777 flight, which crash-landed at Heathrow on 17 January 2008, has prompted a series of research activities on water/ice in fuel by the AAIB. This research project, funded by EASA, represents the pioneer research activity of an agreed common approach between EASA and FAA.

This research project has made a significant advance in understanding the characteristics and physics of water/ice in aviation fuel at temperature below 0°C. However, there are a number of parameters yet to be investigated (see Appendix B.1). More focused research activities to investigate each parameter in detail should be considered. These research activities are best done through a combination of funded PhD studies and post-doc research studies over a longer duration, i.e. 3 years.

In addition to this research project, FAA has recently funded a graduate assistantship to Thomas C. Maloney at Rutgers, the State University of New Jersey, USA, under the supervision of Dr. Tobias Rossmann [32], to investigate ice accretion in pipes. Mr. Maloney completed his MSc graduate programme in 2012 with a thesis titled "The Collection of Ice in Jet A-1 Fuel Pipes" [35]. In the thesis, Mr. Maloney reported ice accumulation observations of tests performed in a re-circulated fuel system. Tests were done at two stages. In the first stage, the tests were qualitative. They were done to better understand the system and variables that effected the ice accumulation. In the second stage, tests were quantitative. They were done to demonstrate the dependence of temperature, Reynolds number and heat transfer on ice accumulation. The results showed that:

- Accumulation of soft ice was greatest when a layer of hard ice had initially formed on the surface
- There was a lack of a preferential accumulation region downstream of a pipe bend
- Stainless steel pipe collected more ice than Teflon coated pipe
- A greater heat transfer from the pipe increased ice accumulation
- Contamination in the fuel from particles was shown to increase ice accumulation
- Lower flow rates contributed to thicker ice layers

A European Union research project “SAFUEL - The SAfer FUEL system” under the Seventh Framework Programme was launched on September 1, 2012 [33]. The project runs for 36 months. A work package within the project, work package 2 – water & ice management, has two sub-tasks [34]. Sub-task 1 of the work package investigates water detection in fuel for water and ice management. A fibre optic based sensor water detector will be developed, tested and validated to accurately detect and measure the presence of water in a fuel tank. The task is led by Aston University with contribution from Airbus Operations Ltd., Cranfield University and Zodiac Intertechnique.

Sub-task 2 of the work package investigates ice in fuel system. Analysis of the findings and test results will be used to develop a system design rules to identify and minimise the potential impact of fuel ice build-ups in the fuel system. The task is led by Cranfield University with contribution from Airbus operations Ltd., Zodiac Intertechnique and Technische Universitaet Hamburg-Harburg. The key deliverables of the work package are [34]:

- System scale icing test bench
- Report on characterised optical water in fuel sensor technology
- Micro scale investigation test report
- Test bench for ice release and ice accretion in non-accessible areas (e.g. pipes)
- Optical water in fuel sensor prototype
- System scale investigation test report on ice in fuel system
- Report on test results for ice release and ice accretion in non-accessible areas (e.g. pipes)
- Report on test results of optical water in fuel sensor
- Ice predictive modelling tool
- Medium scale investigation test report for icing
- Fuel system design rules for preventing ice hazards

Through Airbus Operations Ltd. and Cranfield University participation in SAFUEL, the research findings and the knowledge gained from WAFCOLT may be passed on and applied in SAFUEL. For an example, darkening of the ViPA field of view reported in Part 1, Section 4.4, of this report, may have an implication to optical sensing. Causes of the darkening have not been categorically identified. Having an awareness of this darkening phenomenon would be helpful when developing the optical sensor. Compensation can be built in the hardware and the software of the sensor to ensure the darkening does not affect the accuracy of the sensor.

Experience and knowledge gained on test rig setup, test rig procedures, ice property measurements (porosity and adhesion strength) detailed in Part 2 of this report would be a valuable input to the icing tests in SAFUEL. The WAFCOLT provided a comprehensive study of fuel icing in a pseudo-static environment and allowed SAFUEL to build on it with fuel icing in a dynamic environment.

The Institution of Mechanical Engineers (IMechE) is holding a one-day seminar on “Managing Water and Ice in Aviation Fuel under Cold Temperatures” on Wednesday 29 May 2013 at the IMechE headquarter in London [36]. The seminar is aimed to

disseminate research findings of the initial research studies in response to the AAIB recommendations. The intension is to share this knowledge with those working in aviation and related industries to advance towards a safer future in aviation. It will provide a good network opportunity to those working on this topic to share ideas and collaborate. Figure 15 shows the provision event details on the IMechE website. The event brochure is given in Appendix D.



**Institution of
MECHANICAL
ENGINEERS**

Improving the world through engineering

Forgotten password? or Not a member?.

Home | About us | Events | Knowledge | Learning and development | Membership and registration | Near you | News | Services

Event

Overview	▶ S1773 - Managing water and ice in aviation fuel under cold temperatures
Prices	1 day Seminar Active Wednesday 29 May 2013
Programme	Institution of Mechanical Engineers
Location	Lecture Theatre 1 Birdcage Walk London
Contact	SW1H 9JJ United Kingdom
Sponsorship and Exhibition Opportunities	
Download Documents	<input type="button" value="Book/Register Now"/>
Download Brochure	Paying by invoice? Please download the event brochure and complete the invoice option.

IMechE Events

Events Home	A recent incident on a twin engine, large, commercial aircraft has led the UK Aviation Accident Investigation Branch (AAIB) to make recommendations towards airworthiness authorities for further research into aspects related to water/ice in fuel. Both the European Aviation Safety Agency (EASA) and the US Federal Aviation Administration (FAA) have agreed a common approach to tackle the AAIB recommendations.
Search	
Basket	EASA launched an initial research project titled "WAFCOLT - Water in Aviation Fuel Under Cold Temperature Conditions" in response to the AAIB recommendations.

MY SHOPPING BASKET

My basket is empty

Overview

A recent incident on a twin engine, large, commercial aircraft has led the UK Aviation Accident Investigation Branch (AAIB) to make recommendations towards airworthiness authorities for further research into aspects related to water/ice in fuel. Both the European Aviation Safety Agency (EASA) and the US Federal Aviation Administration (FAA) have agreed a common approach to tackle the AAIB recommendations.

EASA launched an initial research project titled "WAFCOLT - Water in Aviation Fuel Under Cold Temperature Conditions" in response to the AAIB recommendations.

This seminar will disseminate research findings of the initial research studies in response to the AAIB recommendations. The intention is to share this knowledge with those working in aviation and related industries to advance towards a safer future in aviation.

Attending this event will help you:

- Learn the latest research findings on icing in fuel systems
- Understand the key parameters on ice accretion and growth
- Examine the current and future uses of fuel tank materials to reduce icing risk
- Find out more about icing rig for fuel system testing
- Gain an appreciation and understanding of the risk of icing in fuel systems and the implication that it has on safety
- Appreciate the certification rules and methods of compliance
- Explore design innovation in reducing icing risk in fuel system

Technical Advantages

Delegates:

1. High quality content: update on the latest understanding of the formation and characterisation of ice in aviation fuel from experts
2. Be able to design aircraft fuel systems of reduced icing risk

Employer:

1. Hear from experts on implication on certification compliance
2. Reduce aircraft fuel system icing risk
3. Understand the airworthiness directives and adhere to European legislation

Who should attend

- System engineers
- Fuel engineers
- Aerospace engineers
- Airworthiness engineers
- Airline operators
- Certification engineers

Sponsorship and Exhibition Opportunities

If you have a product or service to promote you can enhance brand awareness through our range of exciting sponsorship / exhibition opportunities.

For details of how we can tailor a package to suit your needs, contact Aman Duggal on:

telephone: +44 (0)20 7973 1309
 email: sponsorship@imeche.org
 or complete the [online form](#)

[Contact us](#) | [Site map](#) | [Site help](#) | [Disclaimer](#)

© 2013 Institution of Mechanical Engineers. IMechE is a registered charity in England and Wales number 206882

Figure 15 A snapshot of the provision event details of the one-day IMechE seminar on “water and ice in aviation fuel under cold temperatures”.

REFERENCES

1. M. Wetterwald, C. P. Lawson and J. K.-W. Lam. *Dehydration of Liquid Fuel*, Patent Application no. GB1012988.0, Intellectual Property Office, UK, 3 August 2010.
2. M. Wetterwald, C. P. Lawson and J. K.-W. Lam. *Feasibility Study of OBIGGS for Water Contamination Control in Aircraft Fuel Tanks*, 10th AIAA Aviation Technology, Integration, and Operations (ATIO) Conference, Texas, USA, 13-15 September 2010.
3. O. Merkulov, V. Zherebtsov, M. Peganova, E. Kitanin, J. K.-W. Lam and A. Satori. *OBIGGS for Fuel System Water Management – Proof of Concept*, SAE 2011 AeroTech Congress & Exhibition, paper no. 11ATC-0084/2011-01-2793, Toulouse, France, 18-21 October 2011.
4. *WAFCOLT Water in Aviation Fuel Under Cold Temperature Conditions – A Literature Review*, edited by J K-W Lam, Airbus Report to EASA under the contract EASA.2010.OP.07, Report no. RP1115500, issue 1, May 2010.
5. J. Downey. *Fuel as a Heat Sink – Review of Current and Past Aircraft Types*, Airbus Technical Report, Report no. X28RP1115934, issue 1, July 2011.
6. R. D. Woods. *Long Range Aircraft Fuel System Icing Risk Investigation – Water Icing in Fuel Summary Test Report*, Airbus Technical Report, Report no. SCF/SYS/P/17/15659, issue 1, April 2011.
7. E. C. Ware, D. M. Schultz, H. E. Brooks, P. J. Roebber and S. L. Bruening. *Improving Snowfall Forecasting by Accounting for the Climatological Variability of Snow Density*. *Weather and Forecasting*, vol. 21, p. 94-103, February 2006.
8. P. J. Roebber, S. L. Bruening, D. M. Schultz and J. V. Cortinas, Jr.. *Improving Snowfall Forecasting By Diagnosing Snow Density*. *Weather and Forecasting*, vol. 18, p. 264-287, April 2003.
9. I. Dubé. *From mm to cm... Study of Snow/Liquid Water Ratios in Quebec*. Meteorological Service of Canada, EWSO, Rimouski, Canada, December 2003.
10. The Engineering ToolBox. *Air – Absolute and Kinematic Viscosity*. http://www.engineeringtoolbox.com/air-absolute-kinematic-viscosity-d_601.html [accessed on 9 November 2011].
11. MetEd. *The Ice-Crystal Process*. http://www.meted.ucar.edu/norlat/snow/micro_ice/1.1.crystal_growth.htm#03 [accessed on 30 November 2011].
12. M. D. Carpenter, J. I. Hetherington, L. Lao, C. Ramshaw, H. Yeung, J. K.-W. Lam, S. Masters and S. Barley. *Behaviour of Water in Aviation Fuels at Low Temperatures*, 12th International Conference on Stability, Handling and Use of Liquid Fuels, Sarasota, USA, October 2011

13. SnowCrystals.com. Your Online Guide to Snowflakes, Snow Crystals, and Other Ice Phenomena . <http://www.its.caltech.edu/~atomic/snowcrystals/> [accessed on 1 December 2011].
14. H. R. Byers. *Elements of Cloud Physics*. University of Chicago Press, 191 pp, 1965.
15. R. Rosenberg. *Why Is Ice Slippery?* Physics Today, p. 50-54, December 2005.
16. B. F. Ryan, E. R. Wishart, and D. E. Shaw. *The Growth Rates and Densities of Ice Crystals between -3°C and -21°C*. Journal of the Atmospheric Sciences, vol. 33, no. 5, p. 842–850, May 1976.
17. Chemical.net. *Toluene Properties*. http://www.chemical.net/home/toluene_chem_prop.htm [accessed on 5 December 2011].
18. *Aviation fuel quality control procedures*, editor J. Gammon, 4th edition, ASTM International, PA, USA, 2009.
19. Advance Petrochemicals Ltd. Fuel System Icing Inhibitor – Dicing. <http://www.advancepetro.com/fsii.htm> [accessed on 8 December 2011].
20. *A Review of the Flammability Hazard of Jet A Fuel Vapor in Civil Transport Aircraft Fuel Tank*, edited by Richard Hill, Report no. DOT/FAA/AR-98/26, Federal Aviation Administration, June 1998.
21. J. K.-W. Lam, F. Tichborne, S. Masters and D. Parmenter. *Aircraft Fuel System*. US Patent Application Publication, Publication No. US 2011/0084171 A1, 14 April 2011.
22. The Engineering ToolBox. *Dielectric Constant of Some Common Liquids*. http://www.engineeringtoolbox.com/liquid-dielectric-constants-d_1263.html [accessed on 9 December 2012].
23. J. H. Jiang and D. L. Wu. *Ice and Water Permittivities for Millimeter and Sub-Millimeter Remote Sensing Applications*. Atmospheric Science Letters, vol 5, p. 146-151, 2004.
24. J. K.-W. Lam, F. Tichborne, S. Masters, D. Parmenter. *Aircraft Fuel Tank Ventilation Having a Dehumidifying Device*. World Intellectual Property Organisation, International Publication No. WO 2011/010124 A1, 27 January 2011.
25. J. K.-W. Lam, D. Parmenter and S. Masters. *Aircraft Fuel Tank Ventilation Having a Dehumidifying Device*. World Intellectual Property Organisation, International Publication No. WO 2011/010123 A1, 27 January 2011.

26. J. K.-W. Lam, F. Tichborne, D. Parmenter and S. Masters. *Coalescing Filter*. World Intellectual Property Organisation, International Publication No. WO 2011/117609 A1, 29 September 2011.
27. J. K.-W. Lam. *Cyclonic Separator*. World Intellectual Property Organisation, International Publication No. WO 2010/103305 A2, 16 September 2010.
28. L. Lao, C. Ramshaw, H. Yeung, M. D. Carpenter, J. I. Hetherington, J. K.-W. Lam and S. Barley. *Behavior of Water in Jet Fuel Using a Simulated Fuel Tank*. SAE 2011 AeroTech Congress & Exhibition, paper no. 11ATC-0156/2011-01-2794, Toulouse, France, 18-21 October 2011.
29. CRC. *Handbook of Aviation Fuel Properties*, 3rd Edition. CRC Report No. 635, 2004.
30. A. B. Crampton, R. F. Finn and J. J. Kolfenbach. *What Happens to the Dissolved Water in Aviation Fuels?* SAE Summer Meeting, Atlantic City, New Jersey, USA, 7-12 June 1953.
31. K. G. Libbrecht. *The Physics of Snow Crystals*. Reports on Progress in Physics, vol. 68, no. 4, p.855-895, 2005.
32. T. Rossmann. *Private Communication*, at the SAE 2011 AeroTech Congress & Exhibition, Toulouse, France, 18-21 October 2011.
33. *EU research project: SAFUEL – The SAfer FUEL system*:
<http://cordis.europa.eu/projects/index.cfm?fuseaction=app.details&TXT=safuel&FRM=1&STP=10&SIC=&PGA=&CCY=&PCY=&SRC=&LNG=en&REF=104057>
[accessed on 18 March 2013].
34. *SAFUEL – The SAfer FUEL system, Annex I – Description of Work*, Project no. 314032, call (part) identifier FP7-AAT-2012-RTD-1, April 2012.
35. Thomas C. Maloney. *The Collection of Ice in Jet A-1 Fuel Pipes*, FAA Technical Thesis, DOT/FAA/TC-TT12/29, July 2012. <http://www.fire.tc.faa.gov/pdf/TC-TT12-29.pdf>
36. *S1773 – Water and ice in aviation fuel under cold temperature*, 1-day seminar, Wednesday 29 May 2013, Institution of Mechanical Engineers, London, UK. <http://events.imeche.org/EventView.aspx?EventID=1910> [accessed on 18 March 2013].

Appendix A: Response to Comments on the Literature Review – RP1115500, Issue 1

APPENDIX A RESPONSE TO COMMENTS ON THE LITERATURE REVIEW – RP1115500, Issue 1

#	Part	Page	Section	Other Identification	Comment	Recommendation	Response	Status
1	1	12	2.4	Conventional Jet Fuel – Impurities and contaminants	In real life fuel are not perfect as in laboratory conditions or even at early stage delivery from the refining, how is considered into the proposed testing activities the natural 'contamination' effect for ice formation? For instance the fuel on the BA B777 event may fall into this category.		Very difficult to assess effects of liquid constituents/contaminants, due to the large number of different chemical species which are found in kerosine in trace amounts and in different proportions. Might be able to assess indirectly for a particular fuel, e.g., by use of KF tests (which is part of the current test programme) but tests would need to be carried out on a large number of samples from that source to obtain meaningful data. Bacteria and other fine particulates are believed to pay a part in ice particle nucleation, but it is difficult to replicate these additions in a lab situation.	

#	Part	Page	Section	Other Identification	Comment	Recommendation	Response	Status
2	1	16	2.5	Jet Fuel Additives	Among the list of additives the most interesting, within the frame of the icing scope of the study, is the consideration of FSII.	Add	<p>Agree that FSII is interesting, but really outside the scope of the current project (time/money constraints).</p> <p>FSII is a jet fuel additive. It is added to the fuel at about 0.10% to 0.15% by volume at refuel. It is not widely used by commercial operators.</p> <p>FSII potentially can offer a solution to reduce the risk of icing in aircraft fuel systems. Its pros and cons have been discussed in the final report.</p>	
3	1	17	2.6		<p>A second synthetic fuel spec has been approved by ASTM (D7566) as drop-in fuel (max 50pc): hydro-processed ester and fatty acids (HEFA) SPK is the official name.</p> <p>Summary of changes to D7566 added in an attachment.</p>	Update	<p>This fuel spec was not approved at the time the literature review was prepared, but details of the new specification can be added.</p> <p>The rationale for the revision of the fuel spec is given in Appendix A.1 of this report. An up issue of the Literature Review is not planned.</p>	
4	1	20	3.1	Solid Phase of Water	Ic for "cubic ice" is not represented on the chart.	Add	A new water phase diagram is given in Appendix A.2 of this report. An up issue of the Literature Review is not planned.	

#	Part	Page	Section	Other Identification	Comment	Recommendation	Response	Status
5	1	23	3.3	Formation of Ice	Is the literature from [8] And [9] dealing for ice formation in air, in liquids or specifically in fuel? Are there any variations from the surrounding environment of the water that affect the ice formation?	If any consideration to this aspect, then I suggest to make a specific paragraph on it.	<p>These references mostly relate to ice formation in air and water. Not specifically fuel-related, although crystal formation processes are believed to be similar. Factors important to ice formation include ambient temperature, rate of heat abstraction, degree of agitation, solution thermal conductivity and the presence of nucleating particles.</p> <p>Literature on ice formation in other fluid media is limited and not well studied.</p> <p>In this report, characteristics of snow in fuel were discussed in detail. The variability of the snow-to-liquid ratio (SLR) of snow in fuel and of atmosphere was compared. The effect of the fluid medium on SLR was discussed.</p>	

#	Part	Page	Section	Other Identification	Comment	Recommendation	Response	Status
6	1	23	3.3	Formation of Ice	<p>There is no specific cross reference to the conditions of the B777 event in terms of free water / dissolved / entrained water assumed to be present from samples testing, thermal modelling and estimation of moisture from fuel venting. In general a paragraph could be dedicated to a comparison of conditions of water icing in fuel between a) what has been found in literature and b) event. Were there any conditions already explored? Are fuel/water data from science literature and scientific experiments far away from the fuel/water data practically and realistically encountered on the B777 event?</p>		<p>Regarding the B777 event, the probable cause was believed to be due to ice accretion/release/FOHE blockage; this was simulated in large-scale fuel system tests, but the exact cause cannot be categorically known.</p> <p>Boeing experienced difficulties in maintaining the required concentration of water in the fuel during lab tests (artificial nature of SAE ARP 1401 and AIR790C?); they had to try very hard to create ice and anything that might resemble a fuel system blockage. This may be due to a misunderstanding about what conditions are critical to ice formation (points to need for fundamental research) or that simulation test rigs do not accurately represent real-life conditions.</p>	

#	Part	Page	Section	Other Identification	Comment	Recommendation	Response	Status
7	1	23	3.3	Formation of Ice	<p>There is no specific consideration of the existing aircraft requirement for certification to fulfil (for large airplanes) the CS 25.951e (see below). Is there any consideration for the water contents relevant versus the literature review?</p> <p>FUEL SYSTEM CS 25.951 General (a) Each fuel system must be constructed and arranged to ensure a flow of fuel at a rate and pressure established for proper engine functioning under each likely operating condition, including any manoeuvre for which certification is requested and during which the engine is permitted to be in operation. (b) Each fuel system must be arranged so that any air which is introduced into the system will not result in –</p> <p style="text-align: right;">.../cont.</p>		<p>In FAA FARs, Part 25, Section 971 – Fuel tank sump, it states that:</p> <p>“(a) Each fuel tank must have a sump with an effective capacity, in the normal ground attitude, of not less than the greater of 0.10% the tank capacity or 1/16 of a gallon unless operating limitations are established to ensure that the accumulation of water in service will not exceed the sump capacity.”</p> <p>For a tank of, say, 1,000 ltr (1,000,000 cm³) capacity, the sump would be 1 ltr (1,000 cm³). If the sump is full of water and the water is mixed with the fuel, the concentration of free water in fuel is about 1 cm³ of free water per litre of fuel, i.e. 1000 ppm. This concentration of free water is much higher than the requirement in CS 25.951.</p> <p style="text-align: right;">.../cont.</p>	

#	Part	Page	Section	Other Identification	Comment	Recommendation	Response	Status
					<p>.../cont.</p> <p>(1) Reserved. (2) Flameout. (c) Each fuel system must be capable of sustained operation throughout its flow and pressure range with fuel initially saturated with water at 26,7°C (80°F) and having 0.20 cm³ (0.75 cc) of free water per liter (US gallon) added and cooled to the most critical condition for icing likely to be encountered in operation.</p>		<p>.../cont.</p> <p>Depending on the fuel composition, the saturated dissolved water content of kerosines will be around 60 ppm by volume of water at 27°C for a typical Jet A-1 fuel. With the addition of 200 ppm free water, the total water content will be around 260 ppm by volume.</p> <p>R. Langton et .al., 'Aircraft Fuel Systems', Wiley, 2009, p51, suggests that fuels systems and engines should be able to cope with 600 ppm water (but not necessarily under icing conditions).</p> <p>It is not clear how the certification requirements were derived; possibly proposed as realistic limits that could be addressed by current systems?</p>	

#	Part	Page	Section	Other Identification	Comment	Recommendation	Response	Status
8	1	38	4.4		Identify which methods are standardised and when available the reference ASTM doc.	A brief discussion of strengths/weaknesses (and magnitude of required times and costs) for each test would be helpful.	A brief discussion of the sensitivities, i.e. water detection levels, of the methods has been given in Section 4.4 of the Literature Review. Further detail is contained in Appendix A.3 of this report.	

#	Part	Page	Section	Other Identification	Comment	Recommendation	Response	Status
9	1	14	2.4.2	Sulphur Impurities	There is a recommendation at the end of this paragraph as for §2.5 – 2.6 – 3.1 .Please at a table at the end of the literature review for Part 1 which each recommendation and proposed activity to comply with the recommendation.	Add	<p>These are all wish-list items; it is difficult to procure small quantities of aviation fuels and extremely difficult to procure fuels with the specified characteristics.</p> <p>§2.4.2: Regarding sulphur in fuels, it is very difficult to obtain fuels with specified sulphur levels. Jet A-1 specification max is 3000 ppm, but kerosines are typically supplied with a sulphur content of ~500 ppm. Fuels for the current test programme range in sulphur content from <100 ppm to <1000 ppm.</p> <p>§2.5: SDA is often added to fuels before dispatch for safety reasons - may be difficult to obtain fuel without SDA. Lubricity additive is also of interest, but is usually added to fuels with low sulphur content, e.g., those with large proportions of hydroprocessed or synthetic constituents.</p> <p style="text-align: right;">.../cont.</p>	

#	Part	Page	Section	Other Identification	Comment	Recommendation	Response	Status
							<p>.../cont.</p> <p>§2.6: n-octane, methylcyclohexane and toluene are available (representing n-paraffins, cycloparaffins and aromatics respectively) for such tests within this programme.</p> <p>§3.1: This is interesting, but well outside the scope of the current programme. Cranfield does not have the equipment to evaluate the presence of ice Ic, so it is difficult to know whether we are actually observing ice Ic or ice Ih.</p> <p>A MPhys (Master of Physics) project with the University of Bristol to investigate the crystalline structure of ice in fuel has been proposed by Airbus. The project will use electron scattering technique to identify the crystalline structure. The project is proposed to start in October 2012.</p>	

#	Part	Page	Section	Other Identification	Comment	Recommendation	Response	Status
10	2	53	1.2		Role of fuel heaters in engines (oil to fuel exchangers) is not addressed.	Add	The primary function of FOHE is to cool the engine oil. As oil is pumped around in the engine lubricating gears, bearings, valves and other components, its temperature rises. To make sure the oil stays within the operating limits, it will need to be cooled by running it through an oil cooler. Fuel is used as a coolant in the oil cooler (FOHE) because it is a convenient heat sink. As a side effect, fuel is warmed by the oil in the FOHE. Any ice particles suspended in the fuel will be melted and thereby reduce the risk of blockage in the engine fuel system.	

#	Part	Page	Section	Other Identification	Comment	Recommendation	Response	Status
11	2	56-57	2.1.2		Is there any literature on the shape effect of the surface (flat, curved, ...) ?.		<p>The shape and the fluid dynamics effects are closely linked. There are a number of literature in the field of wing icing.</p> <p>The shape and the fluid dynamics affect the flow stream and play a primary role in wing icing since the density ratio of water to air is close to 1000. Water droplets moving with an airflow stream would have relatively large momentum inertia. They cannot change their motion (i.e. accelerate, decelerate and change direction) in the same way as air. As a result, the water droplets do not follow the airflow stream and are found frequently impinging on the surface if there is a change in the airflow stream.</p> <p>However, the effects of shape and fluid dynamics are small for water droplets in fuel. This is because the density ratio of water to fuel is close to 1. Water droplets in fuel would follow the fuel flow stream very closely.</p> <p>.../cont.</p>	

#	Part	Page	Section	Other Identification	Comment	Recommendation	Response	Status
							<p>.../cont.</p> <p>The frequency of water droplets impinging on the surface in a fuel flow is likely to be very small.</p> <p>From a previous project, Airbus Fuel and Inerting R&T WISDOM, it has been identified that the primary mechanism of ice accretion in a fuel tank is through the Bergeron process. This process takes place in the boundary layer and is therefore independent of the shape and fluid dynamics effects to certain extent.</p>	
12	2	56-57	2.2.2		Is there any literature on the fluid dynamics effect?		See previous response.	
13	3	71		Part 3 Title	The term 'miscellaneous topics' is too broad.	Suggest to rename 'Additional topics related to water/ice in jet fuel'	Since the project title is "WAFCOLT – Water in Aviation Fuel Under Cold Temperature Conditions", the subtitle "Miscellaneous Topics" implies additional topics related to water in jet fuel at cold temperature conditions. It was therefore felt not necessary to echo the project title in the subtitle.	

#	Part	Page	Section	Other Identification	Comment	Recommendation	Response	Status
14	3			General	<p>Is there any leverage to be taken for the phenomenon understanding from a) the Long Range in-service occurrences (similar events to the B777) and b) from the on-going activities associated to the in-service corrective actions?</p> <p>Is there any leverage to be taken for the phenomenon understanding from the activities on-going for the A350XWB certification (CRI Special Condition) ?</p>	<p>It is EASA objective for the research project to have an exhaustive and comprehensive view on the ice/water in fuel by taking any leverage from data sourcing either from universities, testing laboratories, industrial, supplier, research centre, national airworthiness authorities and investigation bodies. This list is far from being exhaustive.</p>	<p>Airbus and Cranfield appreciate the EASA's aspiration for the project. Airbus and Cranfield would do our best with limited time and limited budget to achieve this aspiration.</p> <p>Many organisations are very protective of data that they have, particularly if they have invested money and time to obtain the data. As such they are not always willing to share proprietary data with us.</p> <p>Some Airbus water/icing test data have been presented in Part 3 of this report.</p>	

Appendix A.1 Rationale For The Recent Revision To ASTM D7566



Standards Worldwide - Home

Other Languages

[Login](#) | [Home](#) | [About ASTM](#) | [Site Map](#) | [Support](#) | [Contact](#) | [Web/IP Policies](#) | [Copyright/Permissions](#)



ASTM WK30833

[\(What is a Work Item? / How to Input to a Work Item\)](#)

Work Item: ASTM WK30833 - Revision of D7566 - 10a Standard Specification for Aviation Turbine Fuel Containing Synthesized Hydrocarbons

Active Standard: D7566 - 11a

Developed by Subcommittee: [D02.J0.06](#) | Committee [D02 Home](#) | Contact [Staff Manager](#)

More D02.J0.06 Standards

Copyright/Permissions

Related Products

Work Item Status:

Date Initiated: 10-29-2010

Technical Contact: George Wilson

Item: 005

Ballot: D02 (11-04)

Status: Ballot Item Approved as D7566-2011 and Pending Publication

[Standards Tracker](#)

[Standards Subscriptions](#)

1. Rationale

ASTM D7566-09 Specification for Aviation Turbine Fuels Containing Synthesized Hydrocarbons was issued in September, 2009. This specification was issued in response to the demand expressed by the USAF and commercial operators of turbine engine powered aircraft for alternatives to conventional petroleum-derived jet fuel. The commercial aviation industry established the Commercial Aviation Alternative Fuels Initiative (CAAFI) in 2006 to facilitate the introduction of these alternative aviation fuels. The USAF, CAAFI, and ASTM Subcommittee J (Section J.06) have been coordinating the evaluation and qualification of candidate alternative fuels. The initial version of this specification included Fischer-Tropsch (FT) hydroprocessed synthesized paraffinic kerosenes (SPK) as the first approved synthetic blending component in Annex A1. An initial ballot to add Annex A2 to incorporate Bio-SPK (or HRJ) as a second approved hydroprocessed SPK blending component was circulated to Subcommittee J in May, 2010. The ballot identified these blending components as hydroprocessed SPK from fatty acid esters or free fatty acids. This ballot was withdrawn due to the submittal of seven negative votes. The inclusion of the hydroprocessed SPK from fatty acid esters or free fatty acids blending component is based on an evaluation of those blending components from six different producers using a variety of feedstocks. The evaluation was conducted in accordance with ASTM D4054-09 Standard Practice for Qualification and Approval of New Aviation Turbine Fuels and Fuel Additives to ensure that fuel blends containing these synthetic components would not adversely impact turbine engine safety, durability, or performance. This evaluation was summarized in ASTM Research Report, Evaluation of Bio-

Product Information

[Get Product Updates](#)

[Request a Free Catalog](#)

[View Catalog](#)

 **RSS News Feed**



Derived Synthetic Paraffinic Kerosenes (Bio-SPKs), prepared by The Boeing Company/UOP/United States Air Force Research Laboratory (AFRL), Version 5.0, May - 2010, ASTM RR D.02:xxxx, that was included in an accompanying ballot. That ballot passed and the Research Report will be filed with ASTM. Since that initial ballot, these blending components have been re-identified as Hydroprocessed Esters and Fatty Acids (HEFA) SPKs. This ballot is intended to address the comments received during the initial ballot. The following is a summary of key changes incorporated into this ballot: The draft specification has been revised to add two new requirements for the HEFA blend component in Table A2.1. These new requirements; existent gum and FAME, are intended to protect against impurities and trace materials that might result from unanticipated process or feedstock issues. Test method D86 (physical distillation) has been specified for distillation criteria for both FT-SPK and HEFA-SPK. Simulated distillation (D2887) remains as a report only criteria for each. The scope of D2887 is not appropriate for narrower boiling range fuels and the conversion to D86 equivalent values has been found to be inaccurate. The Other Detailed Requirements specified in Table A2.2 will be required to be verified on a batch basis, with the intent to transition this to a management of change basis upon gaining more production experience. A section has been added to section 6. Materials and Manufacture, and to Appendix X2 to address concerns with quality control of the synthetic blend components during distribution.

Keywords

aviation turbine fuel; avtur; Jet A; Jet A-1; jet fuel; synthesized hydrocarbons; synthesized paraffinic kerosene; synthetic blending component; turbine fuel; Aviation turbine fuels; Synthesized hydrocarbons; Turbine fuels;

[Citing ASTM Standards](#)

[\[Back to Top\]](#)

[Home](#) | [About ASTM](#) | [Site Map](#) | [Support](#) | [Contact](#) | [Web/IP Policies](#) | [Link to Us](#) | [Copyright/Permissions](#)

[Construction Standards](#) - [Petroleum Standards](#) - [Steel Standards](#) - [Plastics Standards](#) - [Environmental Standards](#) - [Metals Standards](#) - [Rubber Standards](#) - [Textiles Standards](#) - [Paint Standards](#) - [Nuclear Standards](#)

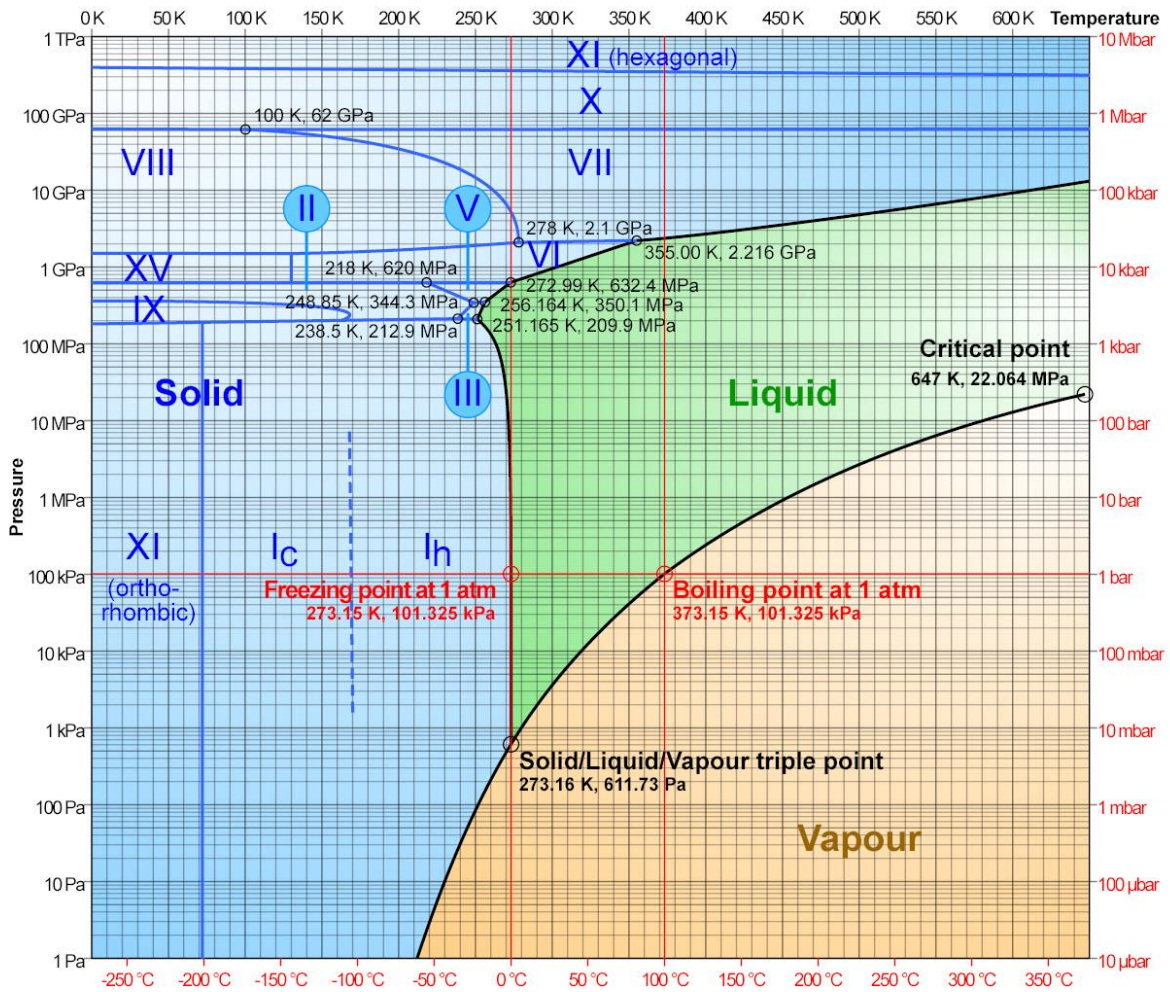
[facebook](#) [YouTube](#) [twitter](#)

Copyright © 1996-2011 ASTM. All Rights Reserved.

ASTM International, 100 Barr Harbor Drive, PO Box C700, West Conshohocken, PA, 19428-2959 USA

Source: <http://www.astm.org/DATABASE.CART/WORKITEMS/WK30833.htm>
[accessed on 5 December 2011].

Appendix A.2 Water Phase Diagram



A water phase diagram with the Ic “Cubic Ice” phase clearly shown on it.

Source: <http://icestructure.com/2011/ice-water-phase-diagram/>
 [accessed on 2 December 2011]

Appendix A.3 Methods Of Detecting Water In Aviation Fuel

Outline details of water monitoring methods were given in Section 4.4 of the Literature Review for the WAFCOLT programme (Airbus report no RP1115500, Issue 1). All of the tests assume that a representative sample of fuel can be acquired and that the sample has not been contaminated by the collection method or sampling container. Tests which use water-detecting pads or capsules are particularly sensitive to atmospheric contamination in humid weather or due to water droplets from rain, sneezing or coughing. Some of the tests require in-line analysis, whilst others require tests on a discrete sample of fuel. For all tests, the operator should wear appropriate personal protective equipment, such as PVC gloves and eye protection. The list below gives details of equipment that is currently available in the UK; price data was that prevailing in December 2011.

Appendix A.3.1 Aqua Glo

The Aqua Glo Series V water detector (model GTP-322) is available as a portable kit for field or lab use. It can operate from internal batteries or an external power source. The most reproducible results are achieved by in-line sampling of fuel. The equipment is instrumented 'to eliminate human error', but the operator will need training in order to achieve consistent results. The actual test takes about 2 minutes, but additional time is required for setting up, making connections and cleaning the equipment. One water detector pad is required per test; test pads have a finite life and need to be checked before use to ensure they have not deteriorated in storage. Tests should be conducted in accordance with ASTM D3240-10. The instrument can be user-calibrated using a 'calibrating standard'.

GTP-322 kit	£1968.00
Water detector pads, GTP-25	£62.96 (box of 50)
Other accessories and consumables are available	

Appendix A.3.2 Shell Water Capsule

The Shell water detector is a simple, low cost laboratory or field test that requires no power and requires minimal operator training. Care needs to be taken in sampling fuel to avoid contamination and/or inadvertent water pick-up. Apart from the detector capsule, the only other items required are a 5 ml syringe and a clean glass or metal sampling container. The test takes less than 30 s and the result, a simple go/no-go test, can be assessed immediately. One water capsule is required per test; test capsules have a finite life and need to be checked before use to ensure they have not deteriorated in storage. Tests should be conducted in accordance with the kit instructions - there is no test standard governing their use. No user calibration is possible since the capsules are one-off use devices.

Shell Water Capsules	£36.00 (box of 80)
----------------------	--------------------

Appendix A.3.3 Karl Fischer Coulometry

Karl Fischer (KF) coulometric titration is a long-established method of measuring water in many types of materials. Suitable equipment is available from various suppliers but Metrohm and Mettler Toledo are probably the two best-known brands in this field. Sigma Aldrich maintain the widest range of KF chemical consumables under their Hydranal brand, but some anolytes and catholytes are available from other suppliers. Of the tests for water listed in the Literature Review, this is the most accurate, but care needs to be taken in acquiring and sampling fuel if optimum precision is to be achieved. It is a laboratory test only and the operator will need to be trained in the safe handling of chemicals, as well as experienced in operating the coulometer. The chemical consumables are sensitive to background moisture and will require replacement at regular intervals. Each test takes about 10 - 15 minutes, allowing time for sampling, injection and instrument settling. A clear digital reading of the water content is given. The combined operator and instrument precision can be checked by the use of calibrated water standards. There are a number of test standards covering the use of KF coulometers, but the most relevant in the context of fuel testing are ASTM E203-08 and D6304-07. The instrument can be user-calibrated using calibrated water standards. A range of extras is available to increase the flexibility of the basic unit.

Typical basic hardware (Metrohm 831KF)	£4500.00
Chemical consumables (typical cost per test)	£2.00 – 3.00

Appendix A.3.4 Microseparator Test

This test is based around the Emcee Model 1140 Microseparator. It is supplied as a portable kit for field or laboratory use. It is normally operated from mains electricity, but can be used with an internal battery pack. The test evaluates the water shedding characteristics of a discrete sample of fuel; like the previous tests, care should be taken not to contaminate the fuel sample. The equipment is designed to minimise human error, but the operator will need training in order to achieve consistent results. The actual test takes about 5 minutes, but additional time is required for setting up, making connections and cleaning the equipment. Coalescing filter elements are available in standard (Alumicel) and MCell variants; the latter coalescer is more suited to testing fuel with low surfactancy properties. One set of consumables is required per test. The test produces a numerical (MSEP) rating that relates to the likelihood of a particular fuel deactivating a filter-separator element. Test standards are ASTM D3948-11 for fuels with strong surfactancy properties and ASTM D7224-08 for fuels with weaker surfactancy properties. The instrument should be recalibrated annually.

Model 1140	£12840.00
Annual recalibration	£695.00
Consumables (either Alumicel or MCell)	£141.00 (for 6 tests)

Appendix A.3.5 Particle Counting Techniques

There are various instruments that are capable of detecting and measuring particles in fluid streams, but the ones currently approved for use with aviation fuels are supplied by Parker Hannifin and Stanhope Seta. Both firms offer variants of their basic design, some of which are detailed below. The equipment is suitable for lab or field use and can be operated via internal batteries or mains electricity. One version of the Parker design is ATEX rated for explosive and hazardous area use. The equipment is normally intended to be operated with discrete samples of fuel, but high pressure in-line versions of the test equipment are available. The units measure particulates in the fluid flow and categorise measurements into the following size bands: >4 µm, >6 µm, >14 µm, >21 µm, > 25 µm, >30 µm; the Stanhope AvCount2 offers additional particulate bands to >200 µm to meet GOST 17216-71. The Parker units claim to complete a test within 2 minutes whilst the Stanhope units typically take less than 6 minutes; however, realistically, both units will take longer than this when allowing for setting up and cleaning down afterwards. As with the other tests, care needs to be taken in obtaining and preparing fuel samples for analysis and both systems will require a fair degree of operator training in order to achieve the most consistent results. Test standards include ASTM D7619-10, IP 564 and IP-565. The Parker units should be recalibrated by the manufacturer once a year whilst Stanhope supplies 'Verification Fluid' and 'Calibration Fluid' if the user wishes to carry out calibration themselves. Both systems offer a number of accessories to suit end-users operational requirements. Apart from recalibration consumables and occasional replacement parts that have been in contact with the fuel, no other consumables are required for operation of these units.

Parker Hannifin ACM20	
ACM202024UK (lab use)	£9394.00
ACM202032UK (explosive and hazardous areas)	£12342.00
Annual standard recalibration	£635.00
Stanhope Seta AvCount	
AvCount	£11320.00
AvCount2 (newer model, more flexible)	£11148.00
AvCount Calibration Fluid (250 ml)	£315.00
AvCount Verification Fluid (250 ml)	£215.00

Appendix B: Response to Comments on the Proposed Work Programme – PL1101812, Issue 1

APPENDIX B RESPONSE TO COMMENTS ON THE PROPOSED WORK PROGRAMME – PL1101812, Issue 1

#	Part	Page	Section	Other Identification	Comment	Recommendation	Response	Status
1	Summary	3	General	New paragraph	Proposed Work Programme does not provide a compliance matrix between the Literature Review and the proposed Testing Activities. Table should identify which areas need to be investigated (from literature review) and show how the proposed testing will fulfil the objective.	Add	A compliance matrix is given in Appendix B.1.	
2	1	6	1	Introduction	A clear test objective shall be stated. Expected outcomes shall be detailed. Anticipated limitations of the test: conduction, results,...	Add	<p>It is felt that the “Introduction” is OK as it stands.</p> <p>Since there are a number of tests and each test requires different test equipment and procedure, it was felt that the “Introduction” would not be an appropriate place to provide details of expected outcomes, limitations of the test and procedures. These were described in detail in separate sections.</p>	

#	Part	Page	Section	Other Identification	Comment	Recommendation	Response	Status
3	1	6	2	First paragraph	Report is mentioning 'there is no guarantee about how a particular fuel has been processed'. It is now unclear in which basis a fuel can be stated "severely hydroprocessed" vs Merox vs hydroprocessed". Team has to demonstrate how is verified that actual fuel composition is matching the foreseen category. Objective being to avoid drawing conclusion on a category of fuel without knowing to which category it actually belongs.	Add a paragraph on Fuel composition verification	<p>The paragraph is factually correct. We rely on the oil companies to detail how a particular batch has been processed and it is not possible to identify exactly how a fuel was processed by retrospective analysis.</p> <p>Fuel composition variations, even from one refinery, are inevitable, because refineries process vast quantities of fuel and buy in crude oils from lots of different sources to maximise their operating profit.</p> <p>It is extremely difficult to obtain, e.g., 'pure' Merox or 'pure' hydroprocessed fuels for experimental purposes.</p>	

#	Part	Page	Section	Other Identification	Comment	Recommendation	Response	Status
4	1	7	3	First paragraph	Paragraph focuses on fuel saturated with water. Is there any attempt to cover also the problematic of free water on top of the dissolved water?	To comment	<p>No.</p> <p>Previous work looked briefly at settling fuel/water emulsions, but this aspect was not intended as part of this programme. For test purposes, fuels saturated with water at a known temperature are easier to replicate than a particular water content. It represents a worst case situation in, say, a tropical environment. Fuel should be passed through a water coalescer, to remove free water, and tested to ensure that the free water is less than 30 ppm before loading on an aircraft. Free water at point of loading should not be an issue, providing loading procedures are followed correctly.</p> <p>Free water as a result of ineffective water management system and procedure may vary considerably. It is not clear what level of free water is representative.</p> <p>Further comments may be found under Item 7 in Appendix A.</p>	

#	Part	Page	Section	Other Identification	Comment	Recommendation	Response	Status
5	1	7	3	Last paragraph	EASA confirms that added value of investigating impact of very fine particles on ice crystals. Consideration of additives may focus on FSII.	Add	FSII is not included in the test programme. It is desired to complete the main test programme before (possibly) tackling the tasks outlined in this paragraph in the limited time and budget.	
6	1	9	5	Particle size analysis	A focus in the range of "sticky" freezing (0 / -20°C) shall be given during testing.	Add	Test results will include this range of interest.	
7	1	10	6	Other research Equipment	EASA confirms the utility to look at phase changes, separation and freezing characteristics of free water and fuel constituents especially at the "sticky" range transition (in-out)	Add	Interesting, but there are time/money constraints. Would only follow up with these tests if unusual or unexplained test results are encountered.	
8	2	13	1	Introduction	A clear Test objective shall be stated. Expected outcomes shall be detailed. Anticipated limitations of the test : conduction, results,...	Add	See Appendix B Item 2.	

#	Part	Page	Section	Other Identification	Comment	Recommendation	Response	Status
9	2	16	3	Methodology	a. The range of temperature to be detailed b. Is there any consideration to investigate free water injection effect? c. Is there any consideration to investigate The dynamic effect?	Add	<p>Pioneering research was proposed to study the ice strength and ice porosity in fuel. The experimental techniques, test equipment and procedures were still under development at the time of writing of the Proposed Work Programme, therefore it was not possible to provide details at that stage.</p> <p>During the test phase, the experimental techniques, test equipment and procedures had developed to maturity. They are detailed in this report.</p>	
10	2	16	3	Methodology	A more realistic fuel, with impurities/particles shall also be evaluated for ice accretion behaviour, on top of the top "extreme" fuels.	Add	<p>Fuel specifications tightly limit impurities and particles in fuel. However, during transportation and storage, impurities and particles could be picked up. The variability of impurities and particles is large.</p> <p>It is extremely difficult to define a realistic fuel for experimental purposes.</p> <p>See Appendix A Item 1 and Appendix B Item 4 for supplementary comments supporting this response.</p>	

#	Part	Page	Section	Other Identification	Comment	Recommendation	Response	Status
11	2	17	3.2	Ice strength and porosity	a. Methods to be detailed. b. Investigation on water/fuel ice proportion shall also be considered.	Add	See Appendix B Item 9.	

Appendix B.1 Compliance Matrix Between The Literature Review And The Proposed Testing Activities

The part, the page and the section in columns 2, 3 and 4, respectively, in the table below reference to the Literature Review [4].

#	Part	Page	Section	Proposed Parameters To Be Investigated	Proposed Testing Activities
1	1	12	2.3.1	<p>Jet fuel hydrocarbon composition</p> <p>It is important to quantify the effect of the concentrations of different hydrocarbon types in the fuel in dissolving and releasing water over the temperature range experienced in aircraft flight.</p>	Effect of aromatics and various national standards of jet fuels are investigated.
2	1	13	2.4.1	<p>Surfactant contamination</p> <p>Surfactants play a significant role in water stabilisation, droplet formation, and water detection tests in jet fuel. It is probable that surfactants will influence the formation of ice in the fuel. Studying the effect of specific surfactant contaminations such as biodiesel and phenols is recommended.</p>	Not investigated.
3	1	14	2.4.2	<p>Sulphur impurities</p> <p>High and low sulphur fuels should be studied to see if sulphur levels have a significant effect on water shedding, droplet formation and ice formation.</p>	Not investigated.

#	Part	Page	Section	Proposed Parameters To Be Investigated	Proposed Testing Activities
4	1	16	2.5	<p>Jet fuel additives</p> <p>Fuels should be studied both without static dissipater additive (SDA) and with well-characterised amounts of SDA to separate out effects due to fuel composition and operating conditions from additive effects. The effects on water shedding of other additives, in particular the lubricity additive, should similarly be investigated.</p>	Not investigated.
5	1	17	2.6	<p>Semi-Synthetic and Wholly Synthetic Aviation Fuels</p> <p>The solubility of water, droplet formation and ice formation should be studied in model hydrocarbons representing the four types of hydrocarbons found in jet fuel: n-paraffins, iso-paraffins, cycloparaffins, and aromatics.</p>	<p>Not investigated.</p> <p>The solubility of water, droplet formation and ice formation in Toluene (aromatics) have been reported in [12].</p>
6	1	20	3.1	<p>Solid phases of water</p> <p>The significance of phase changes between ice Ic and Ih to ice deposits in fuel systems should be investigated.</p>	Not investigated.
7	1	21	3.2	Clathrates	Not Investigated.
8	1	26, 31	3.5 & 3.6	<p>Growth of ice</p> <p>The crystalline habit of ice grown depends on the degree of supercooling, supersaturation over ice and the type of nucleation.</p>	Effect of cooling rate, degree of supercooling and type of nucleation were investigated.

#	Part	Page	Section	Proposed Parameters To Be Investigated	Proposed Testing Activities
9	1	32	3.7	<p>Effect of gases and vapours</p> <p>The presence of organic vapour can significantly influence the growth habit of ice crystals.</p>	Not investigated.
10	1	32	3.8	<p>Effect of electric fields</p> <p>It has been shown that ice grow habits may be modified in the presence of applied electric fields.</p>	<p>Not investigated.</p> <p>It is unlikely that the electric field strengths within an aircraft fuel system would be of a magnitude to cause a change.</p>
11	1	34	4.2	<p>Free water</p> <p>Water can be present in jet fuel as free water or dissolved water.</p>	Not investigated.
12	1	35	4.3	<p>Dissolved water</p> <p>Water can be present in jet fuel as free water or dissolved water.</p>	Dissolution of dissolved water in fuel as the fuel is cooled and subsequent freezing of the free water from dissolution are investigated.
13	1	46	4.6.2	<p>Fuel systems icing inhibitor</p> <p>Fuel systems icing inhibitor (FSII) is a potential solution to prevent icing in fuel.</p>	<p>Not investigated.</p> <p>The effect of FSII has been studied by DeWitt and Zabarnick (2009).</p>
14	2	54	2	Ice on subcooled surfaces in fuels	Effect of bare aluminium surface, painted aluminium surface and composite surface on ice characteristics and adhesion strengths were investigated.

Appendix C: Test Fuels – Chemical & Physical Data Analysis Reports



Appendix C.1 Air BP Filton Airfield Jet A-1



SGS Oil, Gas and Chemicals
Old Time Building,
Junction Cut, Royal Edward Dock,
Avonmouth, Bristol, BS11 9DH
Tel: +44 (0) 117 937 9080
Fax: +44 (0) 117 937 9081

JET A1 - FULL TEST REPORT
Test Certificate No: AV11-00069.004

PRINT DATE: 21/06/2011

AIR BP UK LTD
GROUND FLOOR, BUILDING D
CHERTSEY ROAD
SUNBURY ON THAMESTW16 7LL

PRODUCT DESCRIPTION:	Jet A1	CLIENT ID:	HAL169	LOCATION:	Hallen
SAMPLE RECEIVED:	20/06/2011	SAMPLE BY:	BIS014	DATE SAMPLED:	20/06/2011
SAMPLE TYPE:	Composite	SAMPLE SOURCE:	Ex Tk25	SOURCE ID:	Tank 5
AIR BP SAMPLE REF:					

	Batch Number	Quantity	Test Certificate Number	Location	Static Dissipator
HEEL	HAL152K	783.800 m ³	Av11.0069.001	Ex Tk26	1.3 mg/l
NEW1	HAL162K	5008.900	Av11.0075.002	Tk25	0.0

	Batch Number	Quantity	Client Seal No.
BATCH	BIS/HAL/11/168	5792.700	BIS014

PROPERTY - AV11-00069.004	Units	MIN	MAX	METHOD	RESULT
Appearance	---	--	--	Visual	C+B
Clear, bright & visually free from undissolved water & particles at normal ambient temperature					
Saybolt Colour	---	--	--	ASTM D156	+30
Density at 15°C	kg/m ³	775.0	840.0	ASTM D4052	791.7
Density at 15°C - Lower	kg/m ³	775.0	840.0	ASTM D4052	792.5
Density at 15°C - Middle	kg/m ³	775.0	840.0	ASTM D4052	792.8
Density at 15°C - Upper	kg/m ³	775.0	840.0	ASTM D4052	792.6
Density at 15°C - Calculated Mean	kg/m ³	775.0	840.0	ASTM D4052	792.6
Abel Flash Point	°C	38.0	--	IP 170	41.0
Existent Gum Content	mg/100ml	--	7	IP 540	2
Freezing Point	°C	--	-47.0	IP 529	-57.0
Initial boiling point (IBP)	°C	--	--	IP 123	147.6
10% Recovered at	°C	--	205.0	IP 123	165.3
20% Recovered at	°C	--	--	IP 123	175.9
50% Recovered at	°C	--	--	IP 123	198.0
90% Recovered at	°C	--	--	IP 123	243.9
Final boiling point (FBP)	°C	--	300.0	IP 123	280.2
% Residue	% (v/v)	--	1.5	IP 123	1.0
% Loss	%	--	1.5	IP 123	0.5
Total Sulphur Content	% (m/m)	--	0.30	ASTM D4294	0.0461
Doctor Test	---	--	--	IP 30	Pos
Mercaptan Sulphur	% (m/m)	--	0.0030	ASTM D3227	0.0004
Kinematic Viscosity at -20°C	cSt	--	8.000	ASTM D445	3.992
Net Heat of Combustion	MJ/kg	42.80	--	ASTM D3338	43.418
Smoke Point	mm	19.0	--	ASTM D1322	27.0
Aromatics	% (v/v)	--	25.0	ASTM D1319	13.7
Copper Strip corrosion (2h / 100°C)	Rating	--	1	IP 154	1
Acid Number	mg KOH/g	--	0.015	ASTM D3242	0.007
MSEP-A (with SDA)	---	70	--	ASTM D3948	96
Observed Temperature (Client Supplied)	°C	--	--	ASTM D2624	16.0
Conductivity (U,M,L Average) - Client Supplied	pS/m	50	600	ASTM D2624	308
Heater Tube Control Temperature	°C	260	--	IP 323	260

Sample and additive information received from client. Sampling not within scope of ISO/IEC 17025 Accreditation.
 The results shown in this test report specifically refer to the sample(s) tested as received unless otherwise stated. All tests have been performed using the latest revision of the methods indicated, unless specifically marked otherwise on the report. Precision parameters apply in the determination of the above results. Users of the data shown on this report should refer to the latest published revisions of ASTM D-3244; IP 367 and ISO 4259 and when utilising the test data to determine conformance with any specification or process requirement. This Test Report is issued under the Company's General Conditions of Service (copy available upon request or on the company website at www.sgs.com). Attention is drawn to the limitations of liability, indemnification and jurisdictional issues defined therein. This report shall not be reproduced except in full, without the written approval of the laboratory.

Authorised Signatory

Phil Hoos
Phil Hoos-Laboratory Supervisor

Page 1 of 2

21062011 1414 0000002625

SGS United Kingdom Ltd

Old Time Building, Junction Cut, Royal Edward Dock, Avonmouth, Bristol BS11 9DH Tel: +44 (0)117 937 9080 Fax: +44 (0)117 937 9081
Registered in England No. 1193985 Rossmore Business Park, Ellesmere Port, Cheshire CH65 3EN www.sgs.com

Member of the SGS Group (SGS SA)



JET A1 - FULL TEST REPORT
Test Certificate No: AV11-00069.004

PRINT DATE: 21/06/2011

SGS Oil, Gas and Chemicals
 Old Time Building,
 Junction Cut, Royal Edward Dock,
 Avonmouth, Bristol, BS11 9DH
 Tel: +44 (0) 117 937 9080
 Fax: +44 (0) 117 937 9081

AIR BP UK LTD
 GROUND FLOOR, BUILDING D
 CHERTSEY ROAD
 SUNBURY ON THAMESTW16 7LL

PRODUCT DESCRIPTION:	Jet A1	CLIENT ID:	HAL169	LOCATION:	Hallen
SAMPLE RECEIVED:	20/06/2011	SAMPLE BY:	BIS014	DATE SAMPLED:	20/06/2011
SAMPLE TYPE:	Composite	SAMPLE SOURCE:	Ex Tk25	SOURCE ID:	Tank 5
AIR BP SAMPLE REF:					

PROPERTY - AV11-00069.004	Units	MIN	MAX	METHOD	RESULT
Heater Tube Deposit Rating	--	--	<3	IP 323	1
<3 Max, no peacock or abnormal tube deposits					
Maximum Pressure Drop	mm Hg	--	25.0	IP 323	<1
Test Time	min	--	--	IP 323	150
Spent Fuel at End of Test	ml	--	--	IP 323	455
Heater Tube Serial No	--	--	--	IP 323	11C10988
Filtration Time	min	--	--	MIL-DTL-83133G (Appendix B)	12
Solids Content	mg/l	--	1.0	MIL-DTL-83133G (Appendix B)	0.3
FAME content of Aviation Fuel by GC-MS					
Total FAME Content	mg/kg	--	5.0	IP 585	<1.8

	Quantity
Non-Hydroprocessed components (% vol)	25.30
Hydroprocessed components (% vol)	74.70
Severely Hydroprocessed components (% vol)	41.85
Anti-Oxidant Content of Hydroprocessed Portion (mg/l)	20.0

	Refinery Certificate	Terminal Addition	Cumulative Static diss
Static Dissipator	0.0	0.9	1.1

Anti-Oxidant Limits: 17.0 mg/l to 24.0 mg/l mandatory for Hydroprocessed fuel. 24.0 mg/l max. overall irrespective of source
Static Dissipator Limits: 3.0 mg/l max. Cumulative Dose 5.0mg/l.

SGS United Kingdom Ltd certify that the above mentioned samples, have been tested in accordance with the methods stated above and that the Fuel Batch conforms to DefStan 91-91 Issue 7 and AFQRJOS Checklist 25.

Sample and additive information received from client. Sampling not within scope of ISO/IEC 17025 Accreditation.
 The results shown in this test report specifically refer to the sample(s) tested as received unless otherwise stated. All tests have been performed using the latest revision of the methods indicated, unless specifically marked otherwise on the report. Precision parameters apply in the determination of the above results. Users of the data shown on this report should refer to the latest published revisions of ASTM D-3244; IP 367 and ISO 4259 and when utilising the test data to determine conformance with any specification or process requirement. This Test Report is issued under the Company's General Conditions of Service (copy available upon request or on the company website at www.sgs.com). Attention is drawn to the limitations of liability, indemnification and jurisdictional issues defined therein. This report shall not be reproduced except in full, without the written approval of the laboratory.

Authorised Signatory

Page 2 of 2

21062011 1414 0000002625

Phil Hoos-Laboratory Supervisor

SGS United Kingdom Ltd

Old Time Building, Junction Cut, Royal Edward Dock, Avonmouth, Bristol BS11 9DH Tel: +44 (0)117 937 9080 Fax: +44 (0)117 937 9081
 Registered In England No. 1193985 RossmoreBusiness Park, Ellesmere Port, Cheshire CH65 3EN www.sgs.com

Member of the SGS Group (SGS SA)

Appendix C.2 Chinese No. 3

ORIGINAL

ANALYSIS REPORT

No.: DL110519-1

Client : PetroChina International (Hong Kong) Corporation Ltd.

Order No. : OGCDL110519	Date sampled : Apr.28, 2011
Product : JET A-1	Date Tested : Apr.29&May.03, 2011
Vessel : MT FPMC 17	Date Reported : May.04, 2011
Source : Ship's Tanks 1~6 P/S	Sample No. : DL11-0789.001
	Beach No. : WEPEC 4-25
Type of Sample : Composite	Page No. : 1/2

The mentioned sample has been tested and following results have been obtained:

ANALYTICAL ITEMS	UNIT	METHOD	SPECIFICATIONS		RESULTS
			MIN	MAX	
Appearance					
Visual Appearance		Visual		*	*
Color, Saybolt		GB/T 3555	+25		+30**
Composition					
Total Acidity	mgKOH/g	GB/T 12574		0.015	0.004**
Aromatics	%(V/V)	GB/T 11132		20.0	16.4
Olefins	%(V/V)	GB/T 11132		5.0	0.7
Total Sulfur	%(m/m)	GB/T 17040		0.20	0.0359**
Sulfur, Mercaptan	%(m/m)	GB/T 1792		0.0020	0.0005**
Volatility					
Distillation		GB/T 6536			
Initial Boiling Point	°C			Report	151.9**
10% V/V recovery	°C			205.0	167.1**
20% V/V recovery	°C			Report	172.6**
50% V/V recovery	°C			232	190.4**
90% V/V recovery	°C			Report	224.5**
End Point	°C			300.0	246.2**
Residue	%(V/V)			1.5	1.1**
Loss	%(V/V)			1.5	0.6**
Flash Point	°C	GB/T 261	38.0		41.0**
Density @ 20°C	kg/m ³	GB/T 1884	775.0	830.0	785.1**
Refining Components, at point of manufacture					
Hydroprocessed Components in batch	%(V/V)			Report	73.5
Severely Hydroprocessed Components	%(V/V)			Report	26.5

Remark: 1) * clear, bright and visually free from solid matter and undissolved water at ambient temperature.
 2) All above tests were tested in subcontract lab(** tested in SGS-CSTC lab).

The above reflects our findings at time, date and place of above mentioned only and does not refer to any other matters.
 (To Be Continued)

Authorized Signature
Oil, Gas & Chemicals Services

1) Precision parameters apply in the determination of the above results. Also refer to ASTM D3244, IP 367 & Appendix E of ISO Standards Methods for analysis & testing, for utilization of test data to determine conformance with specifications.
 2) This report shall not be reproduced, except in full, without the written approval of the laboratory.

This document is issued by the Company under its General Conditions of Service accessible at http://www.sgs.com/terms_and_conditions.htm. Attention is drawn to the limitation of liability, indemnification and jurisdiction issues defined therein. Any holder of this document is advised that information contained hereon reflects the Company's findings at the time of its intervention only and within the limits of Client's instructions, if any. The Company's sole responsibility is to its Client and this document does not exonerate parties to a transaction from exercising all their rights and obligations under the transaction documents. Any unauthorized alteration, forgery or falsification of the content or appearance of this document is unlawful and offenders may be prosecuted to the fullest extent of the law.

OGC/F-010/14/2.0R



ORIGINAL

ANALYSIS REPORT

No.: DL110519-1

Client : PetroChina International (Hong Kong) Corporation Ltd.
Order No. : OGCDL110519
Product : JET A-1
Vessel : MT FPMC 17
Source : Ship's Tanks 1~6 P/S
Date sampled : Apr.28, 2011
Date Tested : Apr.29&May.03, 2011
Date Reported : May.04, 2011
Sample No. : DL11-0789.001
Beach No. : WEPEC 4-25
Page No. : 2/2
Type of Sample : Composite

The mentioned sample has been tested and following results have been obtained:

Table with 5 columns: ANALYTICAL ITEMS, UNIT, METHOD, SPECIFICATIONS (MIN, MAX), RESULTS. Rows include Fluidity, Combustion, Corrosion, Stability, Contaminants, Conductivity, Water Separation Characteristics, and Lubricity.

Remark: 1) * clear, bright and visually free from solid matter and undissolved water at ambient temperature.
2) All above tests were tested in subcontract lab(** tested in SGS-CSTC lab).

The above reflects our findings at time, date and place of above mentioned only and does not reflect on other matters.



1) Precision parameters apply in the determination of the above results. Also refer to ASTM D3244, IP 367 & Appendix E of IP Standard Methods for analysis & testing, for utilization of test data to determine conformance with specifications.

2) This report shall not be reproduced, except in full, without the written approval of the laboratory.

This document is issued by the Company under its General Conditions of Service accessible at http://www.sgs.com/terms_and_conditions.htm. Attention is drawn to the limitation of liability, indemnification and jurisdiction issues defined therein. Any holder of this document is advised that information contained hereon reflects the Company's findings at the time of its intervention only and within the limits of Client's instructions, if any. The Company's sole responsibility is to its Client and this document does not exonerate parties to a transaction from exercising all their rights and obligations under the transaction documents. Any unauthorized alteration, forgery or falsification of the content or appearance of this document is unlawful and offenders may be prosecuted to the fullest extent of the law.

OGC/F-010/14/2.0R

Appendix C.3 Coryton High Aromatics Jet A-1



Certificate of Analysis

Fuel Blend No:	CAF-B11/006	Contact:	Rob Illidge
	Jet A-1 High		
Fuel Type:	Aromatics Aviation	Order No:	PO1100063636
	Kerosene		
Customer:	Airbus	Date:	18/06/2011

Test	Method	Unit	Limit		Result
			Min	Max	
Visual Appearance	Visual	Rating	Report		Clear & Bright
Colour	ASTM D156	Rating	Report		+24
Filtration Test	IP 423				
Residue	IP 423	mg/L	Report		0.65
Particulate	IP 564				
> or = 4	IP 564	µm c	Report		1774
> or = 6	IP 564	µm c	Report		273
> or = 14	IP 564	µm c	Report		7
> or = 21	IP 564	µm c	Report		2
> or = 25	IP 564	µm c	Report		1
> or = 30	IP 564	µm c	Report		<1
ISO Code No	IP 564		Report		18/15/10/8/7/>5
Total Acidity	ASTM D3242	mgKOH/g	-	0.015	0.003
Aromatics	ASTM D1319	% v/v	-	25	24.1
Sulphur Content	IP 336	% m/m	-	0.30	0.029
Sulfur Mercaptan	ASTM D3227	% m/m	-	0.0030	0.0003
Distillation					
IBP	ASTM D86	°C	Report		147.2
10% Volume Recovered	ASTM D86	°C	-	205	167.7
20% Volume Recovered	ASTM D86	°C	Report		173.6
30% Volume Recovered	ASTM D86	°C	Report		180.4
40% Volume Recovered	ASTM D86	°C	Report		185.5
50% Volume Recovered	ASTM D86	°C	Report		193.2
60% Volume Recovered	ASTM D86	°C	Report		200.2
70% Volume Recovered	ASTM D86	°C	Report		209.0
80% Volume Recovered	ASTM D86	°C	Report		219.4
90% Volume Recovered	ASTM D86	°C	Report		234.7
95% Volume Recovered	ASTM D86	°C	Report		248.8
FBP	ASTM D86	°C	-	300	262.5
Residue	ASTM D86	% v/v	-	1.5	1.2
Loss	ASTM D86	% v/v	-	1.5	0.7
Flash Point	IP 170	°C	38.0	-	38.5
Density @ 15°C	ASTM D4052	kg/m ³	775.0	840.0	810.8
Freeze Point	ASTM D2386	°C	-	-47	-57.0
Viscosity at -20°C	ASTM D445	mm ² /s	-	8.000	3.547
Smoke Point	ASTM D1322	mm	19.0	-	21.0
Naphthalenes	ASTM D1840	% v/v	-	3.00	1.89
Specific Energy	IP 12	MJ/kg	42.80	-	43.03
Copper Corrosion (2h at 100°C)	ASTM D130	Rating	1	-	1a

**Certificate of Analysis**

Fuel Blend No:	CAF-B11/006	Contact:	Rob Illidge
	Jet A-1 High		
Fuel Type:	Aromatics Aviation Kerosene	Order No:	PO1100063636
Customer:	Airbus	Date:	18/06/2011

Test	Method	Unit	Limit		Result
			Min	Max	
JFTOT Visual Tube Rating @ 260°C	IP 323	Rating	-	3	<1
JFTOT Pressure Difference @ 260°C	IP 323	mmHg	-	25	<1
Existent Gum	ASTM D381	mg/100ml	-	7	1
Water Separation with SDA	ASTM D3948	Rating	Report		92
Conductivity @ 20°C	IP 274	pS/m	50	600	214
Additives					
AO-32 RDE/A/610 Antioxidant Added to Hydroprocessed Hydrocarbon Content	Formulation	mg/L	17.0	24.0	Meets Spec
AO-32 RDE/A/610 Antioxidant Added to Non-Hydroprocessed Hydrocarbon Content	Formulation	mg/L	-	24.0	Meets Spec
Stadis 450 RDE/A/621 Static Dissipator	Formulation - Initial Dose at Manufacture	mg/L	Present	3.0	Meets Spec
Stadis 450 RDE/A/621 Static Dissipator	Incremental Addition	mg/L	Report		1.0
Stadis 450 RDE/A/621 Static Dissipator	Cumulative Total Dose	mg/L	-	5.0	<5.0
RDE/A/650 Metal Deactivator	Formulation	mg/L	-	5.7	Not Added
Lubricity Improver	Formulation	mg/L	-	23.0	Not Added
AL41 Diethylene Glycol Monomethyl Ether RDE/A/630 FSII	Formulation	% v/v	-	0.15	Not Added
Tracer A RDE/A/640 Leak Detector	Formulation	mg/kg	-	1.0	Not Added

Date:	18/06/2011
Signed:	

Coryton Advanced Fuels Ltd
The Manorway
Stanford-le-Hope
Essex SS17 9LN, UK

Tel: +44 (0)1375 665707
Fax: + 44 (0)1375 678904
Email: admin@corytonfuels.co.uk
Website: www.corytonfuels.co.uk

Appendix C.4 Russian TS-1 Aviation Kerosine



Certificate of Analysis

Fuel Blend No:	CAF-B11/019	Contact:	Rob Illidge
Fuel Type:	TS-1 Aviation Kerosene	Order No:	002593
Customer:	Airbus	Date:	09/08/2011

Test	Method	Unit	Limit		Result
			Min	Max	
Reid Vapour Pressure Proc A	ASTM D323	kPa	Report		2.00
Total Acidity	GOST 5985-79	mgKOH/100cm ³	-	0.7	0.11
Water Soluble Acids and Alkalis	GOST 6307-75	Rating	Absent		Absent
Iodine No	GOST 2070-82	gl ₂ /100g	-	3.5	0.9
Naphthenic Acid Soaps	GOST 21103-75	Rating	Absent		Absent
Aromatic Hydrocarbons	GOST 6994-75	% m/m	-	22	13
Sulphur Content	GOST R 50442-92	% m/m	-	0.25	<0.1
Sulfur Mercaptan	GOST 17323-71	% m/m	-	0.005	0.0015
Hydrogen Sulfide	GOST 17323-71	% m/m	Absent		Absent
Distillation					
IBP	GOST 2177-99	°C	-	150	148.5
10% Volume Recovered	GOST 2177-99	°C	-	165	159.0
50% Volume Recovered	GOST 2177-99	°C	-	195	180.0
90% Volume Recovered	GOST 2177-99	°C	-	230	214.0
98% Volume Recovered	GOST 2177-99	°C	-	250	245.0
Flash Point	GOST 6356-75	°C	28	-	37.0
Density @ 20°C	GOST 3900-85	g/cm ³	0.775	-	0.7944
Chilling Point	GOST 5066-91	°C	-	-80	-64
Viscosity at 20°C	GOST 33-2000	mm ² /s	1.250	-	1.407
Viscosity at -40°C	GOST 33-2000	mm ² /s	-	8.000	6.238
Ash Content	GOST 1461-75	% m/m	-	0.003	0.0001
Smoke Point	GOST 4338-91	mm	25.0	-	25.2
Lower Heating Value	GOST 11065-90	kJ/kg	42900	-	43187
Copper Corrosion (3h at 100°C)	GOST 6321-92	Rating	Report		1a
S1 Sediments Content	GOST 11802-88	mg/100ml	-	18	5
Phase Separation After 5min	GOST 27154-88	Rating	1	-	1
Phase Separation After 30min	GOST 27154-88	Rating	1	-	1
Contamination of Admixtures and Water	GOST 10227-98	Rating	Absent		Absent
Gum Content Unwashed	GOST 1567-97	mg/100ml	-	5	1
Conductivity @ 22.3°C	IP 274*	pS/m	50	600	315
Additives					
AO-32 RDE/A/610 Antioxidant Added	Formulation	mg/L	Report		20.0
Stadis 450 RDE/A/621 Static Dissipator	Formulation	mg/L	Report		1.0

* Substitute method to GOST 25950-83

Date:	09/08/2011
Signed:	

Coryton Advanced Fuels Ltd	Tel: +44 (0)1375 665707
The Manorway	Fax: + 44 (0)1375 678904
Stanford-le-Hope	Email: admin@corytonfuels.co.uk
Essex SS17 9LN, UK	Website: www.corytonfuels.co.uk

Appendix C.5 Sasol Fully Synthetic Jet A-1

				A Division of Sasol Oil (Pty) Ltd (Reg No. 52/02850/07) 32 Hillstreet, Ferndale Randburg Telephone (011) 889-7600 Telefax (011) 889-7979		P.O. Box 4211 Randburg 2125	
		NATREF LABORATORY CERTIFICATE OF QUALITY <small>Jan Haak Road, Sasolburg, 1947</small>					
AVIATION TURBINE FUEL (KEROSENE TYPE) A-1 (Fully Synthetic) PRODUCT CODE: 12/32							
Embodying the most stringent requirements of the following of the specifications for the grade shown:							
1. British MoD DEF STAN 91-91 (Issue 5, Amendment 1) dated 25 August 2008, for turbine fuel, (aviation kerosene) Jet A-1. 2. ASTM D1655-08, Jet A-1.							
Date Sampled		: 25 NOV 2010					
Tank No		: F7795Y-Z					
Certificate No		: 10/99/3					
Batch No		: 12/32/Y-Z/1					
Property	Units	Limits	Results	Test method		Note	
				ASTM / IP	Other		
1.1 Appearance Visual		Clear, bright and visually free from solid matter and undissolved water at normal ambient temperature.	Pass				
1.2 Colour		Report	>30	D156		1	
1.3 Particulate contamination	mg/l	1.0 max	0.8	D5452		2	
1.4 Particulate, at point of manufacture, cumulative channel partical count						2	
1.4.1 >= 4µm (c)		Report	844.0	IP564			
1.4.2 >= 6µm (c)		Report	159.1	IP564			
1.4.3 >= 14µm (c)		Report	6.4	IP564			
1.4.4 >= 21µm (c)		Report	1.1	IP564			
1.4.5 >= 25µm (c)		Report	0.3	IP564			
1.4.6 >= 30µm (c)		Report	0.1	IP564			
COMPOSITION							
2. Total acidity	mgKOH/g	0.015 max	<0.001	D3242		3,4	
3. Aromatics:							
3.1 Hydrocarbon Types Aromatics							
- Synthetic component present	vol %	8.0 - 25.0	10.7	D1319		5	
3.2 Total Aromatics	vol %	26.5 max	12.4	IP436		5	
4. Sulfur, Total	mass %	0.30 max	<0.01	D1266 D4294 IP107			
5. Sulfur Mercaptan	mass %	0.0030 max	<0.0001	D3227		6	
or Doctor test		Negative	-	IP 30			
8. Synthetic Jet Fuel component in batch	vol %	Report	100.0		CALCULATION	3	
VOLATILITY							
9. Distillation, corrected to 101,325 kPa							
Initial Boiling point	degC	Report	155.0	D86		8	
10% evap (v/v)	degC	205.0 max	176.0	D86			
50% evap (v/v)	degC	Report	197.7	D86			

Date Sampled : 25 NOV 2010
 Tank No : F7795Y-Z
 Certificate No : 10/99/3
 Batch No : 12/32/Y-Z/1

Property	Units	Limits	Results	Test method		Note
				ASTM / IP	Other	
90% evap (v/v)	degC	Report	244.5	D86		
End Point	degC	300.0 max	261.5	D86		
Residue	vol %	1.5 max	0.8	D86 IP123		
Loss	vol %	1.5 max	0.6	D86 IP123		
T50-T10	degC	20 min	22			
T90-T10	degC	40 min	69			
10. Flash point at 101,325kPa	degC	38.0 - 50.0	46.0	IP170		3,10,23
11. Density@ 20 degC	kg/m3	771.0 - 836.0	810.4	D4052 D1298/04 IP160 IP365/04		23
FLUIDITY						
12. Freezing point	degC	minus 47.0 max	minus 58.1	D 7153		11,23
13. Viscosity at minus 20 degC	mm2/s	8.000 max	5.229	D445		
COMBUSTION						
14. Specific energy, net	MJ/kg	42.80 min	43.25	D3338		12
15. Smoke point	mm	25.0 min	29.0	D1322		
OR Smoke point AND	mm	19.0 min		D1322		
Naphthalenes	vol%	3.00 max		D1840		
CORROSION						
16. Copper Corrosion (2h +/- 5 min@ 100 degC +/- 1 degC)		1 max	1A	D130		
STABILITY						
17. Thermal Stability (JFTOT)						
17.1 -Control Temperature	degC	260 min	-			13
17.2 - Filter pressure differential	mmHg	25.0 max	0	D3241		
17.3 - Tube deposit Rating (visual)		Less than 3, no 'Peacock' (P) or 'Abnormal' (A) deposits	<1	D3241		
CONTAMINANTS						
18. Existent gum	mg/100ml	7 max	0.9	D381		
19. Microseparator - (MSEP) Ratings:						
Fuel with Static Dissipator Additive		70 min	92	D3948		14
OR Fuel without Static Dissipator Additive		85 min	-	D3948		
CONDUCTIVITY						
20. Electrical Conductivity	pS/m	50 - 600	223	D2624		15
LUBRICITY						



Date Sampled : 25 NOV 2010
 Tank No : F7795Y-Z
 Certificate No : 10/99/3
 Batch No : 12/32/Y-Z/1

Property	Units	Limits	Results	Test method		Note
				ASTM / IP	Other	
21. BOCLE Wear scar diameter	mm	0.85 max	0.70	D5001		16
ADDITIVES						
22. Antioxidant: Ocel AO-30 (RDE/A/608) :						
Synthetic Jet Fuel Component (Mandatory)	mg/l	17.0 - 24.0	19.2		SSFJ107	17
Non-Hydrotreated Fuels (optional)	mg/l	24 max				
23. Metal Deactivator (optional):						
23.1 Point of manufacture	mg/l	2.0 max				
23.2 Redoping	mg/l	5.7 max				18
24. Static Dissipator Additive: RDE/A/621:						
24.1 First Doping	mg/l	3.0 max	1.0			19
24.2 Re-doping - same Additive:						20
Cumulative Concentration Static Dissipator Additive	mg/l	5.0 max	-			
24.3 Re-doping or Change of Additive or Original not known						
Additional Static Dissipator Additive	mg/l	2.0				
25. Lubricity additive		None	Nil			
26. Icing Inhibitor		None	Nil			
27. Change management		None				20

NOTES:

1. The requirement to report Saybolt Colour shall apply at point of manufacture, thus enabling a colour change in distribution to be quantified. Where the colour of the fuel precludes the use of the Saybolt Colour test method, then the visual colour shall be reported. Unusual or atypical colours should also be noted and investigated. For further information see An E in DEF STAN 91-91/6 Am1.

2. This limit shall apply at point of manufacture only. For more information refer to An F of DEF STAN 91-91/6 Am1. For guidance on contamination limits for auto plane fuelling refer to 6th edition IA IA Guidance Material (Part III). The implementation date for particle counting is 30th June 2009, the results should be reported as soon as possible. It is the Specification Authorities intention to replace gravimetric membrane filtration test with particle counting at the earliest opportunity. The number of particulates shall be reported as a scale number as defined by Tbl 1 of ISO 4406:1999.

3. Attention is drawn to DEF STAN 91-91 and ASTM D1655 which approves the Semi-Synthetic Jet fuel (SSJF) produced by SASOL under approval reference FS(Air)ssjof1. For SSJF additional testing requirements apply and reference should be made to DEF STAN 91-91/6 Am1, An D. 4.2. Sasol Fully Synthetic Jet Fuel.

D4.2.1 Sasol synthetic kerosene, see clause D4.2.4, is currently the only fully synthetic jet fuel which has been approved for use.

D4.2.2 The aromatic content of Sasol fully synthetic jet fuel shall not be less than 8.0% nor greater than 26.0% by volume when using method IP156, or less than 8.4% nor greater than 26.5% by volume when using method IP436. The fuel shall exhibit a maximum wear scar diameter of 0.65mm when tested by ASTM D5001. Analysis for these properties shall be made at the point of manufacture.

D4.2.3 The flash point shall be no greater than 50°C. The boiling point distribution shall have a minimum slope defined by T50-T10>=20°C and T60-T10>=40°C when measured by IP123/ASTM D86.

D4.2.4 Sasol fully synthetic kerosene is defined as that material blended from light distillate, heavy naphtha and iso-paraffinic kerosene streams manufactured at the Secunda plant as described in the SwRI reports number 06-04439 and 06-04438-2. The batch certificate for the fuel shall state that the fuel contains 100% synthetic components.

4. Concentrations of FAME (Fatty Acid Methyl Ester) greater than or equal to 5.0mg/kg are not acceptable. This does not require mandatory testing of every batch. See section of 5.5 and Annex G of DEF STAN 91-91/6 Am 1 for details.



Date Sampled : 25 NOV 2010
Tank No : F7795Y-Z
Certificate No : 10/99/3
Batch No : 12/32/Y-Z/1

5. Testing for total aromatics has been introduced into DEF STAN 91-91. It is included in Check List to promote the adoption of more modern test methods. The DEF STAN note reads "Round robin testing has demonstrated the correlation between total aromatics content measured by IP 188/ASTM D 1310 and IP 436/ASTM D 6379. Bias between the two methods necessitates different equivalent limits as shown. In case of dispute IP 156/ASTM D1319 will be the referee method."
6. The Doctor Test is an alternative requirement to the Sulphur Mercaptan Content. In event of conflict between the Sulphur Mercaptan and Doctor Test results, The Sulphur Mercaptan results shall prevail.
7. The need to report the %vol of hydroprocessed and severely hydroprocessed components (including "nil" or "100%" as appropriate) on refinery Certificates of Quality for Jet A-1 to Check List derives from DEF STAN 91-91/6 Am1. It relates to:
- a) Antioxidant additives (additive dose rate cannot be interpreted unless the proportion of hydroprocessed fuel is known and therefore recipients of Jet A-1 cannot check or demonstrate that fuel complies with Check List if this information is omitted from refinery Certificates of Quality.
 - b) The requirements to report volume% of severely hydroprocessed components as part of the lubricity requirement of DEF STAN 91-91/6 Am1. Note that "hydroprocessed" includes hydrotreated, hydrofined and hydrocracked. Severely hydroprocessed components are defined as petroleum derived hydrocarbons that have been subjected to hydrogen partial pressure of greater than 7000kPa (70 bar or 1015 psi) during manufacture. The severely hydroprocessed components shall be reported on the certificate of quality as a percentage by volume of the total fuel in the batch.
8. In methods IP 123 and ASTM D 86 all fuels certified to this specification shall be classed as group 4, with a condenser temperature of 0 to 4 deg C.
9. There are different requirements for the use of IP 406 or D 2887 as an alternate method between ASTM D 1655-08a and DEF STAN 91-91/6 Am 1. ASTM allows the use of simulated distillation results directly with different limits while DEF STAN requires a conversion of simulated distillation results to estimated IP 123 results using Annex G IP 406. These different approaches were taken because of operational considerations rather than technical considerations. There is no intent that 1 approach is more restrictive than the other. If IP 406 is the method used to generate IP 123 extrapolated data, there is no requirement to report residue or loss. IP 123 extrapolated may also be used for the calculation of Specific Energy using ASTM D 3338.
10. Subject to a minimum of 40 deg C, results obtained by method ASTM D 56 (T₉₀) may be accepted.
11. These automatic methods are allowed by DEF STAN 91-91/6. IP 16/ ASTM D 2366 remains the referee method.
12. ASTM D4529/ IP 391 may be used where local regulations permit.
13. Examination of the heater tube to determine the Visual Tube Rating using the Visual Tubercator shall be carried out within 120 minutes of completion of the test. It is the Visual Tube Rating that should be reported. Attention is drawn to note 13 in DEF STAN 91-91/6 Am1, which stresses that only approved heater tubes shall be used and lists JFTOT tubes from PAC-Alcor as being technically suitable.
14. Attention is drawn to note 14 of DEF STAN 91-91/6 Am 1 that states "No precision data are available for fuels containing SDA, if MSEP testing is carried out during downstream distribution, no specification limits apply and the results are not to be used as the sole reason for rejection of a fuel." A protocol giving guidelines on actions to be taken following failed MSEP testing can be found in the Joint Inspection Group's Bulletin Number 14, MSEP protocol at www.jointinspectiongroup.org under "Fuel quality".
15. Due to the requirements of DEF STAN 91-91/6 Am1 Conductivity limits are mandatory for product to meet this specification. However it is acknowledged that in some manufacturing and distribution systems it is more practical to inject SDA further downstream. In such cases the Certificate of Quality for the batch should be annotated thus "Product meets the requirements AFQ/IOS Check List 24 except for electrical conductivity". In some situations, the conductivity can decrease rapidly and the fuel can fail to respond to additional dosing with STADIS 450. In such cases, fuel may be released with conductivity down to a minimum of 25pS/m provided that the fuel is fully tested against the specification and the tank Release Note is annotated with the explanation "Product released below 50pS/m due to conductivity loss as per Annex H of DEFSTAN 91-91/6 Am 1.
16. This requirement comes from DEF STAN 91-91/6 Am1. The requirement to determine lubricity applies only to fuels containing more than 95% hydro processed material where at least 20% is severely hydro processed (see note 7 above) and for all fuels containing synthetic components. The limit applies only at the point of manufacture. For important advisory information on the lubricity of aviation turbine fuels see Annex B of DEF STAN 91-91/6 Am 1. CIL/1 additive may be used to improve lubricity, only those additives listed in Table 2 of ASTM D1655-08a are permitted. Refer also to Appendix A.5 of DEF STAN 91-91/6 Am1 for advice on point of addition. When injecting CIL/1 downstream of point of manufacture, care must be taken to ensure that maximum dose rate are not exceeded.
17. Approved antioxidant additives are listed in Annex A.2.4 of DEF STAN 91-91/6 Am 1, together with the appropriate RDE/A/XXX-Qualification Reference for quoting on refinery Certificates of Quality. Where a fuel contain synthetic jet fuel component, or a blend component of the fuel, has been hydro processed and or severely hydro processed, the concentration of active material added to the hydro processed portion of the blend shall be reported on the certificate of quality. If antioxidant has also been added to the non-hydro processed portion of the fuel, the concentration of active material added to this portion should be reported on a separate line on the certificate of quality.
18. The approved Metal Deactivator Additive (MDA) RDL/A/650 appears in Annex A.3 of DEF STAN 91-91/6 Am 1. See also Annex A.3.1. about the need to report thermal stability before and after using when contamination of Jet A-1 by any of these trace metals listed in this Annex is unproven. Note also in A.3.3 that maximum doping at the point of manufacture or on initial doping is limited to 2mg/l.
19. Re-doping limits for static Dissipator additive are:
- | | | |
|--------------------------------|---------------------------|----------|
| (c) Cumulative concentration | Stadis(R) 450 (RDE/A/621) | 5.0 mg/l |
| (d) Original dosage not known: | | |
| Additional concentration | Stadis(R) 460 (RDE/A/621) | 2.0 mg/l |



Date Sampled : 25 NOV 2010
Tank No : F7795Y-Z
Certificate No : 10/99/3
Batch No : 12/32/Y-Z/1

20. Concentrations of Fuel System Icing Inhibitor (FSII) less than 0.02% by volume can be considered negligible and do not require agreement/notification. The assent to allow these small quantities of FSII without agreement/notification is to facilitate the change over from fuels containing FSII to those not containing FSII where the additive may remain in the fuel system for a limited time. This does not allow the continuous FSII addition at these low concentrations.

21. Attention is drawn to the guidance in DEF STAN 91-91/6 Am1 and ASTM D1655-08a concerning the need for appropriate management of change measures in refineries manufacturing Jet Fuel. The implications of any changes to feedstock, processing conditions or process additives on finished product quality and performance need to be considered (for example, experience has shown that some additives might be carried over in trace quantities into aviation fuels).

22. It is normal to certify conformance to specifications with statements like "It is certified that the samples have been tested using the Test Method stated and that the batch represented by the samples conforms to AFQRJOS Check List issue 24. Where applicable Batch Certificates may also confirm, specifically, compliance with DESTAN 91-91 and/or ASTM D 1655.

23. SANAS Accredited method.

Signature : 
T.E.A. Nkitseng
Divisional Manager

Date: 29/11/2010

MO Mahle
Senior Chemist
Natref Laboratory

Appendix C.6 JP-4 Wide-Cut Fuel



Certificate of Analysis

Fuel Blend No:	CAF-B11/023	Contact:	Rob Illidge
Fuel Type:	JP-4 NATO F40	Order No:	6500100079
Customer:	Airbus	Date:	01/09/2011

Test	Method	Unit	Limit		Result
			Min	Max	
Visual Appearance	Visual	Rating	Report		C&B
Colour	ASTM D156	Rating	Report		+30
Filtration Test	IP 423				
Residue	IP 423	mg/L	-	1.0	0.4
Particulate	IP 564				
> or = 4	IP 564	µm c	Report		1307
> or = 6	IP 564	µm c	Report		194
> or = 14	IP 564	µm c	Report		13
> or = 21	IP 564	µm c	Report		5
> or = 25	IP 564	µm c	Report		3
> or = 30	IP 564	µm c	Report		2
ISO Code No	IP 564		Report		18/15/11/10/9/8
Total Acidity	ASTM D3242	mgKOH/g	-	0.015	0.003
Aromatics	ASTM D1319	% v/v	-	25	10.3
Sulphur Content	IP 336	% m/m	-	0.30	<0.01
Sulphur Mercaptan Content	IP 342	% m/m	-	0.0030	<0.001
Hydroprocessed Hydrocarbon Content	Formulation	% v/v	Report		30.7
Severely Hydroprocessed Hydrocarbon Content	Formulation	% v/v	Report		45.3
Distillation					
IBP	ASTM D86	°C	Report		38.8
10% Volume Recovered	ASTM D86	°C	Report		107.1
20% Volume Recovered	ASTM D86	°C	100	-	161.0
30% Volume Recovered	ASTM D86	°C	Report		176.6
40% Volume Recovered	ASTM D86	°C	Report		186.5
50% Volume Recovered	ASTM D86	°C	125	-	192.6
60% Volume Recovered	ASTM D86	°C	Report		198.2
70% Volume Recovered	ASTM D86	°C	Report		205.3
80% Volume Recovered	ASTM D86	°C	Report		213.6
90% Volume Recovered	ASTM D86	°C	Report		225.4
95% Volume Recovered	ASTM D86	°C	Report		234.7
FBP	ASTM D86	°C	-	270	244.0
Residue	ASTM D86	% v/v	-	1.5	1.1
Loss	ASTM D86	% v/v	-	1.5	1.3
Reid Vapour Pressure @ 37.8°C	IP 69	kPa	18.0*	21.0	20.4
Density @ 15°C	ASTM D4052	kg/m ³	751.0	802.0	779.5
Freeze Point	ASTM D2386	°C	-	-58	-58
Smoke Point	ASTM D1322	mm	25.0	-	27.0
Naphthalenes	ASTM D1840	% v/v	-	3.00	0.8
Specific Energy	ASTM D3338	MJ/kg	42.80	-	43.50
Copper Corrosion (2h at 100°C)	ASTM D130	Rating	1	-	1a



Certificate of Analysis

Fuel Blend No:	CAF-B11/023	Contact:	Rob Illidge
Fuel Type:	JP-4 NATO F40	Order No:	6500100079
	AVTAG/FSII	Date:	01/09/2011
Customer:	Airbus		

Test	Method	Unit	Limit		Result
			Min	Max	
JFTOT Visual Tube Rating @ 260°C	IP 323	Rating	-	3	1
JFTOT Pressure Difference @ 260°C	IP 323	mmHg	Report		<1
Existent Gum	ASTM D381	mg/100ml	-	7	<1
Water Separation with SDA	ASTM D3948	Rating	Report		62
Conductivity @ 20°C	IP 274	pS/m	50	600	364
Additives					
AO-32 RDE/A/610 Antioxidant Added to Hydroprocessed Hydrocarbon Content	Formulation	mg/L	17.0	24.0	20.1
AO-32 RDE/A/610 Antioxidant Added to Non-Hydroprocessed Hydrocarbon Content	Formulation	mg/L	-	24.0	20.1
Stadis 450 RDE/A/621 Static Dissipator	Formulation	mg/L	Present	3.0	2.0
RDE/A/650 Metal Deactivator	Formulation	mg/L	Report		
Nalco 5403 RDE/A/664 Lubricity Improver	Formulation	mg/L	12.0	23.0	18.1
AL41 Diethylene Glycol Monomethyl Ether RDE/A/630 FSII	Formulation	% v/v	0.10	0.15	0.126
Tracer A RDE/A/640 Leak Detector	Formulation	mg/kg	-	1.0	0.0

* Customer defined minimum specification

* MSEP specification range only valid for testing at upstream manufacture point. Downstream testing is report only.

Date:	01/09/2011
Signed:	

Coryton Advanced Fuels Ltd
The Manorway
Stanford-le-Hope
Essex SS17 9LN, UK

Tel: +44 (0)1375 665707
Fax: + 44 (0)1375 678904
Email: admin@corytonfuels.co.uk
Website: www.corytonfuels.co.uk

Appendix D: IMechE Event Brochure – Managing Water and Ice in Aviation Fuel Under Cold Temperatures



MANAGING WATER AND ICE IN AVIATION FUEL UNDER LOW TEMPERATURE CONDITIONS.

Institution of
**MECHANICAL
ENGINEERS**

Aerospace Division
Seminar

29 May 2013
London
www.imeche.org/events/S1773



WHY YOU SHOULD BE THERE

A recent incident on a twin-engined large commercial aircraft led the Aviation Accident Investigation Branch (AAIB) to make recommendations to airworthiness authorities for further research into aspects relating to water and ice in fuel.

The European Aviation Safety Agency (EASA) and the US Federal Aviation Administration (FAA) agreed a common approach to tackle these recommendations.

EASA launched the WAFCOLT research project to explore water in aviation fuel under cold temperature conditions. Initial research findings will be presented here, updating you on the latest understanding of the formation and

characterisation of ice in aviation fuel, ensuring reduced icing risk in aircraft fuel systems design as well as certification compliance.

Featuring presentations from the regulators as well as Airbus and Rolls-Royce, improve your understanding of the formation and characterisation of ice in aircraft fuel systems, minimising the challenges that icing may cause in their operation.

KEY TECHNIQUES COVERED:

- Understand the airworthiness directives and adhere to European legislation
- Evaluate the latest research findings on icing in fuel systems
- Understand the key parameters on ice accretion and growth
- Examine the current and future uses of fuel tank materials to reduce icing risk
- Learn more about icing rig for fuel system testing

WHEN	29 May 2013
WHERE	1 Birdcage Walk, London SW1H 9JJ
BOOK ONLINE	www.imeche.org/events/S1773

SUPPORTING ORGANISATIONS


**ROYAL
AERONAUTICAL
SOCIETY**

SPONSORSHIP & EXHIBITION OPPORTUNITIES
GET INVOLVED

Attending this event as either an exhibitor or sponsor will give you the opportunity to display your solutions, services and products to the right people at the right time.

This is an excellent way to enhance your company profile and communicate effectively to your target audience.

BENEFITS OF SPONSORING

- Showcase new products
- Raise awareness of your operation
- Improve perception of your brand
- Influence other organisations' spending plans

For sponsorship and exhibition enquiries, please contact **Aman Duggal** on +44 (0)20 7973 1309 or sponsorship@imeche.org

OTHER EVENTS TO LOOK FOR:

7 May 2013, London

**AN AEROSPACE ARCHIVE
POWERED FLIGHT - FILM
EVENING.**

This second programme of rare archive films tells the story of the first 50 years of powered flight from the Wright Brothers to the modern jet age. For more information email www.imeche.org/events/L321

14 May 2013, London

**THE NEXT GENERATION
OF UAS TECHNOLOGY:
A BAE SYSTEMS PERSPECTIVE.**

Chris Clarkson is responsible for the engineering capability at BAE Systems' Military Aircraft and Information sector and will discuss development of UAS technology and future developments
www.imeche.org/events/L313

29 May 2013, London

**80 YEARS IN AVIATION:
CAPTAIN ERIC "WINKLE"
BROWN.**

From flying in wartime to promoting the safe and efficient operation of helicopters, Captain Eric 'Winkle' Brown's vast expertise spans the 20th century. In this lecture, he introduces highlights from his life in aviation
www.imeche.org/events/L317

If you are interested in any of these events, please contact **Lisa Meenan** on +44 (0)20 7973 1242 or l_meenan@imeche.org

FOLLOW OUR WEEKLY UPDATES
ON WWW.IMECHE.ORG



**SPEAKERS
AND CONTRIBUTORS**

THOMAS MALONEY

FEDERAL AVIATION ADMINISTRATION
Thomas has an MSc and BSc in mechanical and aerospace engineering, where his research focused on fuel icing at the FAA technical centre. He now works within the Fire Safety Research Group.

MARK REID FIMechE

FUEL SYSTEM SPECIALIST,
ROLLS-ROYCE
Mark joined Rolls-Royce in Derby after graduating, working in the Fluid Systems Group supporting fuel, oil and heat management system design and integration for Trent engines.

DR JOSEPH K-W LAM

FIMechE
CFD SPECIALIST, AIRBUS
Joseph's main research focus is water and ice management in fuel systems. He led the 2011 EASA WAFCOLT project and is currently leading the EASA ice accretion and release in fuel systems project.

RÉMI DELÉTAIN

POWERPLANT INSTALLATION AND FUEL SYSTEMS EXPERT, EASA
Rémi's role covers certification aspects of large fixed-wing aircraft and rotorcraft including continued airworthiness, type certification, validation and support to other EASA departments in the fields of fire, fuel system, powerplant and APU installations.

PROGRAMME

WELCOME WEDNESDAY 29/6	9:15	REGISTRATION AND REFRESHMENTS
	10:10	WELCOME AND INTRODUCTION
	10:15	LOOKING FOR ICE Brian McDermid, AAIB
	10:45	CERTIFICATION RULES RELATED TO FUEL SYSTEM ICING Rémi Déletain, Senior Inspector, EASA
	11:15	REFRESHMENTS
	11:45	ENGINE FUEL SYSTEM TOLERANCE TO FUEL-BORNE ICE Mark Reid, Rolls-Royce
	12:15	TITLE TBC TBC, Boeing
	12:45	LUNCH
	13:45	THE LITERATURE REVIEW OF THE EASA WAFCOLT PROJECT Dr Joseph Lam, CFD Specialist, Airbus
	14:15	RESEARCH FINDINGS OF THE EASA WAFCOLT PROJECT ON THE PHYSICAL PROPERTIES OF ACCRETED ICE Dr Liyun Lao, Senior Research Fellow, Cranfield University
	14:45	RESEARCH FINDINGS OF THE EASA WAFCOLT PROJECT ON THE WATER SOLUBILITY IN AVIATION FUEL Mark Carpenter, Postdoctoral Researcher, Cranfield University
	15:15	REFRESHMENTS
	15:45	FAA RESEARCH FINDINGS ON ICE IN JET A-1 Thomas Maloney, Fire Safety Research Group, FAA
	16:15	RESEARCH FINDINGS ON ICE ACCRETION ON PUMP MESH (BASED ON AIRBUS-SPONSORED PHD) Solange Baena, PhD Student, Cranfield University
	16:45	CHAIRMAN'S CONCLUSIONS
	16:50	CLOSE

Find out more about our speakers at www.imeche.org/events/S1773

- This programme is subject to change.
- The Institution is not responsible for the views or opinions expressed by individual speakers.

Aerospace Division Organising Committee:

with assistance from
Dr Joseph Lam, Airbus
Emmanuel Isambert, EASA
Brian McDermid, AAIB

The committee would like to thank the following supporters:

Safety and Reliability Group, Thermofluids Group and Fluid Machinery Group.

BOOKING FORM

AEROSPACE DIVISION
**WATER AND ICE IN AVIATION FUEL
 UNDER LOW TEMPERATURE CONDITIONS.**

29 MAY 2013
 S1773

REGISTRATION Please complete in capitals.

Family Name _____ Title (Mr, Mrs, Miss) _____
 First Name _____ Job Title _____
 Membership No _____ Institution _____
 Name of Organisation (for name badge) _____
 Address for correspondence _____

 Town/City _____
 Postcode _____
 Contact Telephone _____
 Email _____
 Do you have any special requirements? _____

How did you hear about this event? Direct mail Website Colleague Other

The Institution organises a wide programme of events each year. If you would like to receive information about our events, please tick this box

FEEES AND CHARGES Please complete the appropriate box.

Registration fees include entry to the sessions, refreshments, lunch, and a copy of the event proceedings.

1 DAY RATE	Fee	VAT	Total	£
Member, Institution of Mechanical Engineers - early booking	£230.00	£46.00	£276.00	_____
Member, supporting organisation - early booking	£230.00	£46.00	£276.00	_____
Non-member - early booking	£299.00	£59.80	£358.80	_____
Retired Member / Student - early booking	£45.00	£9.00	£54.00	_____
Member, Institution of Mechanical Engineers	£265.00	£53.00	£318.00	_____
Member, supporting organisation	£265.00	£53.00	£318.00	_____
Non-member	£340.00	£68.00	£408.00	_____
Retired Member / Student	£60.00	£12.00	£72.00	_____
EXTRA ITEMS	Fee	VAT	Total	£
Invoice Charging (if applicable)	£10.00	£2.00	£12.00	_____
			Total	_____

PAYMENT DETAILS

Payment must accompany this registration form. Registration will be confirmed only on receipt of full payment.
 Please indicate method of payment: Cheque Credit Card BACS Invoice (see below)
 Cheques should be made payable to IMechE and crossed. Please note international delegates may pay only by credit card, BACS or banker's draft. A copy of the draft must accompany this form. It is the delegate's responsibility to pay any bank charges.

Credit Card: Visa MasterCard (please note we cannot accept American Express, Diners Club or Maestro)

Card No _____ Valid From _____ / _____ Expiry Date _____ / _____
 Name of Cardholder _____
 Billing Address of Cardholder (if different from above) _____

 Postcode _____
 Amount to be Deducted _____ Signature _____

INVOICE DETAILS (UK DELEGATES ONLY)

Delegates wishing to be invoiced must provide an order number. If your company does not use order numbers please include a formal request for invoicing on your company's letterhead. A charge of £10 +VAT will be made to cover additional administration costs. Invoices are payable on receipt and no alterations to these terms will be accepted.

Order No _____
 Contact Name _____
 Name and Address for Invoicing _____

 Postcode _____
 Tel _____ Fax _____
 BACS bank transfers can be made to **IMechE Current Account, NatWest Charing Cross Branch**
 Sort code: **60-40-05** Acc No. **00817767** A copy of the draft must accompany this form.
 Swift Code: **NWBKGB2L** IBAN Code: **GB96NWBK60400500817767**

Early booking discount available until **Wednesday 17 April 2013**
 For added convenience you can also book online at www.imeche.org/events/S1773

Please complete and return this form to:

EVENT REGISTRATIONS
 Institution of Mechanical Engineers
 1 Birdcage Walk, London SW1H 9JJ
 Fax +44 (0)20 7222 9881
 For registration enquiries call
Tina Churcher on +44 (0)20 7973 1258
 or email t_churcher@imeche.org

Please read the information listed below as each booking is subject to the Institution's standard terms and conditions.

CONDITIONS OF BOOKING
 Completed application forms should be returned to the address above, along with the correct payment. Attendance at the event will be confirmed on receipt of the full balance. All participants are advised to bring a copy of their confirmation with them on the day, to ensure the fastest possible entry.

SPECIAL REQUIREMENTS
 Please inform us of any special requirements, ie dietary or access, on the relevant section of this form.

CANCELLATION
 For a refund (minus £25 +VAT admin charge), cancellations must be received at least 14 days prior to the event. Replacement delegates are welcome at any time. The Institution reserves the right to cancel any event. In this case, the full fee will be refunded unless a mutually convenient transfer can be arranged. In the event that the Institution postpones an event for any reason and the delegate is unable or unwilling to attend on the rescheduled date, they will receive a full refund of the fee paid.

The Institution is not responsible for any loss or damage as a result of a substitution, alteration or cancellation/postponement of an event. The Institution shall assume no liability whatsoever if this event is cancelled, rescheduled or postponed due to a fortuitous event, Act of God, unforeseen occurrence or any other event that renders performance of this conference impracticable, illegal or impossible. For purposes of this clause, a fortuitous event shall include, but not be limited to: war, fire, labour strike, extreme weather or other emergency.

Please note that while speakers and topics were confirmed at the time of publishing, circumstances beyond the control of the organisers may necessitate substitutions, alterations or cancellations of the speakers and/or topics. As such, the Institution reserves the right to alter or modify the advertised speakers and/or topics if necessary without any liability to you whatsoever. Any substitutions or alterations will be updated on the event's webpage as soon as possible.

SUPPORTING ORGANISATIONS
 Members of supporting organisations can register at members' rates. See page 2.

VENUE
 This event will be held at 1 Birdcage Walk, London SW1H 9JJ

LIABILITY
 The organisers do not accept liability for any injuries or losses of any nature incurred by delegates and/or accompanying persons, not for loss or damage to their luggage and/or personal belongings.

ACCOMMODATION
 We have arranged special discounted rates at local hotels via The Corporate Team.
 Tel: 0845 604 4060 (UK only)
 or +44 (0)20 7592 3050 (international)
 Email: events@corporateteam.com
 (Quote ID number 8488ME)
www.corporateteam.com/events/8488ME

ENQUIRIES
 For event enquiries, please contact
Lisa Meenan
 on +44 (0)20 7973 1242
 or email L.meenan@imeche.org

The Institution of Mechanical Engineers is a registered charity (no 206882)
 VAT No GB299930493



EUROPEAN AVIATION SAFETY AGENCY
AGENCE EUROPÉENNE DE LA SÉCURITÉ AÉRIENNE
EUROPÄISCHE AGENTUR FÜR FLUGSICHERHEIT

Postal address

Postfach 101253
50452 Cologne
Germany

Visiting address

Ottoplatz 1
50679 Cologne
Germany

Tel +49_221_89990-000

Fax +49_221_89990-999

Mail info@easa.europa.eu

Web easa.europa.eu